
**Modelling and Assessment of Renewable Energy
Systems for Remote Rural Areas in Nigeria**

Christian Akaraka Onwe BEng (Hons), MSc



The thesis submitted to the School of Science and Engineering

University of Dundee

for the degree of Doctor of Philosophy (PhD)

July 2017

Table of contents

Table of contents	i
List of figures.....	vii
List of Tables	xi
Dedication	xiii
Acknowledgements.....	xiv
Declaration.....	xvi
List of Acronyms and Nomenclature.....	xvii
Summary	xxii
1	1
Introduction	1
1.1 Introduction: Background – The Challenges.....	1
1.2 Energy and the World	2
1.2.1 Access to Electricity.....	5
1.2.2 The Big Issue.....	6
1.2.3 Climate Change and Nigeria.....	9
1.3 Aim and Motivation	10
1.4 Potential Research Gaps and Problem Statement.....	11
1.5 Objectives.....	13
1. References	16
2	19
2.0 Literature Review	19
2.1 Review of Nigeria Energy and Electricity Sectors.....	19
2.1.1 Population Growth Vs Gross Domestic Products (GDP)	20
2.1.2 Poverty Metrics.....	23
2.1.3 Justification for Access to Basic Amenities	24
2.1.4 The Electricity Generation Situation in Nigeria.....	25
2.1.5 Electricity Consumption	30
2.1.6 Network and Grid Structure.....	34
2.1.7 Access to Electricity in Nigeria	36
2.2 Review of Nigeria Renewable Energy Resources.....	40
2.2.1 Solar Energy Resources	41
2.2.2 Hydro.....	42

2.2.3	Wind	45
2.3	Present, Past and Future targets of renewable activities in Nigeria	46
2.	References	52
3	56
3.0	Energy Storage System: The Technology and Application.....	56
3.1	Energy Storage Imperative.....	56
3.1.1	Energy Storage Mediums and Methods.....	57
3.1.2	Super-capacitor	58
3.1.3	Flywheel	60
3.1.4	Pumped Hydroelectric Storage	61
3.1.5	Hydrogen Storage	62
3.2	Energy Storage for Renewable Energy Systems	64
3.3	Renewable – Hydrogen Systems.....	65
3.3.1	Solar Photovoltaic Fundamentals	66
3.3.2	Photovoltaic Open Circuit Voltage and Short Circuit Current	69
3.3.3	Governing Equations of the Solar Photovoltaic – The Equivalent Circuit.....	70
3.3.4	Solar Panel.....	71
3.3.5	Photovoltaic Technology and the World – What is the Africa Stand?.....	72
3.3.6	Renewable Technology for Rural Electrification.....	73
3.4	Solar – Hydrogen Storage; the Technologies.....	76
3.4.1	Electrolysis.....	76
3.4.2	Types of Electrolysers	78
3.4.3	Alkaline Electrolyser	78
3.4.4	Solid Proton Exchange Membrane (PEM).....	80
3.5	Hydrogen Storage Mediums and Methods.....	81
3.5.2	Liquid Hydrogen Storage.....	82
3.5.3	Solid - Hydrogen Storage	83
3.6	Fuel Cell.....	84
3.7	Examples of Existing Renewable - Hydrogen Systems and Some Research Activities.....	85
3.	References	90
4	95
4.0	Design and Construction of Renewable Energy Data Logging and Monitoring System	95
4.1	Identifying the Components Used in the Logging System Design	95
4.1.1	Micro SD Card Breakout Board	95
4.2	Measurement Tool.....	96
4.3	How Does the Current Sensing Breakout Board Work?	97

4.4	Increasing the Input	98
4.5	Changing the Shunt Resistor – INA219	99
4.6	Microcontroller	100
4.6.1	Arduino Uno – Atmega328.....	101
4.6.2	Communication.....	101
4.6.3	Programming the Board.....	102
4.7	Current Sensing.....	103
4.7.1	Principles of Current Sensing	103
4.8	Analysing the Hybrid Renewable Power Monitoring Data in Dundee UK	106
4.8.1	PV and Wind Turbine Output Power	110
4.9	Obtaining the Daily Output Power Productions of the PV and Wind Turbine.....	112
4.9.1	Daily Power Outputs of the PV Module and Wind Turbine and Battery Voltage.....	112
4.10	Energy Analysis	116
4.10.1	Energy Productions by Individual Components	117
4.10.2	Solar Panel Energy Productions	118
4.10.3	Estimating the Useful Energy Production of the PV Panel.....	118
4.10.4	Energy Production of the Wind Turbine	119
4.10.5	Discussion.....	120
4.11	The Drain of the Battery and its Implications	121
4.11.1	Battery Discharge Rate.....	122
4.11.2	Determination of Battery Internal Resistance	124
4.12	Monitoring of solar PV system in Abuja Nigeria	127
4.12.1	Daily Power Outputs of the 936W PV Array and Battery Voltage	129
4.12.2	Summary	129
4.	References	131
5	133
5.0	Development of a Modelling and Simulation Tool for Off Grid PV-Hydrogen Energy System 133	
5.1	Introduction	133
5.1.1	Selection of Modelling Tools for RES with Energy Storage System.	134
5.1.2	Renewable Energy Systems Optimisation	135
5.1.3	HOMER	136
5.1.4	iHOGA.....	137
5.2	Justification for the New Software Development.....	139
5.2.1	The Software Development Platform	139
5.2.2	General Description of SOHYSIMO Tool	140

5.3	Component Modelling and Sizing	152
5.3.1	Solar Panel Sizing and Modelling	153
5.3.2	The Solar Resource - Solar Irradiation Model	155
5.3.3	Battery Sizing and Modelling	157
5.3.4	Modelling the Electrolyser	158
5.3.5	Experimental Determination of Dependency of Hydrogen Production on Input Current. 160	
5.3.6	H2 – Engine Genset Model.....	163
5.3.7	Hydrogen as a Cooking Fuel.....	164
5.3.8	Experimental Investigation of Solar Hydrogen Cooking	166
5.3.9	Modelling the Hydrogen Cooker.....	169
5.4	Control Strategies	170
5.5	Analysis and Study of an Existing Off-grid Renewable Energy System – The Isle of Eigg	177
5.5.1	The Electrification of Eigg –a Brief History.....	177
5.6	Evaluation of Power Performance Characteristics of Eigg PV	180
5.6.1	Analysis and Simulation of Power Production Characteristics of 53kW Solar PV at Eigg. 186	
5.6.2	Solar Energy at Eigg.....	186
5.6.3	Simulation of Output Power of 53kW PV at Eigg with SOHYSIMO	189
5.6.4	Comparison and Validation of SOHYSIMO Model Simulation with HOMER and iHOGA.....	198
	Validation 1	199
	Validation 2	209
5.7	Testing and Assessment of Off-grid Solar-Hydrogen Storage System.....	212
5.7.1	Comparison of SOHYSIMO Hydrogen Model with HOMER.	213
	Validation 3	213
5.	References	217
6	224
6.0	Evaluation and Assessment of Solar – Hydrogen system in a Nigerian Rural Area	224
6.1	Introduction	224
6.1.1	Overview	225
6.2:	Okenkwu Village Electrification	225
6.2.1	Site Specifications	225
6.2.2	Okenkwu Load Profile Model.....	227
6.2.3	Component Sizing	229
6.2.4	Simulation Results 1.....	230
6.3	Energy Assessment and Evaluations.....	234

6.3.1	Off-grid Energy System for the Rural Household in Okenkwu Village	236
6.3.2	Simulation Results 2.....	236
6.4	Energy Optimisation	240
6.4.1	Summary.....	245
6.5	Designing the Off-grid Household Energy Access with Solar Home System.....	245
6.5.1	Determination of Series – Parallel Configuration of the Solar PV System.....	246
6.5.2	Obtaining the Cooking Demand.....	249
6.5.3	Cost Evaluations.....	255
6.6	Obtaining Costs of Individual System Components.....	256
6.6.1	Cost of Photovoltaic Panels.....	257
6.6.2	Battery Costs	257
6.6.3	Cost of the Electrolyser	257
6.6.4	The Impacts of a Hydrogen Cooker on Domestic Energy Costs.....	262
6.6.5	Energising the Entire Village	265
6.	References	267
7	270
7.0	Assessment of Solar – Hydrogen Micro-Grid System for Remote Energy Access	270
7.1	DC Micro-Grid an Overview	270
7.1.1	DC Micro – Grid for Rural Energy Access	273
7.1.2	Why DC micro – Grid?.....	274
7.2	DC – DC converter.....	276
7.3	Modelling and Simulation of a DC – DC Micro – Grid Power System for Remote Area Energy Access.277	
7.3.1	Sizing the DC – Micro – Grid Components.....	278
7.3.2	Load Demand Model for Okenkwu.....	278
7.4	Connected Hydrogen Cooking System.....	283
7.4.1	Connected Hydrogen	283
7.4.2	Cooking Demand	284
7.4.3	Simulation Results.....	285
7.4.4	Network architecture of the connected hydrogen village.....	287
7.5	Hydrogen Safety.....	290
7.5.1	Energising the Nation.....	291
7.6	Environmental Impact Assessment of Solar – Hydrogen Cooking.....	294
7.6.1	Carbon Emission Reductions.....	295
7.	References	298
8	303

8.0	Conclusions and Recommendations for Future Work	303
8.1	Conclusions	303
8.2	Recommendations for Future Work	306
	APPENDIX	308
	Appendix 1. Kuje Solar Project Schematic	308
	Appendix 2: Panasonic HIT 240 W Photovoltaic module (VBHN240SA06) specifications	309
	Appendix 3: Daily Solar Resource at Zamfara, Ebonyi, Benue, Taraba, Ondo and Bayelsa	310
	Appendix 4: Specific global existing solar - hydrogen	323
	Appendix 5: Technoeconomic comparisons of ESS	325
	Appendix 6. Empa visit tag	327
	Appendix 7.	327
	7A. The Isle of Eigg AC Micro – Grid Power Characteristics Analysis	327
	7B. Hydro Trip Event on 13 November 2014	328
	7C. Hydro Trip Event 13 Nov 2014 with Synchronised KT and SP Data	331
	7D. Hydro Trip Event 16 February 2015	333
	7E. Buck Converter	336
	7F. Boost Converter	338
	7G. Component Selection	341
	7I. Design and Simulation of DC – DC Converter for Solar – Hydrogen Micro Grid System.	342
	7J. Modelling and Simulation of a DC – DC Boost Converter	343
	7K. Modelling and Simulation of a DC – DC Buck Converter	350

List of figures

Figure 1. Global energy consumption by type 1990 – 2015 [4].....	2
Figure 2. Global energy consumption by type of fuel, 2015 [4][7].....	3
Figure 3. World population 1950 – 2050 World Population Prospects: [8].	4
Figure 4. Access to electricity issues for the most populous Sub-Saharan countries [12].	6
Figure 5. CO ₂ emission profiles from 1950 – 2150 based on projections [15].....	7
Figure 6. CO ₂ concentration from 1960 – 2015 as measured at Mauna Loa Observatory, Hawaii 2015 [16].	8
Figure 7. Map showing the location of Nigeria in Africa [1][2].....	19
Figure 8. Map of Nigeria showing its Geographical spread [2][1].	20
Figure 9. The exponential population growth in Nigeria from 1960 – 2015 [4].	21
Figure 10. Population density of the different federating units in Nigeria [3].	21
Figure 11. Percentage of households with electricity access in the different federating units (states) [16].	25
Figure 12. Map of Nigeria showing the grid distribution [16].	27
Figure 13. Total energy consumption by source in 2014 (%) [16].	31
Figure 14. Percentage energy consumption by sector in 2014 (%) [16].	31
Figure 15. Electricity consumption (million kWh) 1990 - 2010 [16].	32
Figure 16. Per capita energy supply in Nigeria 2007 - 2015 [28][29].....	33
Figure 17. Per capita consumption comparison of countries with comparable populations to Nigeria, highlighting the disparities between developed and developing economies.	33
Figure 18. Map of Nigeria showing existing, ongoing, and proposed generation and transmission (HV) projects Source: Transmission Company of Nigeria [24].	34
Figure 19. Gas pipeline network showing the distribution of generating plants across the country and largely sited in the south [29].	35
Figure 20. Duration of hours of power outage by country in sub-Sahara Africa [32].	37
Figure 21. Map of Nigeria showing the solar energy resources [16].	42
Figure 22. Map of Nigeria showing the water ways [38].	44
Figure 23. Wind energy resource [16].	45
Figure 24. Velkess flywheel energy storage [10].	60
Figure 25. Pumped hydro storage with its technical components [17].....	62
Figure 26. Schematic diagram of off-grid integrated PV-Hydrogen storage [16].	63
Figure 27. Map of Nigeria with the climate showing the mean annual rainfall [21].	65
Figure 28. Solar photovoltaic characteristic configuration [27].	68
Figure 29. Photovoltaic characteristic curve showing the maximum power point [28].	69
Figure 30. circuit representation of the electrical behavior of solar cell.....	70
Figure 31. Solar array formation [29].	72
Figure 32. World photovoltaic installed capacity 2000 - 2016 [31].	72
Figure 33. Cost competitiveness of renewables as at 2015 [37][36].	75
Figure 34. Laboratory size electrolyser [38].	76
Figure 35. Hoffman voltammeter [39].	77
Figure 36. Operational principle of an alkaline electrolysis, showing the electrode reactions [43]. ...	79
Figure. 37 PEM electrolyser with the electrode reactions [43].	81
Figure 38. RE based hydrogen production plant [56].	86

Figure 39. Stand-alone renewable-energy system employing a hydrogen-based energy at West Beacon Farm, in Leicestershire, in UK [61].	89
Figure 40. Adafruit micro SD card breakout board [3].	96
Figure 41. INA219 current shunt monitor.	97
Figure 42. INA219 breakout board [5].	97
Figure 43. INA219 pin configuration [6].	98
Figure 44. Addressing the boards [5].	99
Figure 45. Inner wiring of the monitoring unit showing the 0.034-ohm resistor.	100
Figure 46. Arduino Uno Atmega 328 [1].	101
Figure 47. Implementation of the power monitoring system.	102
Figure 48. Inner view of the monitoring unit box showing the DC-DC converter.	103
Figure 49. Direct current sensing [8].	104
Figure 50. Low side current sensing.	104
Figure 51. High side current sensing.	105
Figure 52. Hall Effect current sensing [9].	106
Figure 53. Schematic diagram of the RE-power monitoring unit showing the wiring connection.	107
Figure 54. Hybrid solar and wind installation with LED lighting.	109
Figure 55. Battery voltage recorded.	110
Figure 56. Output currents of both RE system with battery voltage.	111
Figure 57. Output power in Day 1.	113
Figure 58. Output power in day 2.	114
Figure 59. Output power in day 3.	115
Figure 60. Energy output of solar PV and wind turbine.	116
Figure 61. Total energy productions of solar PV and wind turbine.	118
Figure 62. Battery model showing internal resistance.	121
Figure 63. Battery voltage at load and no-load conditions [16].	123
Figure 64. Obtaining the battery internal resistance.	126
Figure 65. Solar array set up with battery and inverter connection.	128
Figure 66. Solar array installations at Kuje estate Abuja	128
Figure 67. 936W PV array output power performance characteristics.	129
Figure 68. PV sizing User Interface of SOHYSIMO.	143
Figure 69. Data Input user Interface Page of SOHYSIMO.	144
Figure 70. General data user interface page of SOHYSIMO.	145
Figure 71. Cost evaluation user interface page of SOHYSIMO.	147
Figure 72. Energy assessment user interface page of SOHYSIMO.	148
Figure 73. Hydrogen cooking user interface page of SOHYSIMO.	149
Figure 74. SOHYSIMO energy optimisation user interface.	152
Figure 75. NREL Solar radiation model [36].	156
Figure 76. Hydrogen production test rig.	161
Figure 77. Electrolyser I – V characteristic.	162
Figure 78. Characteristic electrolyser dependence of input current for Hydrogen production.	162
Figure 79. Hydrogen cooker at Empa.	167
Figure 80. Hydrogen cooking testing.	167
Figure 81. Hydrogen flow rate vs cooker temperature.	169
Figure 82. Hydrogen cooking decision control in SOHYSIMO.	172
Figure 83. General data page of SOHYSIMO showing the data selection message alert.	175
Figure 84. Input user interface page of SOHYSIMO showing an error reminder for a missing input data.	176

Figure 85. Map of Isle of Eigg showing the sites of the renewable electricity installations [65].	178
Figure 86. Isle of Eigg Renewable AC micro –grid Electricity network schematic [66].	180
Figure 87. Hioki PW3360 data loggers connected at Eigg electric system for data acquisition.	181
Figure 88. Three days of output power of the 53kW Eigg PV measured in 5mins interval from 6 th – 8 th June 2014. Data obtained from SMA Sunny Portal data loggers [67].	181
Figure 89. Limitations of grid frequency on solar PV generation at Eigg.	182
Figure 90. Output power of the 53kW Eigg PV measured in 5mins interval from 6 th – 8 th June 2016 converted to hourly values.	183
Figure 91. Output power of the 53kW Eigg PV measured in seconds interval from 24 th – 25 th February 2015 obtained from Hioki data loggers.	184
Figure 92. Output power of the 53kW Eigg PV measured from 24 th – 25 th February obtained from SMA Hioki data loggers converted to hourly values.	185
Figure 93. Combination of output power for the 53kW Eigg PV measured from 24 th – 25 th 2015 February and 6 th – 8 th June 2016.	186
Figure 94. General page of SOHYSIMO showing a plot of Eigg irradiation data.	188
Figure 95. Simulation page showing the results of the 53kW PV output power computation.	190
Figure 96. 24 th – 25 th February selected data from SOHYSIMO simulation results superimposed on Eigg measured data obtained from sunny portal.	191
Figure 97. 6 th – 8 th June SOHYSIMO simulation results superimposed on Eigg measured data obtained from 6 th – 8 th June.	192
Figure 98. Comparison of SOHYSIMO energy results with Eigg real energy production data.	193
Figure 99. Plot of monthly - hourly output of Eigg 53KW PV for 2014 [67].	195
Figure 100. Plot of monthly - hourly output of Eigg 53KW PV for 2014 [67].	196
Figure 101. Monthly (2014) energy comparison of SOHYSIMO simulation results with Eigg data.	198
Figure 102. HOMER simulation user interface showing the simulated power characteristics of the 53KW PV.	200
Figure 103. HOMER simulation user interface showing the simulated power characteristics of the 53KW PV.	202
Figure 104. Battery performance characteristics in HOMER, showing that they maintain a full state of charge throughout the year. The batteries are just included in the system to allow the simulation to take place.	203
Figure 105. Input data page showing the imported load profile.	204
Figure 106. Main simulation page of SOHYSIMO showing the monthly average power.	205
Figure 107. SOHYSIMO Optimisation results of the 53KW PV.	207
Figure 108. iHOGA simulation user interface showing the imported irradiation data.	209
Figure 109. Simulation user interface showing the simulated power characteristics of the 53KW PV. The large excess production value is simply a consequence of the low load model adopted.	211
Figure 110. HOMER simulation user interface showing the hydrogen productions of the 25kW electrolyser.	214
Figure 111. SOHYSIMO simulation user interface showing the monthly hydrogen productions of the 25kW electrolyser.	216
Figure 112. Average monthly solar irradiation at horizontal surface, adjusted for 10-degree tilt.	226
Figure 113. Daily load demand profile for a household in Okenkwu village.	228
Figure 114. SOHYSIMO user interface showing the input data for load demand, site data and tilt angle entered for simulation, and the graphical view of the load demand.	228
Figure 115. General data page user interface of SOHYSIMO showing the monthly hydrogen production.	230
Figure 116. Hourly output power of 1 kW PV.	231

Figure 117. System annual performance.....	232
Figure 118. Hourly hydrogen production.....	232
Figure 119. Monthly average system performance.....	233
Figure 120. Simulation result showing the energy assessments.	235
Figure 121 . A plot of the system performance over a year period simulated.....	237
Figure 122. Hourly power production of the 930W PV array over a year period.....	238
Figure 123. Hourly hydrogen productions of 400W electrolyser has produced over a year period. .	239
Figure 124. System monthly performance.	239
Figure 125. System annual performance showing 6 kg/Yr of hydrogen produced by the 706 W electrolyser.	240
Figure 126. Hydrogen cooking optimisation results, showing the component configurations that fully satisfies both electric load and the cooking demand.	241
Figure 127. A plot of the system performance over a year period simulated.....	242
Figure 128. Hourly power production of the 1.53kW PV array over a year period.....	243
Figure 129. Hourly hydrogen productions of 400W electrolyser over a year period.	244
Figure 130. System monthly performance.	244
Figure 131. SOHYIMO user interface showing the selected fuel types and results.	252
Figure 132a. Monthly cooking simulation results, Jan -Jun	253
Figure 133. Cost Evaluation.	260
Figure 134. Screenshot of daily cooking demand at Okenkwu village.	264
Figure 135. Schematic representation of solar – battery DC micro – grid system.	272
Figure 136. Campus building at Xiamen University, China, showing the roof top installation of 150 kW PV array for DC micro – grid [13]......	275
Figure 137. Load profile for Okenkwu village micro – grid system.....	279
Figure 138. SOHYSIMO user interface showing the modelled load profile.	281
Figure 139. Cooking demand data.	285
Figure 140. Graph of hydrogen cooker vs cooking demand.....	286
Figure 141. Hydrogen cooker days of energy unavailability.....	287
Figure 142. DC micro – grid network for interconnected hydrogen village.	288
Figure 143. SOHYSIMO cost evaluation display showing the costs for the hydrogen village project.	290

List of Tables

Table 1. Number of people without access to electricity by region in the new policies scenario (million) [1].....	5
Table 2. Nigeria population growth rate, 1960 – 2015.....	6
Table 3. Nigeria GDP growth from 2010 – 2016 [8][9][10].....	22
Table 4. UN Multidimensional Poverty Index [12].....	23
Table 5. Historical electricity generating capacity in Nigeria, 1960 – 1966 (in MW) [18].	26
Table 6. Installed and Actual Generating Capacity (MW) 2004 [6].....	27
Table 7. Comparison of electricity demand projections [21].	28
Table 8. Electricity generation profile 1990 – 1999 [16][6].	29
Table 9. Operational report showing typical daily generation data (from 2015) [24].....	30
Table 10. % electricity production by renewable sources by country from 2010 – 2014 2014 [28]....	36
Table 11. % distribution of households with access to electricity by type of electricity supply [16]. ...	38
Table 12. Renewable energy resources including solar, biomass, wind and hydro [30].....	41
Table 13. small hydro potential in surveyed states of Nigeria [30].	42
Table 14. Exploitable hydro potential [36].	43
Table 15. Existing Installed capacity of small hydro schemes [37].	44
Table 16. Summary of Renewable Electricity Targets in terms of MW capacity [38].....	49
Table 17. Types of electrolyser and their characteristics [42].....	78
Table 18. Higher and lower heating values of gases [49].	81
Table 19. Daily solar radiation and wind speed.	111
Table 20. Energy productions of the hybrid RE system.	117
Table 21. Current consumptions each components of the power monitoring unit.....	124
Table 22. Specifications of solar module and electrolyser.	160
Table 23. Results of hydrogen cooking measurements.....	169
Table 24. Power generators at Eigg [64].....	179
Table 25. The Annual Energy Yield by the Eigg 53kW solar PV [67].	197
Table 26. HOMER simulation results.	201
Table 27. SOHYSIMO simulation results.	206
Table 28. Comparison of HOMER simulation results with SOHYSIMO results.	208
Table 29. Comparison of iHOGA simulation results with SOHYSIMO results.....	210
Table 30. Comparison of HOMER and iHOGA simulation results with SOHYSIMO results.....	212
Table 31. Comparison of HOMER hydrogen (25kW electrolyser) simulation results with SOHYSIMO results.....	215
Table 32. Load profile showing the daily power requirements for a household.....	227
Table 33. Components sizes.....	229
Table 34. Comparison of component sizes to be selected based on initial inputs.....	235
Table 35. Selected component sizes.....	236
Table 36. System component costs used in the energy optimisation.	241
Table 37. Optimised component sizes.....	241
Table 38. List of electrical properties of 85 W Ameresco solar module used in this study [12].	247
Table 39. Estimated daily cooking demand for a typical rural household in Nigeria.	250
Table 40. Components costs.....	258
Table 41. Summary of costs components used in the simulation.	259
Table 42. Calculated system costs.	261
Table 43. Calculated costs at 25 years' electrolyser lifetime.....	262
Table 44. Extended projects costs over the lifetime.....	264

Table 45. Grid connection costs for rural electrification in Bolivia [30].	265
Table 46. Village energy demand data.....	279
Table 47. Micro-grid simulation results.	282
Table 48. Summary of costs components used in the simulation.	289
Table 49. Selection of states in six geopolitical zones with highest number that lack grid access. ...	291
Table 50. Population forecast 2006 -2016 [43].	292
Table 51. Estimated emission savings by selected states if supplied with solar – hydrogen energy system.....	296

Dedication

The Almighty God – The Alpha and Omega, The Beginning and The End, this is for YOU.

To my sweet daughter, Joanne and my darling wife Oluchi for their love and support.

Acknowledgements

I would like to express my special thanks and appreciation to my supervisor, Dr David Rodley, your guidance, support, time contributions, advice, and encouragement throughout this research is exceptional. I would like to thank you for the excellent supervision and for allowing me to grow and develop as a researcher, as you gave me the chance to collaborate with other schools and outside the university (including the school Architecture) and Kinetic Traction Systems Ltd, in the area of off-grid power system, based on renewable energy. Your kind heartedness knows no bounds. To my second supervisor, Dr Stephen Reynolds, I would like to thank you for the opportunity to benefit from your technical expertise around some areas of my research. Your advice and suggestions on several topics, whenever I ask is immeasurable and is greatly appreciated. I would like to thank the technicians, Mr Callum Moore and Mr Grant Kydd for the technical support and for providing me with some electronic components, and granting me access to their facility. I would also like to thank the computing support team, especially Mr David Husband, for his technical assistance.

I also wish to thank Dr Kazeem Dastoori for his assistance and advice on various subjects, especially for providing me with some useful materials. I am grateful to School of Science and Engineering, especially the School Manager Mrs Kathleen Fotheringham, for her kindness and generosity, and particularly for her financial support, when my State Government abandoned my scholarship. I am grateful to her and words are not enough to express my appreciation. My sincere thanks also go to Dr David Keeble and Dr David Mcgloin for their support. Big thanks to Mr Fidelis Mbam the former Secretary to Ebonyi State Government (Nigeria) and his personal assistant, Mr Celestine Egbedike, for their support, and my special thanks go to Chief Martin Elechi, the former Executive Governor of Ebonyi State (Nigeria), for granting me the scholarship to start this research. To my sister-in law Mrs Philomena Onwe, you are wonderful, and I am grateful to you. I would also like to thank Barr Ndubuisi Chibueze Agbo, the former commissioner for education Ebonyi State (Nigeria), for his love and support. I would like to thank Adesuyan Bobby for giving me the permission to conduct a study on the solar array installed in his house at Kuje Abuja. Also, I would like to thank Adam El-Qmache, my PhD colleague and tutor partner. I would also like

to thank the management and staff of Empa Swiss Federal Laboratories for Materials Testing and Research, especially Engr. Benjamin Fumey for granting me access to their system to conduct my research, and for guiding me through the process.

My sincere gratitude and base of my thanks go to my sweet daughter Joanne Onwe and her mum – my darling wife Oluchi Onwe, you are the source of hope, joy and the inspiration that keeps me going throughout this three and half – year journey, and to my mother Mrs Comfort Onwe for all her prayers and to my siblings, I am grateful for all you have done for me. To my brother in-law Dr Paul Emeka Eke and his wife (my sister) Mrs Hope Nkiruka Eke, thanks for everything you have done for me, this thesis is not enough to contain my expression for appreciation and gratefulness from the time of my masters' degree to this PhD.

Declaration

I, **Christian Akaraka Onwe**, declare that I am the sole author of this thesis, titled “Modelling and Assessment of Renewable Energy Systems for Remote Rural Areas” and the work reported in this thesis is original research carried out wholly by myself under the supervision of Dr David Rodley and Dr Stephen Reynolds. All references cited have been consulted by me, and this PhD thesis has not been previously accepted for a higher degree.

Christian Akaraka Onwe.

List of Acronyms and Nomenclature

Ah	Ampere hour
AC	Alternating Current
ADC	Analog to digital converter
AVR	Automatic voltage regulator
Btoe	billion tonnes oil equivalent
Btu/ft ³	British Thermal unit per cubic feet
CBN	Central Bank of Nigeria
CMRR	Common Mode Rejection Ratio
CPU	Central Processing Unit
CO ₂	Carbon dioxide
COP21	Conference of the Parties
DC	Direct current
db	Decibel
DISCOS	Distribution companies
ECN	Energy Commission of Nigeria
ECU	Energy control unit
EEPROM	electrically erasable programmable read-only memory
ESS	Energy storage system
FGN	Federal Government of Nigeria
ft ³	cubic feet
g/l	gram per liter
GENCOS	Generation companies
GW	Giga Watt
GDP	Gross Domestic Product
GMG	Green Mini-Grid

H ₂	Hydrogen gas
HH	Household
HHV	Higher heating value
HOMER	Hybrid Optimisation for Electric Renewables
IDE	Integrated Development Environment
I ² C	Inter-integrated circuit
IEC	International Electrotechnical Commission
IMF	International Monetary Fund
IRENA	International Renewable Energy Agency
IEA	International Energy Agency
iHOGA	Improved Hybrid Optimisation by Genetic Algorithm
I/O	Input and Output
IPPs	Independent Power Producers
IPCC	Intergovernmental Panel on Climate Change
IRVES	Integrated Rural Village Energy Supply
ICEED	International Center for Energy, Environment and Development
kA/cm ²	Kilo amp per square centimetre
kg	kilogram
kt	kiloton
kg/l	kilo gram per liter
kWh/kgLH ₂	kilowatt hour per kilogram of liquid hydrogen
kWh/m ²	Kilowatt-hour per meter square
KV	Kilo-Volt
KJ	Kilo Joule
KW	Kilo Watt
KWh	Kilowatt hour
kWh/Nm ³	Kilowatt hour per normal cubic meter
kWhe/Nm ³ H ₂	Kilowatt hour energy per normal cubic meter of hydrogen gas
KWh/m ²	Kilowatt hour per meter square

KWp	Kilowatt peak
Km	Kilometre
LED	Light emitting diode
LCOE	Levelised cost of Energy
L/min	Litre per minute
LPG	Liquified petroleum gas
LVDC	Low voltage direct current
mA	milliamp
MDG	Millennium Development Goal
MHz	Mega Hertz
mV	millivolt
MW	Mega Watt
m/s	meter per Second
MPa	Mega pascal
MPI	Multidimensional Poverty Index
Mtoe	Million tonnes of oil equivalent
MtCO ₂ eq	Million tonnes of Carbon dioxide equivalent
MDG	Millennium Development Goals
MWhr/yr	Mega Watt hour per year
MJ/m ²	Mega Joule per meter square
MVA	Mega volt Amp
MWh	Mega Watt hour
NA	Not available
N	Naira
NASA	National Aeronautics and Space Administration
NDA	Niger Dams Authority
NEC	National Electric Code
NERC	National Electricity Regulatory Commission
NEP	National Energy Policy

NESCO	Nigeria Electricity Supply Company
NEPA	National Electric Power Authority
NERC	National Electricity Regulatory Commission
Nm ³	Normal cubic meter
NIPP	National Independent Power projects
NOAA	National Oceanic and Atmospheric Administration
NPC	National Population Commission
NPC	Net Present Cost
OPEC	Organisation of Petroleum Exporting Countries
O&M	Operation and maintenance
OH	Hydroxyl
PEM	proton exchange membrane
PHCN	Power Holding Company of Nigeria
Ppm	Parts per million
PV	Photovoltaic
REMP	Renewable Energy Master Plan
RE	Renewable energy
RES	Renewable energy system
Rx	Receive
SDA	Serial data line
SCL	Serial clock line
SEFA	Sustainable Energy Fund for Africa
SELF	Solar Electric Light Fund
SOHYSIMO	Solar – Hydrogen Simulation Model
SWG	Standard Wire Gauge
SSA	Sub-Saharan Africa
TCE	Tonnes of Coal equivalent
TCN	Transmission Company of Nigeria
TW	Terra Watt

TWh/yr	Terra Watt hour per year
TV	Television
TJ/day	Terra Joule per day
Tx	Transmit
TTL	Transistor – Transistor Logic
UART	Universal Asynchronous Receiver and Transmitter
USA	United States of America
USB	Universal Serial Bus
UNFCC	United Nations Framework on Climate Change
UNDP	United Nations Human Development Programme
UNIDO	United Nations Development Organisation
UK	United Kingdom
VBA	Visual Basic for Application
Wp	Watt peak

Summary

Energy production over the years has depended largely on carbon-dense fossil fuels, and these reserves are depleting. Carbon per se is associated with pollution and one of the consequences of over-dependence on this for energy is the observed environmental imbalance causing climate change. There are opportunities to address this situation through widespread adoption of renewable energy (RE), which is a largely environmentally benign means of energy production. Though it has its limitations, RE systems are developing rapidly to tackle these energy and environment issues head-on. RE systems, especially those involving solar and wind energy, depend strongly on weather conditions, and as such they can produce highly variable power outputs. However, due to the limitations, it is crucial that at early RE design stages, that a proper prior study is done to estimate the energy characteristics of the system for the selected location. To do this, it is possible to utilise a computer model and or data monitoring processes. In this research, two RE monitoring and data collection processes have been carried out. From the monitored data, the dynamic system performance characteristics were analysed. A software tool (SOHYSIMO) that can be utilised to simulate, size and estimate the energy performances of a solar-hydrogen system was developed, and this integrated a new approach for calculating the operating and maintenance costs of the system over the lifetime of the project. During abundance solar resource, overproduction usually occurs and the excess energy can be utilised to produce hydrogen as an energy storage medium, which can subsequently produce electricity through a fuel cell or H₂ Genset. Alternatively (or additionally) this hydrogen can be efficiently used to meet a cooking demand. For this reason, and unlike other models, the developed software tool integrates a novel loading which goes beyond the realm of electrical load and includes a hydrogen cooking load facility, as an efficient means of utilising the hydrogen produced, and as a means for displacing current unsustainable fuels such as firewood and kerosene. SOHYSIMO has been validated using two relevant and widely used tools, HOMER and iHOGA. A typical village in Nigeria was selected as case study to evaluate the solar-hydrogen cooking. The idea of utilising a DC micro-grid system instead of the prevalent AC type was also investigated, and the technical challenges inherent in AC grids in an existing RE system with an AC micro-grid network was assessed, and DC micro-grids appear to present a significant opportunity for efficient future renewable power system integration.

Introduction

1.1 Introduction: Background – The Challenges.

Energy is sine qua non in every nation's socio-economic and industrial development. Precisely, living beings cannot do without energy, it is the basis of life. Over the years, the traditional way of energy production has been through the use of fossil fuels. However, there are some environmental issues associated with the use of these for energy production which can be addressed through finding an alternative way of producing energy. This **chapter** presents an introduction and basis of energy production and consumption and the way it affects a typical developing country in sub-Saharan Africa. It also highlights the environmental consequences associated with fossil fuel and the need to seek alternative ways of producing energy. Electricity is basic in our daily activities of life, as we use it to light-up our homes, charge our phones, cook our food, listen to radio and watch television etc. Today about 1.3 billion people in the world still live without access to electricity [1]. The largest (48%) of this share of population is found in the developing countries of sub-Saharan Africa [1]. Nigeria is a sub-Saharan Africa country with a population of over 180 million [2]. Currently about 60% of this population live without access to electricity [2][3]. The Nigerian electricity situation is plagued with a poor grid network, poor maintenance culture, and lack of infrastructural development. Today, 58% of the Nigerian population depend on self-generated electricity (typically ac diesel generators) for their power supply due to the frequent power outages experienced in the country. In 2015, the federal government of Nigeria set a target to expand electricity access in the country and to increase electricity generation up to 115 GW by 2030. It is claimed that 20% of the electricity will come from renewable energy sources.

1.2 Energy and the World

The global energy industry is faced with *challenges of shortage syndrome*. Despite heavy investments and additional generation in the sector every year, easing-up the shortage in the near future still seems unrealistic with the continuous increase in demand due to the growing population of the world and rapid development of traditionally low energy demand economies. Making energy available to meet world demand in a way that will not jeopardise the chances of future generations is a tremendous global challenge. However, an exponential increase seen in the world energy consumption from 1990 to 2016 means that an accumulative estimate of over 13 Giga tonnes oil equivalent (Gtoe) has already been consumed [4][5], this is equivalent to 15,108 Terawatt - hour. The developed countries of the world consumed approximately 75% of this energy [6], while nearly 1.3 billion people in the developing countries, mostly within the tropics, were without access to electricity. As shown in **Figure 1** the vast majority of this energy demand is met by fossil fuel; the shares of energy consumption by fuel type is shown in **Figure 2**; and show that coal, gas and oil account for 86% of all consumption.

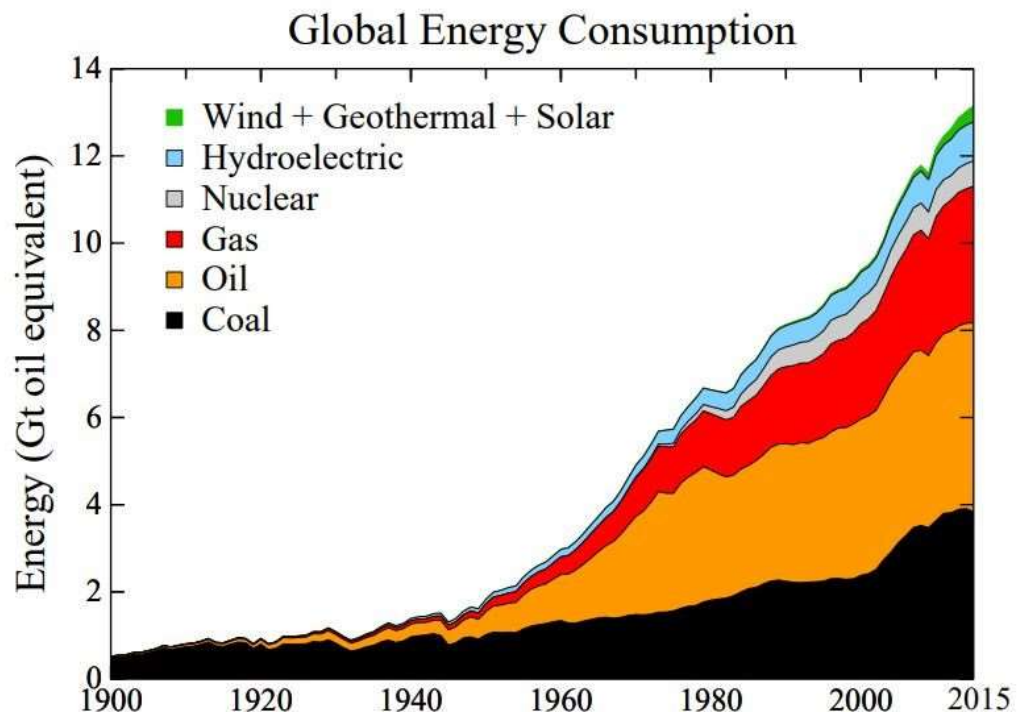


Figure 1. Global energy consumption by type 1990 – 2015 [4].

If this increase in world energy consumption follows historical trends, and the world continues this overdependence on fossil fuel to meet its energy requirements, the twin threats of climate change and depleting resources may have catastrophic consequences.

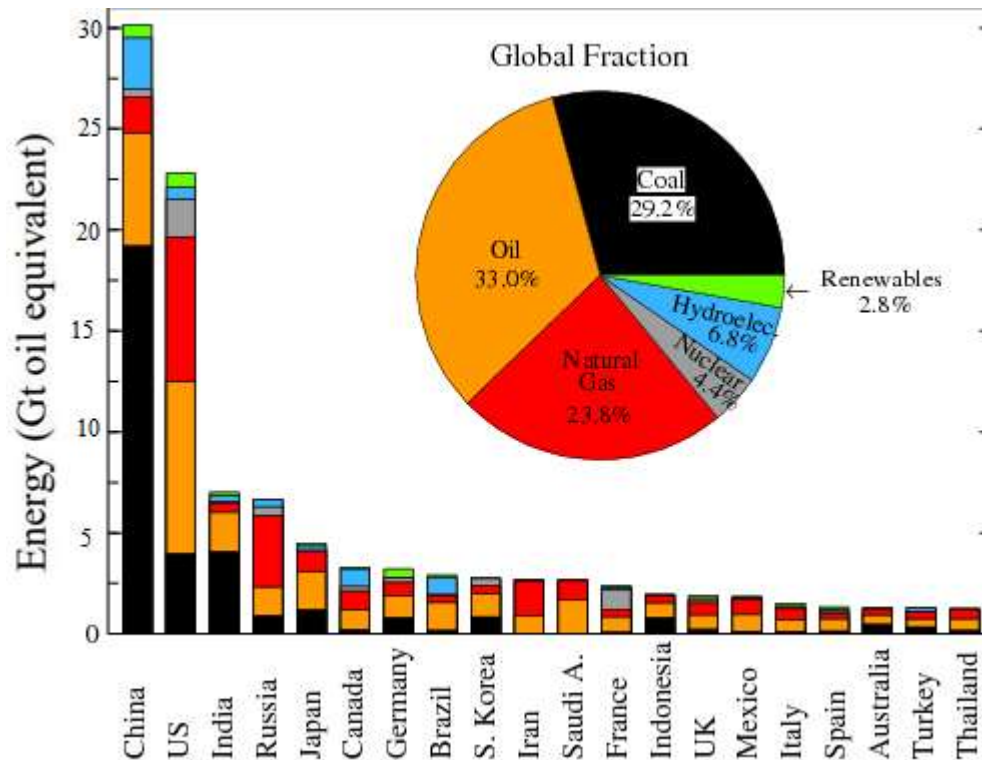


Figure 2. Global energy consumption by type of fuel, 2015 [4][7].

There is a correlation between the rate at which energy is consumed and the rate of increase in population, and it can also be inferred that rise in energy demand is a consequence of rise in people's standard of living. As shown in **Figure 3**, in 2010 the world population stood at 6.8 billion [8], this figure is expected to have increased to around 7.2 billion by 2016, that is 5.6% increase in space of 5 years, and according to a United Nations Department of Economic and Social Affairs report a further rise to more than 9.6 billion by 2050 is projected [8].

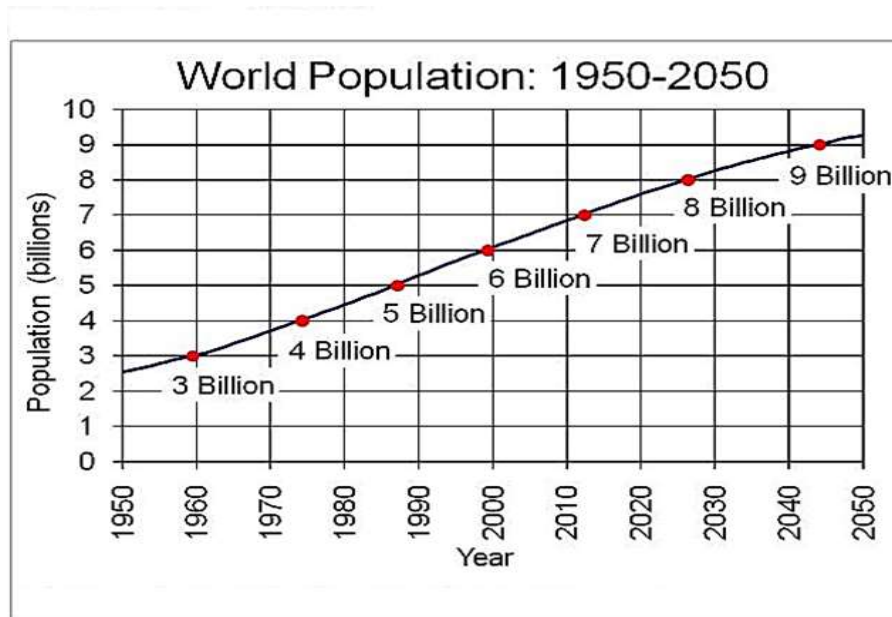


Figure 3. World population 1950 – 2050 World Population Prospects: [8].

This projected increase in world population entails greater pressure and competition for energy resources, and security of supply concerns may lead to greater political and economic instabilities. The demand for energy by sector is classified into four broad categories; the transportation sector (cars, aircraft, train etc), industrial sector (manufacturing machines etc.), agricultural sector, and residential sector (use of energy in cooking, heating, cooling, and all other domestic electricity needs). This gives an insight into the need for a fundamental global shift in ways by which energy is produced and consumed, and to avoid total dependence on fossil fueled energy source which could undermine any chance of slowing down CO₂ emissions. The United Nations have set up Millennium Development Goals (MDG) for environmental sustainability and the creation of a global partnership for developmental access to sustainable electricity [9]. This is a vital tool to help achieve targets outlined in MDG, particularly the interpretation of Goal 7 which includes environmental sustainability and carbon emissions [9].

1.2.1 Access to Electricity

As of 2016, about 18% of the world's population still live without access to electricity, as highlighted in **Table 1** which depicts the 4 major regions of the world still without an electricity supply. The largest percentage is shared between sub-Sahara Africa (48%) [1] and developing Asia (48%) [1], and those mostly affected are the rural dwellers. In sub-Saharan Africa, a 7% increase of this amount is projected by 2030 [10][1]. Hence there is an urgent need for a more diversified way of electricity production in Africa and the world before 2030.

	Population without electricity.	Electrification rate	Urban electrification rate	Rural electrification rate
	millions	%	%	%
Developing countries	1,283	76%	91%	64%
Africa	622	43%	68%	26%
North Africa	1	99%	100%	99%
Sub-Saharan Africa	621	32%	59%	16%
Developing Asia	620	83%	95%	74%
China	3	100%	100%	100%
India	304	75%	94%	67%
Latin America	23	95%	99%	82%
Middle East	18	92%	98%	78%
Transition economies & OECD	1	100%	100%	100%
WORLD	1,285	82%	94%	68%

Table 1. Number of people without access to electricity by region in the new policies scenario (million) [1].

The provision of affordable electricity access is the hallmark of socio-economic growth of any nation. Nigeria has the largest population in sub-Saharan Africa (SSA) without access to electricity [12]. As shown in **Table 2**, the Nigerian population growth has seen a steady increase from 45 million to 180 million by 2015. **Figure 4** highlights the fact that 93 million out of this population lack access to electricity and shows the electrification rates for various SSA countries. Nigeria has one of the least effective electricity grids in SSA and indeed the world. In Nigeria, incessant power outages, low power generation and unstable supply has always been the other of the day, therefore it is important that cultural changes and other means of electricity generation are considered to overcome

these deficiencies. In the summer of 2012, US President Barack Obama announced a \$7 billion *Power Africa* project to support creation of infrastructure that will extend electricity to more than 20 million homes in sub-Saharan Africa [11]. This he did in a bid to help reduce the number of people without access to electricity in Africa, and to encourage sustainability through cleaner electricity generation in Africa.

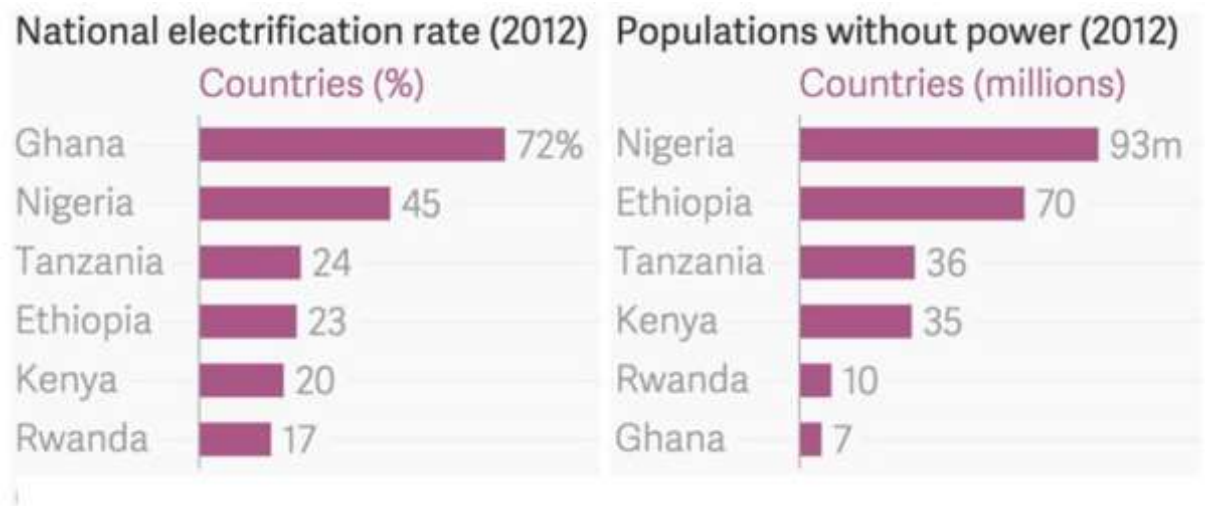


Figure 4. Access to electricity issues for the most populous Sub-Saharan countries [12].

Year	1960	1970	1980	1990	2000	2010	2015
Population(million)	45.2	56.13	73.69	95.62	122.89	159.71	178.84
Growth Rate (%)	N/A %	2.32	2.9	2.62	2.54	2.78	1.94

Table 2. Nigeria population growth rate, 1960 – 2015.

1.2.2 The Big Issue

“The measurements of gas trapped in polar ice and the long-term recordings of remote meteorological stations show unequivocally that the concentration of greenhouse gases in the global atmosphere has increased markedly since the industrial revolution of the 18th century” [13]. There is now overwhelming evidence that this increased concentration of greenhouse gases in the atmosphere is causing significant global warming. Generation of electricity with fossil fuels emit the heat-trapping greenhouse gases i.e. methane, carbon dioxide, nitrous oxide, sulphur dioxide and water vapour, into the atmosphere, and these contribute significantly to the atmospheric

concentrations of these gases. Globally, man-made CO₂ emissions are predominantly from energy production which has been fueled largely from the energy-dense fossil fuels consumed since the Industrial Revolution. One would ask why more attention is placed on CO₂ over other green-house gases listed; this is because of its high abundance and longevity of stay in the atmosphere after its emission. CO₂ lasts longer in the atmosphere compared to other major heat-trapping gases emitted because of human activities [14]. These gases trap heat from the sun, causing a net warming effect.

As shown in **Figure 5**, the impacts a yearly percentage CO₂ emission reduction will have on the climate balance has been recognized; to save the world from danger of climate catastrophe, the rate of reduction in global carbon emission needs to more than double from the current 4% annual reduction to 8% by the year 2050 [15]. The world will need to emit less than one trillion metric tons of CO₂ between now and 2050 to avoid serious climate change. **Figure 6** shows that in the past 60 years CO₂ concentration in the atmosphere has increased steadily from 318ppm to reach 404ppm in 2016 [16].

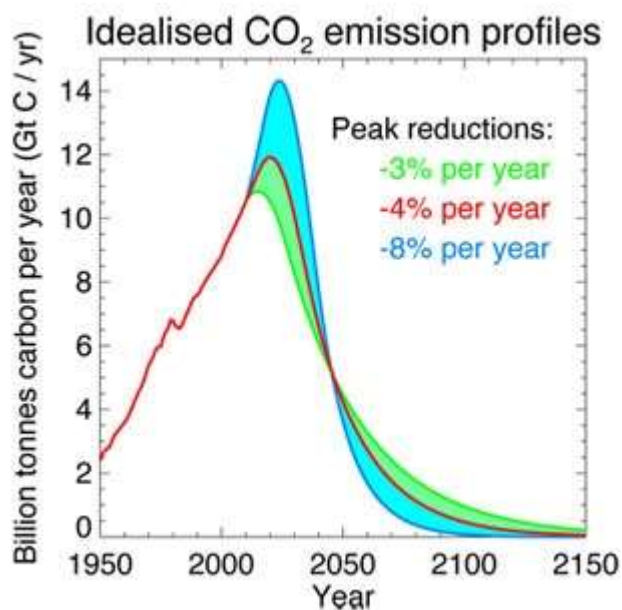


Figure 5. CO₂ emission profiles from 1950 – 2150 based on projections [15].

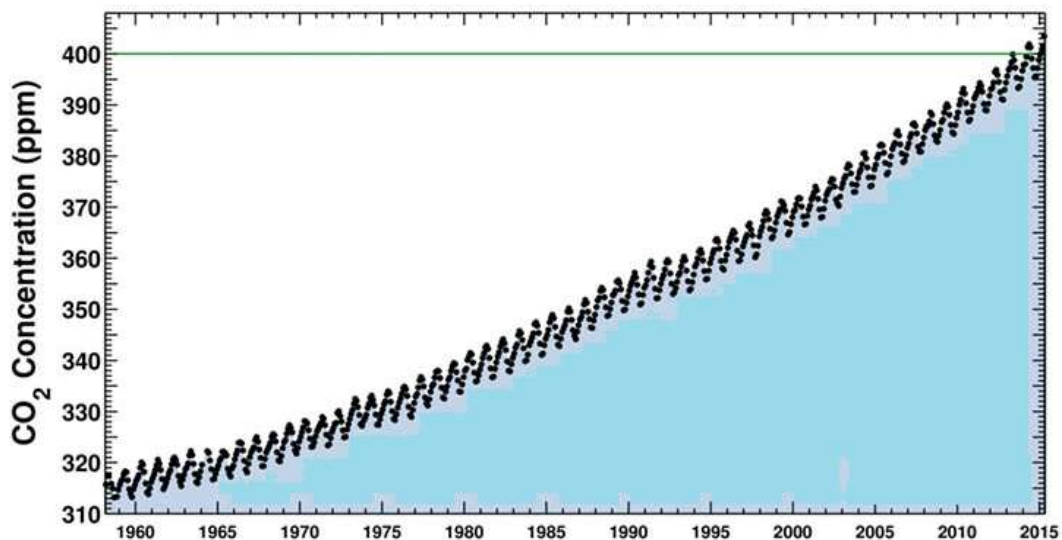


Figure 6. CO₂ concentration from 1960 – 2015 as measured at Mauna Loa Observatory, Hawaii 2015 [16].

To tackle this climate change issue, the United Nation Framework Convention on Climate Change (UNFCCC) adopted the Kyoto protocol in Kyoto Japan in December 1997, to enforce emission reduction commitment on the developed countries by setting internationally binding emission reduction targets. The emission reduction commitments were divided into 3 categories; annex 1 (developed – industrialised countries), annex 2 (provides funding for developing countries), and non – annex (developing countries) [17]. The annex 1 countries are set with emission reduction commitments while annex 2 are the observers. The non – annex countries are not listed for emission reduction commitments. In 2012, the emission reduction commitments were revised and 36 countries were set with binding targets. 13 years after Kyoto protocol, UNFCCC and its parties agreed to commit to not exceed a maximum temperature rise of 2°C above the pre-industrial level and in 2015 a climate change conference was held in Paris termed COP21 (Conference of the Parties) [18]. Here the temperature goal was agreed by all parties to keep the global temperature to “well below” 2°C and to push efforts for a 1.5°C limit. The Intergovernmental Panel on Climate Change have reported the need for urgency in adding more mitigation measures by 2030. According to the IPCC report, the global atmospheric balance will suffer severe damage without additional mitigation efforts beyond those in place today [17][18]. Climate change is a global issue. The consequences of energy production using fossil fuel is a global concern and every nation in the world including Nigeria is aware of the problems associated with its use.

1.2.3 Climate Change and Nigeria

Nigeria joined the United Nations Framework on Climate Change Convention (UNFCCC) in 1992 as Non-Annex 1 country. This position gave Nigeria responsibility to reduce her green-house gas (GHG) emissions, but without externally imposed targets. Based on this development a climate change unit was created within the Federal Ministry of Environment Abuja to implement the activities of the Convention. Nigeria is currently ranked among the lowest emitters of green-house gases [19], but this is largely as a result of its low electrification rate.

In 2003, Nigerian submitted its first national draft on climate change mitigation to UNFCCC [20][21]. Included in the proposals was the reduction of hazardous emissions through the use of alternative energy (renewable) for electricity generation, and rehabilitation of some existing oil refineries and power plants. Also proposed was the introduction of co-generation in the rural and industrial areas [20][21].

However, various pathways have been analysed by which climate change can be mitigated. Among them are;

- Reduction in over-reliance on fossil fuel for electricity production.
- Adoption of cleaner alternative means of electricity generation via renewable energy systems.
- Reduction in deforestation practice.
- Energy saving and efficiency measures

There is a tacit recognition that energy and environment are inextricably linked and that continued large – scale use of energy generation derived from coal, oil and gas will seriously impact on environmental balance and cause global disruption on an unprecedented scale. The International Renewable Energy Agency (IRENA) [22] have stated that “Renewable power generation technologies are now the economic solution for isolated off-grid and small-scale electricity systems, such as on islands, that are reliant on diesel-fired generation”. In this report, they further suggested that renewable energy can go a long way in reducing the dependence on wood for cooking without giving explicit mechanisms. Meanwhile, as of 2015, The Sustainable Energy Fund for Africa (SEFA) approved USD 1 million grant to fund the first phase of a Green Mini-Grid (GMG) Market Development Program (MDP) in Africa to reduce market barriers that

inhibits regional scale deployment of mini-grid green electricity supply in sub-Saharan Africa. The program was geared towards supporting stakeholders such as governments and project developers in creating a favourable environment for scaling up mini-grid investment on the continent and expanding energy access to unserved communities through GMGs [23]. This supports the Sustainable Energy for All (SE4ALL) initiative established by UN Secretary General Ban Ki Moon. A representative from Nigeria (Engr A. Adebisi) attended the inaugural conference in Ivory Coast in 2015. Engr. Adebisi made a presentation illustrating the Nigerian roadmap to expand electricity access to the underserved locations by 2030 [24].

1.3 Aim and Motivation

The federal government of Nigeria recently set a target to increase centralised electricity generation from the present 8.7GW installed capacity in 2016 to reach 115GW by 2030, and to integrate over 20% of renewable generation into the energy mix; 13% hydro, 1% wind, and 9% solar [24]. With forward demand projections, this means 23GW of electricity needs of the country will be sourced from renewables, which is extremely aggressive when compared to the present stand and renewable energy growth of other countries. For example, Germany (with Europe's largest population) has about 32.6% (64.7GW) (capacity factor for solar power range from 10 – 25%) of her 198.45GW electricity installed capacity sourced from renewables as at 2016 [25][26], and is a world leader. To achieve this level of penetration energy storage systems may play a vital role. Energy storage has been identified to be the solution to the unpredictability and variable nature of renewables, so identifying appropriate strategies and developing an appropriate design simulation model for the integration of energy storage systems will add considerable value and quality to the electricity supply system. The problem of intermittency inherent in renewable energy power generation can be addressed by proper consideration of energy storage. This research is concerned only with electrical energy generated from renewable energy sources, and to the integration of a hydrogen storage system for an enhanced energy capture and supply.

1.4 Potential Research Gaps and Problem Statement

Taking a closer look at the Nigerian grid situation, a 20% renewable electricity capacity by 2030 as visualized by the federal government is an important commitment and milestone. Upon adoption of the Sustainable Energy for All initiative (SE4ALL), Engr A. Adebisi – the director of renewable energy and rural power access department of the federal ministry of power, made a presentation in September 2015 where he illustrated the 2030 roadmap [24]. From this presentation, it was apparent that no clear plan is in place to address the issue of efficiently matching supply and demand from renewable energy systems. As in many other developing countries, for low-income rural communities the sources of fuel for domestic cooking are largely centred on firewood, charcoal and kerosene, each of which are associated with health hazards and CO₂ pollution. Renewable energy systems offer the opportunity to utilise excess supply power and harnessing this to provide safe, clean and renewable hydrogen [27][28]. This has considerable potential to provide a sustainable means of cooking [29] for the rural communities, and will help mitigate the climatic consequences which may result from deforestation, as well as giving the villagers a safer and healthier local environment. This tapping into otherwise unused energy associated with over-supply is at the heart of the new software tool that can simulate an optimal solar-hydrogen cooking system.

It is hoped that it will prove to be of value for situations involving off-grid rural energy access. A critical analysis has been made to address some important questions regarding the technical and economic viabilities of such proposed systems. Ideally, to aid prior study of renewable energy systems, software tools are necessary. However, in certain cases the available tools may not meet the requirements of the user, and this suggests new software will be desirable. Currently, there are no renewable energy tools that can simulate and optimise an energy system which goes beyond the realm of electrical load and to integrate a cooking demand. Against this background, developing a new software tool which can do these has become necessary, and this has been addressed in the current research.

Therefore, the specific research questions addressed in this thesis are:

- What is the past and present status of Nigeria in terms of renewable energy and fossil fuels?
- Considering the size and technology, what energy storage configuration is going to be adopted and what are the modalities that inform the choice?
- Will the renewable technology option that is adopted help Nigeria meet her policy goal of sourcing 20% of her electricity generation from renewables by the year 2030?
- What are the benefits associated in using renewables to power rural communities and is renewable electricity the best option?
- What are the attributes required of the target rural area for the implementation of the technology?
- Is there any existing rural community or islanded area which has been powered by this type of technology? If there is, how functional is the renewable energy system in matching the energy demand of the consumers?
- Is there any possibility that villages be powered using a DC micro-grid system?
- What is the likely scalability and transferability of the proposed technologies?
- Is it possible that villages that depend on firewood to meet their cooking needs be supplied with a sustainable and efficient means of cooking?
- In the process, is there sufficient data to carry out prior energy assessment on the selected location?
- If not, is there any available and easily accessible software tool which can be used to perform this assessment?

To help address some of these questions a model for the integration of an energy (hydrogen) storage system by utilising the excess energy that could be generated at times of abundance resource has been developed. This work forms the main thrust of this thesis.

1.5 Objectives

This research will seek to design a renewable energy based electricity generation with a storage system capable of supplying instant access to electricity for a typical rural community currently with no grid access, and laying more emphasis on the electricity demand per household in the rural areas. The factors that could hinder the deployment of the proposed technologies have been investigated. Two basic types of energy storage system; hydrogen and electrochemical battery were investigated. Battery storage was considered for short term storage and system stability, and hydrogen was investigated for coverage of domestic cooking and other energy securities. In the process, a solar – hydrogen energy based simulation tool which can be used by designers interested in this kind of application was developed. The tool has a facility which allows a user to utilise the excess energy to generate hydrogen. Hydrogen is an energy carrier and a portable energy storage method that is manufactured by other energy sources [30]. Traditionally, hydrogen is manufactured using fossil fuels (hydrocarbon, coal, natural gas etc). The storage of hydrogen produced using the fossil fuels greatly increases the concentration of green-house-gases in the atmosphere which makes it ultimately unsustainable. In modern day technology, to make the hydrogen storage completely sustainable it is usually produced using the more environmentally benign renewable energy sources. The most sustainable method of hydrogen production is through the electrolysis of water, with the electrical power required provided by some sort of renewable energy source. The hydrogen obtained in the process will typically be compressed and stored in tanks in different forms [31]. Although an inherently energy-inefficient process, electrolysis provides an excellent means to harness excess renewable energy production. The battery is an established energy storage technology, which when properly harnessed will make great contributions towards future advancements in renewable technology [29][32]. At day time, the solar energy could be captured and stored in a battery to provide back-up power in isolated off-grid electric power system to ensure system stability. The outcome of this research is channelled to an assessment framework for the 20% from renewable energy by 2030 target scenario. This serves a purpose in providing a feasibility study towards finding the best type of system configuration that could be adopted based predominantly on technical and economic factors. This proposed framework could be adoptable by other developing countries towards developing renewable energy systems.

The overall objectives of this research are as follows;

- Review of previous work and related literature around the subject
- Design and construction of a renewable energy monitoring unit to measure the technical performance of solar PV system that will be suitable for remote area power access
- Evaluation of the data obtained from the RE system installed in Dundee UK and Abuja Nigeria via the monitoring unit, and analysis of the results to investigate the accuracy of externally obtained irradiation data
- Development of a novel software tool for simulation and optimisation of a solar-hydrogen system
- Validation of the developed tool with real data and two respected and widely used commercial software models
- Using a typical household in a rural area, development of a load profile model, and based on this, design of an optimised solar – hydrogen system model which can safely satisfy the loading criteria.

The following are contributions made in the current tool;

1. The developed tool introduces a new loading facility which goes beyond the realm of electrical load and include a hydrogen cooking load. Most renewable energy designers do not consider the impacts of cooking demand in the rural household's energy consumptions. Generally, while sizing the energy system for a rural household, RE designers consider the load profile model (for rural areas) with respect to electric load and ignoring the additional requirement to cover the cooking load.
2. Operating and maintenance cost is an important factor in every renewable energy based projects, a novel method for calculating this has been developed and incorporated into the model to obtain an optimal design of a solar PV-hydrogen project. SOHYSIMO has a facility that computes the electrolyser efficiency based on size (electrolyser capacity), no input pertaining electrolyser efficiency is required.

3. Battery is an important cost factor in renewable energy systems, and a new method for determining the days of autonomy (DoA) required from the battery storage has been introduced.
4. The optimisation process introduced in this model, involves an improved approach whereby the battery days of autonomy and its depth of discharge are considered. The optimisation process has two stages, which allows the user to make two decisions; (1) whether to fully satisfy an annual cooking load, (2) or to satisfy part of the cooking load, based on the amount of excess energy generated.

1. References

1. Energy access projections to 2030: IEA, World Energy Outlook; online available at <http://www.worldenergyoutlook.org/resources/energydevelopment/energyaccessprojectionsto2030/> accessed on 23/11/2016.
2. Sustainable energy for All presentation Abidjan Online available at http://www.ecreee.org/sites/default/files/events/presentation_se4all_action_agenda_nigeria.pdf accessed on 28/11/2016.
3. Sustainable Energy for All (SE4ALL) Action Agenda for Nigeria roadmap.
4. Online available at http://www.columbia.edu/~mhs119/EnergyConsump/WorldPrimaryEnergy_line.pdf accessed on 31/08/2017.
5. BP Statistical Review of World Energy June 2016: Online available at <https://www.bp.com/content/dam/bp/pdf/energy-economics/statistical-review-2016/bp-statistical-review-of-world-energy-2016-full-report.pdf> accessed on 24/12/2016
6. Messenger, Roger A., and Jerry Ventre. *Photovoltaic systems engineering*. CRC press, 2010.
7. Online available at <http://www.columbia.edu/~mhs119/EnergyConsump/> accessed on 24/12/2016.
8. Online available at <http://www.un.org/en/development/desa/news/population/un-report-world-population-projected-to-reach-9-6-billion-by-2050.html> accessed on 22/11/2016.
9. Committee for Development Policy - The United Nations Development Strategy Beyond 2015 "Policy note" United Nations publication 2012.
10. The 2015 Revision Key Findings and Advance Tables; Online available at http://esa.un.org/unpd/wpp/publications/files/key_findings_wpp_2015.pdf accessed on 22/11/2016.

11. Online available at <http://www.econlife.com/diminishing-the-worldwide-energy-gap-in-sub-saharan-africa/> accessed on 11/11/2016.
12. Online available at <http://qz.com/422357/charted-how-electricity-problems-are-limiting-growth-in-many-african-countries/> accessed on 11/11/2016.
13. Twidell, J. and Weir, T., 2015. Renewable energy resources. Routledge.
14. Global warming and impacts; Online available at http://www.ucsusa.org/global_warming/science_and_impacts/science/CO2-and-global-warming-faq.html#.VkiFY_nhDIV accessed 13/11/2016.
15. Online available at <http://www.scientificamerican.com/article/limits-on-greenhouse-gas-emissions/> accessed on 26/11/2014.
16. Online available at <http://www.climatechangenews.com/2015/05/06/fossil-fuels-just-pushed-co2-levels-to-a-3-million-year-high> accessed on 24/11/2015.
17. Online available at; http://unfccc.int/kyoto_protocol/items/2830.php accessed on 19/05/2016
18. UNFCC; Adoption of Paris agreement December 2016.
19. Online at <https://unfccc.int/files/adaptation/application/pdf/nigerianeeds.pdf> accessed on 07/07/2017.
20. Sambo, A. S. "Matching electricity supply with demand in Nigeria." *International association for energy economics* Fourth Quarter (2008): 32-38.
21. Online available at <http://unfccc.int/resource/docs/natc/nganc2.pdf> accessed on 10/07/2017.
22. IRENA 2014; Renewable power generation costs in 2014. Online available at http://www.irena.org/DocumentDownloads/Publications/IRENA_RE_Power_Costs_Summary.pdf accessed on 11/11/2016
23. Online available at <http://docs.dgmarket.com/dms/upload/0408131834314-851031508048.pdf> accessed on 16/11/2014.
24. Sustainable Energy for All (SE4ALL) Action Agenda for Nigeria roadmap.

25. Renewable 2016 Global status report REN21; Online available at http://www.ren21.net/wp-content/uploads/2016/06/GSR_2016_Full_Report.pdf accessed on 15/11/2016.
26. Net installed electricity generation capacity in Germany; online available at https://www.energy-charts.de/power_inst.htm accessed on 02/02/2017.
27. Little, M., Thomson, M. and Infield, D., 2007. Electrical integration of renewable energy into stand-alone power supplies incorporating hydrogen storage. *International Journal of Hydrogen Energy*, 32(10), pp.1582-1588.
28. Jain, S. and Agarwal, V., 2008. An integrated hybrid power supply for distributed generation applications fed by nonconventional energy sources. *IEEE transactions on energy conversion*, 23(2), pp.622-631.
29. Hollmuller, P., Joubert, J.M., Lachal, B. and Yvon, K., 2000. Evaluation of a 5 kW p photovoltaic hydrogen production and storage installation for a residential home in Switzerland. *International Journal of Hydrogen Energy*, 25(2), pp.97-109.
30. Dutta, S., 2014. A review on production, storage of hydrogen and its utilization as an energy resource. *Journal of Industrial and Engineering Chemistry*, 20(4), pp.1148-1156.
31. E I. Zoulias, N. Lymberopoulos: *Hydrogen-based Autonomous Power Systems Techno-economic Analysis of the Integration of Hydrogen in Autonomous Power Systems*, 2008 Springer-Verlag London Limited.
32. Dufo-López, R. and Bernal-Agustín, J.L., 2015. Techno-economic analysis of grid-connected battery storage. *Energy Conversion and Management*, 91, pp.394-404.

2.0 Literature Review

2.1 Review of Nigeria Energy and Electricity Sectors

The Federal Republic of Nigeria is a large oil-exporting country located in the Western part of Africa, as shown in **Figure 7**. The country shares borders with Benin Republic, Cameroun and Chad, and is made up of 36 states and the Federal capital territory. **Figure 8** depicts the map of Nigeria showing its neighbouring countries, and its 36 states. It is the most populous country in Africa, and as of 2016, home to Africa's largest economy.



Figure 7. Map showing the location of Nigeria in Africa [1][2].



Figure 8. Map of Nigeria showing its Geographical spread [2][1].

2.1.1 Population Growth Vs Gross Domestic Products (GDP)

The knowledge of a country's population and Gross domestic product (GDP) growth rate is crucial in the identification of the socio-economic and technical factors that can influence the energy demand of the country. As shown in **Figure 9**, the country has seen an exponential increase in population growth since independence was granted in 1960, as at that time the population stood at 45 million [3]. By 1990 the population had reached 95.6 million, which represents a 53% increase in population within 30 years. A continuous increase in population in the country means that by 2015 the population has reached 181 million. As at 2015 Nigeria now accounts for 2.46% of total world population. With this massive population growth, the United Nations has predicted that Nigeria may overtake the United States to become the world's third largest country by population by 2030 [4][5].

In terms of GDP, the country has enjoyed a progressive growth rate in recent years. In 2012 Nigeria was listed as the world's fourth largest exporter of liquefied natural gas (LNG from associated petroleum gas) and as at 2015 Africa's largest oil producer [6]. The GDP growth in Nigeria is shown in **Table 3**. The growth rate in Nigeria averaged 5.8% per annum between 2010 and 2016. According to CBN [7], the revenue from the entire sector had actually declined within this period. However, it was estimated that in 2013 the GDP had increased by 89% from N42.4 trillion to 80.2 trillion Naira (\$510 billion at 1\$ = N160) [8]. Consequently, Nigeria overtook South Africa to become the largest economy in Africa. As highlighted in **Table 3**, compared to the poorest African country – Madagascar, with GDP growth rate at 2.2%, Nigeria GDP is almost 4 times higher. GDP is basically measured by reference to the shape of the economy in a “base” year. From the Central Bank of Nigeria annual report in 2015, the oil revenue received as of 2016 was about US\$31.54 billion [7]. A large percentage of the population still live below the poverty line (less than US\$ 1.90 per day income). However, some fluctuation in oil prices which caused a reduced price of crude oil in 2016 led Nigeria to an unprecedented recession with alarming unemployment and inflation rates which stood at 13.3% and 17.1% respectively.

Macroeconomic indicators							
Year	2010	2011	2012	2013	2014	2015	2016
Nigeria							
GDP, current prices, (US\$ billion)	369.1	414.1	461	515	581.9	597.8	661.4
Real GDP growth (%)	7.8	4.9	4.3	5.4	6.2	5.6	6.5
GDP per capita, current prices, US\$	2,396	2,612	2,835	3,082	3,416	3,677	
Madagascar							
Real GDP growth (%)	0.3	1.5	3.0	2.3	3.3	3.0	
GDP per capita, current prices, US\$	415.8	409.9	755	374.5	415.8	409.9	755

Table 3. Nigeria GDP growth from 2010 – 2016 [8][9][10].

2.1.2 Poverty Metrics

A United Nations Human Development Programme (UNDP) report on Multidimensional Poverty Index (MPI) in 2016 suggested that as of 2013 the increase in population had accelerated the poverty situation in Nigeria. MPI is a new measure of acute poverty that captures the severe deprivations including; education, health and living standards [11]. As shown in **Table 4**, in terms of head count ratio, 50.9% Nigerians live below the poverty line in multidimensional level, while an additional 18.4% live near multidimensional poverty. The multidimensional income poverty is measured by the percentage of the population living below poverty line which is set at US\$1.90 per day [12]. Multidimensional Poverty Index is calculated by taking the percentage of poor people in the country (H) and multiplying this by the average poverty intensity (A) across the poor people; $MPI = H \times A$ [13]. Intensity of deprivations refers to “*average percentage of deprivation experienced by people*” [14].

From the UNDP survey, by improving people’s quality of life, with basic amenities, good education and health care, this will go a long way in alleviating their poverty. These are factors listed by UNDP (indicated in **Table 4**) as major contributors to poverty.

	Survey year	MPI value	Head-count (%)	Intensity of deprivations (%)	Population share (%)			Contribution to overall poverty of deprivations in (%)		
					Near poverty	In severe poverty	Below income poverty line	Health	Education	Living Standards
Nigeria	2013	0.279	50.9	54.8	18.4	30.0	53.5	29.8	29.8	40.4
Congo DR	2011/2012	0.369	72.5	50.8	18.5	36.7	77.1	31.0	15.6	53.4
Ethiopia	2011	0.537	88.2	60.9	6.7	67.0	33.5	25.2	27.4	47.4

Table 4. UN Multidimensional Poverty Index [12].

In Nigeria, as with many developing nations, severe poverty is most associated with those living in the rural areas. This poverty situation and the lack of basic amenities such as electricity supply etc. has contributed to migration from the rural to urban centers, as those living in the rural areas search for a better livelihood for themselves and their families. This in turn puts more pressure on the cities. An indication of this rural - urban migration is the massive increase in the number of people living in Lagos, the largest city

in Nigeria. According to the National Population Commission (NPC), as of 1995 the Lagos population was 9.8 million; and increased to 12.5 million as at 2000 and according to NPC projections it has reached 25 million in 2016 [3].

2.1.3 Justification for Access to Basic Amenities

A country with a booming economy should be able to supply its citizens with at least the basic and essential amenities of life, such as water, electricity and good health care. According to the Centre for Economic League Table research projections, by 2024 Nigeria will boast one of the world's largest economies [15]. This strong economic development coincides within the period stated in the federal government's 2030 electricity generation expansion target roadmap. If this economic climate remains strong, then the country will have no excuse for not using its wealth to provide its citizenry with the necessities of life, including access to electricity.

Access to electricity promotes rural development, education, good health care delivery and micro-enterprise development. Electricity is needed to power health equipment, lighten the school study hall and home, and to facilitate a decent quality of life. **Figure 11** shows the current electricity access rate across the 36 states of Nigeria with Lagos State having the highest rate at 99%. There is a clear disparity in electricity access in certain parts of Nigeria which can be correlated with the population density across the 36 states. Notably, the geographical coverage of the country's transmission line strongly influences the chance of electricity access. Those states in the North – Eastern part of Nigeria are not covered by the transmission network, but most states in the south where gas-powered thermal generating facilities are located are, and the states with lowest access rates are found in the Northern region of Taraba (10.9%) and Yobe (18.1%).

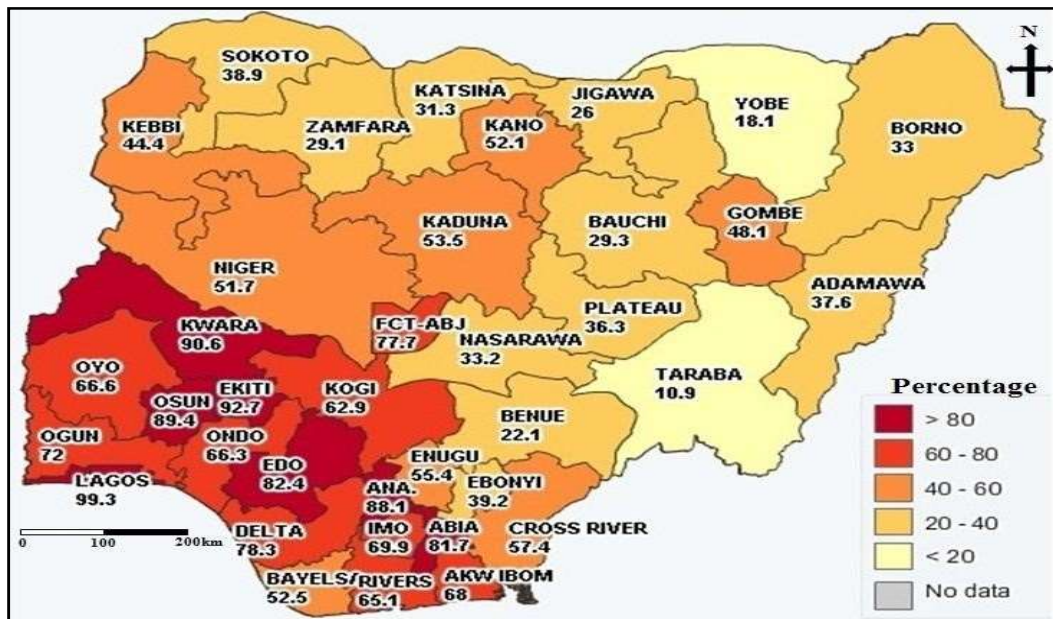


Figure 11. Percentage of households with electricity access in the different federating units (states) [16].

2.1.4 The Electricity Generation Situation in Nigeria

The history of electricity in Nigeria dates to the 19th century when electricity was first produced in Lagos in 1896 [17], fourteen years after electricity was introduced in England. Several statutory bodies have been constituted to handle the electricity supply and development in Nigeria. In 1950, a central body was established by the legislative council, which transferred electricity supply and development to the care of an entity known as the Electricity Corporation of Nigeria (ECN) (now defunct). Other bodies which had licenses to produce electricity in Nigeria at that time were the Niger Dam Authority and the Nigerian Electricity Supply Company (NESCO). They were licensed to generate electricity on a regional basis [17]. By the time of independence in 1960 the total national electricity generating capacity had reached 440 MW.

Table 5 shows the share of installed capacity by the two-major licenced electricity generation companies (ECN and NESCO) in the 1960s. A steady increase in electricity generating capacity took the installed capacity to a maximum of 1208.4MW by 1966, a reflection of the fact that new government was committed in improving the electric power situation from the time of colonial rule. In 1972, the Niger Dams Authority and Electricity co-operation of Nigeria (ECN) was amalgamated which led to the establishment of the National Electric Power Authority (NEPA). Act No. 62 of 1979 of the

federal constitution heralded the establishment of the Energy Commission of Nigeria (ECN), with the mandate for the strategic planning and coordination of national policies in the field of energy including electricity generation and supply [18].

Year	E.C.N.	NESCO	OTHERS	TOTAL	E.C.N. % OF TOTAL
1960	360.7	62.5	17.2	440.4	81.9
1961	520.7	95.3	17.5	633.5	82.2
1962	548.9	101.0	16.0	665.9	82.4
1963	659.4	113.0	13.5	785.9	83.9
1964	795.7	121.2	14.7	931.6	85.4
1965	924.7	126.5	16.0	1067.2	86.6
1966	1056.9	136.2	15.3	1208.4	87.4

Table 5. Historical electricity generating capacity in Nigeria, 1960 – 1966 (in MW) [18].

From 1972 onwards, the power generation capacity took a steep decline. Due to the growing population, there was continuous increase in power demand, but there was little reaction from the government in terms of maintaining the existing power plants or building new ones to meet up with the increasing demand. Sambo [17] highlighted several problems that have plagued electricity generation and supply in the country since 1972. Several changes have occurred in the management of the electricity industry in Nigeria since 2005. The National Electricity Power Authority (NEPA) was disbanded in 2005 and was replaced with the Power Holding Company of Nigeria (PHCN). However, in 2013 the FG disbanded PHCN with the intention of encouraging private sector investment to stimulate development of the electricity sector. The state-owned power entities were unbundled into generation, transmission and distribution companies. It was divided into generation (GENCOS) made up of five generation companies and 11 distribution companies (DISCOS). The physical handover to private tenders in the power sector privatisation process was completed by the Federal Government and handed over to the new owners on 1st November 2013 [19]. **Figure 12** shows the DISCOs established at different zones of the country as well as the mega-wattage allocated to them [19][16]. The skewing of distribution companies to the South reflects the fact that the large thermal stations are predominantly located in the Southern regions.

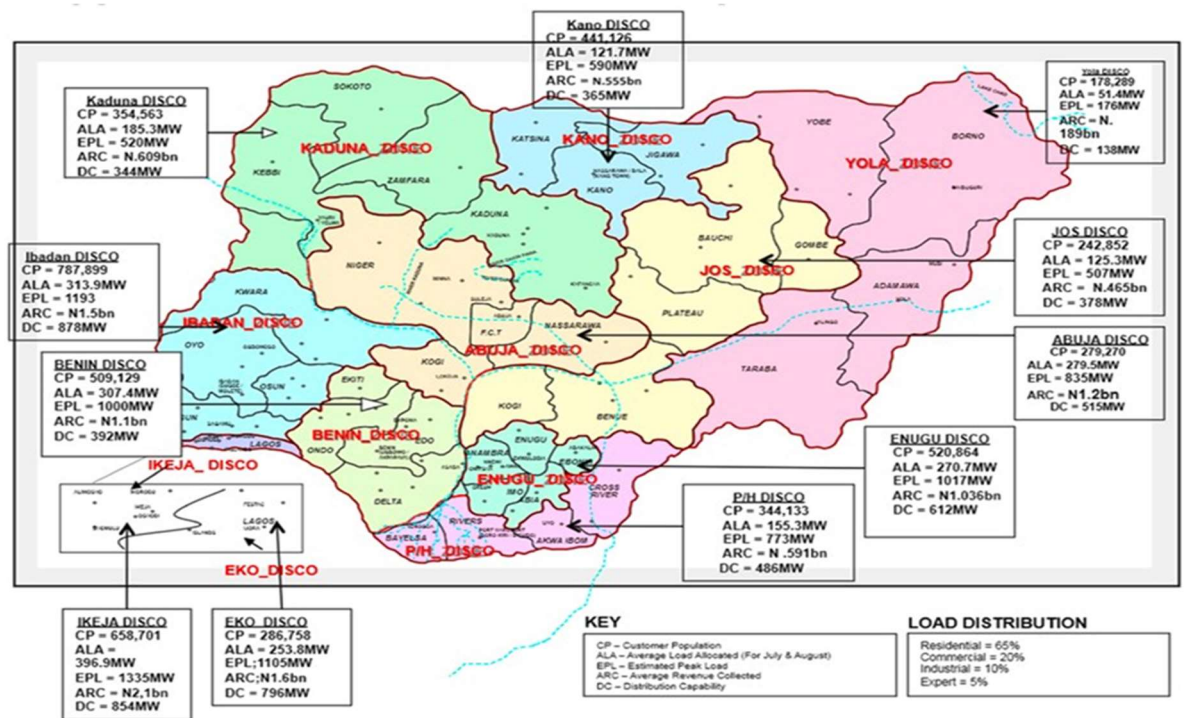


Figure 12. Map of Nigeria showing the grid distribution [16].

Table 6 lists the installed capacity of electricity generating plants in Nigeria and their ages.

Plant	Age	Installed capacity (MW)	Available capacity (MW)	Number of units installed	Number of functional units
Kainji	38-40	760	438.86	8	6
Jebba	25	578.4	529.4	6	4
Shiroro	22	600	488.82	4	4
Egbin	23	1320	694.97	6	5
AES	7	315	233.91	9	9
Ajaokuta	NA	110	24.88	2	2
Sapele	26-45	1020	156.6	10	1
Okapi	3	480	394.56	3	3
Afam	38-45	709.6	82.12	20	3
Delta	18	921	211.67	18	12
Geregu	NA	414	305.14	3	3
Omoku	3	150	87.27	6	4
Omotosho	1	335	256.58	8	2
Olorunsogo	1	335	271.46	8	2
Total		8039	4176.24	93	45

Table 6. Installed and Actual Generating Capacity (MW) 2004 [6].

As at 2010 the installed capacity stood at 5732MW, this was increased to 8,039MW in 2012 to meet the target set by the federal government to meet predicted increase in demand of 10,000MW by 2013. As of 2013 the National Electricity Regulatory Commission (NERC) had issued about 70 licenses to independent power producers (IPPs) to add more generation to the existing generating capacity [19]. The licensed IPPs

include Shell – Afam VI (642MW), Agip – Okpai (480MW) and AES Barges (270MW). These additions took the total installed capacity from 8039MW to 8700MW [19]. As of 2015, only 45 units out of 93 units of the power generators are functional, and a steep decline in capacity utilization was recorded from the performance of the power generating plants. As a result, the usable capacity was about 4176MW (48% of plate capacity) due to the obsolete generating equipment. According to a report by Augusto & Co, as at March 2014 Nigeria’s electricity supply from the national grid stood at 4,306MW, far below the estimated demand of 12,800MW (**Table 7** [20]).

Year	2014	2015	2020	2025	2030	2035	2040
Agusto & Co.	12,800	41,133	88,282	–	–	–	–
Renewable Energy Master Plan (based on 7% growth rate in energy demand)	–	24,380	45,490	79,798	115,674	161,651	213,122
Presidential Task Force on Power (PTFP)	–	12,800	–	–	–	–	–
PTFP, distribution capacity	10,648	–	32,774	–	–	–	–
Tractebel Engineering	–	–	11,433	–	24,208	–	–

Table 7. Comparison of electricity demand projections [21].

However, given the country’s dispersed population and 3.8% urbanisation rate, from Augusto & Co report there is a projection that the electricity demand (consumption) may grow from 12,800MW in 2014 to 88,282MW by 2020. The Presidential Task Force on power have also projected that electricity demand will reach some 115,000MW by 2030 [21]. Ultimately, this is the basis of the 2030 target set by the federal government.

Table 8 shows the Nigerian electricity generation profile from 1990 – 1999 [16]. This portrays the historical energy consumption in Nigeria, and indicates how generation has struggled with losses over those years.

year	installed capacity(MW)	total generation (million kwh)	total consumption (million kwh)	power losses in transmission	Losses (million kwh % of total)
1990	4,548	13,462.90	7,870.50	5,592.40	41.5
1991	4,548	14,166.60	8,292.00	5,874.60	41.5
1992	4,548	14,833.80	8,699.00	6,134.80	41.4
1993	4,586.60	14,504.60	9,998.30	4,506.30	31.1
1994	4,548.60	15,531.60	9,593.90	5,937.10	38.2
1995	4,548.60	15,856.60	9,435.90	6,420.70	40.5
1996	4,548.60	16,242.80	9,051.80	7,191.00	44.3
1997	4,548.60	16,116.80	8,843.20	7,273.70	45.1
1998	5,400.00	15,110.00	8,521.20	6,588.80	43.6
1999	5,876.00	16,088.70	8,576.30	7,512.40	46.7

Table 8. Electricity generation profile 1990 – 1999 [16][6].

On average 40% of total electricity generated each year in the 1990's was wasted due to transmission losses. The higher the generation, the higher is the losses, for example in 1999 where 46.7% losses were recorded. This demonstrates the huge gap that exists between generation and transmission. Improvements in the grid network will minimise losses and hence add to the actual power transmitted and distributed to consumers. Since 1984, the federal government of Nigeria has carried out several reforms in the electricity sector to improve reliability and to increase electricity access, as only 40 percent out of 181 million population have access to electricity. In a recent report [22], regarding the security of electricity supply regime in Nigeria, it was emphasized that a detailed review of the recent privatization of the nation's electricity infrastructures be conducted and the need to broaden the electricity generation mix should also be addressed. It was also recommended that the government update and pass laws supporting development of renewable electricity. The report also highlighted the weak and fragile grid, which presently cannot manage more than 7000 MW of load. The operational report downloaded from the Nigeria electricity system operator's website (shown in **Table 9**) is a snapshot of one day's statistics which shows that out of the presently installed capacity of 11.2 GW only 7.1 GW was available for supply on that day, which at least in part may be due to the non-functionality in some of the generating plants on that date. The maximum generation achieved was 4.8GW, indicating losses of some 32% [23].

SPOTLIGHTS ON GRID OPERATIONS	
Peak Generation	4498.3 MW
Lowest Generation	3881.2 MW
Energy Recorded	99,320.55 MWh
Generation at 06:00Hrs	4429.5 MW
Highest System Frequency	51.375 HZ
Lowest System Frequency	49.992 HZ
Highest Voltage Recorded	348 kV
Lowest Voltage Recorded	300 kV
GRID OPERATIONS MILESTONES	
National Peak Demand Forecast:	14,630.00 MW
Installed Capacity:	11,165.40 MW
Available Capacity:	7,139.60 MW
Current Transmission Capability:	7,000 MW
Network Operational Capability:	5,500.00 MW
Peak Generation Ever Attained:	4,810.70 MW
Maximum Energy Ever Attained:	104,794.26 MWh

Table 9. Operational report showing typical daily generation data (from 2015) [24].

2.1.5 Electricity Consumption

The rate of electricity consumption in Nigeria has been on the increase over the years, and as grid access is inadequate to cover this, some industrial and other consumers have installed stand-alone generators. This capacity is estimated to be at least 50% of the installed capacity of the National grid [25]. Nigeria's total energy production and consumption has traditionally been largely dependent on fossil fuel, such as oil, various forms of petroleum products and natural gas for domestic purposes, industry, transportation and electricity generation [26]. As shown in **Figure 13**, in 2014 116.5Mtoe was the total energy consumed in Nigeria, with 85.3% of this consumption through the use of traditional solid biomass (wood), which translates to 99.3Mtoe.

Total energy consumption: 116.5 Mtoe

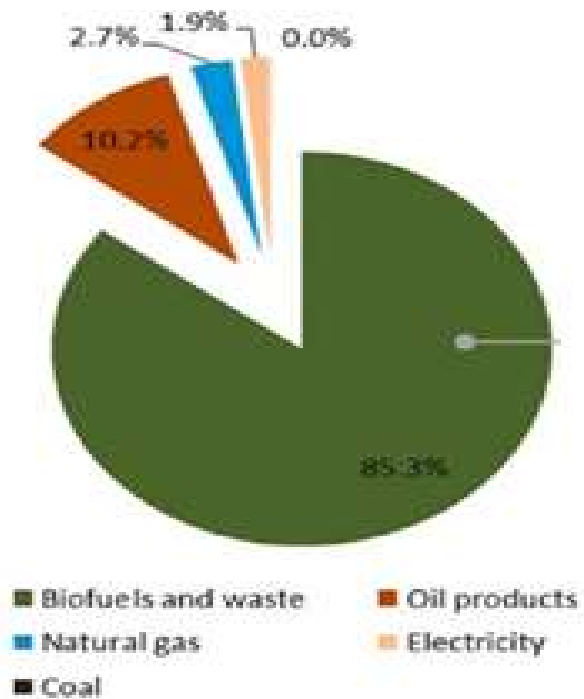


Figure 13. Total energy consumption by source in 2014 (%) [16].

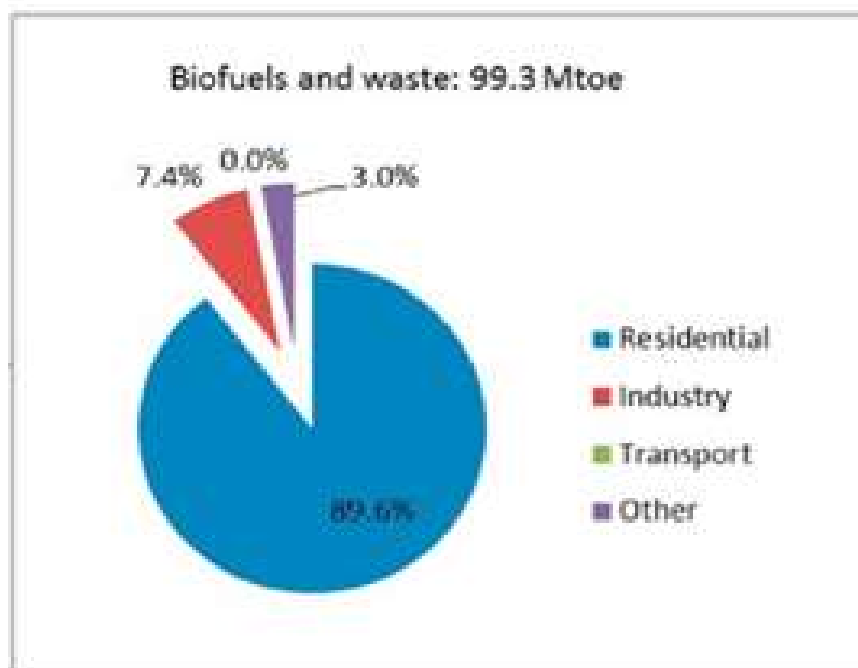


Figure 14. Percentage energy consumption by sector in 2014 (%) [16].

Around 89.6% of that energy is consumed in the residential sector. The largest share of this **residential energy consumption is for cooking purposes** [27]. Comparisons of energy consumption among the three sectors industrial, transport, and residential highlight the problems the industrial sector is facing now, as the residential energy consumption has surpassed that of the industrial sector, which is one of the drivers of the country's economy. **Figure 14** shows the percentage of energy consumption by sector in Nigeria. The heavy dependence on wood for energy has implications on personal health as will be discussed later. A historical electricity consumption by sector in Nigeria is shown in **Figure 15** which highlights the dominance of the domestic sector [16]. In 2010, the residential electricity consumption peaked at 17 TWhr. If compared to the status in 1990, it reflects the dynamics in population and the change in people's way of life within the 20-year period. However, if generation from decentralised privately-owned diesel generators is considered the figure in the industrial sector would be considerably higher than this as presented by the IEA, because data from decentralised diesel electricity generation is not captured.

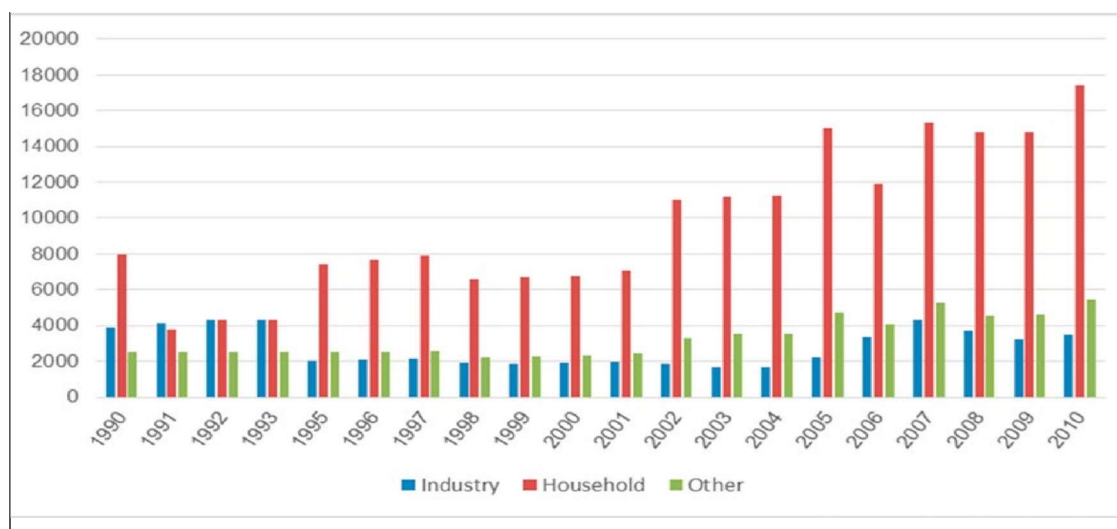


Figure 15. Electricity consumption (million kWh) 1990 - 2010 [16].

In terms of per capita consumption (kWh per person), Nigeria have seen a poor *per capita* consumption rate since 2007. As highlighted in **Figure 16**, in 2015, Nigeria per capita electricity consumption declined to 149 kWh [20][28].

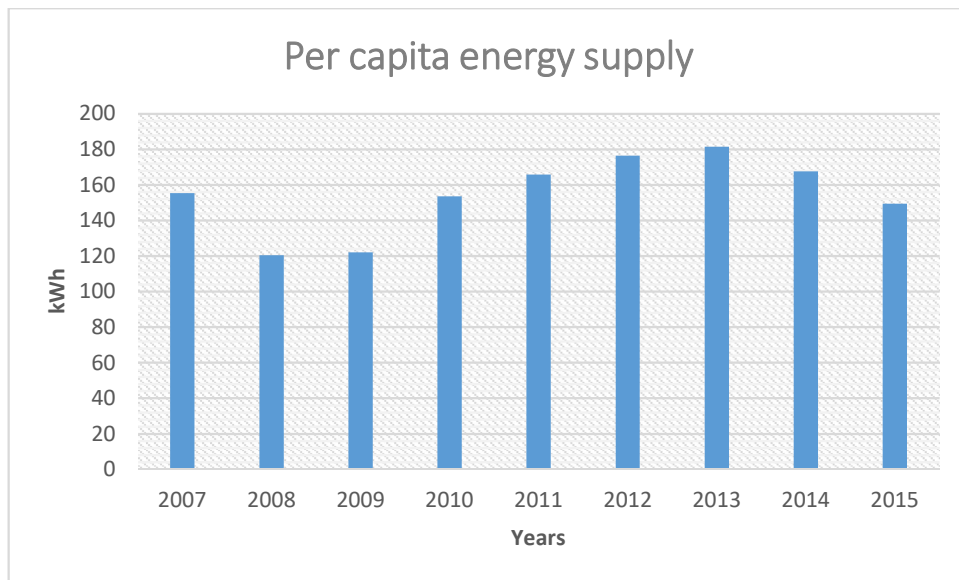


Figure 16. Per capita energy supply in Nigeria 2007 - 2015 [28][29].

Figure 17 highlights the fact that Nigeria's per capital energy consumption is below average when compared to other countries in the world with comparable populations.

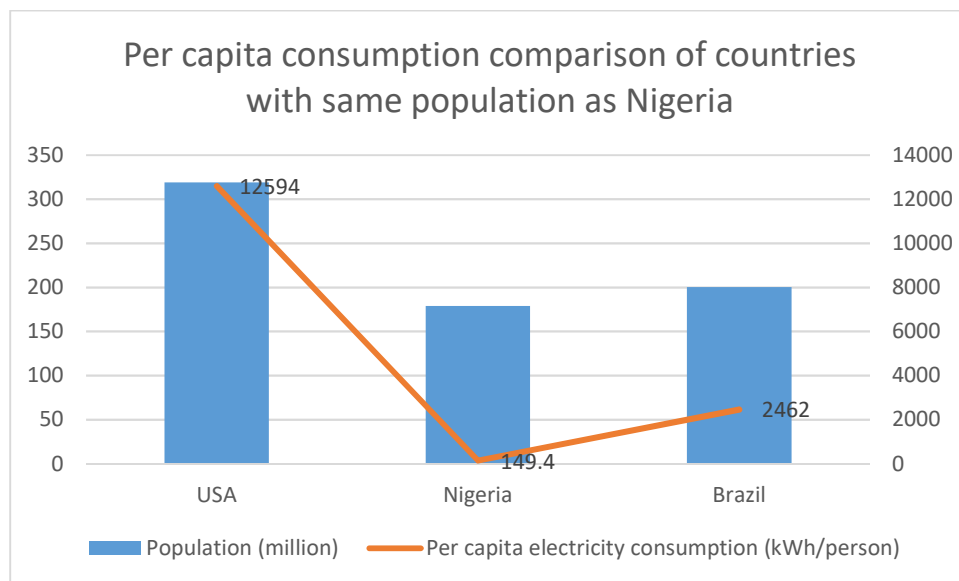


Figure 17. Per capita consumption comparison of countries with comparable populations to Nigeria, highlighting the disparities between developed and developing economies.

Nigeria's population is projected to hit 320 million by 2030 [5]. If the current per capita electricity consumption in Nigeria is compared to that of USA based on current USA population (319 million), realistically, it suggests the Nigerian electricity generation sector has a very daunting task ahead in view of the ambitious 2030 targets set by the

Federal Government. The government will need to oversee an increase in the per capita electricity consumption to a similar value as the USA by 2030, all things being equal. The strong economic growth and increasing urbanisation means that electricity demand in Nigeria needs to be addressed as a matter of extreme urgency.

2.1.6 Network and Grid Structure

The Nigeria national grid is a *radial* network that is prone to low voltage profile and system collapse. This is a somewhat outdated architecture whereby different feeder are radially distributed from a substation and each spoke connected directly to the primary of a distribution transformer. Historically, the adoption of radial network in Nigeria was mainly to minimise investment costs. A major drawback in this system is that the power supply will be interrupted in case of power failure as there would be no other alternative routing, unlike a *ring main distribution system*. **Figure 18** illustrates the structure of the national grid. The transmission lines are shown indicating the existing transmission network coverage areas and ongoing and proposed projects. The Nigeria National grid operates at 330kV and 132kV. About 70% of the total generating plants in Nigeria are stationed in the Southern region. The Northern region of the country has no generating plant and thus very limited grid connection. This is shown in **Figure 19**.

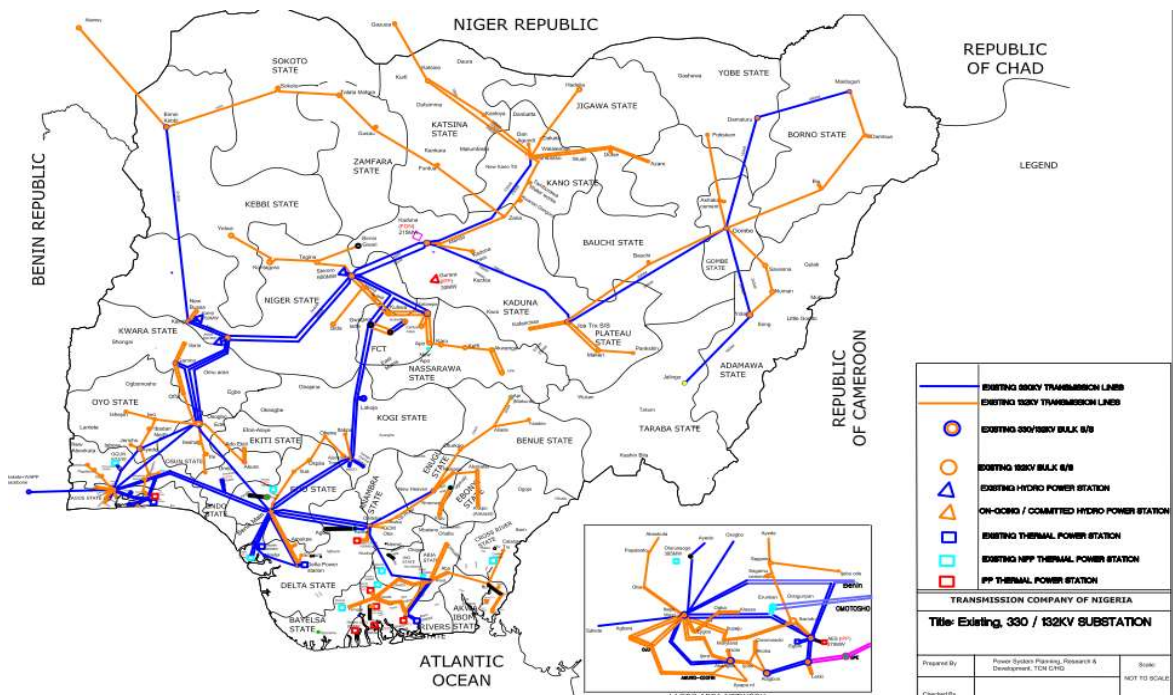


Figure 18. Map of Nigeria showing existing, ongoing, and proposed generation and transmission (HV) projects Source: Transmission Company of Nigeria [24].

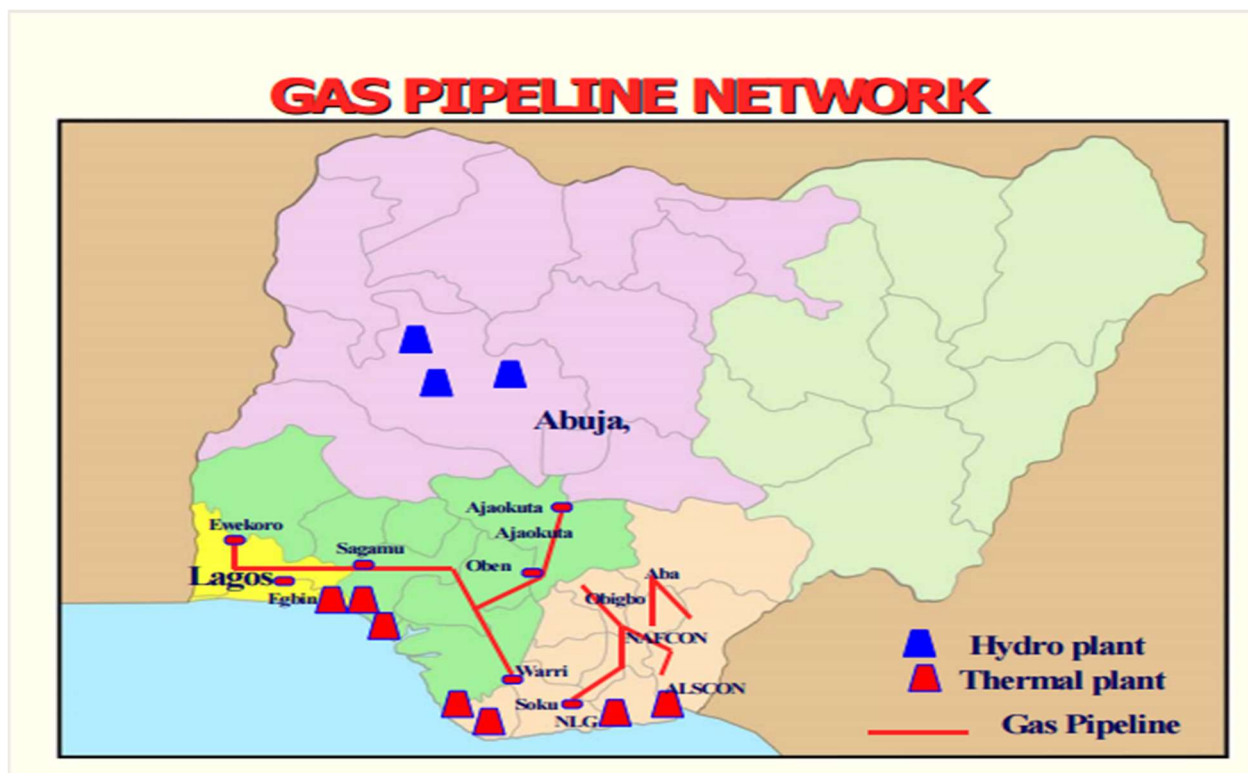


Figure 19. Gas pipeline network showing the distribution of generating plants across the country and largely sited in the south [29].

The grid distribution network consists of 23,753 km of 33 kV lines and 19,226 km of 11 kV line. The transmission network consists of 5,523 km of 330kV line and 6801 km of 132kV lines [30][31]. The 330kV lines feed 23 substations of 330/132kV with 6,000 MVA/4,800 MVA combined capacity rating, at a utilization factor of 80% [30]. The 132kV lines feed 91 substations of 132/33 kV rating with 7,800 MVA/5,800 MVA combined capacity at 75% utilization factor [30][31]. The transmission lines are characterised by high technical and non-technical losses due to overload and other infrastructural issues. The losses incurred in transmission and distribution networks within 15 months after privatization were estimated at 17 – 20%, with around 20 system collapses recorded [25].

2.1.7 Access to Electricity in Nigeria

In **Table 10**, 3 selected countries and their electricity generation profiles over a four-year period between 2010 and 2014 are shown. Brazil generates 73% of its electricity from renewables as at 2014, almost all in the form of hydroelectric power. Kenya has 81.5% of total installed electricity generation capacity met from renewable sources, again mostly as hydropower, while in Nigeria the percentage of renewable energy is falling year on year. A situation which can be explained by the infrastructural degradation as previously highlighted.

Country	2010	2011	2012	2013	2014
Brazil	84.7	87.1	82.4	76.7	73.1
Kenya	69.1	66.9	74.8	69.3	81.5
Nigeria	24.4	21.8	19.7	18.4	17.6

Table 10. % electricity production by renewable sources by country from 2010 – 2014 [28].

A recent study [32], suggests that Nigeria experiences 2,400 hours of power outage in a year (as shown in **Figure 20**), the second-worst compared to other sub-Saharan African countries (only the Central Africa Republic has more). This has led to an estimated 10% loss in annual sales. In 2013, Kabir Usman, the Director-General of Centre for Management and Development in Nigeria, noted in his statistics on the use of diesel generating sets in the country that a total sum of US\$13.6 billion was spent every year by 60 million Nigerians who generate electricity for themselves using diesel generators [25]. In 2012, use of back-up generators accounted for an estimated 11 TWh of electricity consumption across the residential, industrial and service sectors. In the same report, Usman noted that US\$0.40/kWh (N80/kWh at 1\$ = N196 in 2013) was the cost paid by the poorest Nigerians in burning candles, kerosene and firewood, while manufacturers spent between US\$0.23 (N45/kWh) and US\$0.30 (N60/kWh) on diesel generators [25].

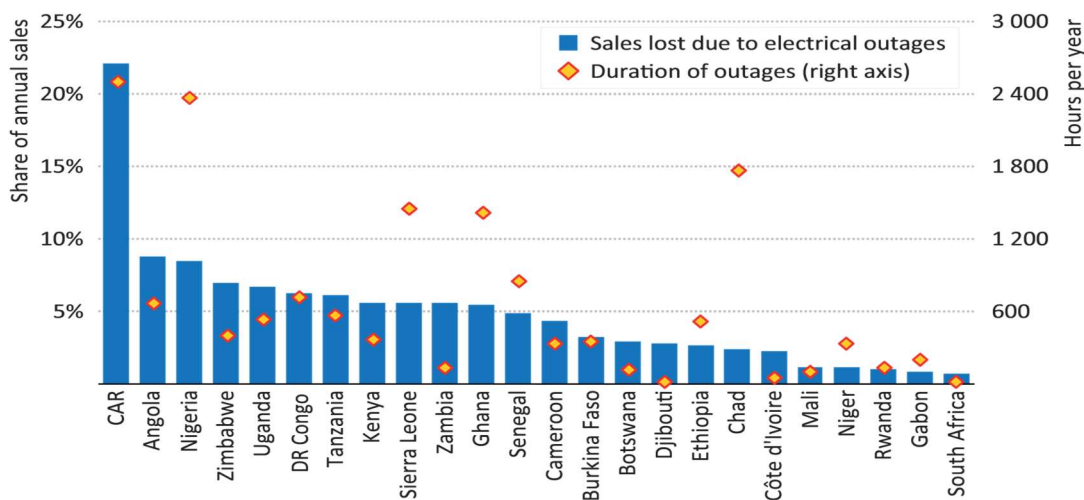


Figure 20. Duration of hours of power outage by country in sub-Sahara Africa [32].

Diesel generators endanger people's health and harm the environment as they emit carbon monoxide gas and nitrous oxide. **Table 11** shows a national sample survey of 38,522 households by the Nigeria Bureau of Statistics (NBS) on the distribution of access to electricity. This data set reflects the fact that electricity access rate in Nigeria currently sits at 55.6%. The states with higher percentage of no grid access present opportunities for alternative energy systems. In the rural areas that have no access to the grid, they live by using the local wood fuel (biomass) for cooking, and locally made lanterns which create pollution hazards and are harmful to the environment [16][27]. Over-dependence on wood fuel for cooking in the villages has a consequence of deforestation.

State of Residence	Have Electricity	No Electricity	Number of household surveyed
North Central	48.7	51.2	5,942
FCT-Abuja	77.7	22	361
Benue	22.1	77.9	1,365
Kogi	62.9	37.1	876
Kwara	90.6	9.1	617
Nasarawa	33.2	66.5	550
Niger	51.7	48.2	1,504
Plateau	36.3	63.7	669
North East	29.3	70.4	5,115
Adamawa	37.6	62.2	726
Bauchi	29.3	70.3	932
Borno	33	66.5	1,560
Gombe	48.1	51.8	464
Taraba	10.9	88.8	634
Yobe	18.1	81.7	799
North West	42.2	57.7	9,992
Jigawa	26	74	1,152
Kaduna	53.5	46.2	1,915
Kano	52.1	47.9	2,606
Katsina	31.3	68.5	1,257
Kebbi	44.4	55.6	1,069
Sokoto	38.9	60.9	898
Zamfara	29.1	70.6	1,096
South East	66.4	33.6	4,687
Abia	81.7	18.3	644
Anambra	88.1	11.8	1,050
Ebonyi	39.2	60.7	978
Enugu	55.4	44.6	920
Imo	69.9	30.1	1,096
South South	68.3	31.3	5,239
Akwa Ibom	68	31.8	892
Bayelsa	52.5	47.3	322
Cross River	57.4	41.4	848
Delta	78.3	21.6	946
Edo	82.4	17.5	702
Rivers	65.1	34.5	1,529
South West	81.1	18.8	7,546
Ekiti	92.7	7.3	376
Lagos	99.3	0.5	2,240
Ogun	72	27.9	1,355
Ondo	66.3	33.7	920
Osun	89.4	10.6	853
Oyo	66.6	33.3	1,802
Total	55.6	44.2	38,522

Table 11. % distribution of households with access to electricity by type of electricity supply [16].

In Nigeria, as at 2016 [27] it was estimated that about 90% of the population depends on traditional biomass (wood fuel) for cooking. Provision of access to sustainable means of cooking could greatly improve the peoples' quality of life. In Nigeria, as in other sub-Saharan Africa countries, there is a desire for grid extension to the un-electrified areas, particularly to rural communities, but grid maintenance, upgrade and extension requires huge investments, particularly when it comes to connecting a location that is far away from the grid terminal point. Following the unbundling of Nigeria power sector, the federal government took over the ownership of transmission facilities and named the company Transmission Company of Nigeria (TCN). TCN is currently being managed by a Canadian firm called Manitoba Management Contractor, Manitoba Hydro International [19]. This acquisition means that the Federal Government will now have the sole

responsibility of maintaining and upgrading the grid as well as constructing new ones. This heralded the establishment of National Independent Power projects (NIPP) geared towards upgrading the existing grid structure and building new ones. In 2014, the NIPP tabled plans to boost the wheeling capacity (transmittable capacity) of the grid as follows; [16].

- Short term: boost the wheeling capacity by 1,300MW.
- Long term plan i: to increase the installed generation capacity to 10 GW by 2014 via grid upgrades. NOTE: the government have not yet implemented this as at the time of writing this thesis in 2017.
- Long term plan ii: to upgrade the grid capacity to 16 GW by 2017 and 20 GW by 2020. NOTE: the 16 GW capacity plan is not yet achieved as at first quarter of 2017.

Other policies, strategies and programmes embarked on by the FG government to date includes;

- Electric Power Sector Reform Act 2005 (which heralded the unbundling of NEPA).
- National Energy Policy 2003 (NEP).
- Renewable Energy Master Plan 2005(REMP).
- Inauguration of Nigeria Electricity Regulatory Commission (NERC) in 2005.
- Integrated Rural Village Energy Supply (IRVES).

Other relevant programmes and policies include;

- Renewable Electricity Action Programme (which established the Renewable Trust Fund (RETF) as an instrument to simulate funding of renewable electricity in the country)
- National policy guideline on Renewable electricity
- Establishment of Centre for Renewable Research in (Usman danfodio University Sokoto, University of Nigeria Nsukka, Federal University of Science and Technology Owerri, Umaru Musa Yar'dua University Katsina etc).
- National Renewable Energy Action Plans (NREAP) 2015 – 2030 [21]; this is the latest policy upon which the 20% renewable target by 2030 is based; this policy

supersedes the previous one made in 2005 (Renewable Energy Master Plan 2005).

2.2 Review of Nigeria Renewable Energy Resources

Renewable electricity generation refers to the technology whereby electricity is produced from inexhaustible clean sources that can be replenished. In Nigeria, the obvious lack of demonstration sites, technical limitations, high capital costs and lack of political will have constrained the large-scale deployment of these low-carbon electricity supply technologies in the country. In future Nigerian electrification projects, renewable energy supply systems may be viewed as a viable option for remote or rural locations where grid extension would not be economically feasible. This approach has been adopted on modest scales in many locations around the world, and such systems can inform the decision-making in developing nations for regions where grid access is an issue. One unique aspect of renewable energy is that its resources could be exploited to function in combi-structure in a hybrid form to provide the required energy loading. Hybrid renewable energy systems comprise two or more renewable energy resources integrated together to provide the required or prescribed amount of energy based on availability of the resource at the selected location/site. One major technical limitation associated with renewable energy system is variability of the resources; the occurrence of wind, sunshine, and rainfall are not entirely predictable. Combining different resource types offers enhanced security of supply. Nigeria is blessed with an abundance of renewable energy resources in solar, hydro, biomass and some amount of wind. The following sections discuss the various renewable energy resources in Nigeria according to their degree of regional concentrations. **Table 12** summarises the renewable energy resource potentials in Nigeria including solar, biomass, wind and hydro.

1	Hydropower large		11,250 MW		0.8 (over 40 yrs)	1938 MW
2	Small Hydropower		3,500 MW		0.34 (over 40years)	30 MW
3	Solar Radiation		3.5 - 7.0 KWh/m ² /day (4.2 million MWh/day using 0.1% Nigeria land area)		5.2 (40 years and 0.1% Nigeria land area)	6 MWh/day Solar PV
4	Wind		(2-4) m/s at 10m height (main land)		0.0003 (4m/s @ 12% speed probability, 70m height, 20m rotor, 0.1% land area, 40 yrs.)	-
5		Fuelwood	11 million hectares of forest and woodland	Excess of 1.2m tonnes/day	-	0.120 million tonnes/day
	Biomass	Animal waste	211 million assorted animals		-	0.781 million tonnes of waste/day
		Energy Crops and Agric Residue	28.2 million hectares of Arable Land (30% of total land)		-	0.256 million tonnes of assorted crops/day

Table 12. Renewable energy resources including solar, biomass, wind and hydro [30].

2.2.1 Solar Energy Resources

The amount of solar energy that strikes the earth's surface in less than an hour is enough to satisfy all energy requirements of the entire human activities on the planet for more than a year (about 3.845×10^{26} W in all directions but only a small fraction reaches the earth) [33]. Solar energy is transmitted as electromagnetic radiation which has a spatial density of about 1.5 kW/m^2 at the boundary of the atmosphere. A square meter of the earth's surface receives as much as 1 kW of solar power, averaging to about 0.5 kW over all hours of daylight. There is enormous solar energy potential in Nigeria. The annual average solar radiation varies from $3.5 \text{ kWh/m}^2\text{-day}$ in the south to about 7.0 kWh/m^2 per day in the far north (see **Figure 21**) [34] adding both and taking the total mean average, it gives 5.25 kWh/m^2 per day and the average annual solar intensity is 1916 kWh/m^2 per year. By way of illustration, if 5% of the $923,768 \text{ km}^2$ Nigerian land area was covered in 10%-efficient solar panels, some 20 TWh of electrical generation (per annum) from solar photovoltaic means could be realised;

$$46 \times 10^9 \text{m}^2 \times 10\% \times 1916 \text{kWh/m}^2/\text{annum} = 20 \text{ TWh.}$$

This figure is comparable to the annual electricity generation in Nigeria at 29 TWh [35], and suggests that solar power could make a very significant contribution to the country's annual electricity demand.

Yearly average of daily sums of global horizontal irradiation
(Helioclim-1/PVGIS data, period 1985-2004)

NIGERIA

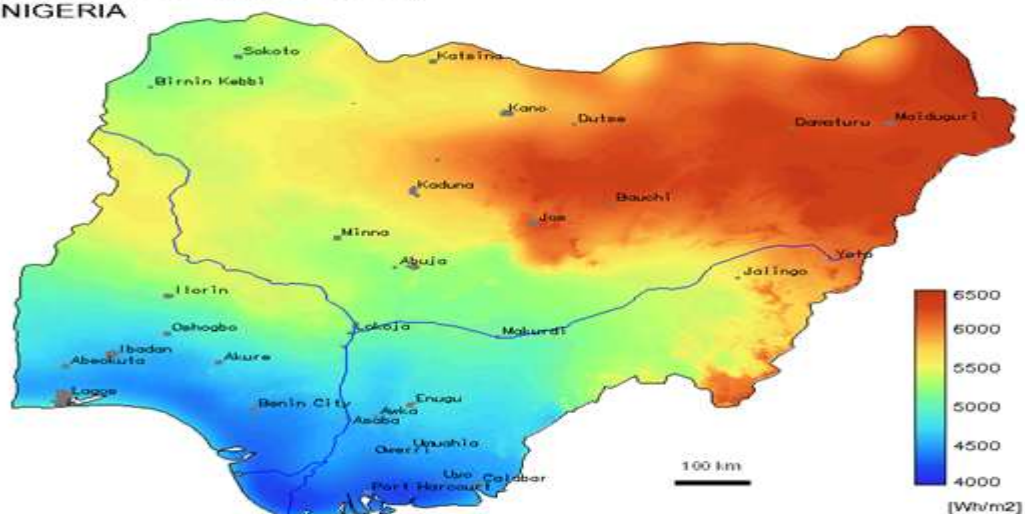


Figure 21. Map of Nigeria showing the solar energy resources [16].

2.2.2 Hydro

Hydropower is one of the oldest methods of electricity generation in the world, and is one of the major sources of electricity in Nigeria. Hydropower potential in Nigeria is significant. From a 1980 survey of 12 old states by NEPA, it was established that 734 MW of small hydropower (SHP) could be harnessed from 277 sites, as listed in **Table 13**.

State	River basin	Total sites	Hydropower potential		
			Developed (MW)	Undeveloped (MW)	Total capacity (MW)
(Pre 1980)					
Sokoto	Sokoto-Rima	22	8	22.6	30.6
Katsina	Sokoto-Rima	11		8	8
Niger	Niger	30		117.6	117.6
Kaduna	Niger	19		59.2	59.2
Kwara	Niger	12		38.8	38.8
Kano	Hadeija-Jamaare	28	6	40.2	46.2
Borno	Chad	28		20.8	20.8
Bauchi	Upper Benue	20		42.6	42.6
Gongola	Upper Benue	38		162.7	162.7
Plateau	Lower Benue	32	18	92.4	110.4
Benue	Lower Benue	19		69.2	69.2
Cross Rivers	Cross Rivers	18		28.1	28.1
Total		277	32	702.2	734.2

Table 13. small hydro potential in surveyed states of Nigeria [30].

A subsequent survey by the Energy Commission of Nigeria (ECN) showed that the total exploitable potential stands at 12,220 MW (see **Table 14**) [36], but another survey by United Nations International Development Organization (UNIDO) has identified an additional 170 potential sites across the country [37]. **Table 15** shows the existing small hydro power with a total of 37 MW installed capacity [37]. If these hydro potentials were technically exploited, and added to the 1930 MW large scale hydros in Kainji Dam, Jeba Dam, and Shiroro Dam the gross hydro potential for the country would be approximately 14,750 MW. Current hydropower generation is about 14% of the nation’s hydropower potential and this represents some 30% of total installed grid connected electricity generation capacity. According to the National Renewable Energy Efficiency Policy 2015 [38], sizes below 100 kW are termed micro-hydro, systems between 100-1000 kW are referred as mini-hydro while those between 1000 – 10,000 kW are classified as small hydro. **Figure 22** shows map of Nigeria indicating the water ways, the thick “Y” line (red ring) shows the two major rivers in Nigeria (River Niger and River Benue), the two rivers join at Lokoja (the confluence). The two Rivers provide Nigeria with great potential for hydropower, but currently only about 20% of this potential is tapped.

Location	River	Capacity (MW)
Donka	Niger	225
Zungeru II	Kaduna	450
Zungeru I	Kaduna	500
Zurubu	Kaduna	20
Gwaram	Jamaare	30
Izom	Gurara	10
Gudi	Mada	40
Kafanchan	Kongum	5
Kura I	Sanga	25
Kurra II	Sanga	15
Richall	Daffo	25
Richal	Mosari	35
Mistakuku	Kura	20
Korubo	Gongola	35
Kiri	Gongola	40
Yola	Benue	360
Karanti	Kam	115
Beli	Taraba	240
Garin Dali	Taraba	135
Sarkin Danko	Suntai	45
Gembu	Dongu	130
Kasimbila	Katsina Ala	30
Katsina Ala	Katsina Ala	260
Makurdi	Benue	1060
Lokoja	Niger	1950
Onitsha	Niger	1050
Ifon	Osse	30
Ikom	Cross	730
Afokpo	Cross	180
Atan	Cross	180
Gurara	Gurara	300
Mambilla	Danga	3960
Total		12220

Table 14. Exploitable hydro potential [36].

S/No.	River	State	Installed Capacity [MW]
1	Bagel (I)	Plateau	1
	Bagel (II)	Plateau	2
2	Kurra	Plateau	8
3	Lere (I)	Plateau	4
	Lere (II)	Plateau	4
4	*Bakalori	Sokoto	3
5	*Tiga	Kano	6
6	*Oyan	Ogun	9
Total			37
* Needs rehabilitation			

Table 15. Existing Installed capacity of small hydro schemes [37].



Figure 22. Map of Nigeria showing the water ways [38].

2.2.3 Wind

For most sites in Nigeria wind speeds generally peak around April to August and on average varies between 1.4m/s and 6m/s in the southern and Northern region of the country respectively [39]. To obtain a useful power from a wind turbine, an average wind speed of 7m/s is required from the location. Hence, a clear indication that Nigeria falls into the poor wind regime. **Figure 23** shows a map of Nigeria with the wind energy resource potentials across the country. Despite the claims of good resource above a 6m/s average wind speed, these figures are heavily skewed by monsoon winds. This will be discussed in a later chapter.

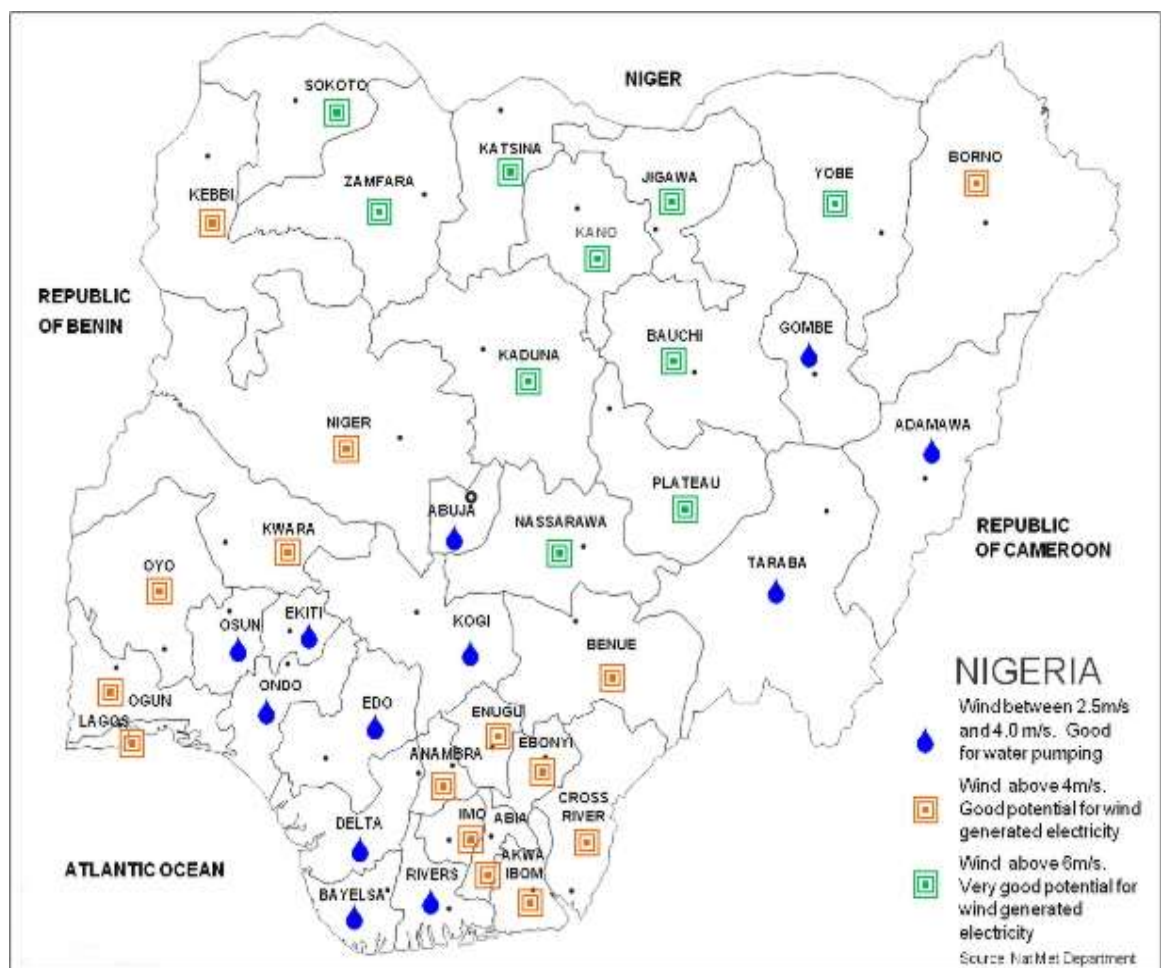


Figure 23. Wind energy resource [16].

2.3 Present, Past and Future targets of renewable activities in Nigeria

In Nigeria, there is great potential for the widespread development of off-grid renewable electricity systems, but there are still some barriers to deployment which will need to be addressed before they are adopted on a meaningful scale. As fossil fuel prices continue their inexorable rise and renewable technologies mature, economies of scale and the urgency for CO₂ reduction may lead to widespread adoption of community scale projects. The UK (especially Scotland) is a world leader in this field, and lessons learned in the development and deployment of community schemes in such regions will help in their future deployment across the globe. For instance, currently (2017) Scotland has some 8GW installed capacity of renewable power, and targets to generate 100% gross annual electricity consumption from renewable generation by 2020 [40]. Scotland's success and deep commitment to sustainable energy have attracted the attention of the United Nations [41] (UN Secretary General Ban Ki Mon global initiative) on Scotland, giving them the responsibility to play a leading role in the quest to addressing the world's electricity issues with renewable energy projects at the local scale.

In 2014, the UN decade of Sustainable Energy for all (SE4ALL) was launched in Glasgow Scotland. SE4ALL was aimed to highlight the importance of energy for economic development, peace and security for both developed and developing world. The choice of Glasgow as launch site was in recognition of Scotland as a world leader in renewable energy developments, especially at the community level, also in part to Scotland's commitment to support access to sustainable energy for communities in Malawi (a developing nation with which it has strong historical connections) [41].

In Nigeria, great resource potentials for adoption and implementation of renewable projects abound, but as yet only hydropower has been developed on a commercial scale. Various studies have reviewed the way forward in renewable resources exploitation to help address the pressing energy issues in Nigeria.

Emodi and Boo [42] have made detailed analyses on the renewable resource potentials in Nigeria, and provided ways by which this technology could be used to expand electricity access to the unserved areas in Nigeria, particularly the rural areas. Okafor and Joe [43], reviewed the power problems in Nigeria and analyzed the potentials for renewable energy solutions, and concluded that diversifying the power sector to include distributed generation sources is the key to the solution. Aliyu, Dada, and Adam [44]

made a thorough review of the slow progress of the Nigerian power industry and compared this with other African countries. They suggested that renewable energy may be the best option in future to transform Nigeria's electricity supply system. Oseni [45] and Uduma, and Arciszewski [46] also analyzed the renewable energy opportunities in Nigeria and suggests that for the country to achieve its electricity targets, renewable energy systems will play a leading role.

Many studies and experiences in different parts of the world have demonstrated that the most viable and economical option in supplying electricity to a location/area where grid connection is impossible is increasingly through the exploitation of renewable resources. A study in India, by Chaurey et al [47] stated that renewables is best for supplying the disadvantaged rural communities with electricity prior to a proposed government reform of the electricity sector. The study further stressed that distributed generation will be most favoured to tackle the technical and economic issues of the electricity sector. Nguyen [48] has illustrated the viability of alternative energy sources in improving electricity access in the rural areas of Vietnam. The study analysed the techno-economic implications of using renewables to power remote locations with dispersed households. It concluded that the initial investment cost is relatively high on an individual scale, and concludes that community scale projects with government policy intervention may help in addressing the economic issues. They may also provide a viable option for communities living at a significant distance from the grid.

Elsewhere, a study by Zahnd and Haddix [49] in Nepal, where about 80% of the total population live in rural areas, suggest that there is great potential in renewable energy, particularly where there are abundant renewable resources. According to the study, Nepal has no fossil fuel resources but is blessed with plenty of renewable resources in hydro and solar, and suggests that by utilising the renewable resources many villages in Nepal can be electrified.

Past solar PV projects in Nigeria since 2000 include [34];

- The solar street lights in Ini Local Government Area of Akwa Ibom State.
- The provision of electricity supply system to 5000 population of Bishop Kodji village (a small fishing and canoe Island close to the Atlantic Ocean off Lagos)

[50]. This solar project was completed in 2006 by the Lagos State Government and costs US\$83,000 (N33.2 million, at N400 = 1 USD exchange rate in 2016) [50]. According to the Engineer who handled this project, as at that time, there was no possibility of connecting this island to the National grid in 50 – 60 years [50]. However, the installed capacity of this solar plant was not made available. The system supplied power to the community building, the primary school, a church, and a mosque. It was also utilised to pump water into an overhead tank in the village [50]. But due to lack of maintenance, sabotage and poor response from the government officials, the solar system failed (stopped working) within three months after installation.

- The construction of 7.2kWp village electrification at kwalikwalawa in Sokoto State by the Sokoto Energy Research Center
- Implementation of 5.5kWp Solar PV plant at Laje in Ondo State.
- Construction of Solar street lighting at Yenagoa in Bayelsa State. 2.85kWp Solar PV plant at Itu mbauzo, Abia State.
- Solar PV internet back up at Nunet Usman Danfodio University Sokoto state.
- 1.87kWp Iheakpu-Awka Village Electrification/TV Viewing project in Enugu State.
- 1.5kWp Nangere Water Pumping Scheme, Sokoto State.
- 2-tonne Solar Rice Dryer, Adani, Enugu State.
- Construction and implementation of a 1.565kWp solar powered borehole and street lighting at Malarin Gamma village, Malam Madori LGA, Jigawa State. Gui in Abuja.
- Construction of a 1.820kWp Village electrification project at Gui in Abuja Municipal council.
- Solar street lighting in Abakaliki, by Ebonyi state Government 2005 (this failed due to poor maintenance)
- Solar street lightings in Ado Ekiti, Ekiti State.

- Bank of Industry (BOI)/UNDP - 24KW micro-grid solar electrification each in Bisanti (a remote village in Katcha Local Government Area of Niger State) and in Ife-North LGA in Osun State and Gombe state to cover 250 households 2015.

Table 16 summarises the short medium and long-term plan of the Nigeria government in implementing renewable energy based electricity, to meet the 2030 target. The table illustrates breakdown of previous activities, the present and future targets.

S/N	Resource	2012	Short Term (2015)	Medium Term (2020)	Long Term (2030)
1	Hydro (LHP)	1,938.00	2,121.00	4,549.00	4,626.96
2	Hydro (SHP)	60.18	140.00	1,607.22	8,173.81
3	Solar	15	117.00	1,343.17	6,830.97
4	Biomass	-	55.00	631.41	3,211.14
5	Wind	10	50.00	57.40	291.92
	All Renewables plus LHP	1,985.18*	2,438.00*	8,188.20*	23,134.80*
	All Energy Resources (On-grid power plus 12,500MW of self-generated power)	21200**	24,380**	45,490**	115,674**
	% of Renewables plus LHP	23%	10%	18%	20%
	% RE Less LHP	0.80%	1.30%	8%	16%

Table 16. Summary of Renewable Electricity Targets in terms of MW capacity [38].

*"From Supply projections based on 7% GDP Growth" [38]

**"Supply projections are based on the addition of on-grid power, and a base capacity of 12,500MW of self-generation (i.e. power generated for own use) including off-grid generation from year 2012 to 2030" [38].

In 2017, the FGN raised the hope of meeting the 2030 target by signing an agreement for 120MW solar power project with two solar developers (Afrinegia Nigeria Limited CT and Cosmos Power Company) [51]. Though, according to the original plan as listed in **Table 16** this action is belated, since the initial target was to generate 117MW of electricity from solar by 2015. This explains the attitude of the Federal Government towards implementing policies and plans.

Having reviewed and analysed the previous renewable energy based projects that have been implemented in Nigeria and elsewhere the following deductions can be made;

- Nigeria presents a huge exploitable market for renewable technology given the resources available
- The target by the federal government of Nigeria to generate 20% of the country's electricity from renewable resources by 2030 can be realizable if the policies already put in place by the federal government are implemented.
- From the experience of off-grid communities in many parts of the world that have already developed renewable electricity systems with demonstrable success, it shows that the technology and know-how are transferrable
- The rural communities and various parts of the Northern region of Nigeria, which have no electricity generation and are remote from the grid will make good candidates for this type of electricity technology. However, this depends on governments commitments to proper planning in the initial stage, as seen in Bishop Kodji village.
- The idea of scalability in a bottom-up scenario will help as a start in the long-term goal. Renewable energy systems, for example solar, are scalable, therefore, in the initial design process, a modest size may be installed, with a view to increasing the size in a modular fashion according to ongoing energy demand.
- There is an opportunity to displace diesel, considering the 58% of electricity that is currently generated off-grid by private individuals.
- Using the income level of the citizens (the people's income level determines the kind of electric appliance they can possess, and hence their energy consumption) and a careful prediction of the rate of population growth, a long-term electricity

demand in Nigeria can be estimated which could be used to make an informed decision in expanding electricity access across the country.

2. References

1. Online available at <http://www.total-facts-about-nigeria.com/physical-map-of-nigeria.html> accessed on 10/07/2017.
2. The world factbook; online available at <https://www.cia.gov/library/publications/the-world-factbook/geos/ni.html> accessed on 22/06/2017.
3. National Population Commission; Online available at <http://www.population.gov.ng/> accessed on 02/11/2015.
4. United Nations World Population Prospects 2017; online available at <https://esa.un.org/unpd/wpp/Download/Standard/Population/>.
5. United Nations; UN projects world population to reach 8.5 billion by 2030, driven by growth in developing countries: online, available at <http://www.un.org/sustainabledevelopment/blog/2015/07/un-projects-world-population-to-reach-8-5-billion-by-2030-driven-by-growth-in-developing-countries/> accessed on 22/06/2017.
6. Africa Development Bank Group; Nigeria Economic and Power Sector Reform Appraisal Report Online available at [The_Economic_and_Power_Sector_Reform_Program__EPSERP__-_Appraisal_Report.pdf](#) accessed on November 2015.
7. Central Bank of Nigeria Economic Report 2016: Online available at <https://www.cbn.gov.ng/out/2016/rsd/cbn%20economic%20report%20for%20first%20quarter%202016.pdf> accessed on 12/11/2016.
8. Online available at http://jreiss.org/jreiss.org/Teaching_files/2015_Week_8.pdf accessed on November 2015
9. Online available at <https://tradingeconomics.com/madagascar/gdp-growth-annual> accessed on 05/07/2017.
10. National Bureau of Statistics; Nigerian Gross Domestic Product Report 2015.
11. Oxford Poverty and Human Development Initiative; online, available at <http://www.ophi.org.uk/multidimensional-poverty-index/mpo-faqs/> accessed on 22/06/2017.

12. Progress, Human. "Reducing Vulnerabilities and Building Resilience." (2014).
Online available at; http://hdr.undp.org/sites/all/themes/hdr_theme/country-notes/NGA.pdf accessed on 01/11/2015.
13. Online available at <http://www.un.org/en/ga/second/65/docs/foster.pdf> accessed on 10/07/2017.
14. Online available at <http://hdr.undp.org/en/content/intensity-deprivation> accessed on 05/07/2017.
15. World Economic League Table; Online available at <http://www.cebr.com/reports/world-economic-league-table-2015/> accessed on 11/11/2015.
16. An Overview with a Special Emphasis on Renewable Energy, Energy Efficiency and Rural Electrification 2nd Edition, June 2015.
17. Sambo, A. S. "Matching electricity supply with demand in Nigeria." *International association for energy economics* Fourth Quarter (2008): 32-38.
18. Olukoju, Ayodeji. *Infrastructure development and urban facilities in Lagos, 1861-2000*. Vol. 15. Institut français de recherche en Afrique, University of Ibadan, 2003.
19. KPMG (December 2013) A Guide to the Nigerian Power Sector.
20. Online available at <http://www.thisdaylive.com/articles/-nigeria-s-electricity-consumption-per-capita-lowest-in-africa-/186796/> accessed on 12/12/2014.
21. National Renewable Energy Action Plans (NREAP) 2015 – 2030 First version.
22. Sambo A.S (2015) The way forward for electricity supply in Nigeria; Online available at <http://voices.nationalgeographic.com/2015/10/20/the-way-forward-for-electricity-supply-in-nigeria/> accessed on 13/07/2016.
23. National grid. National energy policy report 2003
24. Online at <http://www.nsong.org/App Themes/Blue/images/NationalGrid.png> accessed on 03/11/ 2015
25. Nigeria on the brink of electricity self-insufficiency, online available at <https://www.thisdaylive.com/articles/nigeria-on-the-brink-of-electricity-self-insufficiency/163451/> accessed on 13/11/2015.
26. World Energy Council; Online available at <https://www.worldenergy.org/data/trilemma-index/country/nigeria/2014/>.
27. Saad, S. and Bugaje, I.M., 2016. Biomass Consumption in Nigeria: Trends and Policy Issues. *Journal of Agriculture and Sustainability*, 9(2).

28. World Bank (2015): World Development Indicators; Electricity production, sources, and access, Online available at <http://data.worldbank.org/indicator/EG.USE.ELEC.KH.PC> accessed on November 2015.
29. Mobolaji Aluko. The case for an energy emergency in Nigeria again: Essay 2015.
30. Federal Ministry of Power and Steel Nigeria; Renewable Electricity Policy Guidelines, December 2006.
31. Federal Ministry of Power and Steel: Renewable Energy Action Plan 2006.
32. IEA 2014; Africa energy outlook, A focus on energy prospects in Sub-Saharan Africa. Online available at https://www.iea.org/publications/freepublications/publication/WEO2014_AfricaEnergyOutlook.pdf accessed on 19/05/2016.
33. Kapur, V.K., 1999. Photovoltaics for the 21st Century: Proceedings of the International Symposium. The Electrochemical Society.
34. Energy Commission of Nigeria (November 2005); Renewable Energy Master Plan Final Draft
35. The world factbook; online available at <https://www.cia.gov/library/publications/the-world-factbook/fields/2232.html> accessed on 22/06/2017.
36. Manohar, K. and Adeyanju, A.A., 2009. Hydropower Energy Resources in Nigeria. Journal of Engineering and Applied Sciences, 4(1), pp.68-73.
37. Zarma, I.H., 2006. Energy Commission of Nigeria: Hydro power resources in Nigeria. In 2nd hydro power for today conference, China.
38. National Renewable Energy and Energy Efficiency Policy (2015); Online available at <http://www.power.gov.ng/download/NREEE%20POLICY%202015-%20FEC%20APPROVED%20COPY.pdf> accessed on 13/11/2015.
39. Agwu, D.D., Chinaeke-Ogbuka, I.M. and Ogbuka, C.U., Towards effective harnessing of wind energy for power generation in Nigeria.
40. Scottish Government 2020 route-map; online available at; <http://www.gov.scot/Resource/0044/00441628.pdf> accessed on November 2015.

41. Online available at <https://news.gov.scot/news/scotland-hosts-launch-of-un-global-initiative> accessed on 22/06/2017.
42. Emodi, N.V. and Boo, K.J., 2015. Sustainable energy development in Nigeria: overcoming energy poverty. *International Journal of Energy Economics and Policy*, 5(2).
43. Okafor, E.N.C. and Joe-Uzuegbu, C.K.A., 2010. Challenges to development of renewable energy for electric power sector in Nigeria. *International journal of academic research*, 2(2).
44. Aliyu, A.S., Dada, J.O. and Adam, I.K., 2015. Current status and future prospects of renewable energy in Nigeria. *Renewable and sustainable energy reviews*, 48, pp.336-346.
45. Oseni, M.O., 2012. Improving households' access to electricity and energy consumption pattern in Nigeria: Renewable energy alternative. *Renewable and Sustainable Energy Reviews*, 16(6), pp.3967-3974.
46. Uduma, K. and Arciszewski, T., 2010. Sustainable energy development: the key to a stable Nigeria. *Sustainability*, 2(6), pp.1558-1570.
47. Chaurey, Akanksha., Malini Ranganathan., and Parimita Mohanty., 2004. "Electricity access for geographically disadvantaged rural communities—technology and policy insights." *Energy policy* 32.15 (2004): 1693-1705.
48. Nguyen, Khanh Q. "Alternatives to grid extension for rural electrification: Decentralized renewable energy technologies in Vietnam." *Energy Policy* 35.4 (2007): 2579-2589.
49. Zahnd, Alex, and Haddix McKay Kimber. "Benefits from a renewable energy village electrification system." *Renewable Energy* 34.2 (2009): 362-368.
50. National Geographic: Nigeria's solar projects yield, both failure and success, online available at <http://news.nationalgeographic.com/news/energy/2011/11/111102-solar-power-in-nigeria/> accessed on 22/06/2017
51. Vanguard news; Online available at <http://www.vanguardngr.com/2017/04/fg-two-others-sign-120mw-solar-project/> accessed on 25/04/2017.

3.0 Energy Storage System: The Technology and Application

In every renewable energy system design, it is imperative that a detailed study is made on the technological options regarding the choice of system configuration suitable for the purpose of end-user demand. This chapter starts with an overview of different technological options and applications for facilitating the integration of intermittent renewable energy generation sources with an energy storage system (ESS). Energy storage has various functions including meeting peak loads, quick response in providing spinning reserve (this refers to the reserve capacity set in synchronism with grid to meet an unexpected increase in demand to maintain system frequency), load levelling, improving power quality and power stabilization, and providing seasonal storage [1]. These capabilities can be exploited in off-grid renewable electricity generation. Here, a brief review of different energy storage technology options applicable to renewable energy systems are considered. Energy storage technologies for different applications are presented, and based on this an energy storage system that forms the focus of this work will be introduced.

3.1 Energy Storage Imperative

Most renewable energy sources are non-dispatchable by nature. Their intermittency demands that an energy storage facility be integrated into the system to cover electrical demand for those periods where the renewable supply cannot satisfy this alone. Energy storage simply put means the process by which energy can be stored and then be released to perform a useful operation at a later stage. Over the years, the problem of energy storage has been a major issue (technological and cost-wise) in the design of renewable powered systems. The conventional solution has been to employ strings of electrochemical batteries, usually based on a lead-acid technology.

Recent interests in energy storage is informed by several factors and requirements including;

- advancements of power electronics and storage technology
- advent of renewable energy systems; managing the intermittency and development of off-grid renewable electricity
- the problem of improving power quality in terms of grid connected applications; voltage and frequency stabilization
- providing additional capacity in grid-scale applications

3.1.1 Energy Storage Mediums and Methods

Any device or media that can be used to store energy to perform useful work later is referred to as an energy storage medium. Ideally, electrical energy storage is the conversion of electrical energy to an economically feasible form that can be stored and converted back to electrical energy when needed. Energy storage mediums include electrochemical, electromagnetic, electrostatic, mechanical and chemical forms. The type of energy storage mediums discussed in this thesis relates to those used in small scale renewable energy systems. These include;

- Batteries – electrochemical storage
- Super-capacitors (ultra-capacitors) – electrostatic storage
- Flywheels – mechanical (kinetic) storage
- Hydroelectric – Pumped (gravitational) storage
- Hydrogen – chemical storage

Depending on the type of technology employed and the energy network requirements, the energy storage systems can be further classified into short and long-term storage. The functionality of the storage is often defined in terms of these temporal considerations. Hydrogen storage is best suited for long term storage. Flywheels and

batteries are mostly used for relatively short-term energy storage, typically a few seconds to the order of a day.

3.1.2 Batteries

The most widely used small scale energy storage device is the battery. Batteries are made up of basic units which are usually connected in series or parallel strings to achieve a desired voltage and capacity. These basic units are called cells. For a 12V battery each cell is designed to contribute 2V in the 6-cell series stack making up 12V. Batteries are rated in terms of the power (kW) and energy (kWh or Ah) capacity it can deliver at a rated voltage. Some of the characteristics of batteries which defines their mode of performances are; efficiency, operating temperature, energy density, power density, charge and discharge cycle, life span, depth of discharge and the self-discharge rate [2]. Some of the types of batteries mostly used today are lead acid, lithium ion, and valve regulated lead acid. Flow batteries are coming into the mainstream, and novel chemistries to provide high currents at very high-power densities are under research and development. Lead acid batteries are the oldest and most mature electrical energy storage technology. Invented in the 19th century, they are widely used in renewable energy applications [3]. The lifespan of batteries is typically limited to 5 – 15 years [4], depending on technology and usage. This can be a concern as replacement costs at end of life may be considerable. In addition, battery can be viewed as a short term (minutes - hours) energy storage medium due to its limited depth of discharge and self-discharge (discharges about 1-5% of its energy per month if left unused) characteristics [5].

3.1.2 Super-capacitor

Super-capacitors are a relatively new energy storage technology which employs a non-Faradaic charging process as opposed to that used in traditional batteries [6]. They have a high-power density, long life and nearly unlimited cycle-capability and are well suited especially for applications with many short charge and discharge cycles, where their high performance can best be utilised [6]. However, the drawback of supercapacitors is its short discharge duration (seconds), high self-discharge rate (5%), and its low energy density compared to batteries. Recent studies have highlighted the use of

supercapacitors in off-grid electricity environments; Logerais et al [7] studied the storage of photovoltaic energy by means of supercapacitors. One good aspect of their work is that both an experimental and modelling (Matlab/Simulink) approach was used, a data logging/acquisition system with LabVIEW software was also used to obtain physical data which they used in their analysis. They tried to establish the fact that experimental irradiance and supercapacitor charge/discharge cycles can be in good agreement. They measured the global solar irradiance with a Kipp and Zonen CMP6 pyranometer. They used a Photowatt PW1650 PV array which contains 72 polycrystalline silicon cells and connected 16, 2.7V Maxwell BCAP0100 supercapacitors of capacitance 100F in series. From their experiments, they calculated the efficiency of the charging and discharging process. Their results show an error of 1% on the energy stored for a given day atmospheric and irradiance conditions, meaning that the process is almost 99% accurate.

Glavin and Hurley [8] studied a hybrid ultracapacitor – battery system to increase the reliability and improve the cost efficiency of solar PV. To reduce the size of the battery pack and at the same time extend the battery life, the peak power requirements of the load were supplied by the ultracapacitor (a large supercapacitor). However, they proposed a photovoltaic system where an ultracapacitor is used to achieve the high pulse currents that are required by the battery charging algorithm. They also developed an energy control unit (ECU) for a photovoltaic battery supercapacitor hybrid system and performed a simulation using Matlab/Simulink to compare the energy control unit (ECU) under different load conditions to the standard photovoltaic battery storage system. They observed from their simulations that the addition of a supercapacitor bank increases the battery state of charge (SOC) for peak and pulse current loads [8]. This shows the advantages of a hybrid energy system, for instance, as described, the supercapacitor may significantly increase the battery lifetime, and this will help reduce costs that will be incurred in battery replacement.

3.1.3 Flywheel

A flywheel is a mechanical device that depends on a rotating mass to store energy [6]. The basic principle behind the storage mechanism of a flywheel is that the rotating action of the flywheel is achieved (typically) by being driven by an electric motor. Its work is to supply energy in form of torque to the flywheel so it can start rotating, conversely the energy stored is retrieved by the withdrawal of a device that supplies the torque (electric motor), in the reverse order it becomes a generator. The amount of energy the flywheel can store depends on its rotational velocity, according to the equation $E = \frac{1}{2} I \omega^2$, where I is the moment of inertia of the flywheel and ω is the rotational velocity [9][10]. Flywheel storage systems are categorized into two groups, the conventional metal rotor system (with low speed) that is typically used for short and medium-term applications, and the high-speed composite metal systems. Flywheels typically have high charge and discharge rates and relatively low capacity, which is a major limitation to its use for long term storage. This means that it may be best suited for use as standby power [11] or for electrical smoothing. A recent flywheel design (see **Figure 24**) offers possibilities for flywheel storage on a household scale [12]. In the Velkess (stands for Very Large Kinetic Energy Storage System), it is claimed that the new flywheel has an efficiency of more than 80%, and would rival the best energy storage alternatives.



Figure 24. Velkess flywheel energy storage [10].

The flywheel has a fast charging rate, and can charge fully in 5 hours [12] (this means that an average of 6.5-hours sunshine in Nigeria is enough to get it fully charged). A size of 3kW storage system is priced at \$6,000 [10], or \$2,000 per kW. This would be a good match to an off-grid house with a solar photovoltaic (PV) system as it can store up to 15 kWh of energy [10][13]. This means it can store electricity at \$133 per kWh which is cheaper compared to lithium battery at \$400 - \$500 per kWh [14].

Examples of existing systems flywheel storage systems are;

- Integrated flywheel energy storage in Isle of Eigg; the Scottish Island
- Integrated flywheel energy storage in the Fair Isle; the Scottish Island.

Both islands rely heavily on renewables for their electric power supply. The Isle of Eigg uses a combination of various renewable energy sources in hybrid form with a diesel generator, hydro, wind, solar and lead acid batteries. A recent addition is a flywheel which was integrated primarily in order to reduce electrical spiking (which can cause island-wide system trips) and to enhance battery life. Fair Isle is powered by only a wind turbine and diesel backup, and now incorporates flywheel storage. The installations of flywheel energy storage technology in these Scottish Islands are the first time the technology has been used for a stationary application in the energy sector, and was funded by (the then) UK Department of Energy and Climate Change [14].

3.1.4 Pumped Hydroelectric Storage

Pumped hydroelectric refers to a type of storage system whereby water is pumped from a lower elevation reservoir to a higher elevation reservoir where it is stored for future utilization when power demand peaks. This type of storage mechanism (illustrated in **Figure 25**) is most suited for long term storage in off-grid renewable energy systems, and simply makes use of gravitational potential energy in its operation [15].

As an example, in off-grid renewable power system utilising solar as the energy source, the excess energy that could be generated by one or more of these energy sources will be used to pump water from the lower reservoir to the higher reservoir [16]. The stored water will be released to turn the hydro turbine during the period of high energy demand when the hydro resource is low. The main drawbacks in the implementation of

this type of storage system in off-grid renewable energy systems are the site specificity associated with it, and the potentially prohibitive capital costs.

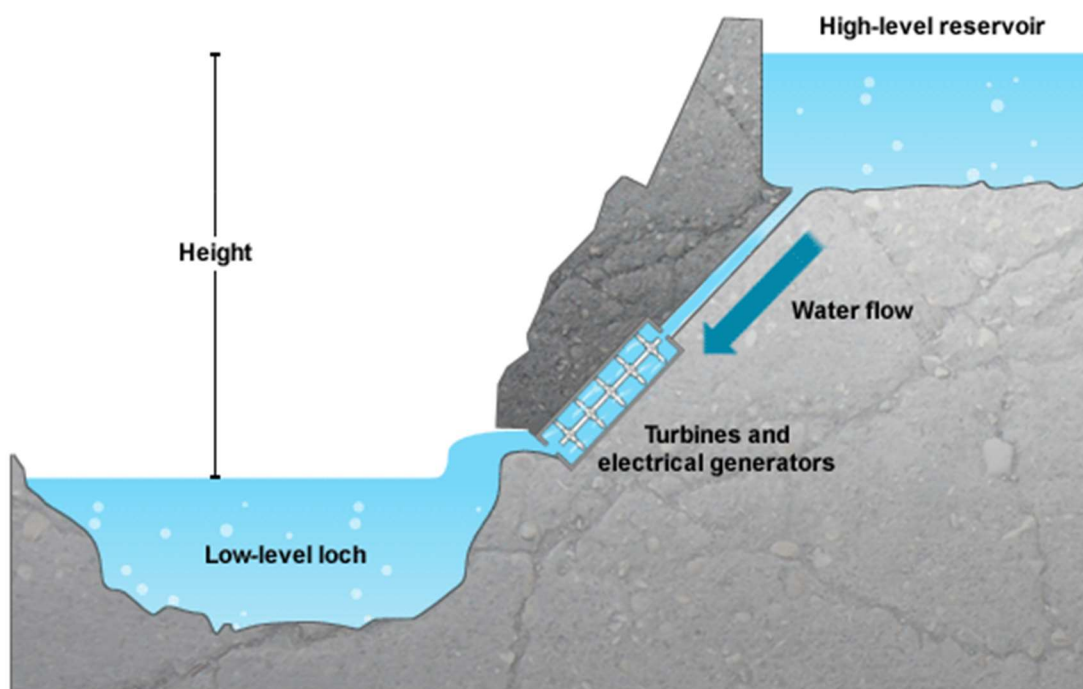


Figure 25. Pumped hydro storage with its technical components [17].

3.1.5 Hydrogen Storage

Jules Verne quotes;

"Yes, my friends, I believe that water will one day be employed as fuel, that hydrogen and oxygen which constitute it, used singly or together, will furnish an inexhaustible source of heat and light, of an intensity of which coal is not capable.... water will be the coal of the future". Jules Verne - Mysterious Island 1874 [18].

Recent advances in hydrogen technologies are unlocking their potential for use as a storage medium in hybrid renewable energy systems, especially those found in remote islands and rural dwelling places. The search for suitable technologies for energy storage to cope with the intermittency of the renewable technologies has become an area of considerable interest, and hydrogen is at the forefront of this research.

The principle by which electricity is used to decompose water into hydrogen and oxygen is called electrolysis and this process is made possible using a device called an electrolyser. The hydrogen produced in the process can be stored in various forms (explained in detail in the later part of this **chapter**) for future use. To convert the hydrogen produced through the action of an electrolyser into electricity a hydrogen fuel cell may be employed. This is an electrochemical device that combines hydrogen with oxygen (air) to produce electricity and water. It is an electrochemical reaction process which can be considered as a reverse electrolysis process, because while energy is needed to produce hydrogen via electrolysis, the recombination of hydrogen and oxygen in the fuel cell releases electrical energy. Production of hydrogen using sustainable energy systems is a zero-emission energy production process. Other common methods by which hydrogen can be produced are;

- Steam reforming of hydrocarbons and gasification of solid fuels
- Thermochemical water splitting at high temperature, photo-biological reactions, biomass conversions, power-ball and others [16].

To make a renewable energy system more reliable in terms of availability of supply, any excess electrical energy generated by the system can be diverted to an electrolyser to produce hydrogen. An electrolyser/fuel cell combo offers a potentially competitive solution to batteries in terms of lifetime and flexible storage capacity [19].

Figure 26 shows the configuration of PV-Hydrogen off-grid electricity with a fuel cell for the conversion of the stored hydrogen into electricity.

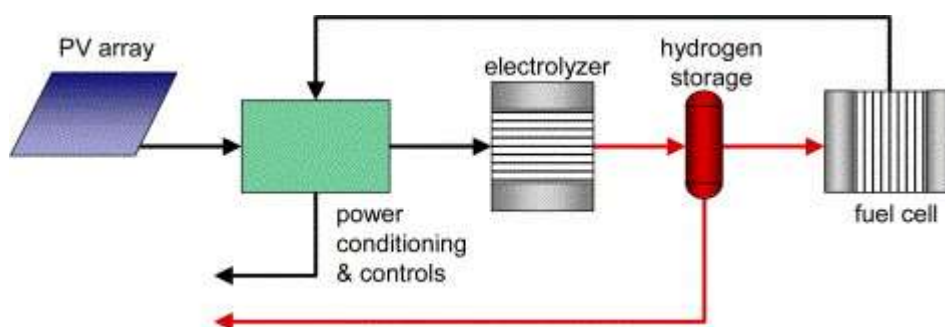


Figure 26. Schematic diagram of off-grid integrated PV-Hydrogen storage [16].

In Nigeria, solar power systems for electrical energy production are likely to predominate, and the integration of this together with hydrogen storage facility forms the main thrust of this research. Experience from elsewhere suggests that there are considerable benefits to be obtained from availability of flexible storage (as opposed to batteries). In the Isle of Eigg system the renewables often generate more power than required, and once the batteries are fully charged excess power is mostly diverted/dumped to heaters, or switched out of the system.

However, instead of diverting this excess power to dump heaters, it could be utilised for hydrogen production. This offers relatively long-term and high-volume storage, and would significantly reduce reliance on the backup diesel generators. This systemic approach is applicable to Nigerian villages; excess energy production from the abundant solar resource can be utilised to produce hydrogen, offering enhanced security of supply and possibilities for utilising the produced hydrogen in a thermal capacity to meet cooking needs. As with the Scottish islands experience they will almost certainly benefit from socio-economic growth and development which electricity can offer. The techno-economic comparisons of various energy storage mediums that finds application in renewables- based electricity systems are presented in **Appendix 5**.

3.2 Energy Storage for Renewable Energy Systems

In RES, the energy produced during periods of high availability may sometimes exceed the energy requirement of the consumers and will need to either be stored or exported to grid. If this is not possible dump heaters may be used to maintain the energy balance for voltage stabilization and to avoid frequency distortion in terms of micro-grid applications. This problem arises because the demand for energy does not always coincide with production especially in off-grid renewable electricity application. The shifting balance between energy supply and demand is a significant challenge to system designers, and resulting efficiencies tend to be quite poor. On the supply side RES outputs are naturally linked to local weather conditions, so these need to be carefully assessed through observation and modelling.

To analyse the opportunities, we first have a look at the weather distribution in Nigeria. The Nigerian climate is tropical. **Figure 27** shows the weather pattern in Nigeria. There are two different seasons; a wet season is from April to September, with lower monthly temperatures and the wettest month being June. Also, a dry season starts from October and ends in March. There is also period in the dry season when the dusty wind from the Sahara sweeps across the North-Eastern area. This period is called harmattan. In the wet season, moisture-laden south-westerly winds from the Atlantic bring cloudy and rainy weather. Those cloudy days imply that the solar generator outputs may be reduced, and thus an energy storage system (or hydrocarbon based generator) will be required as back up [20].

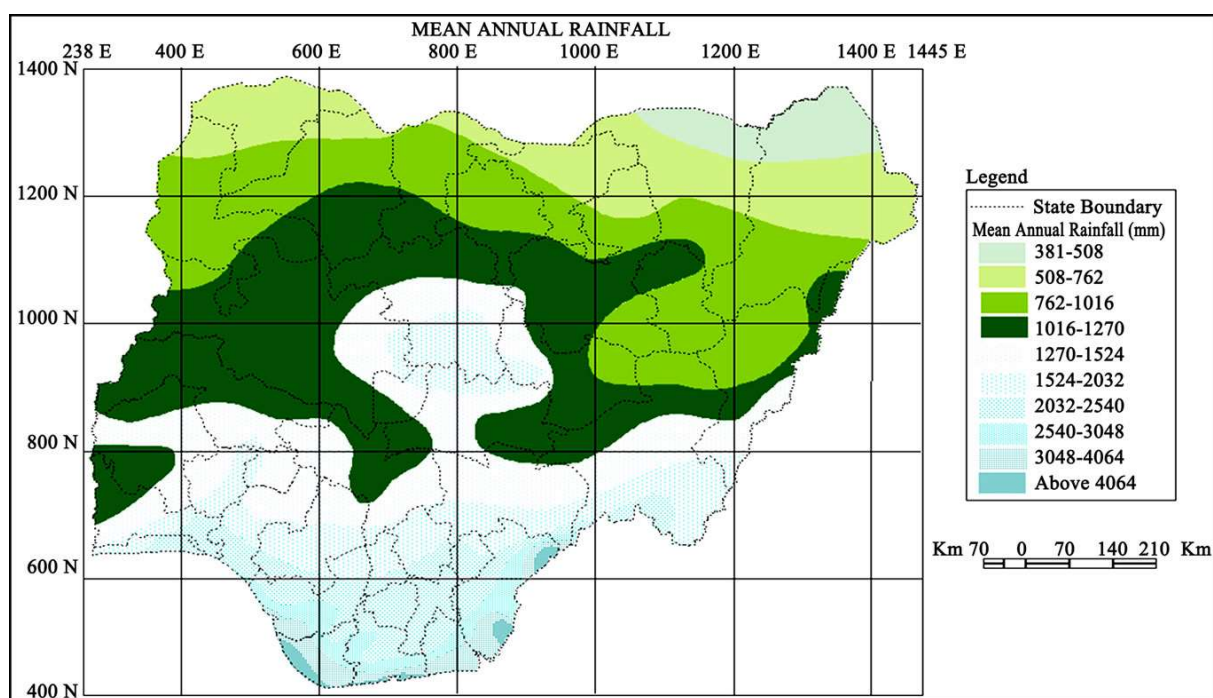


Figure 27. Map of Nigeria with the climate showing the mean annual rainfall [21].

3.3 Renewable – Hydrogen Systems

Unlike electricity, it is possible to store hydrogen in large quantities for relatively long periods of time. The use of hydrogen as part of an energy system is generally referred to as the hydrogen economy [22]. What makes the principle of utilising renewable technologies in the production of hydrogen via electrolysis advantageous, is the environmental friendly nature of it and the fact that water used in electrolysis (which

contains the target hydrogen) is abundant almost everywhere free of charge, and is in theory recyclable [22][23]. Of key interest, however, is the attraction of finding an efficient use for the excess energy generated when system supply outstrips demand. This is energy which otherwise might be wasted.

Recent applications of renewable technologies in the so-called hydrogen economy come in various configuration as follows;

- wind-hydrogen system
- solar PV – hydrogen system
- biomass –hydrogen systems
- hybrid wind, solar PV and hydro – hydrogen systems

Among the listed configurations, the method of most interest in this thesis is **the one that integrates only solar PV technology**. This is because solar energy resource potential is in abundance and is more predictable compared to other RE sources (e.g. wind).

3.3.1 Solar Photovoltaic Fundamentals

The term photovoltaic was coined from Greek word **photos** (light, of the light) and the name of the Italian physicist Alexandro **Volta** (1745 – 1825) who discovered the first functional electro-chemical battery and the unit of electricity – **Volt**. The photovoltaic (PV) effect is the electrical potential developed between two dissimilar materials when their common junction is illuminated with radiation by photons. Solar cells form the building block of photovoltaic system; its characteristics are analogous to the behavior of the p – n junction diode. Typically, photovoltaic materials are semi-conductor materials generally several square centimeters in size that produce electric charge (positive and negative charge) when exposed to sunlight. As light penetrates the photovoltaic material electrons are freed from the atoms into conducting states.

Generally, the choice of semi-conductor materials in photovoltaic applications are based on two basic factors; efficiency and costs. The most widely used semi-conductor material in PV technology is crystalline silicon, broadly divided into two categories; polycrystalline and monocrystalline silicon. Photovoltaic panels made using a

monocrystalline silicon are the most efficient PV technology, averaging 14% to 17% efficiency [24][25]. Polycrystalline silicon has lower efficiencies at 13% to 15% but have a lower cost per watt when compared to monocrystalline silicon [24][25]. Other semiconductors used in photovoltaic system are called thin-film technologies and they are made up of multi-junction materials and include; Gallium Arsenide, amorphous silicon and Copper indium-diselenide. These are less efficient PV technologies when compared to silicon materials, with typical efficiencies ranging from 4 – 8%, but are cheaper and can be manufactured in large area arrays [25]. Recent research activities mean that a high efficient solar cell will be possible in future. This has been demonstrated in the discovery of perovskite solar cells, which may achieve 20% efficiency [26].

These materials are referred as semiconductors because their electrical conductivity lies between the insulators and conductors. According to Fermi-Dirac statistics, the electrical conductivity of a semiconductor increases with temperature. To change the electrical conductivity of a semiconductor, it is usually doped with some impurities. For instance, silicon has the atomic number 14 and belong to the group IV elements, possessing four valence electrons. To change its electrical conductivity, one can introduce a group V element (phosphorous) as a donor atom into the silicon lattice, and the four valence electrons enters a bond with the neighboring atom, freeing the fifth electron which is weakly connected to the nucleus (the innermost shell of the atom). This is called n-type semiconductor.

Similarly, a p-type semiconductor is achieved by doping the silicon crystal with a trivalent element (boron), this leaves only three valence electrons making the bond incomplete, and for boron to attain a noble gas configuration, a movement of the neighboring electron into this open bond occurs and thus creates a positively charged '*hole*'. The trivalent atom is called an acceptor atom. In principle, the formation of a solar cell starts from bringing together these two doped semiconductor materials; n-type and p-type, and when this happens a p – n junction is formed. The structure of a solar cell can be represented as photodiode in its technical realization. **Figure 28** shows a solar cell with its doped front and back metallic contacts. An incident photon is absorbed by the cell and it generates an electron – hole pair. The energy of absorbed photons is transferred

to the electron – hole system of the material, creating charge carriers that is separated at the junction.

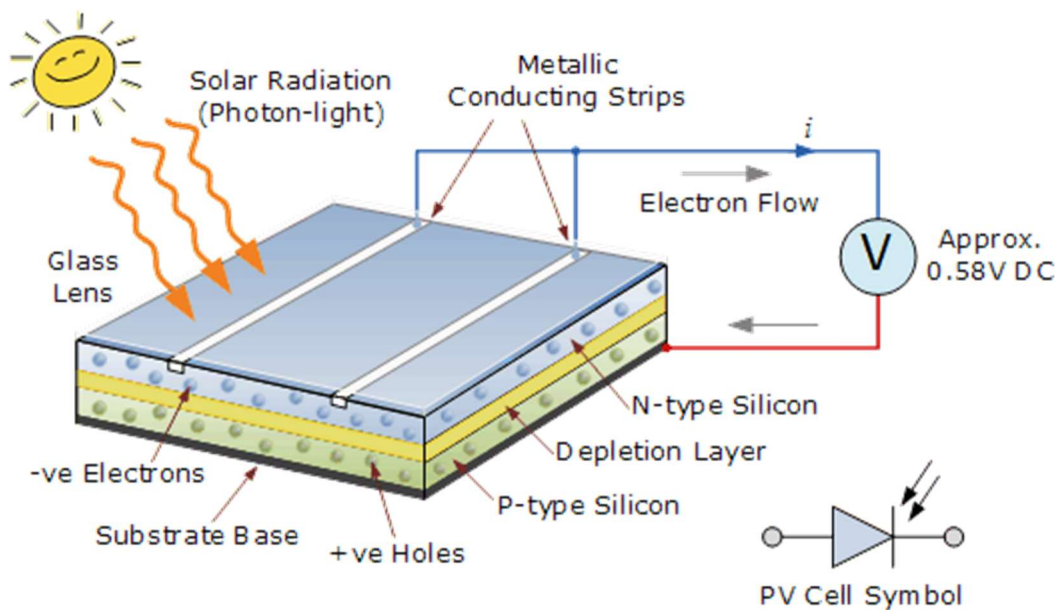


Figure 28. Solar photovoltaic characteristic configuration [27].

Thus, a difference in potential is created in the junction region and gets accelerated under the electric field, the generated electron is transported as current through a connected load (the electric bulb) [24]. The optical and electrical properties of a solar cell material (semiconductor) are critical in defining the efficiency of the absorption/generation process, and hence the cell itself. The two most important optical parameters that are considered when characterizing a solar cell material are the absorptivity of the material and the materials optical bandgap. While *absorptivity* refers to that fraction of incident photons at a given photon energy which the material can absorb to generate the electron – hole pairs, the *optical bandgap* of the solar cell material establishes the necessary energy threshold the incident photon can have to excite an electron from its bound state into a free state where it can participate in conduction. The larger the bandgap the more photon energy that is required for the solar cell to produce electric current. This is because a larger bandgap will make the material absorb only short wavelength of light and thus small photocurrent (current generated by photons). Conversely, the smaller the bandgap the more photocurrent the solar cell can produce but at a lower voltage. As an example, silicon has a bandgap

energy of 1.12eV, any impinging photon on the solar cell must have more than that amount of energy before it could excite electron to the conduction band [24]. From this it can be stated that photocurrent is directly proportional to solar irradiance. One of the challenges photovoltaic cell manufacturers face today is how to maximize the capture of photons, and in turn make the most of the captured photons (visible light particle) in the flow of current in the PV cell.

3.3.2 Photovoltaic Open Circuit Voltage and Short Circuit Current

Under full illumination, solar cell electrical performances are described using two important parameters namely; the open – circuit voltage (V_{oc}) and the short – circuit current (I_{sc}). The maximum voltage available from a solar cell is called the open – circuit voltage (V_{oc}), this occurs when the short – circuit current (I_{sc}) is equal to zero. The short – circuit current (I_{sc}) is the current through the solar cell when the voltage across the solar cell is zero. This is due to the generation and collection of light generated carriers. The short-circuit current is measured by shorting the output terminals and measuring the terminal current. **Figure 29** below illustrates the occurrence of maximum value for power at the points between the short – circuit current (I_{sc}) and the open – circuit voltage (V_{oc}). The voltage and current at this maximum point are denoted by V_m and I_m respectively.

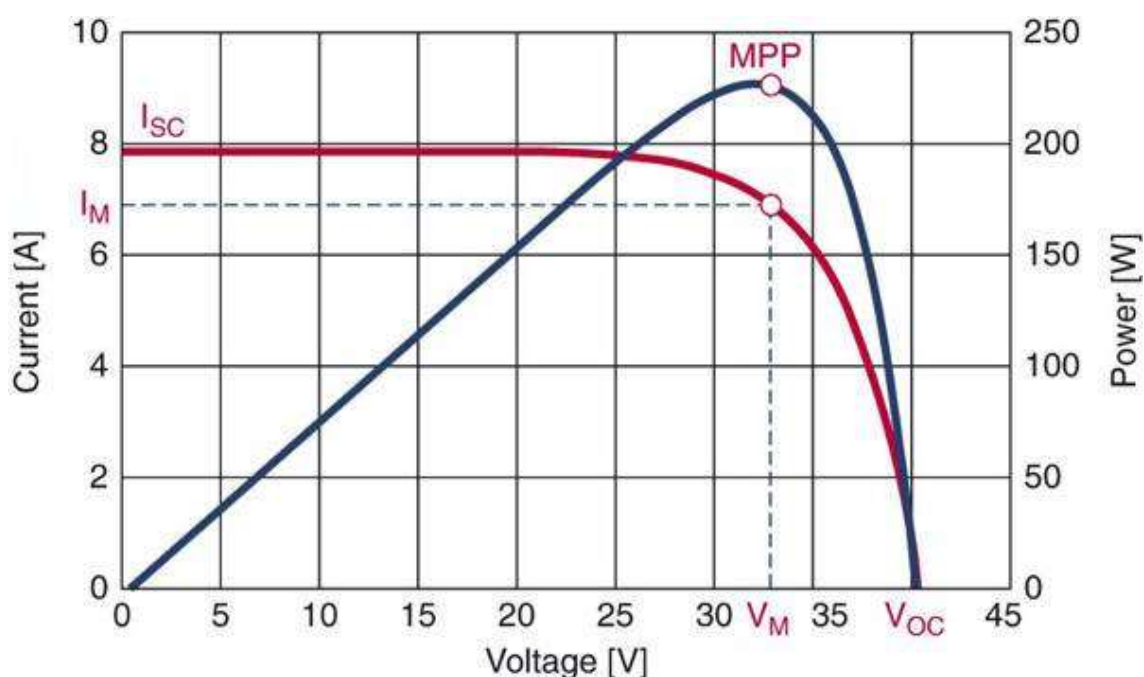
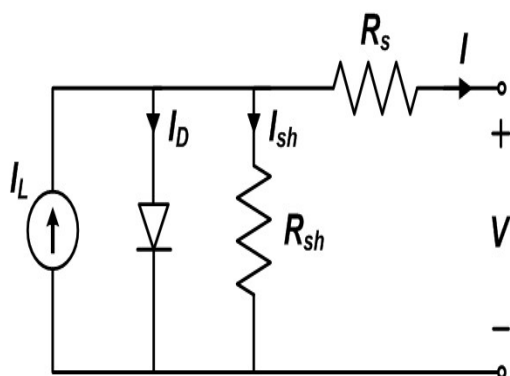


Figure 29. Photovoltaic characteristic curve showing the maximum power point [28].

3.3.3 Governing Equations of the Solar Photovoltaic – The Equivalent Circuit

The electrical behavior of a solar cell can be represented using a diode equivalent circuit as shown in **Figure 30**



Parameters

1. I_L = light generated current.
2. I_D = Diode current - voltage-dependent current lost to recombination.
3. R_{sh} = shunt resistance: this reduces the PV output, by increasing the incidence of leakage current.
4. R_s = series resistance: affects the PV output

Figure 30. circuit representation of the electrical behavior of solar cell.

Using Kirchhoff current law, the equivalent electrical equation has been formulated as follows; [24][25].

$$I = I_L - I_D - I_{sh} \quad (\text{Equation 1})$$

But the open circuit voltage of the solar cell is obtained when the load current = 0; therefore,

$$V_{oc} = V + IR_s \quad (\text{Equation 2})$$

From the diode Shockley equation, we obtain that the current through the diode is;

$$I_D = I_o \left[e^{\frac{qV_{oc}}{nkT}} - 1 \right] \quad (\text{Equation 3})$$

Where

- I_o = reverse saturation current (ampere)
- n = curve fitting factor (1 for an ideal diode)
- q = electron charge; 1.60211×10^{-19} coulombs
- k = Boltzmann's constant; $1.3806488 \times 10^{-23}$ J K⁻¹
- T = absolute temperature

$$\begin{aligned} \text{At } 25^{\circ}\text{C, } \frac{kT}{q} &= \frac{1.3806488 \times 10^{-23} \times (273 + 25)}{1.60211 \times 10^{-19}} \text{ V} \\ &= 0.02586 \text{ V,} \end{aligned}$$

Thus $nkT = 0.02568 \text{ V}$, this factor is described as the solar cell thermal voltage denoted by V_T .

Now, recall Ohms law which states that;

$$V = IR \quad (\text{Equation 4})$$

Then, the current through the shunt resistance is given by;

$$I_{sh} = \frac{V}{R_{sh}} \quad (\text{Equation 5})$$

Substituting equations 2, 3 and 5 into equation 1, we obtain the characteristic equation of a solar cell as;

$$I = I_L - I_o \left\{ \exp \left[\frac{q(V + IR_s)}{AKT} \right] - 1 \right\} - \frac{V + I R_s}{R_{sh}} \quad (\text{Equation 6})$$

Solar cells are low voltage devices; therefore, they are usually connected in series strings to yield useful voltage. The voltage produced depends directly on the irradiation incident on the cells. The combination of solar cells produces a solar module and combining a group of solar modules produces a solar panel, and the combination of solar panels produces a solar array.

3.3.4 Solar Panel

A PV solar panel is a group of several solar modules that are electrically connected in a series-parallel combination to generate electricity within defined current and voltage ranges [29]. **Figure 31** shows the modular solar array formation, which is produced by connecting several groups of this solar module in series – parallel format. By doing so the appropriate voltage and current characteristics are achieved. Modules can be connected in series to make a string, and when this string is connected in parallel format they form an array.

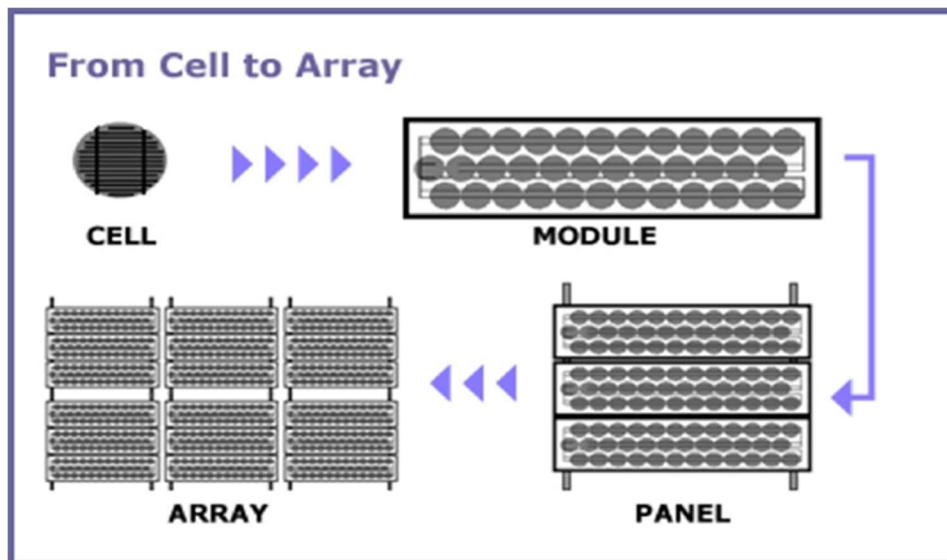


Figure 31. Solar array formation [29].

3.3.5 Photovoltaic Technology and the World – What is the Africa Stand?

In the past few decades, there has been a significant global shift from conventional means of electric power generation, as countries across the world have embraced renewable sources such as photovoltaic technologies. According to the International Energy Agency (IEA) PVS Report [30], since 2000 there has been a steady growth in world grid-connected solar PV installed capacity; this is shown in **Figure 32**, which depicts the world PV installed capacity from 2000 to 2016 [31].

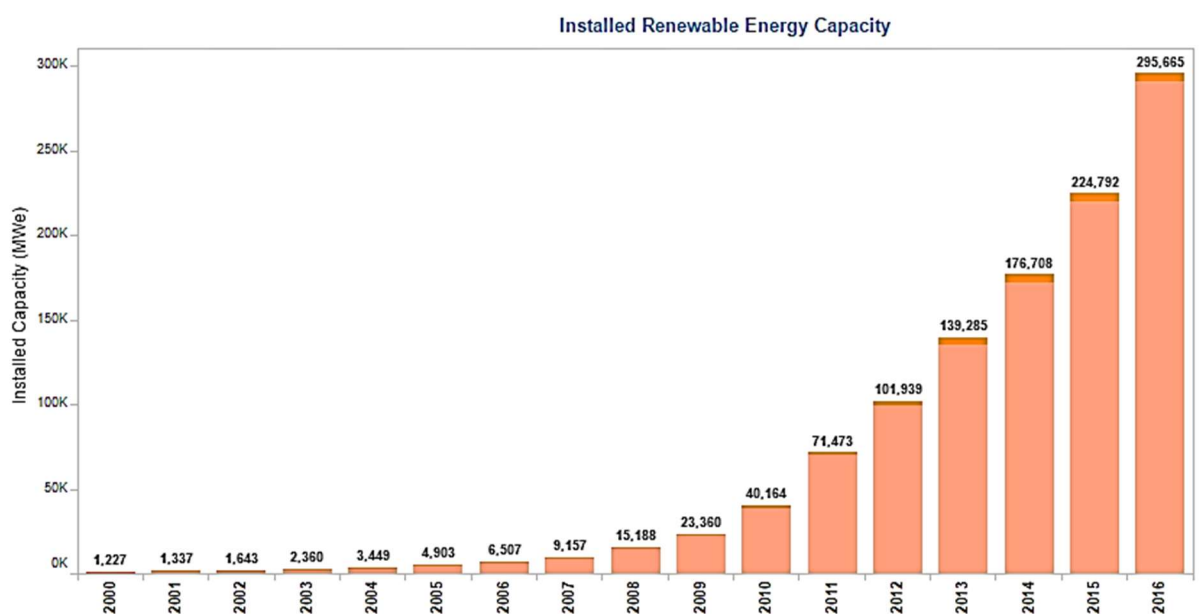


Figure 32. World photovoltaic installed capacity 2000 - 2016 [31].

By the end of 2010 about 40 GW of solar photovoltaic power system had already been installed globally. By way of illustration, this is equivalent to the average power demand of the UK. This grew to about 100 GW in 2012 and at the end of 2016 about 296 GW capacity of solar photovoltaic power system had been installed worldwide. This represents a remarkable 86 % growth between 2010 and 2016, reflecting the fact that tremendous improvements have been made in recent years on the viability of renewable energy sources. The progressive growth of PV can be put in perspective with plummeting prices in last few years. The share of this record level of world PV installations is split between Europe and Asia Pacific, with Africa having very little contribution. Europe and Asia represent the major markets, with Europe accounting for about 104 GW of the total installation and Asia some 140 GW. As of 2015, Germany was the leader in the world PV installations with about 40.9 GW installed capacity, but China's massive solar PV project at 77.43 GW [31] total installed capacity in 2016, means they overtook Germany and are currently the world leaders. Africa represents only 2.9 GW share of the global total installed capacity, at a time when other continents of the world are already producing at least 1% of their electricity needs with solar PV. This means that African governments need to change their current attitude and implement policy, plans and schemes to support the integration of renewables, especially solar PV, into the electricity generation mix of their respective countries.

3.3.6 Renewable Technology for Rural Electrification

Many factors must be considered before a renewable electricity project is implemented in island or other remote areas. The distance of the location from existing grid and the topography of the location are important in establishing whether a grid connection might be feasible economically or technically. The cost of grid connection to remote areas was estimated at USD10000/1km [32], which is prohibitively expensive. Renewable electricity becomes attractive in some areas where the costs of grid extension become too expensive [33].

Major advantages of solar PV power systems are:

- It has short installation time
- Modularity; the system economy is not strongly dependent on size; it is easily adaptable
- It has no moving parts so is silent (and robust)
- It requires little maintenance and has a relatively long lifespan
- When carefully designed its output matches with peak-load demands
- Solar PV power is highly mobile and portable
- It offers clean electric power generation that is free from GHG emissions
- Photovoltaic power systems do not incur fuel costs
- In terms of small scale applications such as in sunny remote locations, photovoltaic systems are cheaper and more viable than other alternatives [34].

The disadvantages of solar power system are;

- Intermittency in energy production: its high dependency on weather conditions means that PV systems are highly unpredictable in their energy performances
- High initial investment cost
- The requirement for a storage system to cover for those periods of low power output (night time and cloudy weather)
- Degradations in performance due to dust accumulation on the cell surface over time. However, this can be solved by frequent cleaning maintenance

The cost competitiveness of renewable electricity: The drop in oil prices starting from end of 2014 till 2016 is not representative of historical trends and the climate consequences associated with electric power generated from fossil fuels are now well understood and widely accepted. As at 2015, the cost competitiveness of renewable power generation has improved greatly when compared to the cost in 2008. As of 2008, the average levelised cost of energy (LCOE) of residential solar photovoltaic systems was

estimated at 0.38 – 0.68 \$/kWh [35]. Germany as an exemplar PV adopter with “the most competitive small-scale residential rooftop systems in the world. Germany’s residential system costs have fallen from just over USD 7200/kW installed capacity in the first quarter of 2008 to USD 2200/kW in the first quarter of 2014” [35]. However, installed costs of both solar photovoltaic and wind power have continued to fall as tremendous improvements has been made in their efficiency of build, with economies of scale significantly lowering the cost of electricity from these sources. On a regional scale for instance, in 2015 the levelised cost of ‘utility-scale solar PV’ electricity (LCOE) fell as low as 0.11 and 0.12 \$/kWh in North and South America, the highest was in Central America with 0.36 \$/kWh [36]. In Africa and Asia, the LCOE of utility-scale solar PV stood at \$0.20 kWh and 0.18 \$/kWh respectively compared to the 0.10 \$/kWh costs of fossil fuel as depicted in **Figure 33**. If the costs of CO₂ emissions are added the combined costs of fossil fuel power may reach up to 0.13 \$/kWh [36].

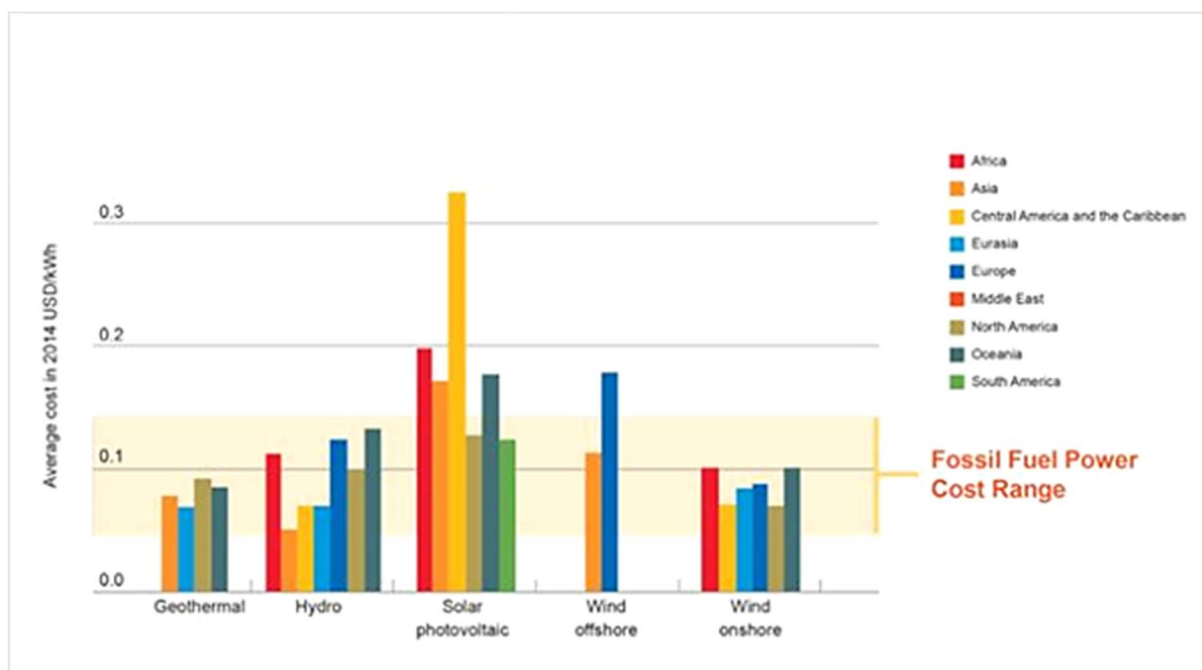


Figure 33. Cost competitiveness of renewables as at 2015 [37][36].

3.4 Solar – Hydrogen Storage; the Technologies

The physical basis of hydrogen production and storage technology relevant to this thesis is the electrolysis of water. This section explores electrolysis in some detail.

3.4.1 Electrolysis

The principle by which electricity is used to decompose water into its constituents of hydrogen and oxygen is called electrolysis, and this process is made possible using a device called an electrolyser (**laboratory example pictured in Figure 34**). This device is an electrolytic cell where the oxidation – reduction reactions occur to decompose water. Ideally, water in its pure form is non-conductive, and therefore an electrolyte in the form of acid (HCl), base (NaOH) or salt (NaCl) is usually added to increase its conductivity. These electrolytes react with the water and splits it into negative and positive ions. Industrial electrolysers usually consist of more than one electrolyte [16].



Figure 34. Laboratory size electrolyser [38].

A simple electrolyser is the type invented in 1866 by August Wilhelm von Hofmann called Hoffman's voltammeter (**shown in Figure 35 below**). This consists of anode and cathode electrodes inside a container. When direct electric current is passed through the voltammeter hydrogen gas is produced at the cathode (the negatively charged electrode) and oxygen gas is produced at the anode (the positively charged electrode).

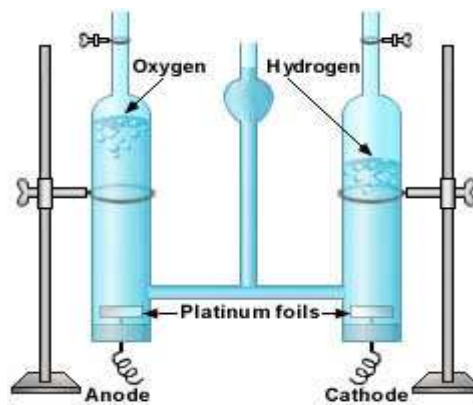
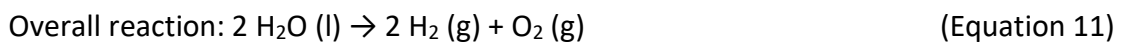
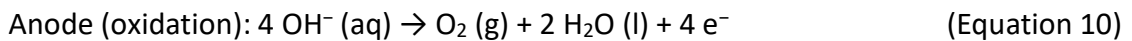
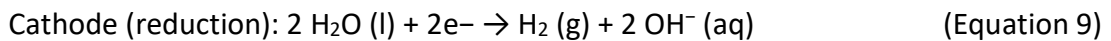
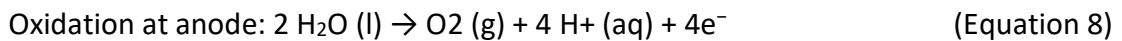
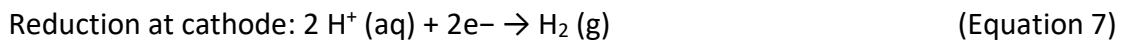


Figure 35. Hoffman voltammeter [39].

The general equation representing the reactions at the electrodes are as follows;



In principle, electrolyzers are normally constructed by connecting several cells in series to increase its productivity. This process also helps to evenly distribute the voltage drop across the cells. The efficiency of an electrolyzer is normally expressed in kWh/Nm³H₂ and 1 Nm³ (one normal cubic meter) of hydrogen gas has a higher heating value (HHV) of 3.54 kWh. This implies that for an electrolyzer to be considered 100% efficient in its electricity – hydrogen conversion, its input requirement must be 3.54 kWh/Nm³ H₂ [40][41]. The efficiency of electrolysis can be calculated as the ratio between the chemical energy contained in the yielded hydrogen and the electric power employed to the process [41]. In RES applications, the sizing of an electrolyzer is ideally determined using the maximum excess power that the renewable energy systems can produce. This is achieved by considering efficiencies of the power conditioning devices associated to the electrolyzer, (e.g the dc/ac converter), and the auxiliary power consumptions, for example the compressors.

3.4.2 Types of Electrolysers

Electrolysers (listed in **Table 17**) are generally described based on the kind of electrolytic solution used and its technology. Basically, electrolysers are key component of renewable-hydrogen systems and they account for a substantial portion of the cost of such systems. Three types of electrolysers commonly in use are;

1. Alkaline electrolyser
2. Proton Exchange Membrane Electrolysers
3. Solid – Oxide Electrolyser

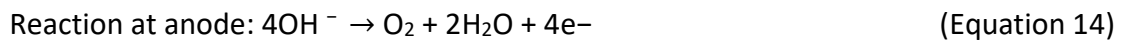
Types	Alkaline Electrolyser	PEM Electrolyser	Solid Oxide Electrolyser
Electrolyte/Membrane	Potassium hydroxide (KOH)/NiO	Solid, proton exchange polymer membrane (Nafion)	a) Zirconia ceramics (0.91ZrO ₂ -0.09Y ₂ O ₃) b) Zirconia Oxide ceramics
Electrodes/Catalyst	Anode: Ni/Ni alloys, metal oxides Cathode: Steel + Ni / Ni-Co	Anode: Graphite-PTFE + Ti / RuO ₂ , IrO ₂ Cathode: Graphite + Pt / Pt	Anode: Ceramics (Mn, La, Cr) / Ni Cathode: Zr & Ni cermets / CeOx
Global Reaction	Anode: $4HO^-(aq) \rightarrow O_2(g) + 2H_2O(l) + 4e^-$ Cathode: $4H_2O(l) + 4e^- \rightarrow 2H_2(g) + 4HO^-(aq)$	Anode: $6H_2O(l) \rightarrow O_2(g) + 4H_3O^+(aq) + 4e^-$ Cathode: $4H_3O^+(aq) + 4e^- \rightarrow 4H_2(g) + 4H_2O(l)$	a) Cathode: $2H_2O(g) + 4e^- \rightarrow 2H_2(g) + 2O^{2-}$ Anode: $2O^{2-} \rightarrow O_2(g) + 4e^-$ b) Anode: $2H_2O \rightarrow 4H^+ + O_2(g) + 4e^-$ Cathode: $4H^+ + 4e^- \rightarrow 2H_2(g)$
Operational Temperature	50 – 100 °C	80 – 100 °C	800 – 1000 °C
Operational Pressure	3 – 30 bars	1 – 200 bars	??
Capacity	10 – 200 Nm ³ /h H ₂	0.01 – 10 Nm ³ /h H ₂	1 – 10 Nm ³ /h H ₂
Conversion Efficiency	75 – 95 %	80 – 90 %	80 – 90 %
Operational Life	15 – 20 yrs	15 – 17 yrs	??
State of Development	Marketed	Marketed	Research

Table 17. Types of electrolyser and their characteristics [42].

3.4.3 Alkaline Electrolyser

Alkaline electrolysers, as shown in **Figure 36** are composed of an electrolytic cell in which two electrodes are immersed in a liquid alkaline electrolyte solution of potassium hydroxide KOH of around 20 – 30 % concentration at approximately 85°C, [43][44]. Alkaline electrolysers operate at electric current density in the range of 0.2 – 0.4 A/cm² with an efficiency ratio between 75 - 85% [40]. Current density refers to current per

surface of electrode area of the electrolyser. The following electrochemical reactions take place inside the alkaline electrolysis cell:



Three major issues are normally associated with alkaline electrolysers. These include low partial load range, limited current density and low operating pressure. First, the diaphragm does not completely prevent the product gases from cross-diffusing through it. The diffusion of oxygen into the cathode chamber reduces the efficiency of the electrolyser, since oxygen will be catalysed back to water with the hydrogen present on the cathode side [43]. A porous diaphragm, permeable to OH^- ions and water allows water and the ionic electric current to pass through while keeping the hydrogen and oxygen gases from mixing with each other. This enables the system to store the two gases separately [43].

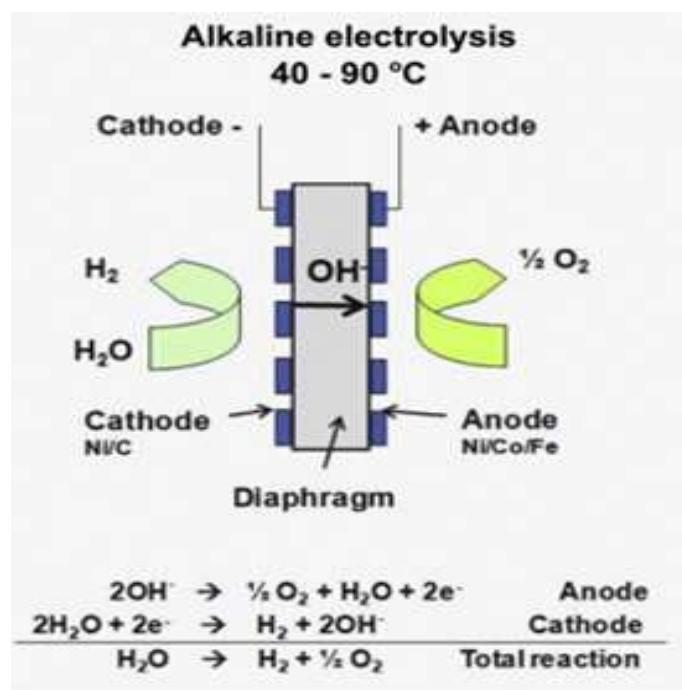


Figure 36. Operational principle of an alkaline electrolysis, showing the electrode reactions [43].

3.4.4 Solid Proton Exchange Membrane (PEM)

The potential problems associated with the alkaline electrolyzers can be addressed using proton exchange membrane electrolyzers. In this, the electrolysis of water takes place in a cell containing a solid polymer electrolyte (SPE). Unlike alkaline electrolyser, in SPE, the electrolyte is contained in a thin solid ion-conducting membrane. This electrolyte (SPE) bears three responsibilities in the reaction process as follows;

1. The conduction of protons
2. The separation of gases
3. The electrical insulation of the electrodes [43].

In PEM electrolyser the hydrogen ion transfers from the anode side of the membrane to the cathode side, this process effectively separates the hydrogen and oxygen gases. Oxygen is produced at the anode side and hydrogen is produced at the cathode. Most commonly used PEM membrane is a Nafion made by DuPont [22][43]. As the reaction proceeds the H₂ gas is channelled separately from the cell stack and is captured, while O₂ gas remains behind in the water (see **Figure 37** below). Oxygen that accumulates in the separation tank can be removed from the system by recirculating the water [45]. 39.4 kWh per kilogram is the energy required at the theoretical efficiency limit of any water electrolysis. This efficiency limit can only be achieved by PEM electrolyzers operating at low current density. However, at low current densities, the quantities of hydrogen produced are relatively small, resulting in very high capital costs per unit hydrogen produced [22]. PEM electrolyzers have the capacity to operate at current densities above 1.6 A/cm² [22][46]. However, its cell stack efficiencies decrease at higher current densities [22][46].

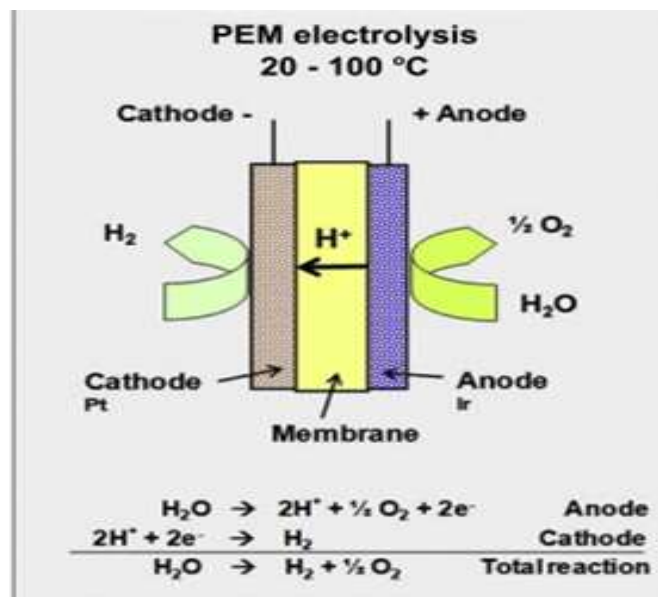


Figure. 37 PEM electrolyser with the electrode reactions [43].

3.5 Hydrogen Storage Mediums and Methods

To ensure sustainability of hydrogen as an energy carrier in hybrid – renewable hydrogen energy systems, the hydrogen produced through the processes mentioned in **section 3.4** should be stored in such a way that it could occupy a smaller volume as efficiently and conveniently as possible for future use. However, there is a tension between compactness of storage and system efficiency associated with compression processes. The most commonly employed method of hydrogen storage is as a compressed gas (the simplest method). Other methods of hydrogen storage are solid storage – in metal hydrides, and cryogenic hydrogen storage – liquid hydrogen. Fuel's energy content is normally stated in two distinct heating values, namely the higher heating value (HHV) and lower heating value (LHV) [47]. **Table 18** illustrates the energy content of hydrogen gas. The HHV of 1 kg of hydrogen gas is 142 MJ (39.4 kWh) at -286 kJ/mol and the LHV is 120MJ (33.3 kWh) at -242 kJ/mol [48]. The lower heating value (LHV) at 33 kWh/kg is the heat of formation of steam.

Lower and Higher Heating Values of Gas (LHV and HHV)			
Fuels	Lower Heating Value (MJ/kg)	Higher Heating Value (MJ/kg)	Density (g/ft ³)
Gaseous fuels at stp			
Natural gas	47.14	52.23	22
Hydrogen	120.21	142.2	2.55
Still gas (in refineries)	46.9	50.95	32.8

Table 18. Higher and lower heating values of gases [49].

Hydrogen has a poor energy density by volume (0.08988 g/l in gaseous state, i.e. 7 % of the density of air; 70.8 g/l as liquid (at 253°C), i.e. 7% of the density of water; and 70.6 g/l as solid (-262°C) [41]. For this reason, it must be compressed to very high pressures to store a sufficient amount of hydrogen for many practical applications. Two types of compressor available to raise the pressure to at least 15 MPa are: (i) reciprocating piston compressors and (ii) diaphragm compressors [22]. Usually compression of hydrogen gas is carried out in multiple stages with the first stage providing a pre-pressurisation from 1-atm to several atmospheres. In this process, the pressure level can be selected based on the maximum permitted pressure the storage tank can withstand, but is relatively energy intensive [41]. High-pressure hydrogen is stored in thick-walled tanks (mainly of cylindrical or quasi-conformable shape) made of high strength materials to ensure durability [41]. Hydrogen is a carbon free energy carrier, therefore its wide utilization as an energy storage medium will go a long way in contributing to the global fight for carbon-free power generation, provided that the input energies for hydrolysis and compression are from renewables. The next section discusses some hydrogen energy storage technologies suitable for off-grid or micro – grid renewable energy generation.

3.5.1 Gaseous Hydrogen Storage

The volumetric density of hydrogen gas under normal conditions is 0.0823 kg/m³ with a correspondingly low energy density. In view of this some work needs to be done on the hydrogen to store it compactly in small pressurised tanks. Standard pressures achievable in the current literature are 350 and 700 bar [49] when applied to industrial scale hydrogen storage. The challenges and difficulties associated with increasing stored energy density are the energy required for the compression of the gas, the cost involved, the storage cylinders, and the safety risks [22]. For domestic applications, hydrogen storage requires pressure at less than 30 bar, and ultimately between 10 bar – 17 bar.

3.5.2 Liquid Hydrogen Storage

When hydrogen gas is cooled below its boiling point (temperature of -253°C) it liquefies, with this process brought about using a device called a liquefier. The liquid hydrogen has a high purity and high storage density [22]. The high tendency of liquid to evaporate

implies that the liquefied hydrogen must be stored in a well-insulated tank of a dual-walled stainless-steel vessel with vacuum super-insulation between the inner and the outer vessel [22]. The shape and volume of the storage tank used affects the rate of the evaporation of the liquid hydrogen, specifically a spherical tank is normally preferred. This is because the evaporation rate is proportional to surface to volume ratio and a linear function of the total heat flux [22]. The losses due to evaporation and boil-off can be minimised by increasing the volume of the tank. The energy requirement for hydrogen liquefaction is a downside of liquid hydrogen storage, even though it has a much higher volumetric capacity than gaseous hydrogen at (0.070 kg/L compared to 0.030 kg/L for 700 bar gas tank) [47][48]. This constitutes a loss in the overall system as the energy utilised in the liquefaction cannot be recovered. This seriously reduces the final efficiency of the system, about 30% of energy is lost when liquid hydrogen is produced in a large scale and 10% of energy is lost at medium scale production [49]. Therefore, it can be stated that the ideal work for the liquefaction of hydrogen from 300K at 1 bar to 20K at 1 bar is equal to an electric energy requirement of 3.9 kWh/kgLH₂ [22], but if the hydrogen gas is compressed at 30 bar, this energy requirement may decrease to about 2.8 kWh/kgLH₂ [22].

3.5.3 Solid - Hydrogen Storage

Hydrogen is the lightest and one of the most abundant elements on earth, but it does not exist in its natural form. The gas is found in combination with other elements, a feature which makes it easier for it to react with some metal atoms (host lattice) to form metal-hydride (MH) compounds. Under moderate temperature and pressure, hydrogen forms metal-hydride with light metals such as Li, Be, Na, Mg, B and Al. The process involves the metallic absorption of hydrogen gas at constant pressure, which results to the hydrogen atoms (H₂) contributing their electrons to the band structure of the metal, this in turn, exothermically dissolves the hydrogen into the metal. The desorption of hydrogen involves the thermal dissociation or release of the hydrogen atom from the metal. The chemical behaviour or physical characteristics of every alloy or metal used in solid hydrogen storage has a direct link with the value of hydrogen it could store [50]. An optimum hydrogen storage material should be able to store and release its hydrogen content at minimal application of temperature, pressure, energy and at lower cost [50],

and have high hydrogen capacity per unit mass and unit volume [51]. Another requirement for a good metal-hydride renewable hydrogen storage is the perfect charge and discharge cycle [52]. The following equation defines the reaction process involved in forming a metal – hydride [51];



Where M = metal and x = 1,2,3...

Because metal – hydrides have the advantage of higher hydrogen storage density compared to other methods previously mentioned (liquid and gas) it has been a subject of research interest in the area of hydrogen storage materials in recent years [53][54][55].

3.6 Fuel Cell

Fuel cells are electrochemical devices that can utilise the hydrogen gas produced via the electrolyser described in **section 3.4.1** to generate electricity. In a fuel cell, a spontaneous reaction involving oxygen as the oxidiser (anode) and hydrogen (cathode) as the fuel takes place. The result of this reaction process is water, electricity and heat. Fuel cells play a significant role in the hydrogen energy concept. In the cell reaction, hydrogen diffuses at the anode by penetrating through the electrode pores. A catalytic reaction enables the adsorbed hydrogen to be ionized and then passed through the solution where it releases an electron at the electrode [22].

The equation describing the reaction process is as follows;



Other means by which hydrogen can be utilised to produce electricity is through direct combustion in internal combustion engines, but fuel cells have a potential for being more efficient and more silent. Fuel cells types are categorized per the kind of electrolyte they contain and their ranges of operating temperature [22].

Briefly, the main types of fuel cells currently in use are;

- **Alkaline fuel cell** – mainly contains potassium hydroxide in a water solution with the operating temperature between 60–100°C.

- **Phosphoric acid fuel cell** – its electrolyte is phosphoric acid and it can be operated at temperatures up to 200°C, and has a service life in the order of 40,000 hours.
- **Proton exchange membrane fuel cell** – contains carbon electrodes separated by a polymeric membrane of chlorinated sulphuric acid and operates at temperatures between 80 – 120°C.
- **Molten carbonate fuel cell** - carbonated alkaline liquid solution (mainly KCO_3) and the cell operation temperature is between 600 – 850°C.

The energy sizing of a fuel cell can be determined by identifying the peak load power required. It is finalised by considering the efficiencies of the power conditioning devices associated to the fuel cell, (e.g. the DC/AC converter), and the auxiliaries' consumption. This research is not concerned with utilising the produced hydrogen in fuel cell for electricity and so detailed descriptions and explanations of the operations of each of the mentioned fuel cell types is not considered further.

3.7 Examples of Existing Renewable - Hydrogen Systems and Some Research Activities

The use of hydrogen energy production from renewables- based electrolysis has been researched in some detail in recent years, and several renewable energy systems with hydrogen storage plants have been discussed in the literature. Santarelli, Michele and Sara [56] have demonstrated a hydrogen storage-based renewable electricity project in an isolated residential building in Valle dell'Euglio-Locana, Italy serving an electricity demand of 3 MWh/yr during a complete year of operation. **Figure 38** shows the configuration they used in the research. The system was comprised of a 6.37 kW PV array, three 1 kW electrolyzers placed in parallel formation, a battery pack for short term energy supply, a pressurized gas storage tank, and a 3 kW proton exchange membrane fuel cell (PEMFC) operating at 80 °C. The hydrogen stored was utilised in a PEM fuel cell to supply power when there was an insufficient renewable generation for the electricity needs of the user. The basic aim of their analysis was to highlight the differences between the systems using different renewable energy sources. They proposed that wind-hydrogen energy storage system needs an enormous wind generator (30 kW) as

compared to the capacity required for the solar PV. This is partly a consequence that power productions from the PV can be less variable and more predictable when compared to wind power, and this shows the if a PV system is properly sized and installed in a location that has no seasonal weather variation (for example day length), a high energy performance from the PV is possible.

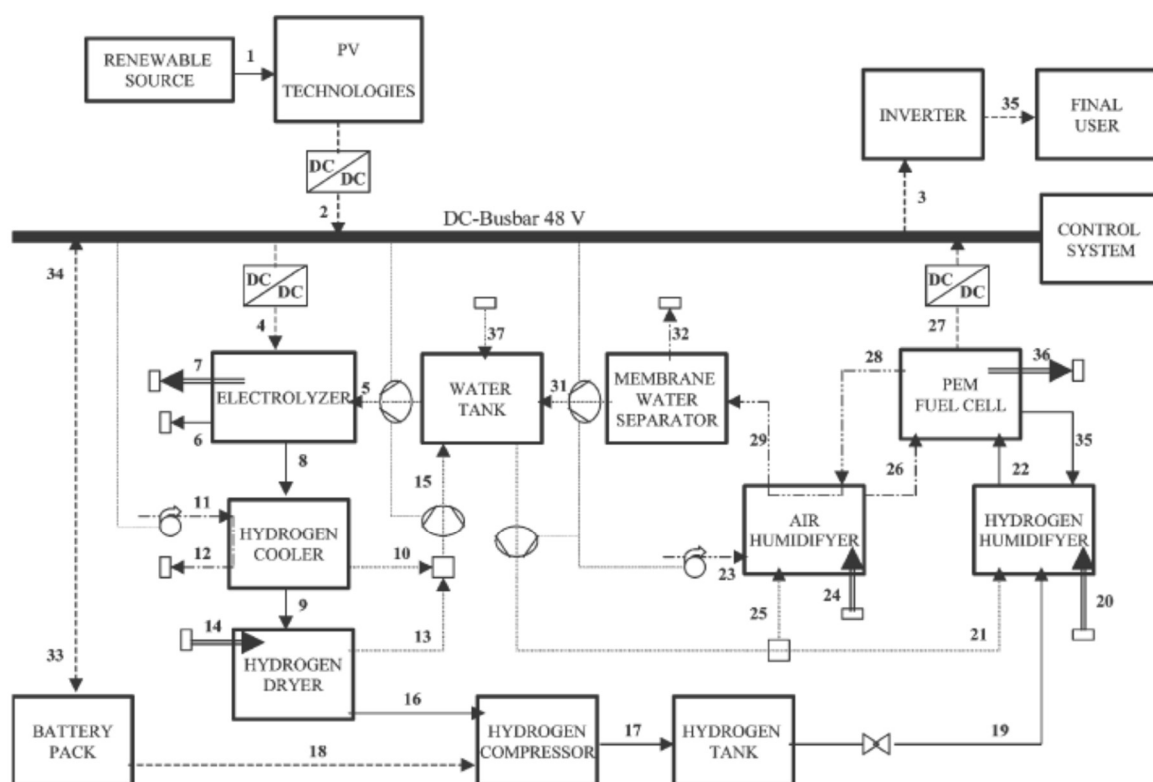


Figure 38. RE based hydrogen production plant [56].

Muneer, Asif and Munawwar [57] describes a modular energy network in India based on a solar – hydrogen system. After thorough investigation of the solar energy resource and estimated performance of 1m^2 PV area over 5 years, they found that an energy network aimed at connecting six major cities in India with a solar electricity grid could be a viable option, and that in future, utilising the excessive solar electricity production in a hydrogen storage – fuel cell arrangement may improve the energy capture, giving the plummeting price trend of solar electricity.

In 2012 Africa's first wind-hydrogen system was launched by PURE energy, a UK based renewable energy and energy storage company. They installed a hydrogen storage system in Morocco to capture excess wind energy via electrolysis. This project was

completed in collaboration with Saharan Wind Inc and Al Akhawayn University in Morocco. The system consisted of a hydrogen electrolyser, hydrogen storage tanks and a fuel cell [58]. However, it cannot be ascertained whether the system is still functional at the time of writing this thesis. Agbossou et al [59], have reported a stand-alone RE system based on hydrogen storage installed in at the Hydrogen Research Institute (HRI) in Canada.

According to their report, the system consisted of a 10 kW wind turbine generator, 1 kWp PV array, a 5 kW electrolyser and 5 kW fuel cell utilised to produce electricity on demand. The excess available renewable energy was fed into an electrolyser (with 71% efficiency at 55°C) to produce hydrogen and then pressurised using an external compressor. However, because of lack of RE sources in their location owing to climatic conditions, they have used a 10-kW programmable power source to simulate the typical intermittent power output patterns for days with no RE power available. They recorded the 6-hour daily operation of the system from December 3rd, 2001 to April 17th, 2002. Based on the success they have achieved in the work, they summarised with a proposal that a system of that kind would be useful in remote power applications.

In Europe, small islands are proving to be excellent test beds for renewable energy electricity since connection of the islands to the continental European energy network can be prohibitively expensive. The literature discusses possibilities of utilising an energy storage system with renewable electricity in these areas. Neven and Maria [60] have proposed a RE-hydrogen storage system at an island in Porto Santo Portugal inhabited by 5000 residents. The system was based on what they called H₂RES model. This used an hourly time series analysis of electricity demand, wind potential, solar insolation and precipitation. They designed their storage module such that any input into the storage system that exceeded the storage capability of the storing facility would be diverted (rejected or dumped). The efficiency of the storage facility was around 50 - 60% for the electrolyser. According to the authors, in 2001 the 28.4 GWh energy demand of the island was mostly supplied from a thermal source (26.1 GWh). The only renewable source mentioned in the project was wind energy which was provided by a combination of 1.1 MW Vestas wind turbine and 2.9 MW_p solar PV. They observed that when the wind turbine operated at full rated power there was an over-supply. They concluded

that the potential solution to this problem was introduction of a hydrogen storage and generation system. They modelled such a renewable – hydrogen system using two scenarios. In one scenario, a peak shaving technique was utilised with only wind as a renewable source. In the other scenario, a wind – solar hybrid mix was utilised and their results shows that while wind – solar mix might be more effective the 100% wind system would be more cost effective.

At West Beacon Farm, in Leicestershire, in UK [61], a stand-alone renewable-energy system employing a hydrogen-based energy storage system was commissioned in 2006 (HaRI project). This is shown schematically in **Figure 39**. The system consisted of 13 kW solar PV, a 1 kW cross-flow hydro turbine and 2.7kW Turgo hydro turbine, and two 25kW wind turbines. The system was installed to supply both single and three-phase power to a residential house and a set of offices. The hydrogen storage tanks of 22.8m³ capacity were installed. These were rated for up to 137bar, which gives a maximum storage of 2856Nm³ hydrogen gas. Two fuel cells based on PEM rated 5 kW and 2 kW totalling 7 kW capacity was also installed to convert the hydrogen gas into electricity. They also reported an electrolyser rated at 34kW at 25 bar which can produce up to 8 Nm³ of hydrogen gas per hour [61]. Ultimately, electrolysers undergo some degradations when they are subject to frequent ON and OFF cycling, to avoid this problem, they mentioned that a 120 kWh Zebra battery manufactured by Beta batteries was installed to provide steady power to the electrolyser, they quoted that the energy density of the battery is approximately three times that of lead acid battery (100 Wh/kg).

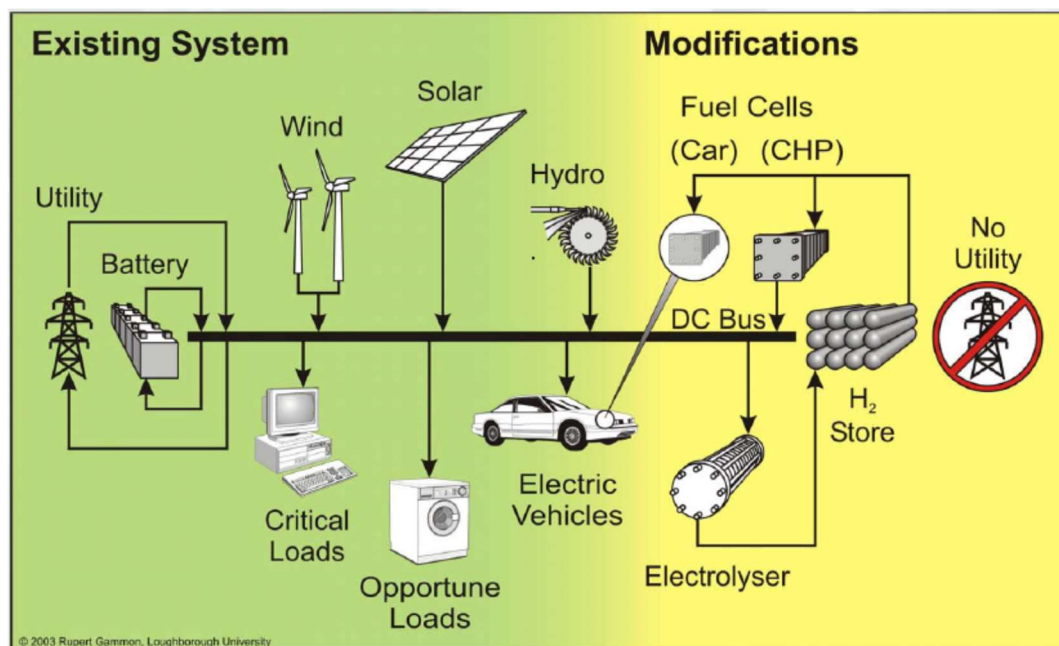


Figure 39. Stand-alone renewable-energy system employing a hydrogen-based energy at West Beacon Farm, in Leicestershire, in UK [61].

This project is a typical example of a hybrid RES on a scale that can be applied to remote locations in Nigeria. The summary of existing renewable – hydrogen systems is presented in **Appendix 4** with specific comments on the configurations of the systems. It is strongly recommended that at the initial stages of the design process appropriate power performance measurements are carried out using a monitoring system. This facilitates critical decisions over the choice of the system sizes and configurations and is the subject of **chapter four**.

3. References

1. Energy storage technologies for wind power integration, Université Libre de Bruxelles Faculté des Sciences Appliquées Service BEAMS groupe Energie March 2010.
2. Dunlop, James P. "Batteries and charge control in stand-alone photovoltaic systems: Fundamentals and application." Sandia National Laboratories (1997).
3. Dell, Ronald M., and David AJ Rand. "Energy storage—a key technology for global energy sustainability." *Journal of Power Sources* 100.1 (2001): 2-17.
4. Energy storage opportunities and challenges: A west Coast perspective white paper, 2014.
5. Kemsley, R.H., McGarley, P., Wade, S. and Thim, F., 2011, September. Making small high-penetration renewable energy systems work—Scottish Island experience. In *Renewable Power Generation (RPG 2011)*, IET Conference on (pp. 1-7). IET.
6. B.E Conway, 1999; *Electrochemical Supercapacitors Scientific Fundamentals and Technological Applications* ISBN 978-1-4757-3058-61.
7. Logerais, Pierre-Olivier, et al. "Study of Photovoltaic Energy Storage by Supercapacitors through Both Experimental and Modelling Approaches." *Journal of Solar Energy* 2013 (2013).
8. Glavin, M. E., and W. G. Hurley. "Ultracapacitor/battery hybrid for solar energy storage." *Universities Power Engineering Conference, 2007. UPEC 2007. 42nd International*. IEEE, 2007.
9. Medina, P., et al. "Electrical Energy Storage Systems: Technologies' State-of-the-Art, Techno-economic Benefits and Applications Analysis." *System Sciences (HICSS), 2014 47th Hawaii International Conference on*. IEEE, 2014.
10. Online available at <http://www.velkess.com/> accessed on November 2016.
11. Online available at <http://phys.org/news/2013-04-velkess-flywheel-flexible-energy-storage.html> accessed on November 2016.
12. Online available at <http://www.scientificamerican.com/article/new-flywheel-design/> accessed on November 2016
13. Digikey, Maximizing the Output from Solar Modules; Online available at <https://www.digikey.com/en/articles/techzone/2013/dec/maximizing-the-output-from-solar-modules> accessed on 13/11/2016.

14. Online available at <http://www.imeche.org/news/project-profile-flywheel-energy-storage>.
15. Online available at <http://www.tva.gov/power/pumpstorart.htm> accessed on [December 2016](#).
16. Gabriele Zini, Paolo Tartarini: Solar Hydrogen Energy Systems, Science and Technology for the Hydrogen Economy.
17. Online available at http://www.bbc.co.uk/bitesize/standard/physics/energy_matters/generation_of_electricity/revision/3/ accessed on 05/072017.
18. Verne, Jules. *The mysterious island*. Penguin, 2004.
19. Rodrigues, E. M. G., et al. "Energy storage systems supporting increased penetration of renewables in islanded systems." *Energy* 75 (2014): 265-280.
20. Online available at http://www.geog.ox.ac.uk/research/climate/projects/undp-cp/UNDP_reports/Nigeria/Nigeria.hires.report.pdf accessed on [December 2016](#).
21. M Rafee, Majid. "X-Raying rainfall pattern and variability in Northeastern Nigeria: impacts on access to water supply." *Journal of water resource and protection* 2010 (2010).
22. Leon, Aline. *Hydrogen technology: mobile and portable applications*. Springer, 2008.
23. Twidell, John, and Anthony D. Weir. *Renewable energy resources*. Taylor & Francis, 2006.
24. Mertens, Konrad. *Photovoltaics: Fundamentals, Technology and Practice*. John Wiley & Sons, 2013.
25. Messenger, Roger A., and Jerry Ventre. *Photovoltaic systems engineering*. CRC press, 2010.
26. Online available at <http://science.sciencemag.org/content/345/6196/542.full> accessed on [31/08/2017](#).
27. Electronic tutorials; Online available at <http://www.electronics-tutorials.ws/diode/bypass-diodes.html> accessed on [02/11/2016](#).
28. Digikey, Maximizing the Output from Solar Modules; Online available at <https://www.digikey.com/en/articles/techzone/2013/dec/maximizing-the-output-from-solar-modules> accessed on [13/11/2016](#).
29. Patel, M.R., 2005. *Wind and solar power systems: design, analysis, and operation*. CRC press.

30. PVPS, I., 2012. Trends in photovoltaic applications. Survey report of selected IEA countries between 1992 and 2011. Report IEA-PVPS T1–21.
31. IRENA: Online available at <http://resourceirena.irena.org/gateway/dashboard/?topic=4&subTopic=16> accessed on 15/03/2017.
32. Wade, H.A., 2003. Solar photovoltaic project development. Unesco.
33. Onwe C.A. Plan for the development of off-grid electricity in Nigeria rural area which takes into account climate change issues; MSc Thesis 2011.
34. Online available at <http://www.vaclavsmil.com/wp-content/uploads/smil-article-ieee-20120700.pdf> accessed on December 2016.
35. Online available at http://www.irena.org/documentdownloads/publications/irena_re_power_costs_2014_report.pdf accessed on November 2016.
36. PVPS, I., 2012. Trends in photovoltaic applications. Survey report of selected IEA countries between 1992 and 2011. Report IEA-PVPS T1–21.
37. Renewable energy world online available at <http://www.renewableenergyworld.com/bg/geothermal-energy-association/blog/geothermal-visual-costcompetitive-geothermal-can-stimulate-economy.html> accessed on 11/11/2015.
38. Online available at http://www.uniterm.pl/ogniwa_paliwowe/electrolyser.html accessed on 13/11/2016.
39. The World encyclopedia, electrolysis of water; online available at <http://www.newworldencyclopedia.org/entry/Electrolysis> accessed on 13/11/2016.
40. Wang, C., 2006. Modeling and control of hybrid wind/photovoltaic/fuel cell distributed generation systems (Doctoral dissertation, Montana State University-Bozeman, College of Engineering).
41. Tzimas, E., et al. "Hydrogen storage: state-of-the-art and future perspective." (2003).
42. Online available at http://www.esru.strath.ac.uk/EandE/Web_sites/08-09/Hydrogen_Buffering/Website%20Electrolyser.html accessed on November 2016.
43. Marcelo Carmo David L. Fritz Jürgen Mergel Detlef Stolten: A comprehensive review on PEM water electrolysis.

44. E I. Zoulias, N. Lymberopoulos: Hydrogen-based Autonomous Power Systems Techno-economic Analysis of the Integration of Hydrogen in Autonomous Power Systems, 2008 Springer-Verlag London Limited.
45. Sen, P. K., et al. *Electrolysis, Information and Opportunities for Electric Power Utilities*. National Renewable Energy Laboratory, 2006.
46. Rajeshwar, K., McConnell, R. and Licht, S., 2008. Solar hydrogen generation. Toward a renewable energy future. Springer: New York.
47. Kutz, M. ed., 2014. Mechanical Engineers' Handbook, Volume 4: Energy and Power. John Wiley & Sons.
48. Board on Energy and Environmental Systems National Research Council, Division on Engineering and Physical Sciences National Research Council, and Washington National Academy of Engineering. The hydrogen economy: Opportunities, costs, barriers, and R&D needs. National Academies Press, 2004.
49. Satypal, S., 2011. US Department of Energy Hydrogen and Fuel Cells Program 2011 Annual Merit Review and Peer Evaluation Report (No. DOE/GO-102011-3384). National Renewable Energy Laboratory (NREL), Golden, CO.
50. Gray, Evan, et al. "Hydrogen storage for off-grid power supply." *International Journal of Hydrogen Energy* 36.1 (2011): 654-663.
51. Sakintuna, B., Lamari-Darkrim, F. and Hirscher, M., 2007. Metal hydride materials for solid hydrogen storage: a review. *International Journal of Hydrogen Energy*, 32(9), pp.1121-1140.
52. Züttel, A., 2003. Materials for hydrogen storage. *Materials today*, 6(9), pp.24-33.
53. Tozzini, V. and Pellegrini, V., 2013. Prospects for hydrogen storage in graphene. *Physical Chemistry Chemical Physics*, 15(1), pp.80-89.
54. Xia, Y., Yang, Z. and Zhu, Y., 2013. Porous carbon-based materials for hydrogen storage: advancement and challenges. *Journal of Materials Chemistry A*, 1(33), pp.9365-9381.
55. Niaz, S., Manzoor, T. and Pandith, A.H., 2015. Hydrogen storage: Materials, methods and perspectives. *Renewable and Sustainable Energy Reviews*, 50, pp.457-469.
56. Santarelli, Massimo, Michele Calì, and Sara Macagno. "Design and analysis of stand-alone hydrogen energy systems with different renewable sources." *International Journal of Hydrogen Energy* 29.15 (2004): 1571-1586.

57. Muneer, T., Asif, M. and Munawwar, S., 2005. Sustainable production of solar electricity with particular reference to the Indian economy. *Renewable and Sustainable Energy Reviews*, 9(5), pp.444-473.
58. Online at: <http://pureenergycentre.com/first-african-wind-hydrogen-system-launched/> accessed on 6th November 2016.
59. Agbossou, Kodjo, et al. "Performance of a stand-alone renewable energy system based on energy storage as hydrogen." *Energy Conversion, IEEE Transactions on* 19.3 (2004): 633-640.
60. Duić, Neven, and Maria da Graça Carvalho. "Increasing renewable energy sources in island energy supply: case study Porto Santo." *Renewable and Sustainable Energy Reviews* 8.4 (2004): 383-399.
61. Little, Matthew, Murray Thomson, and David Infield. "Electrical integration of renewable energy into stand-alone power supplies incorporating hydrogen storage." *International Journal of Hydrogen Energy* 32.10 (2007): 1582-1588.

4.0 Design and Construction of Renewable Energy Data Logging and Monitoring System

Data logging is the act of data collection over a period. Electronic logging systems are typically designed to monitor a process using sensors linked to a micro-controller or PC. The inclusion of a monitoring system in renewable power design provides an understanding and flexibility in characterising the performance of the system (RE-system). This chapter describes the design and construction of a basic RE-power monitoring system in which current, voltage, and output power of a simple RE-system have been monitored, recorded and analysed. Arduino Uno (Atmega328) [1][2] formed the basis of this power monitoring system, and an INA219 current sensor was utilised in the design to facilitate the measurements of the output parameters.

4.1 Identifying the Components Used in the Logging System Design

This section and its subsections present a chronological overview of the components used in the construction of the data logging system.

4.1.1 Micro SD Card Breakout Board

It is desirable that a logging system be capable of handling large amount of data, and retaining this for a sufficient time-period. Most micro-controllers, especially Atmega328 upon which this design was based, has a very limited built in storage (EEPROM). Arduino Uno (Atmega328) has 1KB EEPROM (Electrically Erasable Programmable Read Only Memory) [1], which requires augmented storage. For this purpose, a secure digital card (SD card or micro-SD card) was utilised to provide the necessary storage required. SD cards has high storage capability up to 2TB range (Terabyte). The Micro-SD card breakout board shown in **Figure 40** below, made by Adafruit [3], and that was designed for easy use in Arduino-based data logging projects was selected. One of the things to consider when building a logging system is the power requirements of the device. SD

cards are strictly 3.3V devices and the power draw when writing to them can be quite high, about 100mA or more. Therefore a 3.3V power supply is necessary, and a 3.3V logic is needed to interface to the pins. According to the manufacturers, the breakout board used in this project design has an on-board ultra-low drop-out voltage regulator that can convert voltages from 3.3V - 6V down to equivalent of 3.3V [3]. This provides the opportunity for the board to interact with 3.3V or 5V micro-controllers without damaging the micro-SD card when writing data to it. Also, the regulator provides up to 150 mA current for the power-hungry SD cards. This voltage regulating capability in the board ensures its safe use on either a 3V or 5V systems.

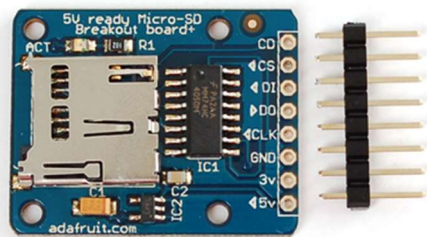


Figure 40. Adafruit micro SD card breakout board [3].

4.2 Measurement Tool

The voltage and current sensing apparatus that can give out a pure reading with maximum accuracy was desired, and therefore analogue measuring current sensors were avoided. A digital current sensor (INA219 manufactured by Texas Instruments [4] (shown in **Figure 41** below) was utilised in this design. According to the manufacturer's specifications the device incorporates an internal ADC (Analog to Digital Converter), is completely programmable and has an I²C (digital serial protocol used to communicate data between integrated circuits) interface. The I²C interface features 16 programmable addresses. They provide the digital current, voltage, and power channels necessary for accurate decision-making in precision-controlled systems. The current sensor has a programmable calibration value, combined with an internal multiplier, and this enables direct read-out of measured currents in amperes.



Figure 41. INA219 current shunt monitor.

The sensor measures both the high side voltage and DC current draw over I²C with 1% precision [5]. The INA219B chip can handle high side current measuring up to +26V even though it is powered with 3V or 5V [4]. Adafruit [5] has assembled an easy to use breakout board with this sensor as shown in **Figure 42** below. This breakout board was used in the monitoring system design.

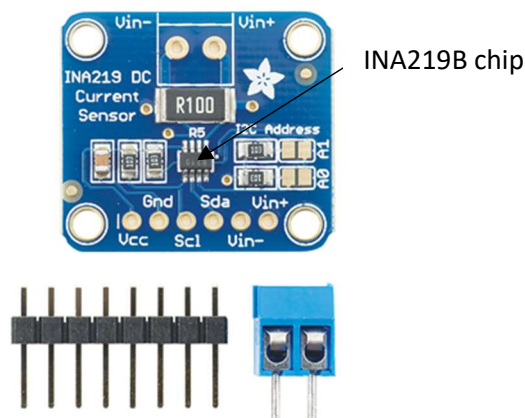


Figure 42. INA219 breakout board [5].

4.3 How Does the Current Sensing Breakout Board Work?

The precision amplifier (INA219) measures the voltage across the sense resistor connected between the two differential voltage inputs. The board came with an inbuilt 0.1-ohm sense resistor, but the amplifier maximum input difference of the sensor is $\pm 320\text{mV}$, which means it can only measure up to ± 3.2 Amps. To enable it to measure up to the required amount of current, this resistor was removed and replaced with a more suitable one. **Figure 43** below depicts pin configuration and wiring of the sensor. SDA and SCL are the clock and data lines tied to pull-up resistors. A0 and A1 are the addressable bus which can be modified, addressed to suit the desired inputs to be

measured. VIN⁻ is the negative differential shunt voltage, this connects to the negative side of shunt resistor. The bus voltage is measured from this pin to ground. VIN⁺ is the positive differential shunt voltage that connects to the positive [5].

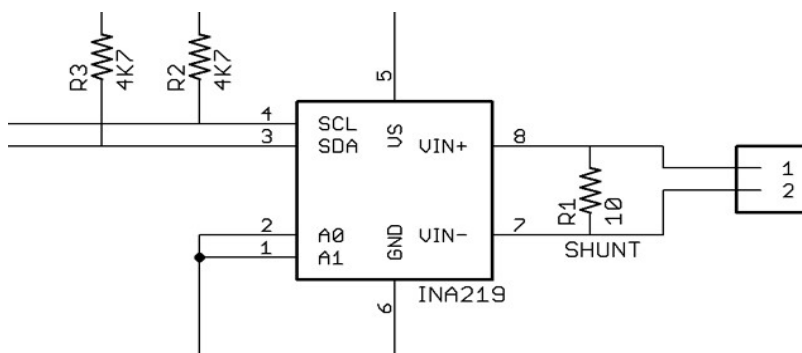


Figure 43. INA219 pin configuration [6].

4.4 Increasing the Input

Three measurements were desired (battery voltage, solar output power and wind turbine output power), therefore three INA219 breakout boards were connected with each board assigned a unique address. This was done with the address jumpers on the right edge of the board as shown in **Figure 44** below. The I²C base address for each board was 0x40. A drop of solder was used to bridge the corresponding address jumper for each binary '1' in the address to program the address offset. Each of the three INA219B current sensors breakout boards was assigned a unique address as illustrated below.

Board 0: Address = 0x40 Offset = binary 00000 (no jumpers required).

Board 1: Address = 0x41 Offset = binary 00001 (bridge A0 as shown).

Board 2: Address = 0x44 Offset = binary 00100 (bridge A1).

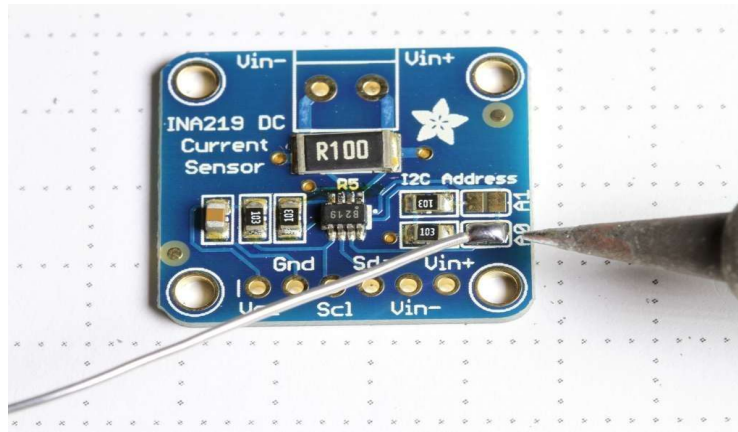


Figure 44. Addressing the boards [5].

4.5 Changing the Shunt Resistor – INA219

The maximum current rating desired was 8 Amps. A range between 5.4 Amps and 6.0 Amps was taken into consideration, for a 72 W and 85 W rated solar panel and wind turbine tied to a nominal 12V battery. This was scaled up to 8 Amps to improve the sensing capability of the INA219. The INA219 current sensor breakout board has an on-board 0.1-ohm sense resistor, this limited the measurement to a maximum of 3.2Amps since the amplifier maximum input difference was 320mV (the maximum voltage drop across the sense resistor). However, the 0.1-ohm current sense resistor was removed and replaced with a suitable resistor in order get the sensor to improve the measurement range above 8 Amps. This was deduced from the following calculations,

$$\text{Voltage} = \text{current} \times \text{resistance},$$

(Equation 18)

$$\text{Maximum voltage drops across the sense resistor} = 320\text{mV}$$

$$\text{Desired current to be measured} = 8 \text{ Amps}$$

Resistance = $320\text{mV}/8\text{A} = 0.04\text{Ohm}$. This value of sense resistor will allow measurements up to 8A). The power rating that would match this sense resistor (0.04 ohm) can be obtained from the following relation,

$$\text{Power (mW)} = \text{Voltage (mV)} \times \text{current (A)},$$

$$\text{Power (mW)} = (320 \times 8)/1000$$

$$\text{Power} = 2.56\text{mW}$$

Based on the above a 0.04 Ohm, 3W sense resistor was selected for the desired measurement range, and a handmade 0.034-ohm sense resistor was fabricated using a 20cm length of 28 S.W.G diameter (0.376 mm) of copper wire. The constructed resistor was tested by passing a current of 2.0A. The voltage across the resistor was measured at 68mV giving a resistance of 34mOhm as required. **Figure 45** shows the fabricated sense resistor. The wires from the resistor were connected close to the differential amplifier to avoid any drop.



Figure 45. Inner wiring of the monitoring unit showing the 0.034-ohm resistor.

4.6 Microcontroller

This design demands an extensive use of microcontrollers to handle the data from all current sensors used in the monitoring system. The requirement was that these should handle all essential codes for the parameters (voltage, current, power) used in the system and get their respective values stored in a data logging system. A total of three sensors was used to monitor and measure the specified power generation parameters. Ideally, a chosen microcontroller should have enough flash memory available for programming in order to be able to accommodate the codes needed to properly manipulate and handle the data to be utilised. Therefore, a choice of micro-controller that would have at least a 16KB of flash memory available for programming was made. Micro-controllers that possess all desired specifications are the ATmegaXX8 series manufactured by Atmel [2]. The Atmega328 has a 32-pin count and 32KB programmable flash memory, 8-bit AVR CPU (Automatic Voltage Regulator, Central Processing Unit), 20MHz maximum clock speed, and 23 I/O pins [2]. Atmega328 will offer high performance advantage to the monitoring unit. The choice of a board that supports Atmega328 was considered and the Arduino Uno was selected. AtmegaXX8 series is the

central component of the open-source electronics prototyping platform manufactured by Arduino [1].

4.6.1 Arduino Uno – Atmega328

The Arduino Uno shown in **Figure 46** is a project development board based on the Atmega328 micro-controller. The microcontroller can be programmed using the Arduino programming language (based on wiring) and the Arduino development environment (based on processing). Power supply to Arduino Uno can be via the USB connection or with an external power supply (AC-to-DC adapter or battery). According to the manufacturers the board can operate on an external supply of 6 to 20 volts [1]. The recommended voltage range is 7 to 12 volts to avoid overheating the regulator, and using more than 12V may damage the board.



Figure 46. Arduino Uno Atmega 328 [1].

4.6.2 Communication

Arduino Uno can communicate with a computer, another Arduino, or other microcontrollers through several facilities. The serial monitor facilitates exchange of textual data in the Arduino board. The RX (Receiver) and TX (Transmitter) LEDs on the board will flash when data is being transmitted via the USB-to-serial chip and USB (Universal Serial Bus) connection to the computer. Arduino software includes a wire library that facilitates use of the I²C bus [1]. For Uno, SDA and SCL are the I²C pins, they are directly connected to analog pin A4 and pin A5 respectively.

4.6.3 Programming the Board

Arduino programmes are written in C++, this is based on the integrated development environment (IDE) platform. Arduino software can be downloaded freely from their website. The Atmega328 on the Arduino Uno comes pre-burned with a boot-loader, that allows upload of new codes to it without the use of an external hardware programmer [1]. The programming language, which may consist of mathematical operations, expressions, variables and functions, allow users the freedom to manipulate the communication protocols [1]. Coded programs can be written and uploaded into the Arduino Uno to make it perform a desired specific function and operation. The codes used in this renewable energy data logging design were written in C++ and uploaded to the board. **Figure 47** shows the power monitoring unit as it was designed and constructed. Power supply to the board was via the RE-system battery storage, and a 5V DC-DC converter made by Traco power [7] was utilised to convert the battery voltage (12V) to 5V for Arduino and other connected components. **Figure 48** illustrates the point where the DC-DC converter was placed in the board.

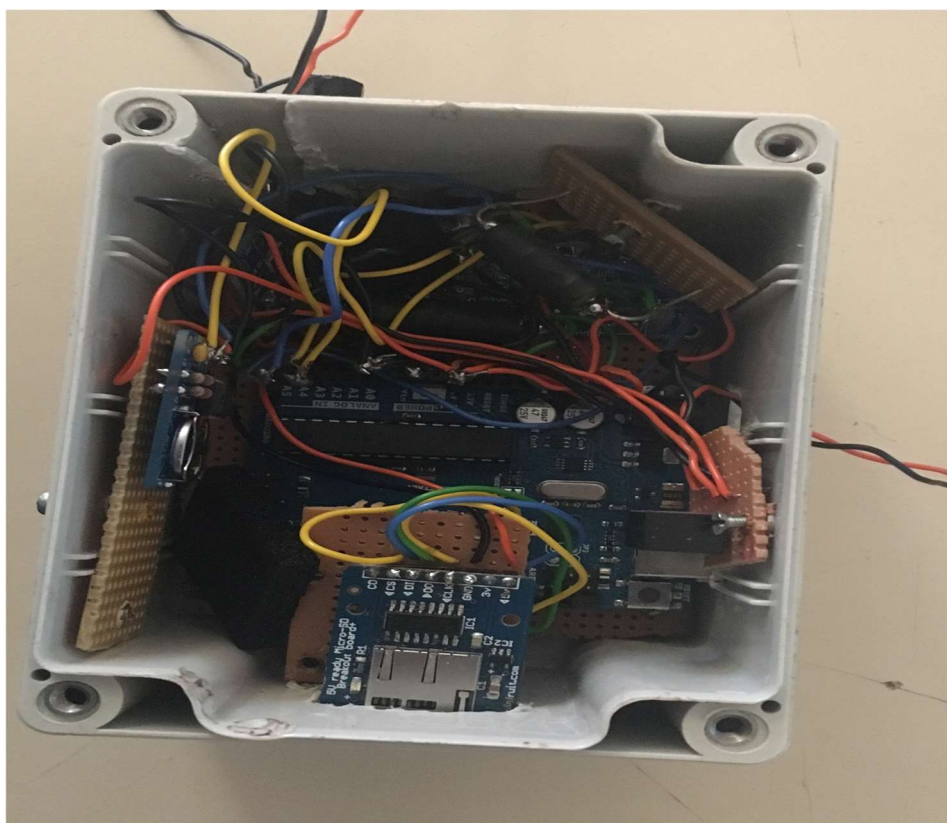


Figure 47. Implementation of the power monitoring system.

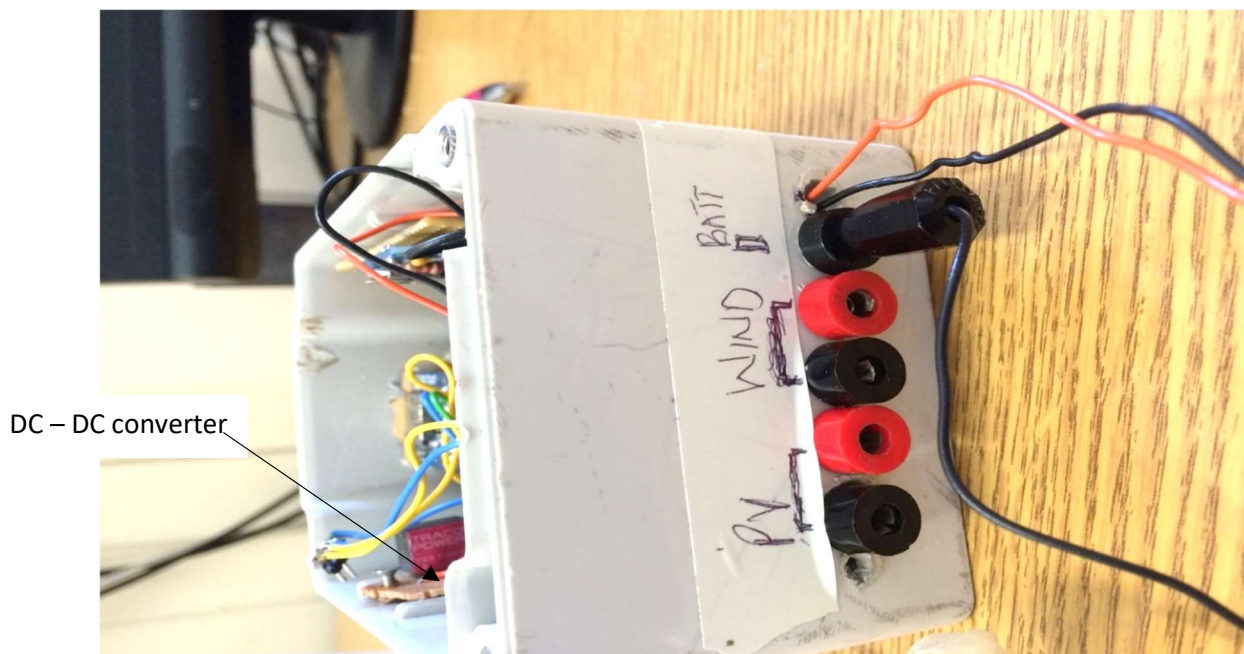


Figure 48. Inner view of the monitoring unit box showing the DC-DC converter.

4.7 Current Sensing

It is important that current and voltage be monitored in a RES to understand the system's impact on the battery life. Current sensors are devices that detect and converts current to a measurable output voltage, which is proportional to the current measured path. This is discussed in the next section.

4.7.1 Principles of Current Sensing

There are two basic ways into which current measurement techniques are categorized, they are direct and indirect. Both are direct applications of Ohms law, Faradays law and Amperes law. They obey the law which stipulates that: (1) there is always a voltage drop whenever a current flow through a wire or in a circuit. (2) An electric current generates a magnetic field around a carrying conductor.

Direct sensing as shown in **Figure 49** is based on Ohms law that reads:

$$V_2 - V_1 = R_{shunt} \cdot I$$

(Equation 19)

Where:

R_{shunt} = shunt resistor inserted through which a current flow, and the voltage drop across this is measured.

$V_2 - V_1$ = the voltage difference between two terminals of the shunt resistor. This voltage drop ($V_2 - V_1$) will be amplified by differential amplifier. This amplifier in INA219 current sensor amplifies the voltage drop ($V_2 - V_1$) across the sense resistor and feeds this to an analog-to-digital converter (ADC) which outputs a digital value proportional to the current being measured. Two basic ways of implementing this direct current sensing technique are 'High side' and 'Low side'.

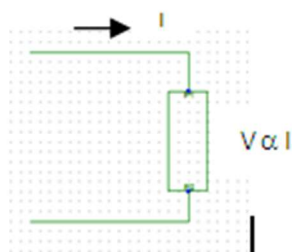


Figure 49. Direct current sensing [8].

Low side current sensing: this technique has the sensing resistor placed between the load and the ground shown in **Figure 50**. A simple precision amplifier is used to measure the voltage drop across the sense resistor placed between the load and ground. The challenges encountered in implementing this technique is that load is lifted from direct ground to connection, and this makes the whole circuit vulnerable to RF disturbances. It can also leave accidental load shorts to ground undetected.

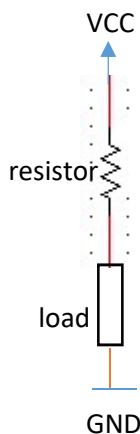


Figure 50. Low side current sensing.

High side current sensing: In this scheme, the sense resistor is inserted between the load and source, as illustrated in **Figure 51**. Traditionally, in high side current measurement, a differential amplifier, amplifies the difference between the two-input voltage across the sense resistor and measures the output. It is difficult to achieve an accurate capture in high side current sensing because of the resistor matching issues which is required in order to obtain a high common mode rejection ratio (CMRR) of the IC being used. CMRR measurement measured in decibels describes the capability of an instruments to reject a voltage common to both sides of a differential circuit [4], and this is acceptable when it is above 90dB [4]. A 1% deviation for a selected sense resistor has the effect of reducing the CMRR to around 46dB. Current shunt monitors are designed such that the resistors used for the differential amplifier are placed inside the IC, this eliminates the CMRR issue associated with high side sensing. The INA219 chip used in this power monitoring system design is a high side current shunt monitor manufactured by Texas Instruments. The chip offers accurate measurement as detailed below [4];

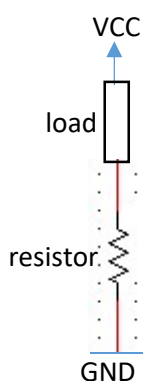


Figure 51. High side current sensing.

High accuracy: For high accuracy, Texas Instrument's INA219B chip used in this work is an ideal one with an offset voltage as low as $35\mu\text{V}$ [4], making the chip an ideal choice for this project.

Indirect current sensing: this technique is based on electromagnetics and is associated with the early moving coil meter. When a current-carrying conductor is placed in a magnetic field perpendicular to the path of the electrons, the electrons are deflected from its straight-line path and the conductor becomes polarised. This charge separation process continues until electric field force balances with the magnetic force. This process

measures the transverse Hall) voltage. No shunt resistor is required and accordingly there is no voltage drop. As illustrated in **Figure 52** it only performs the direct measurement of the magnetic field of the conductor. The whole process is called Hall effect sensing, and the devices used in the sensing processes are Hall sensors. This approach of current sensing is prone to temperature drift and they may be affected by interference from an external magnetic field.

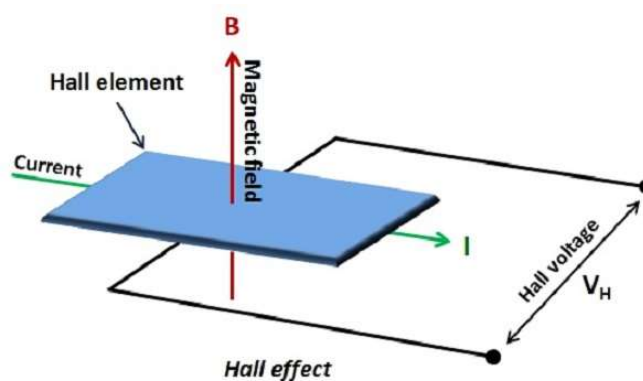


Figure 52. Hall Effect current sensing [9].

4.8 Analysing the Hybrid Renewable Power Monitoring Data in Dundee UK

A power monitoring/data logging unit was designed and constructed according to the procedures presented in **sections 4.0 – 4.6**, to monitor in real time the performances of RE-power sources (solar, wind and battery) installed as a system at a location in Dundee. **Figure 53**, is a schematic diagram illustrating the wiring connections during the design phase and its implementation of the monitoring system. Analysing the data obtained from the hybrid renewable energy system is beneficial as it helps to know the efficiency level of the system, which could be used to determine the characteristics performance and impacts of the system on the battery. The monitoring system was installed to obtain the performance characteristics of the system. This is essential as results obtained will be used to determine how a renewable energy system with battery and hydrogen storage (solar-hydrogen) might perform, and this will be used to make an informed decision about transferable aspects of the renewable energy system to developing countries in sub-Saharan Africa. How transferable this could be depend on several factors, typically the geographical location and the weather conditions of the area. The

climatic condition at the location - Dundee area (UK) where the RE-lighting system is installed, is temperate maritime which is subject to the moderating influences of the Gulf Stream. If compared to the tropical climate in sub-Saharan Africa it will influence the characteristic performance of the renewable energy system when sited in Africa based on data and designs obtained from Europe. Therefore, another data monitoring process was conducted at a location in Nigeria, and this will be discussed in a later section of this **chapter**.

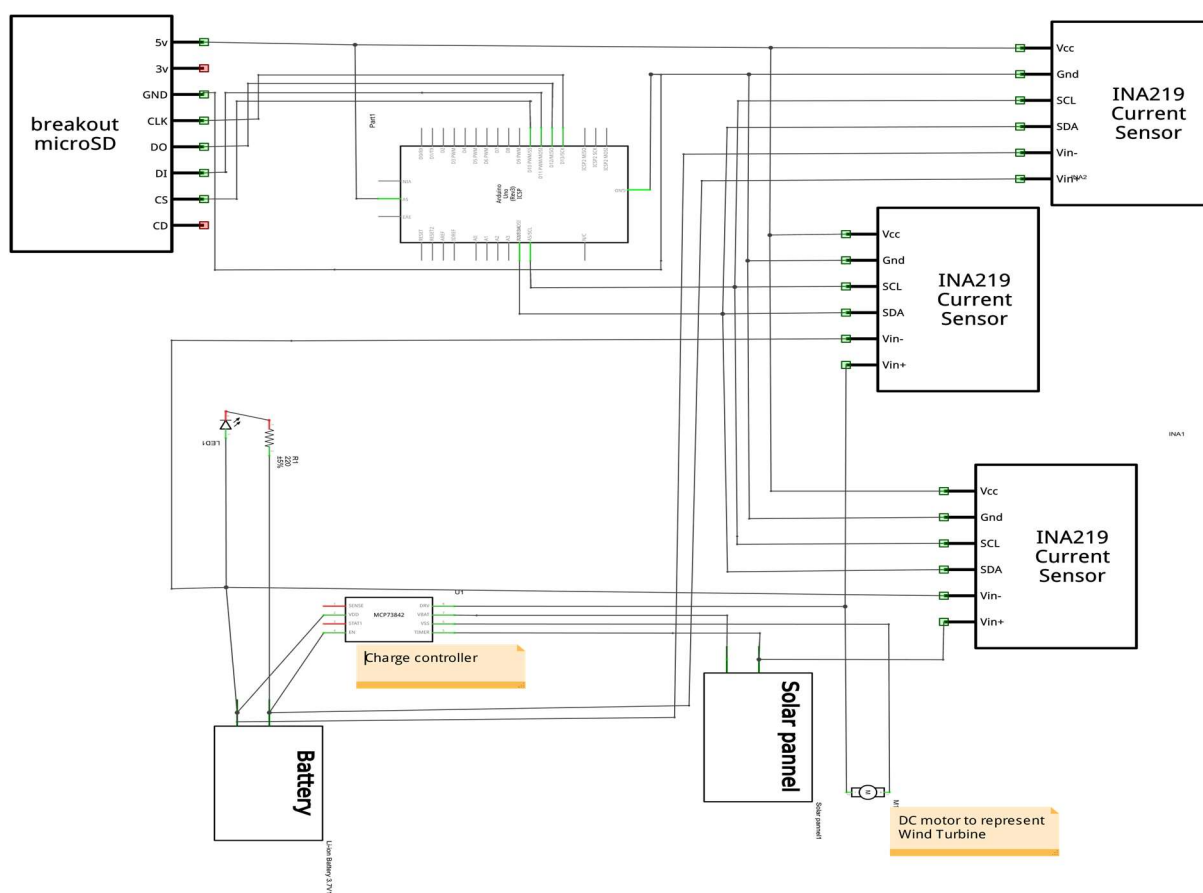


Figure 53. Schematic diagram of the RE-power monitoring unit showing the wiring connection

The installed hybrid RE system is shown in **Figure 54** and consists of 85W solar PV, 18W LED light, a 12V gel lead-acid battery and 72W wind turbine. All of them are connected to a Marlec charge controller, to regulate the battery charging process [10]. The purpose of the system is to provide controllable off-grid lighting. The power monitoring unit was installed on the RE system to obtain the power production of the system and to visualize

its battery charging regime. A summary of the hybrid RE power system installed and their component specifications are as follows;

- 85W Ameresco solar module (0.65m² area).
- 72W Ruthland 910 wind turbine
- 12V 70Ah AGM battery
- 18W lighting system
- Marlec HRDi charge controller

A data set at 5-minutes data interval was collected from the monitoring unit via the integrated SD card.

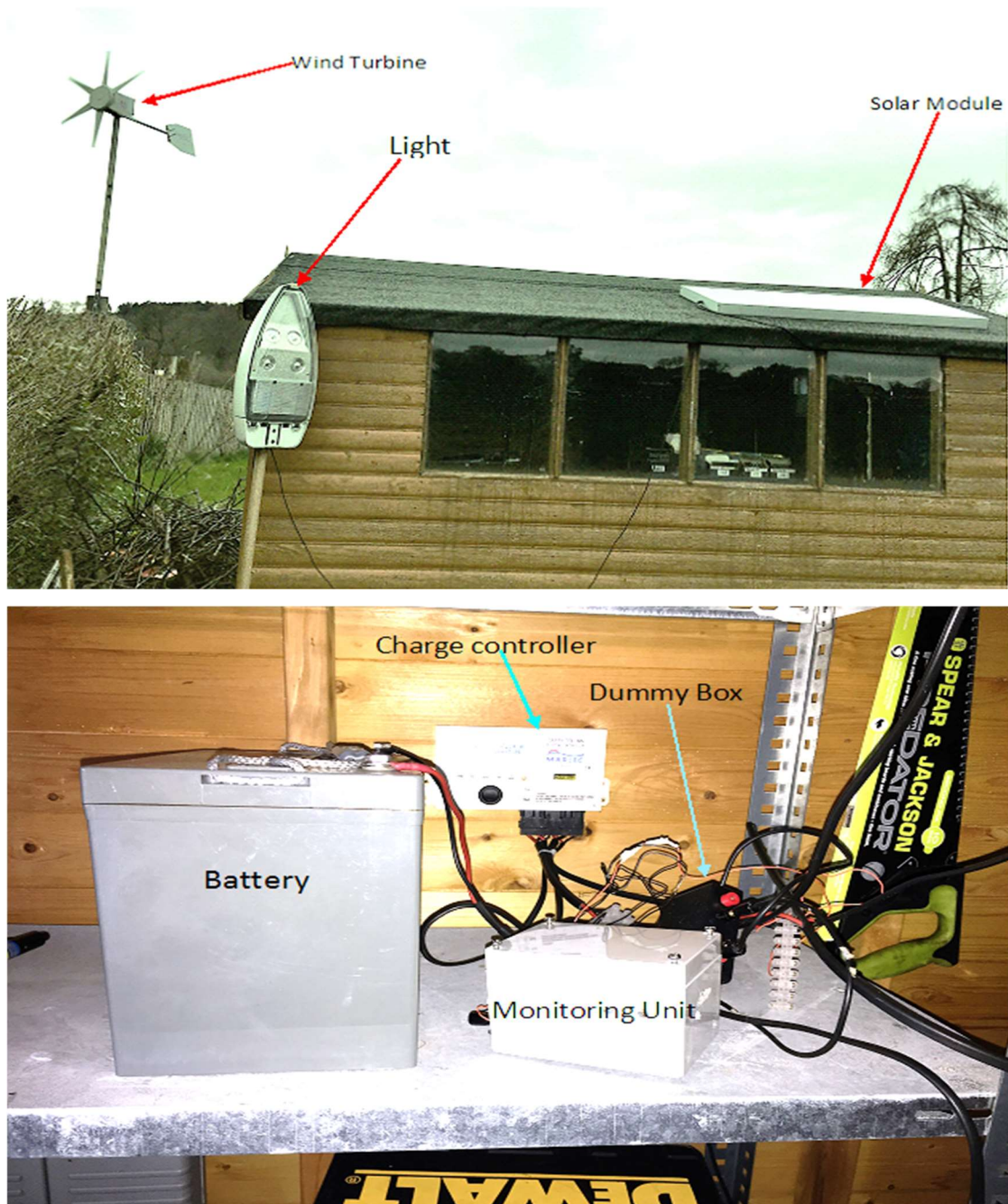


Figure 54. Hybrid solar and wind installation with LED lighting.

Figure 55 shows the state variation of the battery over the 3 days period recorded, a fluctuation in battery voltage can be observed within this period.

Ideally, at full state of charge of the battery voltage may vary between 14 – 15V, but for this work 13.3V will be used as reference in this analysis, to reflect the upper limit of the battery state of charge seen over the 3-day period.

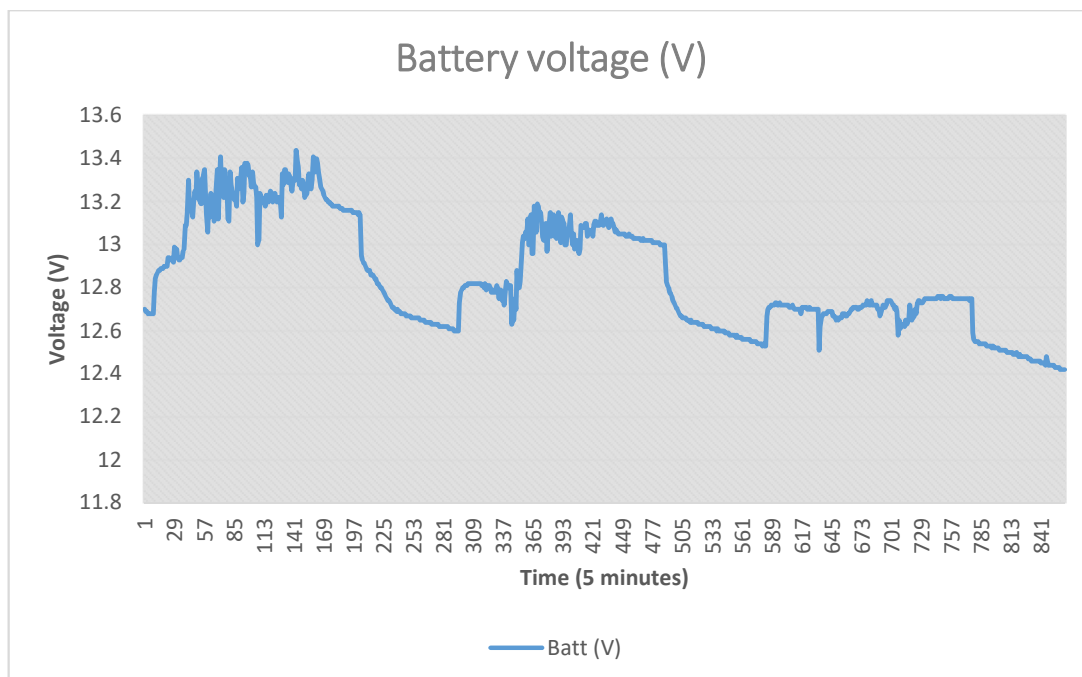


Figure 55. Battery voltage recorded.

According to the configuration of the system a drop in battery voltage is observed when the lights are activated, in accordance with simple circuit theory. The battery state of charge (SoC) or terminal voltage is intimately linked to the competing charge and discharge rates. For example, under no load (lights off) and strong solar charging the open circuit voltage of **14.4V** might be expected to be observed. However, there are always drains on the system, including the control electronics and LC display. Under wind-only charging a rather variable terminal voltage is observed, reflecting the fluctuating wind strength (and hence turbine output voltage). Because the turbine is tied to the battery wind speed increases will tend to produce more torque (i.e. current) for little increase in voltage. Some example plots will be shown in subsequent sections of this **chapter**.

4.8.1 PV and Wind Turbine Output Power

The PV and wind turbine output power over the period recorded are shown in **Figure 56**. From this we can clearly observe the daily cycle of the solar PV whereas the wind turbine outputs are less predictable, as to be expected. The red lines in plot depicts when the light come on.

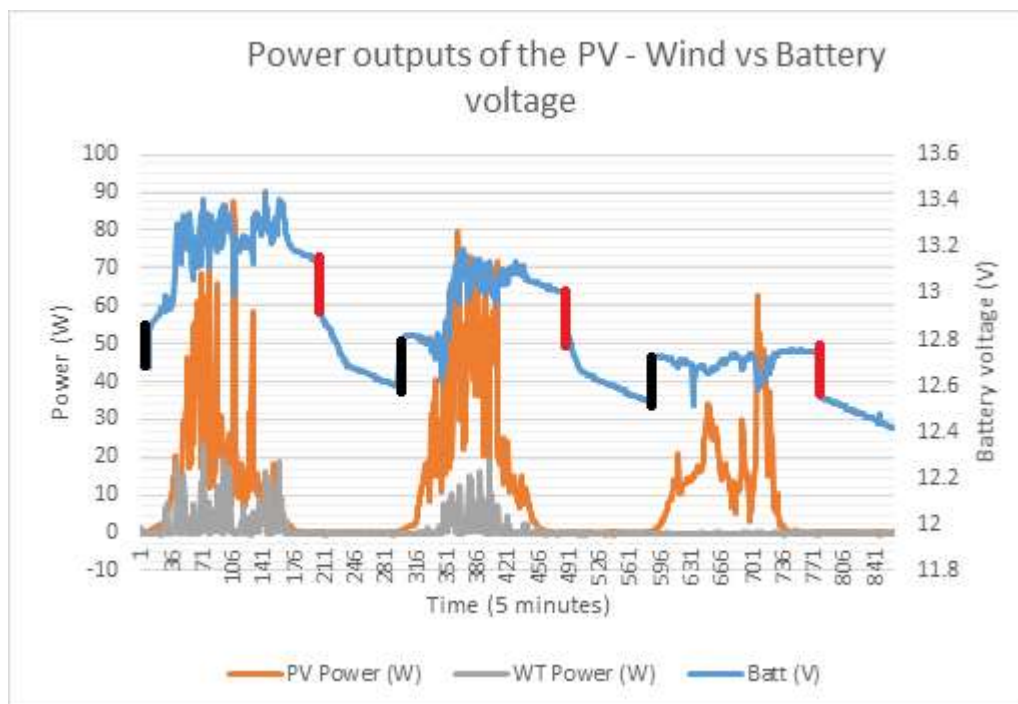


Figure 56. Output currents of both RE system with battery voltage.

Ultimately, variations in weather conditions have significant impact on the characteristic output production of renewable power generators. These data were recorded from 29th August – 31st August 2015. To validate the performances and data obtained from the RE components with the installed monitoring unit within this period, a real-time weather data spanning from 29th August – 31st August for wind speed and solar irradiation related to the location – Dundee United Kingdom with coordinates 56.4640° N, 2.9700° W was downloaded from the NASA website via RETSCREEN PLUS software. To obtain a more accurate weather data, good practice is to install a local weather station at the project site. However, due to the unavailability of the weather station at the project site, the option of downloading the time series data from NASA website was adopted, **Table 19** shows the wind speed and solar irradiation at the project location.

Date	Daily solar radiation - horizont	Wind speed (m/s)
	kWh/m ²	m/s
29/08/2015	3.73	6.15
30/08/2015	3.91	4.2
31/08/2015	3.01	2.63

Table 19. Daily solar radiation and wind speed.

4.9 Obtaining the Daily Output Power Productions of the PV and Wind Turbine

A graph with the 3- days output of the RE system components has been shown in **Figure 56**, however, the graph was clustered, and that makes it difficult to view properly the performance of the PV and wind turbine. To obtain a visible plot that shows clearly the daily output power of the RE components, the graph was split into sections representing the daily power productions of the PV and wind turbine (including the battery voltages) and plotted in hourly values.

4.9.1 Daily Power Outputs of the PV Module and Wind Turbine and Battery Voltage

In this section, the daily output performance characteristics of the RE-system is presented.

DAY 1

In the first day (29th August) the wind turbine produced a maximum output power of 5.28 W. **Figure 57** shows the power outputs of the PV and wind turbine. From the graph, a variation in power output can be seen in both system components, PV power outputs increased in the early hours of the day (sunrise) and peaks at 46 W at 6 am and diminishes as night time hours approached.

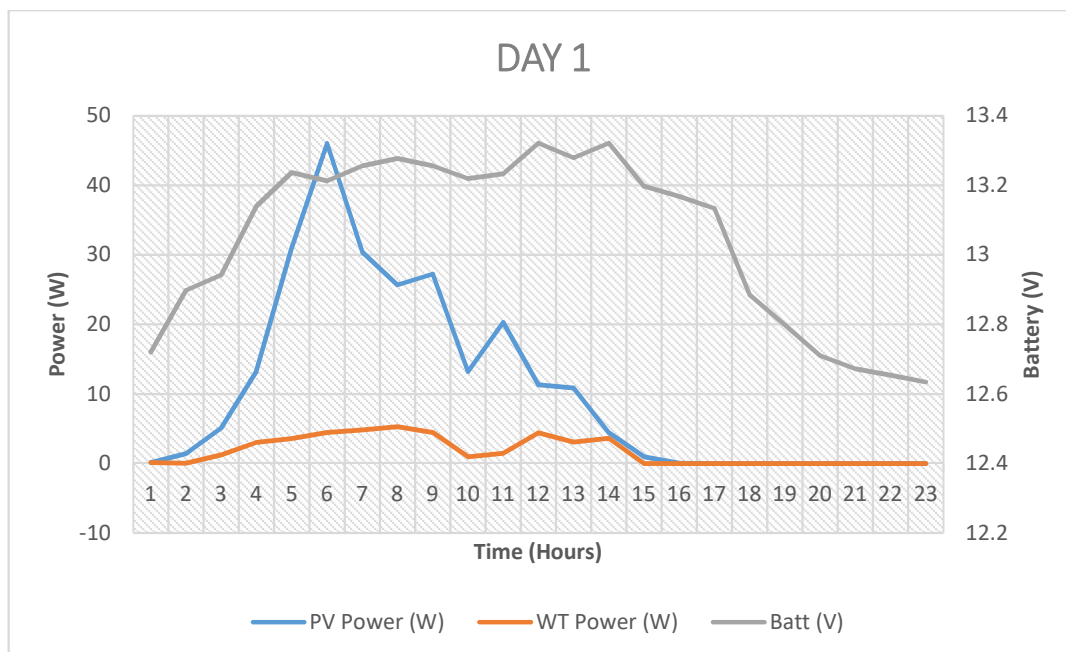


Figure 57. Output power in Day 1.

A similar pattern was also seen in the wind turbine, a factor which will be discussed in the later part of this chapter. The initial state of the battery voltage was 12.72V, inputs from the PV and wind turbine ensured that the battery voltage increased steadily up to maximum 13.3V, and this eventually declined to 12.63V. From the graph, it can be observed that the decline in battery voltage happened at the period when outputs from both RE components dropped.

DAY 2

On the second day (30th August), the PV module produced a maximum of 54 W, and the wind turbine power peaked at 4.5 W. The outputs from PV and wind turbine for “Day 2” is shown in **Figure 58**, a 7.6 W more in peak output power in PV panel, but there was a 0.78 W drop in wind turbine output compared to the power productions seen in ‘Day 1’.

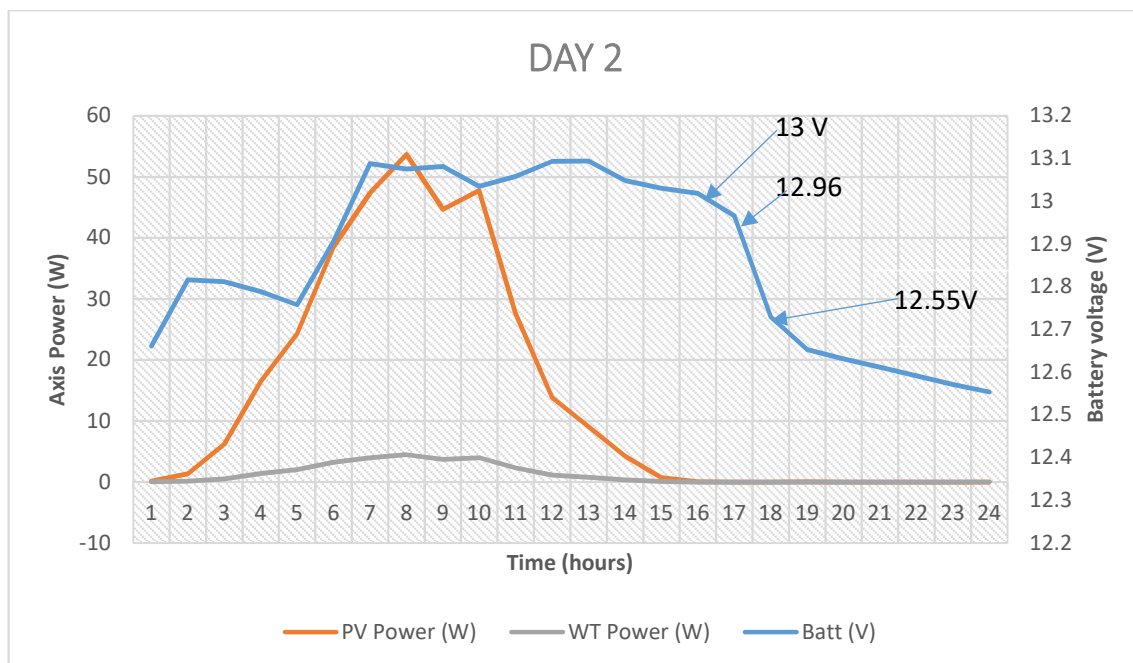


Figure 58. Output power in day 2.

The battery state of charge which remained at 12.6V over the night of 'Day 1' was charged up by the RE components. The output currents from the RE components had trickle charged the battery from 12.6V up to 12.8V, also it can be observed that PV output power have fluctuated within this period, as it did not produce useful amount of power (6 W - 16 W). The wind turbine also did not produce useful amount of power within this period. A factor which accounts for the voltage drop is the lighting load, which was activated in this time frame. At morning time, the battery voltage increased steadily up to a maximum of 13.0V. This rise in battery voltage can be related to the power productions from the RE components, it can be observed that the battery voltage was stable at 13.0V on this day and this had occurred in the around 8 am when the PV power peaked at 54W. The wind turbine did not contribute useful charging current to the battery. The maximum power output from the wind turbine within this period was 4.4W.

However, there was a steady decline in battery voltage afterwards, the voltage can be seen to have dropped from 13.0V to 12.9V and down to 12.55V. This can be attributed to the output performance characteristics of the RE system components. Viewing the RE power output plot shown, it can be seen that the lower battery voltage was because of the night long outage of PV and wind turbine. This coupled with the current drain from the lighting load which came on within this period (18:00 hours) could have caused the battery to struggle all night and could not cope with the system.

DAY 3

Figure 59 shows a plot of output power recorded from the PV and wind turbine on day 3 (31st August). From the graph, no output production from the wind turbine was seen on this day, but, the solar PV generated some amount of power over the course of the day.

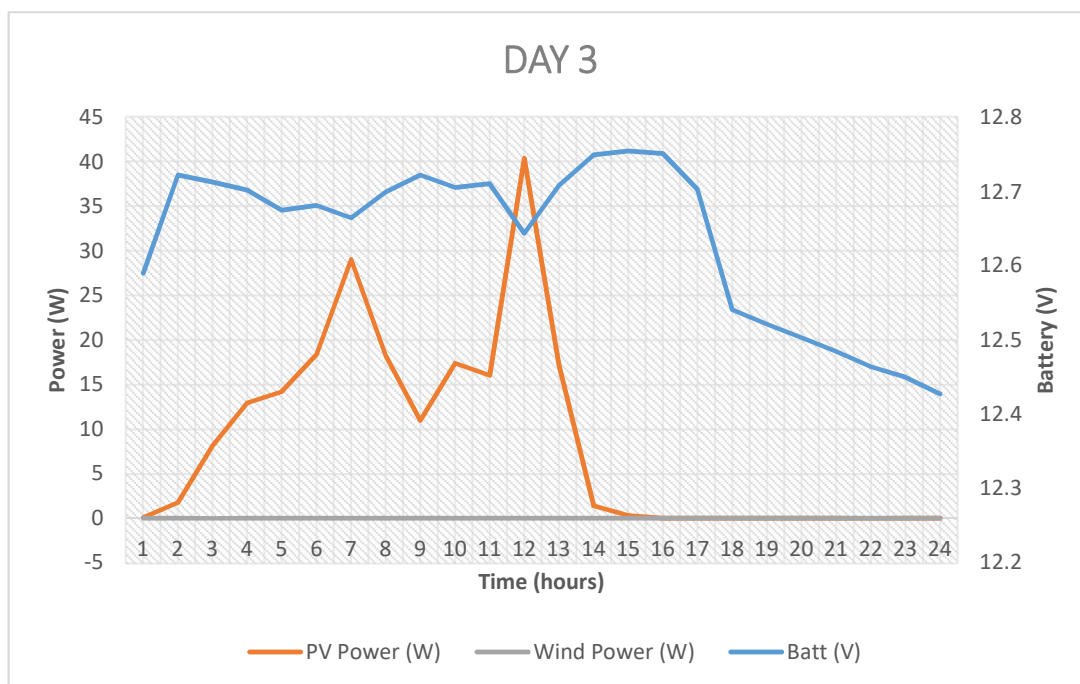


Figure 59. Output power in day 3.

The PV power was maximum at 40.4 W. There is a 25% decline in outputs from the PV system when compared to its day 2 performances. There is a variation in power production from the PV, this is normal for renewable power system. The trend in battery state of charge in “Day 3” is the highest state of charge recorded shows the voltage sitting at 12.7V which indicated a slight increase in voltage from the initial 12.5V it was at night of day 2, from this it can be inferred that the RE components had trickle charged the battery. A drop in voltage of 12.4V was seen to occur at night time due to the unavailability of solar energy resource.

4.10 Energy Analysis

Energy is the power produced or expended over a period of time. It is important to determine the total amount of energy that is produced by a renewable power system over a set period, in order to evaluate the capability of the RE system in supplying the daily amount of energy required for a domestic or commercial setting. The power produced by each of the system components has been described with the graphs in the previous sections (4.8 – 4.9). Here the energy performance and characteristics of the RE system will be discussed.

The energy produced by the hybrid RE system can be determined using the following equation;

$$\text{Energy} = \text{Power} \times \text{Time} \quad (\text{Equation 20})$$

With power plots as a function of time the energy flows over a period can be found through integration of these plots. The calculated energy supplied to keep the 12V battery charged over the 3-days period is shown in **Figure 60**. From the graph, the daily energy performances of the hybrid renewable power system were clearly visible. The hybrid RE system produced more energy in 'Days' 2. The total energy productions from both renewable energy systems over the 3 days was 0.846 kWh as listed in **Table 20** and shown in **Figure 60**.

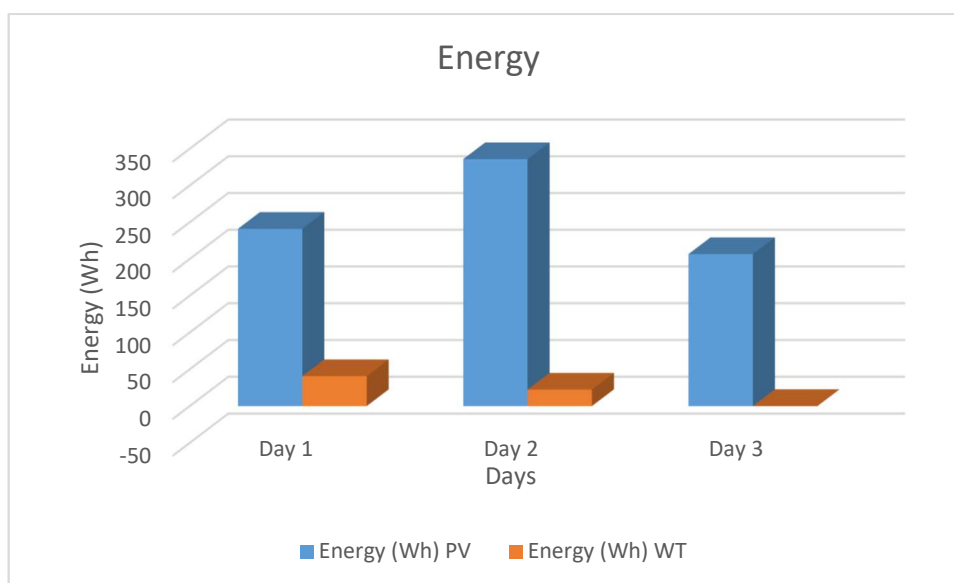


Figure 60. Energy output of solar PV and wind turbine.

The variability nature of the wind turbine was clear, the energy contributions from the wind turbine was **62.7 Wh** as listed in **Table 20**, a mere **7.4%** of total energy productions was seen, and this validates the need for a hybrid combination of different renewable power sources to meet the load demand.

Days	PV (Wh)	WT (Wh)
Day 1	241.2	40.6
Day 2	335.9	22.3
Day 3	206.6	0.14
Total	783.8	62.7

Table 20. Energy productions of the hybrid RE system.

4.10.1 Energy Productions by Individual Components

A graph of the total energy productions from both RE system is shown in **Figure 61**, however, it is important that the energy performances by each of the component is presented in order to properly visualise the contributions of each component and to verify the energy performance of each component based on the daily energy resource at the selected location. By doing so, the energy, power production and efficiency characteristics of the renewable power generators as specified by the manufacturers will be evaluated. Also, it will help to know when the power generators are not producing up to their optimum output level due to age degrading factors and losses.

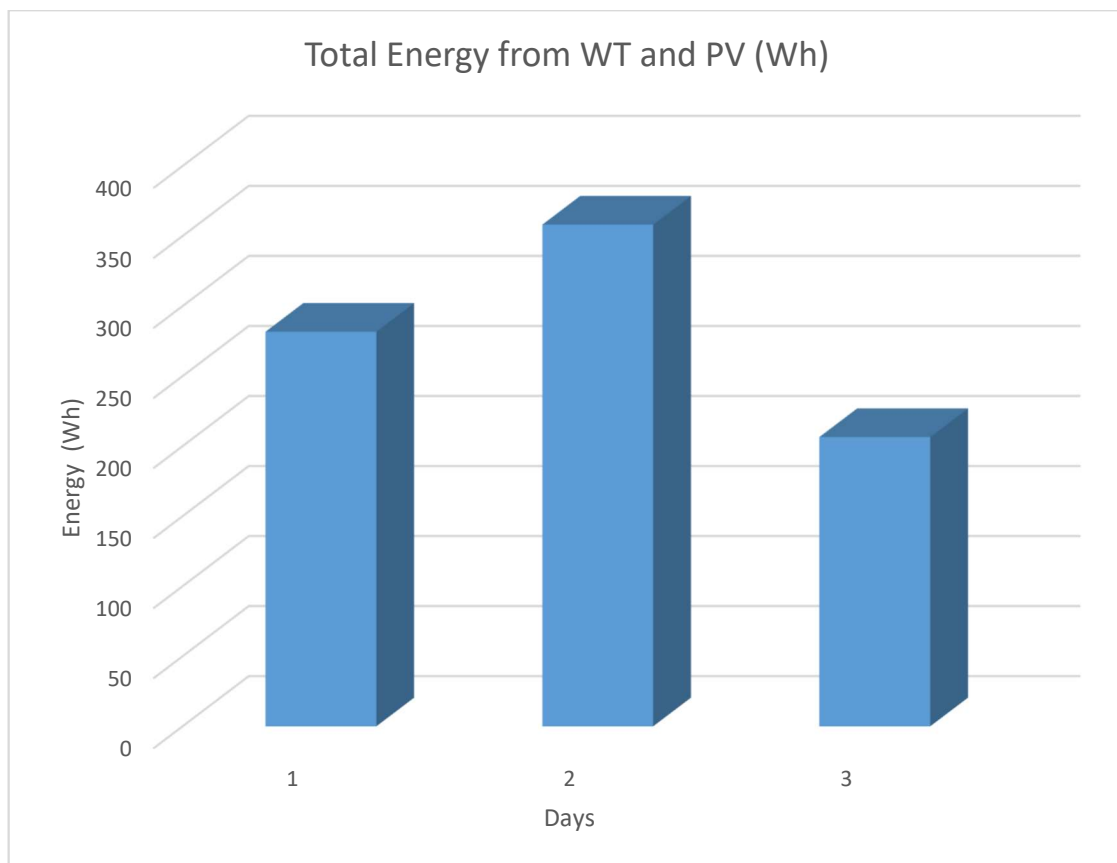


Figure 61. Total energy productions of solar PV and wind turbine.

4.10.2 Solar Panel Energy Productions

From the graph of **Figure 61**, it was calculated that the solar PV generated total of 336 Wh in the second day.

4.10.3 Estimating the Useful Energy Production of the PV Panel

The average daily solar irradiation available at the location within the period this data was recorded has been shown in **Table 21** of **section 4.8.2**. The day of interest here is “Day 2” as the PV produced more energy, and we can compare this to what can be obtainable using the solar radiation data. Day 2 was selected because more solar irradiation (3.91 kWh/m²) was seen on Day 2 than other days. However, the formula to estimate the energy generated is given as;

$$E = \text{Rated} \frac{\text{power}}{\text{Area}} \times \text{Daily solar irradiation} \times \text{performance ratio} \quad (\text{Equation 21})$$

Performance ratio is a measure used to describes how efficient a PV plant will be in terms of power production, irrespective of the location where it is installed. In this work, a 75% performance ratio was assumed.

Thus, inputting the downloaded daily solar radiation values and solar PV data presented earlier we obtain as follows;

$$\text{Energy produced at day 2} = \frac{85}{0.65} \times 3.91 \times 0.75$$

Hence the estimate of total energy the solar PV would produce at Day 2 =
384 Wh

Comparing this value (384 Wh) with the energy obtained from recorded data for “Day 2” (336 Wh) we can see that there is a **12%** difference, that is, the theoretical PV output power is about 12% more than its actual power. This is very close, and it shows that the solar panel was operating at efficiency close to its optimum.

4.10.4 Energy Production of the Wind Turbine

In **Figure 60**, the daily energy productions from the 72W wind turbine, and a trend which was clearly visible in the energy production graph is the variability of the wind resource, it was up in “Day 1” showing strong energy production by the wind turbine on this day, this can be explained by the moderate wind speed seen at ‘Day 1’ 6.15m/s (**refer to Table 19**), being so unpredictable, the wind speed was low at ‘Day 2’ 4.2m/s, a 31.7% drop compared with the wind energy resource seen at ‘Day 1’. Essentially, to draw a proper comparison a power curve for this wind turbine should be used, but in this thesis, a detailed review of wind energy analysis is not dealt with. However, ‘Day 3’ was the worst of all days recorded in terms of energy production, a zero-energy production. A point for highlight as the wind speed (2.63m/s) seen on this day was not enough for the wind turbine to kick in, and it remained this way for the whole day.

4.10.5 Discussion

The 3-days data collected from the **85 W** solar PV and the **72 W** wind turbine has been analysed and their energy and power performances presented. Here, some interesting observations made in the analysis is discussed. The following observations have been noted;

- The agreements and disagreements of the hybrid RE system components performances with the real-time wind speed data downloaded from NASA via RETSCREEN software tool [11].
- The difference in intermittency observed in both systems.
- The complimentary characteristics of the hybrid RE system, means that increasing the capacity of the wind turbine can improve the performance of the hybrid system, but this is only a 3-day snapshot though, and that wind will be much more productive than PV in the winter. However, the usual way to compare this is to carry out another measurement in winter but this was not possible due to time constraints.
- The efficiency of both RE components.
- The persistent drop in battery voltage observed whenever the light came on
- The battery losses caused by the connected monitoring unit observed when the lights were off but no renewables inputs were recorded
- The importance of taking proper and real-time measurements of the renewable energy resources at any selected project location.

The importance of having the knowledge of distribution of the renewable energy resources available at the selected project site cannot be over-emphasized. This has been shown in this thesis, in the energy calculations carried out using the downloaded resource data. The power production from the solar panel was in good agreement with the one calculated using the downloaded solar irradiation data, same can be said in wind turbine where it did not produce any power in “Day 3” because of the low wind speed seen on that day. Having instantaneous measurements of energy resources at a project location will be very beneficial. Solar PV systems can generate moderate amount of power with the few hours of sunshine in the winter months, considering the less

variability nature of sunshine compared with wind speed, and this will help in keeping the battery charged all the time. The cause of persistent drain in battery voltage is discussed in the next section.

4.11 The Drain of the Battery and its Implications

The issues related to the battery drain have been commented on previously, but in this section, we will discuss the reasons for this battery drain and how the problem could be solved. In a hybrid, renewable energy system that integrates battery as its energy storage medium, it is always good practice to select a battery of appropriate capacity, and to understand the charge – discharge regime of the battery. One important characteristic of the battery that defines these characteristics is the internal resistance of the battery. Resistance is the opposition to the flow of current. **Figure 62** shows a representation of battery internal resistance with a battery modelled as electromotive force (ϵ) connected in series with a resistor (r).

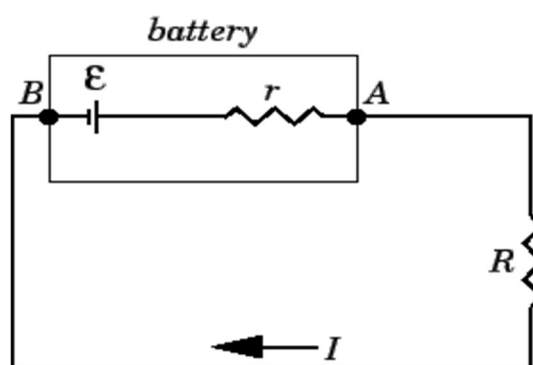


Figure 62. Battery model showing internal resistance.

Battery internal resistance denoted by ' r ' is composed of two basic components; the electronic resistance and ionic resistance. The battery electronic resistance is caused by some electronics integrated into the battery architecture. The ionic resistance refers to the opposition in the flow of current inside the battery due to the various electrochemical factors; such as the mobility of the ions, the electrolyte conductivity and the surface area of the selected electrode. The voltage drop of a battery is a function of

total effective resistance and current drain rate. However, relating these factors to the 12V battery used in this analysis, it was found that the 18W light would drain the battery at a rate of approximately 1.3A (18/13.5). However, while discharging the voltage of a battery is defined by;

$$V = \varepsilon - Ir \quad (\text{Equation 22})$$

This equation explains the relationship that; electrical potential difference increases by $+\varepsilon$ (*volts*) and decreases by Ir . This means that increasing the current draw (load) increases the voltage drop of the battery. In practice, the internal resistance of a battery is influenced by several factors which include age, chemical properties, size, charging - discharge current and temperature. However, in relation to the persistent battery drain highlighted in this thesis, age and charging – discharging current is of paramount importance. The internal resistance of a battery increases with age. However, a significant build-up of internal resistance over the years may have impacted on the battery performance. Battery failure results from inability of the battery to supply useful amount of power to the load. Essentially, when a load is connected to a battery the terminal voltage of the battery will drop drastically; a situation which can be explained as ‘the battery dropping most of its voltage across its internal resistance’ with no power available for the external load (resistance). Ideally, the internal resistance of a 12V lead acid battery may be around 2 – 11 m Ω depending on the battery Ampere-hour capacity (Ah), the higher the capacity the lower the internal resistance. It has been reported that the value for internal resistance of a 12V 70Ah battery as described in this thesis is approximately 4.5m Ω [13][14].

4.11.1 Battery Discharge Rate

Batteries (e.g. Lead acid batteries) used in renewable power applications need to be charged regularly to ensure that the battery is always in good operating condition. Essentially, the selection of batteries is based on the charge and discharge cycles of the battery. Discharge rate refers to the rate at which current is drawn from the battery. A battery discharges quickly when it is subjected to a high discharge rate [15]. For a current to flow from the battery to the load there must be a voltage difference, this is obtained as the potential difference between the two electrode terminals of the battery.

The duration of the battery discharge determines how much current can be drawn from the battery. **Figure 63** shows a typical example of what goes on inside the battery at load and no-load conditions. At no load, the battery voltage is referred to as electromotive force (emf) denoted by ε . For a nominal 12V battery ε is typically about 14.4 Volts. The battery voltage drops whenever an external load is connected, due to the Ir factor. The rate at which the battery is discharged and depth of discharge (DOD) are also critical in the life cycle performance of the battery [15].

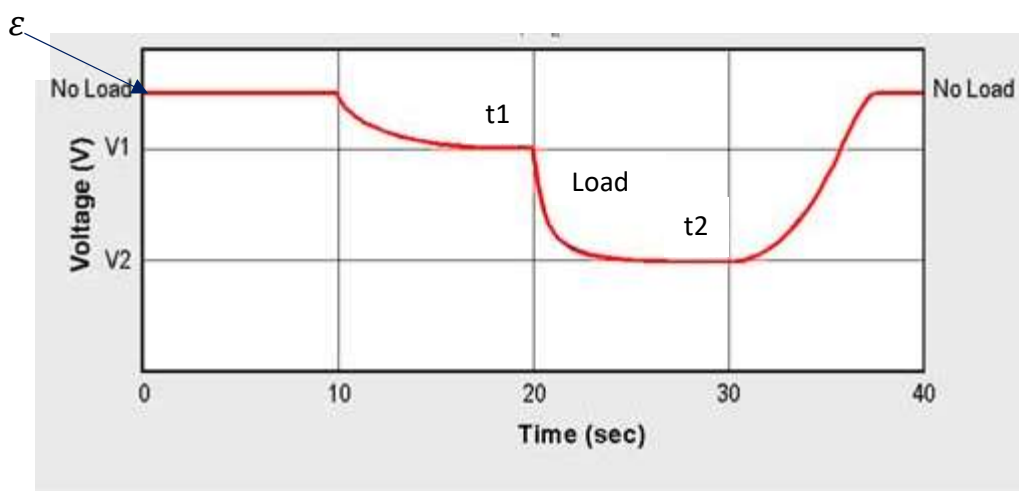


Figure 63. Battery voltage at load and no-load conditions [16].

t_1 = time at initial discharge

t_2 = time after discharge

Ideally, battery is known to be a voltage source and not a current source. In Day 3, the battery voltage can be seen to have decreased linearly in the negative direction when the 18W light load was on, but a linear discharge continued even when the lighting load was disconnected from it. The linear negative decrease in voltage may be because of the discharge current adjustments the battery was forced to make in order to maintain a steady voltage across its terminals. However, this make battery go a long time before it picks up to a steady voltage when it has stopped discharging (when the load has been disconnected or turned off) [17].

4.11.2 Determination of Battery Internal Resistance

'Day 3' was selected for the battery drain rate analysis because of the unavailability of wind power on this day, to isolate the power contributions from the solar panel. However, from the power performance analysis of Day 3, spikes were seen in the battery discharge. This scenario, can be attributed to the current drawn from the battery by the monitoring unit, because the load was seen to be constant at 18W on this day. **Table 21** lists the summary of the current consumptions by individual circuit components of the power monitoring unit.

Component	Quantity	Current consumption (mA)
INA219 current sensor	3	3
MicroSD card Breakout board	1	150 approx.
Arduino	1	40
Total	5	193

Table 21. Current consumptions each components of the power monitoring unit.

From the table, the total current consumption of the monitoring unit is approximately 200mA (0.2A). An expression used to determine the current draw from the battery is given as follows;

$$Current = \frac{Ampere-hou \text{ capacity}}{Discharge \text{ duration}} \quad (Equation 23)$$

Now, to determine the current consumption by the load, it follows that discharge duration can be obtained from the plotted points previously shown in **section 4.8.1**;

But, battery nominal capacity = 70Ah

$$Discharge \text{ current} = \frac{70}{6} = 11.7A \text{ (discharge duration} = 6 \text{ hours)}$$

Now, the load resistance R_L can also be determined using;

$$Power = \frac{V^2}{R} \quad (Equation 24)$$

$$\text{Hence, } 18 = \frac{12^2}{R_L}, \text{ (at 12 V)}$$

$$R_L = 8\Omega,$$

The battery internal resistance can be deduced by extrapolating the voltage slope to the beginning of the discharge pulse from the battery curve as shown in **Figure 64**, using the following equations;

$$Y = mX + c \quad (\text{Equation 25})$$

This is an equation for a straight-line graph used to determine these parameters; m = slope of the graph which gives the battery internal resistance.

$$= \frac{\Delta y}{\Delta x} = \frac{V}{I \times t} \quad (\text{Equation 26})$$

But, comparing the straight-line graph to equation representing voltage of a battery at discharge, gives;

$$V = -rI + \varepsilon \quad (\text{Equation 27})$$

$$Y = mX + c \quad (\text{Equation 28})$$

However, since battery manufacturers do not provide information that will be key in obtaining the battery electromotive force (open circuit voltage), therefore this makes it difficult to accurately predict the battery electromotive force (emf) upon termination of discharge. Studies have suggested that this varies approximately 0.2V/cell from fully charged to fully discharged [18]. However, using this value may result to some errors but an accuracy of $\pm 1\%$ for a voltage measurement may be acceptable [19]. Therefore, in this design, the emf is deduced using the following equation;

$$\varepsilon = \varepsilon_v + 0.2 * 6 \quad \text{Equation 29}$$

Where $\varepsilon_v = y - \text{intercept}$ of the battery voltage – time graph

From the battery curve $\varepsilon_v = 12.9V$ {c = y (V) = intercept and $\varepsilon = 1.2V + 12.9V = 14.1V$.

The current that flowed when the light was turned on = $I = \frac{\varepsilon}{r+R}$ (Equation 30)

Therefore, $I = \frac{14.1}{(0.0045)+(8)}$

$$I = \frac{14.1}{8} = 1.76A$$

Then total load current = $(1.76\text{A} + 200\text{ mA}) = 1.76 + 0.2 = 1.96\text{A}$.

$$\text{Internal resistance} = \frac{\Delta V}{I t} = \frac{\text{Change in voltage}}{\text{Current} \times \text{time}} = \frac{0.20}{1.96 \times 6} = \frac{0.20}{11.78} = 16.98\text{m}\Omega$$

Consumption for 6 hours = $1.96 \times 6 = 11.76 \cong 12\text{ Ah}$.

And the voltage drop is $(I r) = 12\text{ A} \times 0.0169\text{ Ohm} = 200\text{ mV}$.

Therefore, the battery voltage which dropped from 12.75V to 12.55V when the light turned on, can be verified as; $12.75 - 0.200 = 12.55\text{ V}$, which is equal to 12.55V as shown in the graph, and this confirms the value of the internal resistance obtained from this calculation to a considerable level of accuracy.

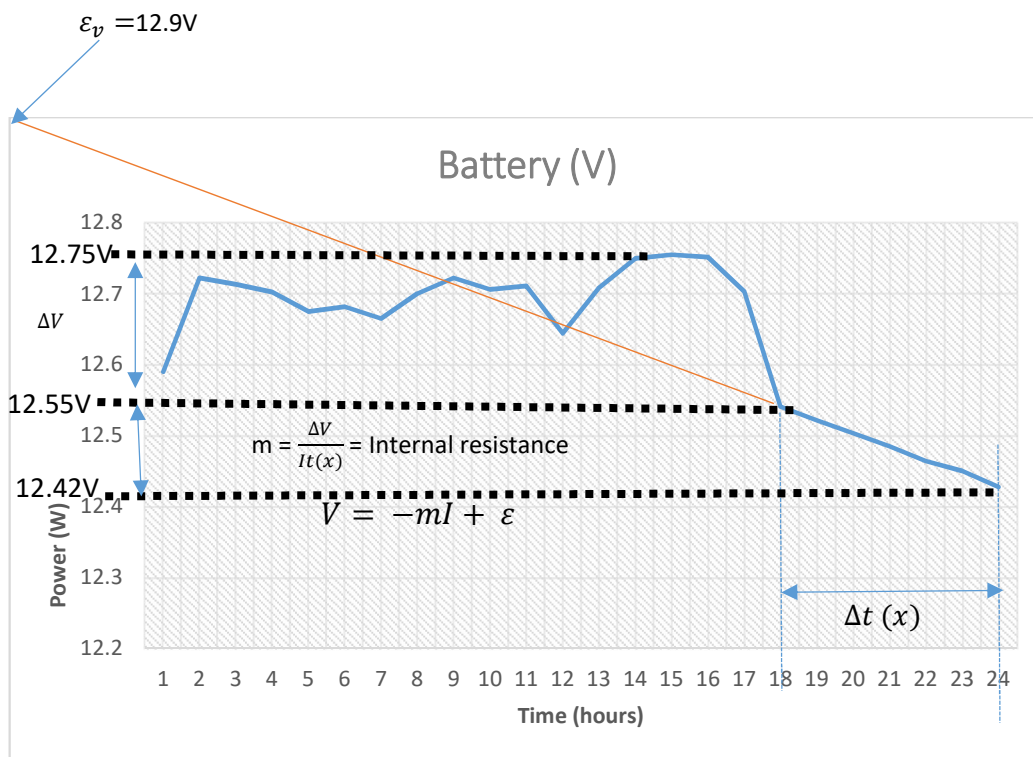


Figure 64. Obtaining the battery internal resistance.

From the calculations, it was found that the battery emf was 14.1V reading from the y-intercept when the battery was on no load, and the battery internal resistance was found to be $16.98\text{ m}\Omega$. As described earlier, the emf of a nominal 12V battery is typically about 14.4 Volts, and this is close to the calculated emf value at 14.1V, and this shows the accuracy of the process. The battery voltage dropped from 12.75V to 12.55V when the 18 W light load was connected. Hence, an inference that the terminal voltage was

12.55V. It was clear that the battery internal resistance had increased over the years and have significant impact on the current delivery of the battery when it was connected to a load. The increase in the internal resistance of the battery can be calculated as $16.98 - 4.5 = 12.5m\Omega$, this is approximately 3 times the recommended value for internal resistance of a 12V 70Ah battery, meaning the active components of the battery had declined as can be seen in dip voltage drop of the battery, whenever it is connected external to load (when the light come on).

4.12 Monitoring of solar PV system in Abuja Nigeria

This chapter concludes with a brief section discussing a solar PV system installed in Abuja, Nigeria. The data obtained from the system is analysed here. The system consists of 4 Solarland solar PV panels rated 240 W x 2, 220 W and 250 W, and 2 x 220 Ah@24V battery bank in series connection, with 2 panels in series and 2 panels in parallel. The PV system is connected in series – parallel form and has a total capacity of 936 W (15.6A Imp x 60V Vmp). The panels are interlocked to a **Fangpusun MPPT 45A/150v 12-24-48v** charge controller to regulate the battery charging process. Unlike the system described previously where the power monitoring unit was designed and constructed by the author of this thesis, the monitoring equipment used in this current system is a commercially available **Victron** energy monitor. The PV system is connected to the battery via the charge controller and then to the household appliances (load) via an inverter. The inverter is bi-directionally connected to the grid, and this means it imports power from the grid to charge the battery when the PV is not operational. The energy from the grid is not monitored, and power imports from the grid cannot be quantified. The battery voltage and load characteristics are therefore not considered in this analysis. The schematic with the complete system configuration plus the costs of individual components of the system is shown in **Appendix 1. Figure 65** depicts the actual installation with the monitoring unit. The solar panels are ground mounted, with orientation facing south at 81° vertical tilt (shown in **Figure 66**). The system is installed in Kuje Abuja Nigeria, with coordinates at 8.8764° N, 7.2437° E. A series of data was collected for two months, this is based on daily energy yield of the PV system. Analysis of the data collected are presented in the following section.

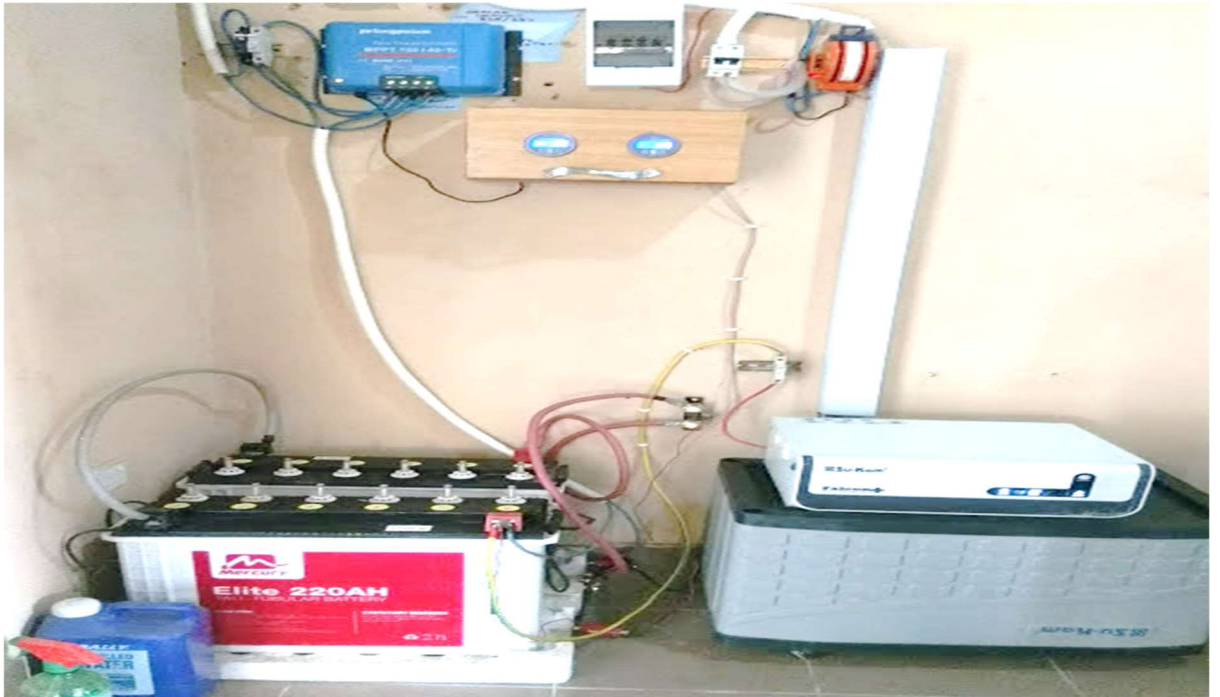


Figure 65. Solar array set up with battery and inverter connection.



Figure 66. Solar array installations at Kuje estate Abuja

4.12.1 Daily Power Outputs of the 936W PV Array and Battery Voltage

Data were recorded from 20th January to 19th February 2017, and plotted as shown in **Figure 67**, there are variations in the output power over the period recorded. The worst day was on the 22nd of January 2017, at 104W.

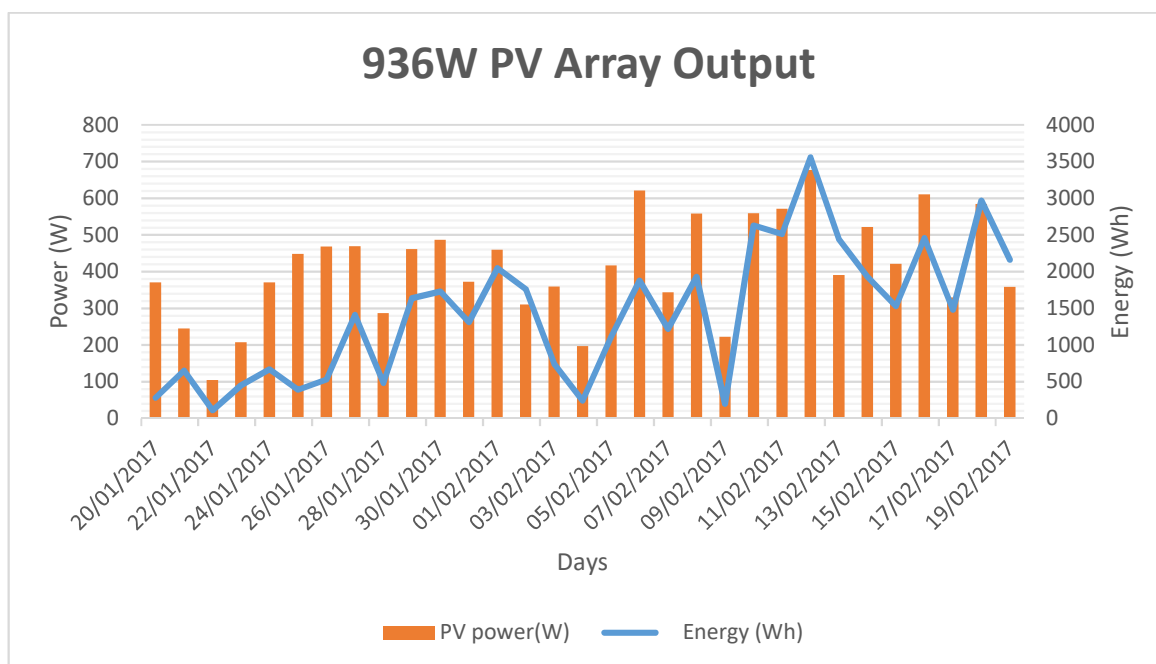


Figure 67. 936W PV array output power performance characteristics.

Over the 30 days, for the clear weather conditions noted during the period, the PV array seemingly did not produce to its optimum power capacity, its power performance was highest on the 12th February 2017, when it peaked at 677W. The daily energy productions averaged at 2.5 kWh. However, this system described here and the power performances seen will be considered later in this thesis to investigate the sizing of a PV system capacity for a typical household in Nigeria.

4.12.2 Summary

It has been shown the importance of monitoring in the early stages of capacity sizing, especially for intermittent power sources such as the solar photovoltaics. In actual sense, designing a RE systems requires careful handling, to avoid over sizing or under – sizing the system. Ideally, for solar power system designs, it may be difficult to size a

system to avoid an excess energy or over – production due to the variable nature of the solar energy resource. However, it is possible to store this excess energy in the battery, but it is also possible that when this battery is full and there are still some excess available it could be used to generate hydrogen. In future, hydrogen could be a viable solution to intermittency inherent in renewable energy. The solar- wind analysis has shown the difference in variability of wind as compared to solar, however, it can be deduced that, on predictability scale, solar energy has an edge over wind energy system. This data monitoring has shown that these are possible. These are shown in detail in later part of this thesis.

4. References

1. Arduino Uno; online available at <https://www.arduino.cc/en/main/arduinoBoardUno> accessed on 21/05/2016
2. Microchip Atmel; online available at <http://www.atmel.com/devices/atmega328.aspx> accessed on 22/05/16.
3. Adafruit microSD card breakout board; online available at <https://www.adafruit.com/product/254> accessed on 21/05/2016.
4. Texas instrument INA219 current sensor; online available at <http://www.ti.com/lit/ds/symlink/ina219.pdf> accessed on 21/05/2016.
5. Adafruit INA219 high side current sensor; online available at <https://www.adafruit.com/product/904> accessed on 22/05/2016.
6. Online available at <http://www.johngineer.com/blog/?p=1178> accessed on 22/05/2016.
7. Traco power; DC-DC converter, online available at <http://www.tracopower.com/home/> accessed on 22/05/2016.
8. Online available at <https://www.engineersgarage.com/articles/current-sensor> accessed on 12/12/2016.
9. Online available at <http://dangerousprototypes.com/blog/2012/01/27/interfacing-a-pic-microcontroller-with-the-acs712-hall-effect-current-sensor/> accessed 02/12/2015.
10. Marlec charge controller; online available at <http://www.marlec.co.uk/product/hrdi-controller/> accessed on 22/05/2016.
11. NASA, online available at <https://eosweb.larc.nasa.gov/sse/> accessed on 07/09/2015.

12. Online available at <http://farside.ph.utexas.edu/teaching/302l/lectures/node57.html> accessed on 22/09/2015
13. Online available at <http://hyperphysics.phy-astr.gsu.edu/hbase/electric/dcex6.html> accessed on 24/09/2015
14. Internal resistance; Online available at <http://www.unionbattery.com/images/1.7.pdf> accessed on 07/10/15
15. Foster, R., Ghassemi, M. and Cota, A., 2009. Solar energy: renewable energy and the environment. CRC Press.
16. Online http://batteryuniversity.com/learn/archive/rapid_testing_portable_batteries accessed on 21/07/2016.
17. Texas instrument application report; Single-cell Battery Discharge Characteristics Using the TPS61070 Boost Converter: online available at <http://www.ti.com/lit/an/slva194/slva194.pdf>
18. Colson, C.M., 2012. Towards real-time power management of microgrids for power system integration: a decentralized multi-agent based approach. Montana State University.
19. Duryea S, Islam S, Lawrence W. A battery management system for standalone photovoltaic energy systems. In Industry Applications Conference, 1999. Thirty-Fourth IAS Annual Meeting. Conference Record of the 1999 IEEE 1999 (Vol. 4, pp. 2649-2654). IEEE.

5.0 Development of a Modelling and Simulation Tool for Off Grid PV-Hydrogen Energy System

5.1 Introduction

Modelling refers to mathematical or logical analysis of a system, as a basis for simulation of physical or empirical processes that occur within the system. This is usually based on developing an algorithmic representation that mimics the real life behavioural characteristics of the system. A Solar-hydrogen system consists of various components, which by way of either physical or chemical interaction within the limits imposed by certain strategies used to control the system, produces a desired result. However, during the design phase of a solar-hydrogen system, it is important to implement a model representation of the system to have a feel of how it will behave before the actual real-life testing. A well-optimised renewable energy system with incorporated energy storage will improve the energy yield and likely extend its service. However, with storage facilities it is crucial that at early stages proper prior studies are done to ascertain or estimate the energy characteristics of the system for the selected location. To do this, it is possible to utilise a software modelling approach and/or data monitoring processes. The choice of such tools depends largely on the criteria and the kind of load the system will serve. Modelling allows optimisation of the system elements in terms of sizing and cost. This chapter presents the development of a software tool for modelling, sizing and simulation of solar – hydrogen system for remote power access. The primary objectives are to obtain the optimum system component sizing which addresses properly the needs of the system end user, as defined by the desired load characteristics. Several software tools are available for use in this type of application, and these will be discussed in the following section.

5.1.1 Selection of Modelling Tools for RES with Energy Storage System.

Of the many RE modelling and sizing software tools available, most are commercially licensed to the end user, and some of these may have basic versions available to trial or for free download. A limited number are freely available with no licensing restrictions. Using such tools enables comparison of different scenarios to evaluate the best possible solution for RE-configuration. The list below summarises those software tools which can be used to size and model a RES with hydrogen production capability;

- HOMER – Hybrid Optimisation model for Electric Renewables
- iHOGA – Improved Hybrid Optimisation by Genetic Algorithm
- TRYNSYS – Transient System simulation
- HYDROGEMS (Hydrogen energy Models Suitable for Simulation of Integrated Hydrogen Energy Systems - this package is incorporated into the TRYNSYS software),
- UniSyD3.0
- ARES (Autonomous Renewable Energy Systems).
- RET Screen
- Matlab/Simulink

In the system design, modelling tools are selected based on the objectives they can serve. HYDROGEMS can simulate the performance and thermal characteristics of the hydrogen production process, also simulate the hydrogen mass flows and electrical and production of renewable energy based stand – alone power systems. One of the drawbacks with this tool is that it is not designed to simulate a system that integrates hydrogen as a storage medium, rather, it is limited to the RE based hydrogen production [1]. The UniSyD3.0 tool bears same similarity with HYDROGEMS in terms of application. A simulation that involves UniSyD3.0 will consider a hydrogen – electricity cogeneration option but no direct electricity storage will be simulated [2].

ARES simulates a RE system with battery storage. It is a software tool developed at the School of Engineering, University of Cardiff. The software requires an input of the basic weather profile and load before it can calculate the system loss of load probability and the system autonomy. HOMER, iHOGA and Matlab/Simulink software tools can simulate a renewable energy system that integrates hydrogen as a storage medium. While HOMER and iHOGA are dedicated software tools for RE-systems modelling and

simulation, the Matlab/Simulink software tool has the capacity to model and simulate multi-domain dynamic systems. This flexibility of approach means its modelling and simulation capabilities are not limited to RE-systems only.

In recent years a number of studies have been carried out in modelling and simulation of solar – hydrogen power systems, in order to size and determine the system reliability and to evaluate seasonal performances and cost minimisation [3]. Uzunoglu, Onar and Alam [4] describe the integration of different energy sources, utilising a 5kW photovoltaic, 10kW electrolyser, 5kW fuel cell, 165F supercapacitors and power converters to meet sustained load demands of stand-alone residential micro-grid users, while testing the sensitivities under various natural conditions. The authors have argued that variability of weather conditions and the difficulty in storing electric power generated during favourable weather conditions demand that a hydrogen-based energy storage system be integrated into the mix. The stored energy is released on demand (usually at night) via a hydrogen fuel cell. Bernal-Augustin and Dufo Lopez [5] summarized the most relevant research papers over the past decade on solar-hydrogen power systems, especially in terms of cost minimisation and optimum power performance. According to their findings, a stand-alone hybrid renewable power system is more suitable for off-grid applications than systems that have only one power source (e.g. PV). It is desirable at the design stage of every renewable based power system to ascertain the suitability of the selected choice of technology for the specified location. Also, the assessments of seasonal weather variation and density of renewable energy resources and the associated type of load at the location is crucial in enhancing the power and efficiency performances of the selected RE source. Ideally, this can be done through modelling of the individual system components with the use of the aforementioned software tools before the actual implementation.

5.1.2 Renewable Energy Systems Optimisation

The sizing process involves finding an iterative method that best defines a solution of a given problem under a predefined termination criterion. For renewable energy systems, this is characterised by definition of possible system components and finding the optimum blend which best satisfies load demand. This will probably also be constrained

by cost considerations. In the RES optimisation process, an input of data for example, the number of PV panels, the battery bank, etc can be used to represent the decision variables. The objective function can be expressed using a mathematical equation that relates these decision variables. It could be represented in form of minimising the cost per kWh of the hybrid RE system components including installation and maintenance costs, or maximising the available energy resources to satisfy the load demand. The constraints can be one or several factors imposed on the system using inequalities as a requirement set out as conditions that must be satisfied. Some notable optimisation methods include; linear and nonlinear programming, probabilistic and dynamic programming. Optimisation can be linear or nonlinear depending on the problem and algorithm adopted in solving the problem. A standard optimisation problem is of the form [6];

$$\text{minimise } f_o(x),$$

subject to;

$$f_i(x) \leq b_i, i = 1, \dots, m$$

Where x = optimisation variable of the problem, f_o is the objective function, f_i are the inequality constraints and constants b_i are the limits imposed on the constraints. HOMER and iHOGA are RES optimisation software tools.

5.1.3 HOMER

Hybrid Optimisation Model for Electric Renewables (HOMER) is a computer model that simplifies the task of designing hybrid renewable micro-grids. The sensitivity and optimisation analysis algorithms integrated in the software enables the user to evaluate the economic and technical feasibility of many technology options and to account for variations in technology costs and energy resource availability [7]. This software tool was developed at the National Renewable Energy Laboratory USA in 1993, over a span of 20 years. It was initially developed without the ability to simulate on demand, so all systems appear to have hourly data. This later became the first improvement that was added in HOMER. It is the most widely used software tool for modelling a hybrid renewable energy system, both on-grid and off-grid. The latest updated version of

HOMER is the HOMER Pro version 3.8.4 (March 2, 2017) [8]. This software uses windows as a computer platform with visual C++ as a programming language.

Features of HOMER;

- The software can simulate a renewable energy system over an annual cycle.
- It can suggest the design of various systems based on economic parameters.
- HOMER can generate results and list them per feasibility and sorts them by the net present cost.
- HOMER does not allow multi-objective function for minimising the net present cost, it uses only a single objective function in the optimisation process. Also, the software does not rank the results of the hybrid system configurations in terms of levelised energy cost, and this is a potential drawback.

5.1.4 iHOGA

Improved Hybrid Optimisation by Genetic Algorithm (iHOGA) is a software tool developed at the Electrical Engineering department of the University of Zaragoza Spain, by Dr. Rodolfo Dufo-López. The earlier version 2.0 was called HOGA [9]. The software was developed in C++ for the simulation and optimisation of hybrid renewable energy systems for generation of electrical energy (DC or AC), and included hydrogen. According to the developers, the tool can be utilised to simulate and optimise energy systems of any size. Both grid and off-grid systems, with or without load, and different cases of Net metering can be defined [10]. Optimisation is dependent on obtaining the minimum system costs that satisfy the load over the lifetime of the project, and this defines the mono-objective optimisation in iHOGA. Similarly, multi-objective optimisation can be achieved where additional variables (which includes CO₂ emissions or unmet load) may also be minimised [10]. A simulation algorithm based on an enumerative method is also available in the tool. In the enumerative method, all possible combinations for both components and control strategies can be evaluated. However, this approach is very heavy on processing time, since the number of components and strategies may require extreme iterative sequences [10].

Features of iHOGA

- After optimisation iHOGA ranks the results of the hybrid system configurations in terms of levelized energy cost and the net present cost.
- Any energy system design process that involves a high number of variables can take considerable time to obtain convergence in the optimisation process. Heuristic optimisation techniques are the best design technique to be used when high number of variables are involved, as it allows low computational requirements, and hence obtains results in a relatively short calculation time. One of the most widely used heuristic techniques is the so-called genetic algorithm. Genetic algorithms (GAs) refers to the use of computer programs to facilitate a processes that mimic the biological evolution in order to solve problems [11]. This idea stem from creating an initial population of possible solutions, in the process the fittest members among the population survives, and combine amongst themselves to form the next possible solutions, to achieve better results [11]. One major advantage of a GA is its ability to code an infinite number of system parameters [12]. iHOGA uses genetic algorithm to carry out optimisation, both for system components (main genetic algorithm), and for the control strategy (secondary genetic algorithm).
- iHOGA considers battery depth of discharge in its optimisation process.
- iHOGA allows for different loads, AC and DC systems, and hydrogen storage.
- The software optimises RE system on an hourly basis, over an annual cycle (8760hr).
- The choice of enumerative method is also available in iHOGA, but this approach suffers from long computational times when potentially complex systems are being considered [10]
- iHOGA allows the option of selling electricity to the grid.

5.2 Justification for the New Software Development


When considering adoption of a software tool for RES optimisation care is needed to ensure that the chosen package can satisfy the requirements of the job, especially as there may be a significant cost involved. For a pre-defined specific project, it might be that the tool available may not have all the necessary facilities required by the RES designer. In addition, some of these software tools are not user-oriented and could be highly complex to use for someone without a deep technical or engineering background. In addition, and despite the wide proliferation of renewable energy-based software tools now available, little attention has been paid to the development of a software tool that includes a facility for addressing cooking problems especially in the rural areas of developing countries. For this emerging application area, the development of a project specific software tool becomes necessary. The modelling tool developed in this research simulates solar-based systems with energy storage and hydrogen facilities for cooking purposes.

5.2.1 The Software Development Platform

In this thesis, a software tool called **SOHYSIMO** for design, simulation and optimisation of a solar hydrogen power system developed by the author is presented. The software is based on Excel Visual Basic for Application (VBA). The choice of Excel VBA is based chiefly on its very wide availability. Excel Visual Basic is an easy way to perform some task in Excel which the standard Excel user interface environment does not seem to address, especially, some tedious repetitive tasks [13]. Two ways by which a specified task can be accomplished in Excel VBA are with VBA Macro and VBA Userform. VBA Macro is based on the standard Excel environment, while VBA Userform can be utilised to create a customisable user interface program. VBA Userform was employed in the development of this current software, as it presents an easy way to create a custom dialogue box, which is an important advantage of Excel VBA. Previous modelling tools developed over the past decade have successfully used Excel VBA as a platform for development of software tools for off-grid renewable energy systems. Ali and Salih [14] proposed a tool for a sizing model of RES components of a photovoltaic power system in Iraq. Vladimir and Suchanek [15] developed a comprehensive software model they called expert system, which can be used to simulate and optimise an off-grid hybrid

renewable power system comprising solar, wind and battery storage. Kuo et al [16] describes the use of VBA for development of a tool which may be used to assess system operating conditions and characteristic behaviour of a solar and wind energy system. Mhalas et al [17] demonstrated a modelling tool for visual energy performance assessment and decision support for dwellings. Among all studies in literature only Vladimir and Suchanek [15] tried to address the issue of balancing the energy supply, but their model did not seem to include a system by which the excess power which can be generated from these energy sources (especially solar and wind) can be utilised. This thesis introduces a user-oriented software model for simulation and optimisation of renewable power system where the excess energy can be utilised. Renewable energy systems, especially solar sometimes generate more power than is required, this over – production usually occurs in standalone RE power system when the load is satisfied and the battery has attained its full state of charge (SOC), in this situation any energy that is generated becomes a surplus. As already highlighted, utilising this surplus energy in an efficient way in hydrogen energy forms the main thrust of the developed software tool.

5.2.2 General Description of SOHYSIMO Tool

‘SOHYSIMO’ is an acronym for **Solar Hydrogen Simulation Model** . It was developed by Christian Onwe (the author of this thesis) for modelling and simulation of solar – hydrogen production for remote power access. It is a DC power simulation software optimised for low power consuming households, especially rural dwellers. The software has a facility which can help a designer to make an informed decision on how the hydrogen produced by the solar PV can be utilised. Another important feature which is available in SOHYSIMO is multi-simulation capability. This facility enables the user to fast-toggle between simulating with imported resource data and simulated/modelled resource data after the first complete system simulation. The tool stores the imported and simulated/modelled data into different locations, and uses an integrated control block to switch between the two resource input data simultaneously. Ultimately, this means that the user only need to click a button and the simulation will change from imported data to simulated data. It ensures quick visual comparisons. This facility is presently unavailable in most RE modelling and simulation tools. The following describes step-by-step development process of the present software tool;

The tool is implemented in modular form to enhance its simulation accuracy and speed, based on multipage User form object. For energy optimisation, the Generalised Reduced Gradient (GRG) nonlinear optimisation available in the Excel SOLVER Add-in facility was utilised. For a given optimisation problem, optimisation methods can be categorised based on the following parameters;

- The constraints type
- Nature of variables
- How these variables are determined
- Problem structure
- Nature of the equations
- Number of objectives

Optimisation can be broadly split into multivariable search process, single variable search process and stochastic process. Multivariable search process can be classified into constrained and unconstrained search methods thus [18];

1. Unconstrained multivariable search methods include; Newton's and quasi-Newton's method, conjugate gradient and logical methods.
2. Constrained multivariable search methods, include; Successive linear programming and linear quadratic method, generalised reduced gradient method, augmented Lagrangian functions, and Newton's (equality constrained).

Detailed explanation or descriptions of each of the above methods is out the scope of this work. In solving engineering problems, constrained nonlinear programming optimisation is often a preferred choice. The two well-known and most used nonlinear optimisation methods are sequential quadratic programming methods and generalised reduced gradient methods [19].

These two methods have been described by researchers as the best deterministic nonlinear optimisation methods [20]. The two methods always search for optimum either local or global that is closest to the starting initial guess. Therefore, the method adopted in the developed tool is gradient based optimisation, which fall under the category of constrained multivariable search method. In gradient based optimisation

method problems can be solved by iteratively searching a minimum of a dimensional target function and this target function can be approximated by a Taylor series expansion and computed in loops to obtain a minimum [21].

Newton's method is also a gradient based optimisation, in which a set of constrained optimisation problem is reduced to solving a sequence of quadratic problems [6]. Generalised Reduced Gradient nonlinear optimisation adopted in the tool, and this has the capacity to transform inequality constraints into equality constraints by introducing slack variables. This option was selected because it is a robust nonlinear programming method.

In the following narrative, each of the programme screens are described sequentially, with additional front-end screenshots as visual aids to better visualise the operation of the software. The detail behind the interface will be discussed later in this section.

PAGE 1 - PV sizing: This page contains a PV sizing block where a user or RE designer can estimate PV power capacity required for a project based on inputs such as; load, peak sun hours (PSH) of the site, PV module efficiency and power conditioning equipment. The page also has a facility for manufacturer's data fitting, where a designer can enter a PV data specification by manufacturers to determine a modified PV panel characteristic based on local atmospheric conditions. **Figure 73** shows the PV sizing page of the **SOHYSIMO** software user interface (UI). These features have more functionality than most RE simulation software, and has been designed to be accessible to both engineers and those with little technical background to do a pre-size and determine the system size specifications for their solar project. As a further aid to accessibility each screen of the software has a 'help' facility where the user can click to view additional documentation which contains guidelines more detailed information.

Figure 68. PV sizing User Interface of SOHYSIMO

PAGE 2 - Input data: It is in this page that all input data dialogue boxes for the system simulation are contained. The tool provides two options for input of solar irradiation, imported or simulated/modelled data. A user will need to input data pertaining **time zone, latitude, and longitude** and the slope angle of the solar PV for the site or location at which the project will be implemented. However, the slope angle depends on the roof (if it is a roof mounted design) and for ground based the system can be optimised. There is no default value for slope angle in the developed tool. An error control block integrated into the tool ensures that all input boxes must be completed before the simulation will execute. Clicking the 'ok' button initiates acceptance of the inputted data. The "save simulation" button transfers the simulated data to a location where it will be stored. The simulation process will not complete until 'save simulation data' button is clicked. For the load profile input data, the software provides an easy and user-friendly method. A user can either import a handy hourly load profile data or input a load profile in the box area provided. 5 different loads (appliances) can be entered at a time in the space provided. The 24-hour load profile model derives from the complexities in predicting the variations in energy consumption for a household. It entails that, a single 24 – hour load profile entry is spread to represent a steady daily load demand pattern over a year. The user need just enter zeros for the period when the load will be turned off. After the last load data is entered, a click on the 'Click to

Accept Data' button records the load profile, while 'Total (Wh/day)', button transfers and stores the data and makes it available for simulation. It will display an error message if a box is left empty. If a user wishes to simulate the temperature effects on the PV output power, the user must click on the 'Model temperature effect' Checkbox. A graphical visualisation of load profile is also available. **Figure 69** shows the input data page of the developed tool UI.

The screenshot shows the 'SOHYSIMO' application window with the 'Input data' tab active. The main area is titled 'ENTER 24 - HOURS LOAD DATA' and contains a table with 24 columns (hours 1-24) and 5 rows (LOAD 1-5). Below the table are several control panels:

- Left Panel:** A 'Click to Accept Load Data' button, a 'Help' button, and a blue box labeled 'DISPLAY TOTAL DAILY LOAD DEMAND' with a 'Click Here - Total (kWh/day)' button and an empty input field.
- Center Panel (ENTER LOCATION DATA):** Fields for 'Enter Latitude', 'Enter Longitude', 'Enter Time Zone', and 'Enter PV Tilt Angle', each with an 'OK' button. A 'START' button is also present. A warning note states: 'NB: Do not click on 'START' or 'SAVE SIMULATION DATA' buttons unless you want to simulate Irradiation'. Below are 'SAVE SIMULATION DATA' and 'kWh/m²/day' buttons.
- Right Panel (HAVE HOURLY SOLAR IRRADIATION DATA ??):** An 'Import' button, a 'kWh/m²/day' input field, and a 'Modified Irrad at Tilt' button with another 'kWh/m²/day' input field.
- Bottom Panel (HAVE HOURLY LOAD DATA??):** An 'Import Load' button and a 'kWh/day' input field.
- Bottom Center:** A checkbox for 'Model Temperature Effect' and three input fields for 'Temp coeff of power (%/°C)', 'NOCT (°C)', and 'Eff at STC (°C)'.

Figure 69. Data Input user Interface Page of SOHYSIMO.

Page 3 – General data: This is the main page where details regarding the sizing capacity of major components (Solar PV, Battery, Electrolyser and H₂-Genset), of the solar-hydrogen power system will be input into the **SOHYSIMO** software tool. Simulation can be initiated by clicking the 'start simulation' button. It will display an error message if a user forgets to select a solar resource option, this control was implemented with an embedded error control algorithm, which will be discussed in the later part of this **chapter**. Graphical visualization of simulation results is also available on this page. The software can simulate hourly power performance of the RE-system for a year period; a user can view month by month or annual power characteristics of the simulated system by a click on the requisite button. Simulation results can also be exported and saved on the desktop. **Figure 70** shows the general data page of **SOHYSIMO** tool UI.

SOHYSIMO

PV Sizing | Input data | General data | Cost Evaluations | Energy Assessment | Cooking Decision on Hydrogen Use

SYSTEM REQUIRMENTS

Enter DC Voltage (V)

Enter Depth of Discharge (%)

Enter PV Derate Factor (%)

OK

Use Imported Solar Data

Use Simulated Solar Data

Simulate H2-GENSET Power

Simulate ELECTROLYSER

Start Simulation

COMPONENTS

Enter Size of Solar Panels (kW)

Enter Battery Size (Ah)

Enter Size of Electrolyser (kW)

HAVE ELECTROLYSER PARAMETERS??

Power Consumption Parameters
A (kW/kg/h) B (kW/kg/h) **OK**

Display H2 Mass Flow (kg/h)

Display Electrolyser Efficiency (%)

ENTER GENSET PARAMETERS

Enter H2-Genset Size (kW)

H2-GENSET CONSUMPTION

A B

OK

Click To Accept Entries

Export Simulation Result

Help

CLOSE

O H

PLOT GRAPHS

Plot Simulated Irradiation

Plot Imported Irradiation

Plot Sys Monthly Av. Power

Plot Annual Totals

Plot Monthly Average PV

Plot Daily H2 prod (kg/day)

SELECT HOURLY GRAPHS BY COMPONENT

OK

VISUALIZE HOURLY PV SYSTEM GRAPH PER MONTH

JAN	JUL
FEB	AUG
MAR	SEP
APR	OCT
MAY	NOV
JUNE	DEC

Figure 70. General data user interface page of SOHYSIMO.

Page 4 – Cost evaluations: Cost calculations for all system components (Net present cost and levelised cost of energy) can be determined by entering in this page, the costs (capital, operating and maintenance (O&M) and auxiliary components) of individual system components of the solar-hydrogen power system. A click on the start button executes the computation. **Figure 71** shows the user interface (UI) for cost evaluations in SOHYSIMO. The tool uses the following formulas to calculate the Net Present Cost and levelised cost of energy (LCOE) of the Solar based hydrogen system;

$$NPC = \frac{Tot_{AnnC}}{CRF(interest, N)} \quad (\text{Equation 31})$$

$$LCOE = \left[\left\{ \sum_{n=1}^{n=25} \frac{(Capex + O\&M)}{\sum kW} \right\} * CRF \right] \quad (\text{Equation 32})$$

$$\text{Where } CRF = \sum_{n=25} \frac{interest\ rate * (1 + interest\ rate)^n}{[(1 + interest\ rate)^n - 1]} \quad (\text{Equation 33})$$

$$Tot_{AnnC} = \text{Total Annualised cost of system}$$

n = time, in years

$Capex$ = capital expenditure

$O \ \& \ M$ = operation and maintenance cost entered by the user

Figure 71. Cost evaluation user interface page of SOHYSIMO.

Page 5 – Energy assessment: In the **SOHYSIMO** energy assessment page the component configurations that may aid in maximising the number of days the load will be supplied with steady electric power will be obtained. This algorithm was implemented with codes that assess the number of hours in a year which the solar photovoltaic will not be operational, and relate the difference with battery capacity and state of charge, and automatically computes the required ‘Days of Autonomy (DoA) of the battery system and displays the result. This process ensures a more efficient way of calculating the DoD in renewable power system design. In this process, the present developed software also suggests the capacity of system components (solar PV and Battery) which is expected (in a typical weather year) to cover the selected load profile with no shortfall. A facility for calculating the system carbon savings is also included. This requires entry of parameters of data regarding carbon and hydrogen emission factors, defaults values for these are; 0.541 kgCO₂/kWh for solar PV, and 0.700 kgCO₂/kWh for hydrogen cooker. These factors are used to calculate the carbon savings for each kilo watt-hour of energy produced from solar PV and clean cooking fuel respectively. It should be noted that these factors vary by country, therefore, a user may need to check for this. **Figure 72** shows the energy assessment user interface.

Figure 72. Energy assessment user interface page of SOHYSIMO.

Page 6 – Cooking decision on hydrogen use: One of the significant differences between the **SOHYSIMO** tool developed in this thesis and other tools is that it has a hydrogen cooking simulation package. In the simulation process, the user inputs a 7-day cooking load in kilo gram for firewood and litres for kerosene once, and **SOHYSIMO** repeats this demand for a one-year period. The user also has an option on whether to use hydrogen to meet cooking demand or use it on H₂-genset for power generation. This latter option effectively enhances the energy storage capability of the system, with associated sizing changes for the other system components.

The tool computes the amount of hydrogen required to meet the cooking need of the specified period and compares it to the load demand with H₂-genset. If the hydrogen produced is not enough to generate electric power for that period, the software will display a message with a decision, and vice versa. There is an additional facility to display graphically the computed hourly hydrogen usage of the cooker. **Figure 73** shows the hydrogen cooking page of the user interface.

Figure 73. Hydrogen cooking user interface page of SOHYSIMO.

Page 7 – Energy optimisation: in this page the optimisation of the RE system, as briefly described in **section 5.1.2**, is implemented. Optimisation is achieved by minimising the cost per kW of the total system capacity that can satisfy a required daily load demand over the lifetime of the project. The optimisation algorithm is implemented in SOHYSIMO as illustrated below;

$$\text{minimise } f\left(\frac{\text{Cost}}{\text{kW}}\right) = f(PV(\text{kW})) + f(PBatt(\text{kW})) \quad (\text{Equation 34})$$

subject to

$$P_{pv} \geq P_{load} * 1.09$$

$$P_{batt} \geq P_{load} * \left(\frac{\text{COUNTIF}(P_{pv}, <3)}{24} * \frac{52}{52} * DoD \right) / 1.9$$

$$P_{pv} \geq P_{batt} * 1.16,$$

$$P_{batt} \geq P_{load},$$

$$P_{pv} + P_{batt} \geq P_{load}$$

$$f(PV(\text{kW})) = P_{pv} * \text{Cost}Pv, \quad (\text{Equation 35})$$

$$f(P_{Batt}(kW)) = P_{batt} * CostP_{batt} \quad (Equation 36)$$

where P_{pv} = PV output power, P_{batt} = battery capacity,
 $CostP_{batt}$ = battery capital cost, $CostP_v$ = PV capital cost, P_{load}
= load power

For cost optimisation, operating and maintenance cost is an important component, a novel method has been developed, which can be used to compute the annualised operating and maintenance cost over the lifetime of the project as illustrated in **equation 37**;

$$O \& M_{Life} = \left\{ \frac{P_{life}}{Comp_{life}} \right\} * \left\{ \frac{Comp_{cost}}{P_{life}} \right\} + OM_e \quad (Equation 37)$$

Where, $O \& M_{Life}$ = Lifetime Operating and Maintenance cost

P_{life} = Project lifetime

$Comp_{life}$ = system component lifetime

$Comp_{cost}$ = cost of system component

OM_e = Operating and maintenance entered by user

The tool uses the following algorithm to facilitate hydrogen cooking optimisation
 $H_2Cooker > (P_{pv} - P_{load}) * (kWh/day) * 0.2$

To set this up in Excel Solver built in tool, the target cell can be specified as the objective to minimise, the cells that changes its values during optimisation process and this corresponds to the decision variables that need to be specified [22]. After this, the optimisation constraints were implemented. In Excel Solver, an optimisation method can be selected based on numbered algorithm, each of the three optimisation algorithms defined in Excel Solver (GRG Nonlinear, LP Simplex and Evolutionary) has a number that is associated to it. For example, GRG Nonlinear = 1, LP Simplex = 2, and Evolutionary = 3. The following codes selects a GRG optimisation adopted in the current tool;

Engine: =1, EngineDesc: ="GRG Nonlinear" (Selects Solver optimisation method). There are 3 Solver optimisation method methods available, they include simplex linear optimisation method, evolutionary optimisation method and GRG nonlinear optimisation method.

The whole optimisation process was implemented in SOHYSIMO using the following codes with description;

SolverOk SetCell: ="\$BY\$17", (Initialises Solver and the target cell was set to "\$BY\$17" by SetCell: ="\$BY\$17")

MaxMinVal: =2, (This minimises the target cell and number '2' selects minimisation, but if maximisation is sought number '1' can be selected as MaxMinVal: =1)

ValueOf: =0, (tells Solver to set the target cell to zero, the target cell or the objective cell must contain a formula)

ByChange: ="\$BZ\$3, \$CA\$3", _ (tells Solver to vary the decision variables)

Engine: =1, EngineDesc: ="GRG Nonlinear" (Selects Solver optimisation method)

SolverOk SetCell: ="\$BY\$17", MaxMinVal: =2, ValueOf: =0, ByChange: ="\$BZ\$3, \$CA\$3",

–

Engine: =1, EngineDesc: ="GRG Nonlinear"

SolverSolve UserFinish: =True (Stops Solver from displaying a result dialogue box)

SolverFinish KeepFinal: =1 (Tells Solver to keep the optimal result or solution found).

Figure 74 shows the 'Energy optimisation page'. The user will need to enter data pertaining the system capacity, the installed cost (all cost components must be entered in US dollars) and lifetime of each component considered. Also, the project lifetime will need to be defined for each component considered. Then click on the OK button to accept your entry. However, an error message will be displayed if a user leaves an empty box, or forgets to fill all boxes provided for these components. After optimisation, SOHYSIMO sorts the results based on low costs per KWh (LCOE) of the system. After optimisation, the tool allows the user to make two decisions whether to fully satisfy an annual cooking load or to satisfy part of the cooking load, based on the amount of excess energy generated. To facilitate this process, the user will need to click the 'click for 100% cooking' button, after one optimisation process.

SOHYSIMO

PV Sizing | Input data | General data | Cost Evaluations | Energy Assessment | Cooking Decision on Hydrogen Use | Energy Optimisation

ENTER PV PARAMETERS

Enter PV Capital Cost (\$)

Enter PV O&M Cost (\$)

PV Replacement Cost (\$)

Enter PV Lifetime (Yr)

OK

ENTER BATTERY PARAMETERS

Enter Battery Cap Cost (\$)

Enter Battery O&M Cost (\$)

Enter Batt Replacement Cost (\$)

Enter Project Lifetime(Yr)

OK

ENTER ELECTROLYSER PARAMETERS

Enter Electrolyser Cap Cost (\$)

Enter Electrolyser O&M Cost (\$)

Enter Elec Replacement Cost (\$)

Enter Elect Lifetime (Yr)

OK

Start Optimisation Help

Click For 100% Cooling

EXPORT OPTIMISATION RESULT

OPTIMISATION RESULTS

#	PV (kW)	Batt. (kWh)	Elec. (kW)	Init. Cap. Cost (\$)	O&M (\$/Yr)	Total NPC (\$)	CH2 (\$/kg)	LCOE (\$/kWh)
1								
2								
3								
4								

Figure 74. SOHYSIMO energy optimisation user interface.

5.3 Component Modelling and Sizing

The unpredictability in renewable power sources usually demands that some form of energy storage system be integrated into the mix. For instance, in a solar power system, energy that is stored during daytime hours can be utilised at night time when there is no direct supply but may be a considerable demand. This may be referred to as deferred supply. In this study, the system is designed such that after satisfying the load demand and charging the battery to its full SOC, any excess energy generated by the solar power system will be utilised to produce hydrogen via an electrolyser. The hydrogen produced in the process can be utilised as fuel in a hydrogen engine generator set (genset) to power the house or to meet cooking demand. Conventionally, fuel cells are used to provide the generation, because they are more efficient than a H₂-genset, but the choice of hydrogen engine in this thesis is due to the wide availability of petrol engine generators in the rural areas considered, as this will minimise cost and complexity of the system, and such generators can be modified to run on hydrogen.

With this scheme, the components to be modelled include the solar PV array, electrolyser, H₂-powered generator and battery storage. Considerable previous work in modelling sizing methods for renewable power systems is in the literature. For example, Zhou et al [23] extensively reviewed different sizing methods and suggested that optimum resource allocation based on load demand is essential for reducing the hybrid

system's initial cost and operation cost. Chadid et al argued [24] that the major concern in the design process is the accurate selection of components that can economically satisfy the load demand. To this end they developed a linear programming unit sizing method for rural power access system. In the literature several authors have proposed different optimal sizing methods based on artificial intelligence models [25][26][27]. However, among all these sources only Diaf et al [27] have proposed a way by which excess energy generated would be minimised by utilising a third energy source. In this thesis, a sizing model whereby the general governing equations of each component can be used to obtain the system size is proposed, and the selected component sizes are simulated.

5.3.1 Solar Panel Sizing and Modelling

In principle, the power output of the solar PV can be calculated as follows;

$$P_{pv} = \left(\frac{I_t}{I_{stc}} \right) * PV \text{ rated power (kW)} * \text{Derate factor (\%)} \quad (\text{Equation 38})$$

where; P_{pv} = PV power, I_t = incident solar radiation (kW/m²) on the PV array at time t, I_{stc} = solar radiation in kW/m² at standard test conditions.

The equation used for PV power calculations of the software tool developed in this thesis is based on **equation 38**. De-rate factor represents the anticipated losses due to dirt or ageing of the PV panel. A user will need just to input the de-rate factor and nominal power capacity of the solar panel and the tool calculates the output power based on hourly solar irradiation of the selected location or site. However, temperature has large impact on the performance of PV cells [28]. The open circuit voltage of a crystalline silicon solar cell decreases by 2.3mV per degree rise in temperature. Module manufacturers usually report the nominal operating cell temperature (NOCT) at 0.8kW/m² irradiance conditions in an ambient temperature of 20°C [29]. A user may wish to select the option to model temperature effects (by selecting the 'Model Temperature Effect' Checkbox), in that case the following formula is used to compute (estimate), thus [29];

$$T_C = T_A + \left(\frac{NOCT-20}{0.8} \right) \left(1 - \frac{\eta_c}{0.9} \right) \quad (\text{Equation 39})$$

T_C = Cell temperature, T_A = Ambient temperature, $NOCT$
= nominal operating cell temperature, η_c = cell efficiency.

Then PV power can be obtained as;

$$P_{pv} = \left(\frac{I_t}{I_{stc}} \right) * [1 + \alpha_p(T_c - T_{c(STC)})] * PV \text{ rated power (kW)} * DF (\%) \quad (\text{Equation 40})$$

Where, α_p = temperature coefficient of power

$T_{c(STC)}$ = temperature at standard test conditions

DF = Derate factor

A user may need to enter values for these (α_p , $T_{c(STC)}$, T_c) in order to model the temperature effects. Also, for optimum power production a user may need to enter the slope or tilt angle as desired (in future version of this tool, a default value for this based on the latitude entered will be made available). SOHYSIMO utilises this to modify the solar irradiation based on tilt based on the following equations;

$$\alpha = 90 - \phi + \delta \quad (\text{Equation 41})$$

Where

α = Angle of elevation, ϕ = location latitude, δ = declination angle = 23.5°

Then sum of angle of elevation and module tilt angle gives;

$$Sum = \alpha + \beta \quad (\text{Equation 42})$$

Where β = module tilt angle (to be entered by the user)

Therefore, by combining equations 41 and 42 we obtain the panel transposition factor as follows;

$$\text{Transposition factor} = \text{Sin} \left[\frac{Sum}{\alpha} \right] \quad (\text{Equation 43})$$

5.3.2 The Solar Resource - Solar Irradiation Model

The process by which the energy radiation from the sun is utilised to produce electricity is called the photovoltaic effect. For a solar electricity project, it is often important that a detailed study regarding the solar resource at the selected location is carried out, especially if the solar element is part of a wider system. This can be achieved through local meteorological data collection or from NASA, which maintains a useful global database of meteorological information. A synthetic model which mimics the solar radiation behaviour of the selected site be studied can also be used [30]. In recent year much effort and progress has been made by researchers in the area of solar radiation modelling [31][32][33]. To calculate this solar radiation, the basic trigonometric equations defining the relationships between the sun's position and the earth coordinates are usually employed [33]. This method was adopted by The National Oceanic and Atmospheric Administration (NOAA) to produce a solar radiation model which can simulate the solar resource characteristics of any location. According to NOAA, in the model, the sunrise and sunset results are theoretically accurate to within a minute for locations between +/- 72° latitude, and within 10 minutes outside of those latitudes. They also note that the observed values may vary from calculations due to some factors including variations in atmospheric composition, temperature and pressure [34].

The solar irradiation simulation model adopted in developing this present software is based on NOAA's model [35]. It is an Excel VBA translation of their JavaScript solar position calculator [36]. This has several inputs that represent 3 models; Brass solar model, Bird & Hulstrom's solar model, and Ryan & Stolzenbach solar model. Among the three models specified the Ryan & Stolzenbach model was adopted in the current software as it needs just one input 'atmospheric transmission factor (0.70-0.91, default 0.8)' and as depicted in **Figure 75** [36] Ryan & Stolzenbach solar radiation model seems more convenient, yet all three models produce similar results.

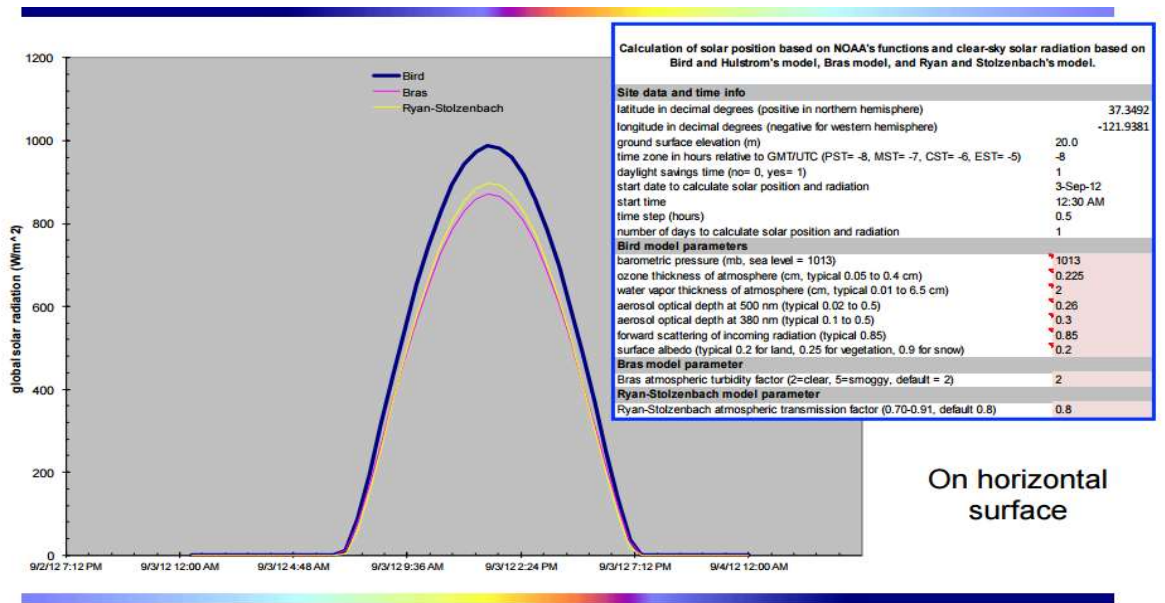


Figure 75. NREL Solar radiation model [36].

To adapt this for use in **SOHYSIMO** the Ryan & Stolzenbach model was modified by translating its standard Excel VBA code to Excel Userform adaptable codes. This is because an input to Excel Userform is based on TextBox object whereas that of standard Excel VBA is based on the regular Excel cell. The start date, start time, ground elevation, time step, number of days and day light saving time were each integrated into the codes with default values of 01/01/00, 00:00:00, 1, 1, 365 respectively, to reduce the number of inputs a user need enter. This reduced the inputs to 3 (latitude, longitude and time zone). The day light saving time was modified using the following codes;

```
Dim MyDay As Integer ' ENTER DAY LIGHT SAVING TIME
```

```
Dim MyTime As Integer
```

```
MyDay = 1
```

```
MyTime = 0
```

```
dIstime = MyDay
```

```
If lat > 20 Then
```

```
dIstime = MyTime
```

```
Else
```

```
End If
```

Two options for solar insolation data are available in the software tool developed in this thesis. The user can choose either to generate a synthetic hourly solar irradiation data or import an already made hourly solar irradiation data. This facility adds flexibility to the developed tool as the tool's solar irradiation simulation model can generate 8760 hours of solar data, thus covering a full annual irradiation required to carry out a complete PV energy simulation for the selected location.

5.3.3 Battery Sizing and Modelling

Energy can be stored in the battery during the period when excess renewable energy supply is available, and released when the resource dips. There are different types of storage batteries for small and large scale renewable energy applications [37]. Nair and Garimella [38] have made a comprehensive review and assessment of different types of battery storage systems for small scale applications. The battery model developed in this thesis was designed such that a user has the choice of adopting a load following method, and to charge the battery when the PV power exceeds load demand. When battery has attained a full state of charge, the remaining power from the PV will then be sent to electrolyser, the surplus power will then become excess power. The equation used to model the dynamics of the power delivery is as follows;

The battery bank capacity ($Batt_{cap}$) is given by the expression:

$$Batt_{cap} = \frac{P_{load} * DA * DM}{V_{batt} * DOD} \left(\frac{Ah}{day} \right) \quad (Equation 44)$$

where,

DA: Days of Autonomy, the following codes was used to implement the days of autonomy

DA =ROUND (COUNTIF (J2:J8760,"=0")/24/52*0.5,1). This computes the number of days of solar photovoltaic unavailability.

DM: Design Margin (this is a factor usually introduced by RE designers to account for some losses or balance the effects of unexpected circumstances, for example, load transients, poor maintenance, and discharge transients)

DOD: Depth of Discharge (this describes how deeply or a percent limit to which a battery can be discharged)

If $P_{pv} > P_{load}$ Battery charging

$$Batt_{SOC} = Batt_{initial\ SOC} (t - 1) + P_{pv} - P_{load} (t) \times BattEff \quad (Equation\ 45)$$

If $P_{pv} < P_{load}$ Battery discharging

$$Batt_{SOC} = Batt_{initial\ SOC} - P_{load} (t) \times \left(\frac{1}{BattEff} \right) \quad (Equation\ 46)$$

Where P_{pv} = Total power from solar PV

$$Batt_{SOC} = \text{Battery state of charge at time } (t)$$

$$Batt_{initial\ SOC} = \text{Battery state of charge at time } (t - 1)$$

$$P_{load} = \text{Load demand}$$

Minimum battery state of charge can be deduced by multiplying the battery nominal capacity by the battery depth of discharge, and subtracting the result from the nominal capacity.

5.3.4 Modelling the Electrolyser

In RE systems applications electrolysers are normally sized based on the total maximum power the RE generators can produce. Researchers have proposed different algorithms for sizing electrolysers. Castañeda et al [39] have proposed four different sizing methods, in the first they have used basic equations to determine the appropriate sizes of the RE system components and in the second method they have used a Simulink design optimisation method to technically match demand with supply. The other two methods were based on the use of a software tool (HOMER) to optimize the hybrid system components for proper demand – supply matching, with a view to realizing the best strategy that offers the minimum system cost. The whole system was designed such that the hydrogen can feed the fuel cell to deliver power to the load in periods of high demand. Hydrogen production using RES involves energy consumption, especially when a compressor is used to raise the energy density of the stored hydrogen. The determination of appropriate storage procedures ensures that these parasitic energy

consumptions are minimised. Kaviani, Riahy and Kouhsari [40] have designed an optimal system where they have used low and high-pressure storage tanks. The compressor was designed to pump hydrogen into the high-pressure storage tank only when the low-pressure storage tank is fully charged. In that process, the energy consumption was reduced, thereby improving the efficiency of the hydrogen production process and storage system. In this study, the equation used for hydrogen generation is based is given by the following;

$$mH_2 = \frac{P_{excess} * \eta_e}{39,400} \left(\frac{kg}{h} \right) \quad (\text{Equation 47})$$

Where mH_2 = mass of hydrogen produced,

η_e = electrolyser efficiency,

P_{excess} = electrolyser input power (W),

The excess power produced by the PV panel is compared with the nominal power capacity of the electrolyser. All excess power that falls below the capacity will be utilised to generate hydrogen. The higher heating value (HHV) which describes the energy content of hydrogen (147000 kJ/kg = 39400 Wh/g) is used in the above equation. The electrolyser efficiency was modelled based on the following illustrations [41];

$$\text{Efficiency (\%)} = \left\{ \frac{HHV \left(\frac{kWh}{kg} \right)}{E \left(\frac{kWh}{kg} \right)} \right\} * 100 \quad (\text{Equation 48})$$

$$E \left(\frac{kWh}{kg} \right) = \frac{P_{Max}}{(H_{2Mass} \left(\frac{kg}{h} \right))} \quad (\text{Equation 49})$$

Where E = energy consumed, HHV = Higher heating value of hydrogen (39.4kWh/kg). This considers the electrolyser energy consumption per hydrogen mass flow rate. The hydrogen mass flow rate per hour is deduced from the following equation [10];

$$H_{2Mass} \left(\frac{kg}{h} \right) = \frac{P_{Max}}{(A \left(\frac{kW}{kg} \right) / h + B \left(\frac{kWh}{kg} \right) / h)} \quad (\text{Equation 50})$$

Where P_{Max} = Electrolyser rated power (kW), $(A \frac{kWh}{kg} / h + B \left(\frac{kW}{kg} \right) / h)$ and $\left(\frac{kW}{kg} \right) / h + B \left(\frac{kWh}{kg} \right) / h$ = electrolyser power consumption represent the parameters required for the simulation process. The hydrogen production rate depends on the level of input current from the PV. A default power consumption value adopted in this design was

53kWh/kg, but the tool also provides an option where a user can enter measured consumption parameters. In practice, the electrolyser efficiency range is between 70% - 80%. A value of 75% has been adopted for the electrolyser model developed in the current software tool. It has been reported that if the power consumption by the auxiliary devices such as DC-DC converters are included, the electrolyser energy requirements may be up to 53.4 kWh/kg [42]. For this reason, a 53 kWh/kg was adopted in the current software tool.

5.3.5 Experimental Determination of Dependency of Hydrogen

Production on Input Current.

As previously mentioned, it is useful to measure the behaviour of hydrogen per input voltage and current input on electrolyser to get a practical idea of how these systems perform in real life. To do this a test rig was set up as shown in **Figure 76**. The set up consists of a heliocentris electrolyser, a solar module, a 120W lamp, and two digital voltmeters. Specifications of the solar module and PEM electrolyser are given in **Table 22**.

Solar module	Electrolyser
Dimension = 200mm x 310mm x 130mm	Dimension = 200mm x 297mm x 125mm
Voltage = 2.3V	Operating voltage = (1.4 – 1.8) V
Current = 1A	Current = 4A
Rated power = 1.7W	H ₂ production rate = 28ml/min at 4A
Short circuit current = 1A	Storage tank = 64ml

Table 22. Specifications of solar module and electrolyser.

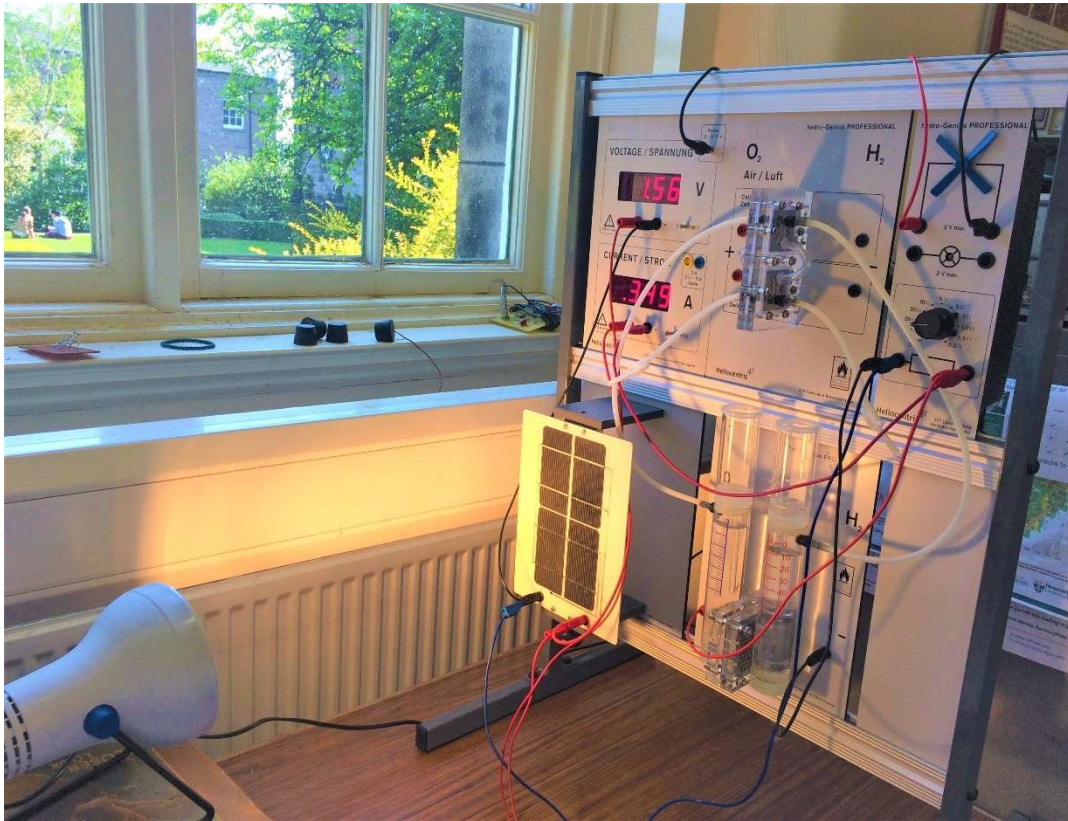


Figure 76. Hydrogen production test rig.

The experiment was conducted to determine the dependence of hydrogen gas production on a given power supply. In **chapter 3** the effects of light intensity on the output current of a solar module is shown, when light is incident on a solar cell current is produced. However, output current is directly proportional to light intensity, therefore current increases with increase in light intensity. Due to the effects of shunt resistance, at low light intensity [43], a decrease in the bias point occurs, and this would result to a decrease in current through the solar cell. A 120W lamp was used to simulate the incident light (to act as sunshine incident on the solar cell) by adjusting its distance to approximately 20cm in front of the solar module, and currents were obtained at different applied voltages, from 0 – 2V. Firstly, the I – V characteristics of the electrolyser was obtained and is shown in **Figure 77**. This is to determine the voltage threshold for a water electrolysis to start. As described in chapter 3, at standard conditions (25°C), the standard thermodynamic voltage for electrolysis of a liquid water is $E^o = 1.229V$ [43], and for electrolysis without heat exchange with the surroundings, it is referred as thermoneutral voltage E_{TN} and this is approximately equal to 1.48V [44], and slightly depends on operating pressure [44]. At standard

conditions, the cell voltage U applied to the electrolysis cell must be significantly larger than these for the electrolysis to start (for the electrolyser to start producing hydrogen gas) [44]. As shown in **Figure 77**, current began to flow at 1.5 V threshold voltage, and this increased linearly afterwards.

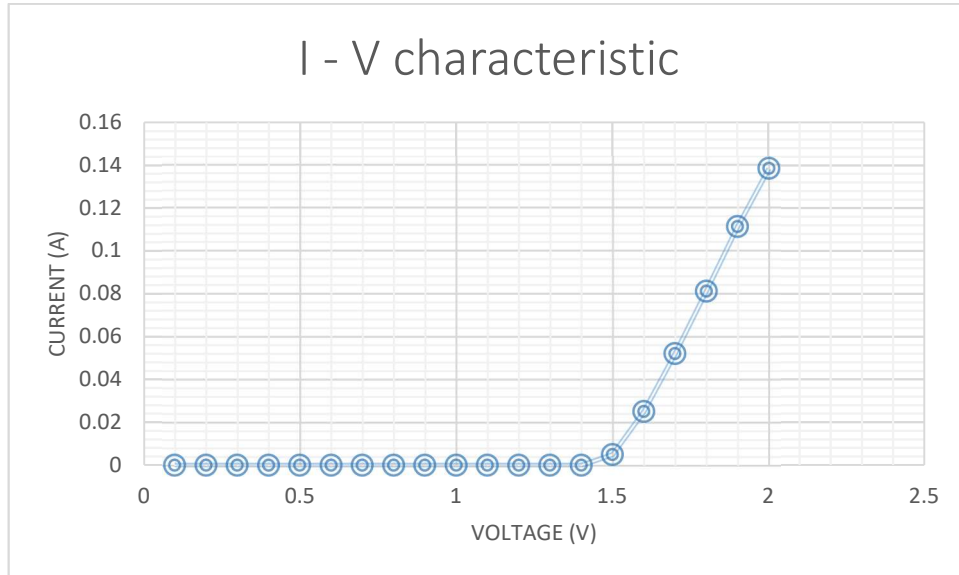


Figure 77. Electrolyser I – V characteristic.

To determine the dependence of Hydrogen gas production was noted and data was recorded, **Figure 78** shows the plot of current against hydrogen produced.

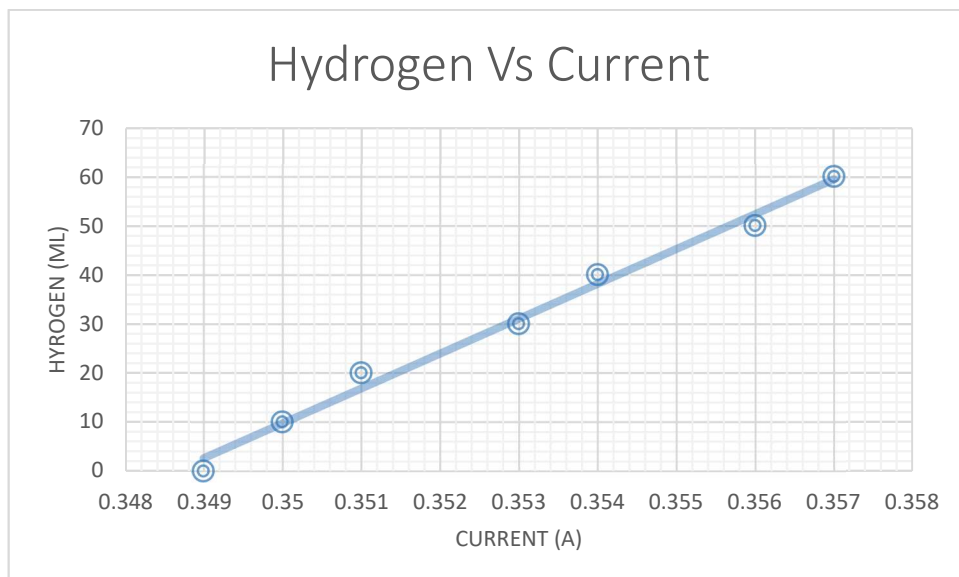


Figure 78. Characteristic electrolyser dependence of input current for Hydrogen production.

The relationship between the hydrogen gas produced and the current per flow rate of gas, demonstrates that hydrogen production increases linearly with input current.

5.3.6 H₂ – Engine Genset Model

It has been reported that conversion of a diesel-powered generator set to hydrogen-powered generator can be relatively straight-forward [45]. A typical and existing example of this type of a system has been installed at the Island of Utsira in Norway [46]. The installed system at Norway comprises of a 600 kW wind turbine, 10 Nm³/hr electrolyser, 2400 Nm³ – 200 bar hydrogen gas storage, 10 kW Fuel cell (not in use) and 55 kW hydrogen engine (H₂ – genset). From their investigation, the system gave 2 – 3 days of full energy autonomy with the 55 kW H₂ – genset, which they reported was a diesel engine rebuilt for using hydrogen as fuel [46]. However, due to the poor efficiency performance of the hydrogen engine at **25%**, they had considered increasing the capacity of the fuel cell to 55 kW, with a reduced size of electrolyser and H₂ storage capacity. However, their economic analyses show that total investment costs for the main components for either fuel cell or H₂ - genset system arrangement are comparable. Ideally, there must be a compromise in power generation system modelling, and this can be based on efficiency or cost depending on the user's requirement. The choice of H₂ – genset is based on its wide availability, and the fact that the H₂ – genset will be used sparingly based on an imposed control strategy which will be explained later in this thesis. Efficiency savings are therefore considered secondary compared to availability and capital costs of engines over fuel cells. The hydrogen powered generator set considered in this study was assumed to have a similar efficiency to the one installed in Utsira, that is **25%**. In similar fashion, the power generated by a H₂ – engine generator with a rated power (P_{rated}) is described as follows [47];

$$mH_{2min} = 0.2476 * P_{gen} + 0.07391 * P_{rated} \quad (\text{Equation 51})$$

where;

A and B = Genset fuel consumption parameters

P_{gen} = Generator output power (kW)

P_{rated} = rated power (kW)

$mH_{2\text{min}}$ = H_2 – Genset hydrogen consumption

For gensets in the range of 1 kW – 10 kW capacity default values A and B are; A = 0.2476 l/kWh, B = 0.07391 l/kWh, otherwise a user will need to input data pertaining to this. These default values are assumed based on the parameters determined in an experiment described by Yamegueu, D et al [47] and they obtained these from a 9.1 kW diesel genset.

5.3.7 Hydrogen as a Cooking Fuel

The recent advances in renewable technologies has proffered various energy provision opportunities, especially for currently unserved rural areas. Renewable energy systems can provide cost effective solutions where grid extension costs are prohibitive. Anything but the most rudimentary system will incorporate energy storage for addressing inherent problems in matching supply with load. In RES, this storage can be via batteries, hydrogen, supercapacitors, flywheels and so on. The hybrid system of most interest here involves both battery and hydrogen storage. To make the energy system more reliable in terms of availability of supply, it can be connected to an electrolyser such that the hydrogen generated during periods of excess energy production can be recovered when demand outstrips (solar) energy supply, and electricity re-generated through a fuel cell arrangement. In this study, which incorporates both battery and hydrogen storage, it is proposed that excess hydrogen (once the electrical demand has been met) to be used to meet cooking demand, which has efficiency, pollution and sustainability benefits which is discussed later in this section.

The conversion of hydrogen to heat is a very energy efficient process compared to its use in electrical energy production. The use of hydrogen for domestic heating has attracted important interest in recent years. According to a recent report [48], a potential for hydrogen as a safe efficient fuel source in the domestic setting and sure replacement for natural gas has been demonstrated. The study has also proved that the safety risks in hydrogen is just the same the risks seen in other flammable gases currently used [48]. Research has reported different important numerical and experimental

studies on the utilisation of renewable generated hydrogen for cooking in the household. Topriska et al [49] describe a numerical model developed in TRNSYS for a large-scale solar powered hydrogen production for domestic cooking in Jamaica. Their model took a holistic approach in developing a cooking demand profile by source, but most rural dwellers do not use LPG and this has made their model to be more applicable to the urban dwellers than the rural. In addition, their model did not consider the use of excess energy that could be generated from the renewable energy system, rather it was based on utilising all energy generated to produce hydrogen without an integration of an additional storage medium in battery. This means that they also did not take the cost implications of an electrolyser into consideration. The installation of a solar plant for the sole purpose of generating hydrogen seems an unrealistic proposition and would have very limited appeal, is capital and energy intensive, and has relatively low efficiency.

In other reported works, a possible application of hydrogen for domestic cooking has also been proposed [50][51]. A clear and practical representation of opportunities in hydrogen cooking has been demonstrated by Fumey et al [52][53]. This is an existing solar – hydrogen cooking system at EMPA Switzerland which they call a self-sufficient living and working unit (SELF). The system consists of a solar array, lithium ion battery storage, and a hydrogen storage system. According to EMPA the excess energy generated during the summer time is utilised to generate hydrogen, in the process they found that electric cooking was unfeasible due to the high-energy consumption involved, and they developed a hydrogen fuelled stove to meet their all year-round cooking needs. This highlights one of the key advantages of hydrogen over solar-derived electricity for cooking, in that hydrogen can be stored easily in relatively large quantities, whereas electric cooking will involve considerable expense in appropriate sizing of the battery stack to meet the required loading demands.

A recent report by the UK Daily Telegraph describes a possible shift from the current use of natural gas for domestic cooking and heating to hydrogen in the city of Leeds in UK by 2030 [54]. Hydrogen derived from excess renewables is increasingly seen as a means of addressing thermal loading, in particular by blending with existing natural gas supplies in a 2% to 10% mix [55] In the worldwide domestic energy sector, energy requirements for heating and cooking dominates. Developing countries may source a considerable

portion of their cooking needs from the highly outdated, inefficient and health risk firewood, charcoal and kerosene, especially in rural areas. The two most conventional sources of fuel for domestic cooking in Nigeria are kerosene and firewood [56]. A report in 2013 by the WHO estimated that 98,000 Nigerian women die each year because of indoor cooking with firewood [57]. Providing the villagers access to sustainable clean electricity, with hydrogen cooking facilities as a relatively low-cost add-on, would be a powerful attractor. However, it has been demonstrated that PV electricity can as well be used for cooking by directly connecting the PV to an electric heater [58]. Unfortunately, this system is limited by the high-power required to raise the temperature to a level that is sufficient for a complete cooking process.

5.3.8 Experimental Investigation of Solar Hydrogen Cooking

To characterise the hydrogen applications for cooking, a brief experimental assessment of hydrogen for domestic cooking was conducted in Empa Urban Energy Systems laboratory in Switzerland. The composition of the hydrogen cooking facility and the integration is described in [59]. The hydrogen is generated using a Schmidlin 400W PEM electrolyser with 0.8 NI/min hydrogen output at 17bar. This is connected to a 3 kW PV array and 16 kWh lithium battery bank. The generated hydrogen is stored in a metal-hydride storage tank with 4 kg total storage capacity. A simple experiment was conducted using the test facility in order to gather numerical data on the basic heating conditions of a hydrogen cooker, and to establish a feel for the dynamics and the rate of hydrogen consumption in the cooking process. **Figure 79** shows the hydrogen cooker developed at Empa.



Figure 79. Hydrogen cooker at Empa.

A measurement was done using a covered cooking pot filled 3.0 litres of water at 25°C. The cooker was turned on with the hydrogen flow rate set to 10.9 NI/min. Measurements of hydrogen consumption by the stove per temperature rise was taken. The test procedure is shown in **Figure 80**.



Figure 80. Hydrogen cooking testing.

A stop watch was used to record the period elapsed before the water starts boiling. The cooking duration was measured at exactly 22 minutes. However, it is fundamental that the thermal conductivity of the materials used to make the pot be established. It is a stainless-steel pot and thermal conductivity of stainless steel ranges from 12 W/mK to 45 W/mK (watts per meter-kelvin), and because there are various kinds of stainless steel and unfortunately the exact type used in making the pot used in this test cannot be determined.

Results

Table 23 lists the test parameters and **Figure 81** shows the hydrogen flow. For the cooker to achieve a hot temperature the hydrogen flow increased steadily from 1.7 NI/min (normal litre per minute) to 10.9NI.min, correspondingly, the temperature of the cooker increased from 42.9°C to 600°C. The difference between the initial water temperature and final water temperature was noted at 77°C. From **Figure 81**, the hydrogen cooker temperature was 549°C when the hydrogen flow was raised to 10.9 NI/min. Now, to calculate the hydrogen cooker efficiency, the energy content in hydrogen per unit volume at 10bar is around 0.53kWh per normal litre [59], for 17bar the energy content is about 0.84kWh/NI. Therefore, at 10.9NI/min flow rate the hydrogen consumed is 10.9NI/min x 22 minutes = 239.8NI. Dividing these by the pressure at 17bar in order to convert the values to litre, we obtain 14.1L of hydrogen flow. But 1 litre of hydrogen has a mass of 0.08234g and this means that the total amount of hydrogen consumed in the process is 1.16g in the test conducted. Irrespective of some errors encountered in the testing process, it has now been established the quantity of hydrogen required for basic cooking process. Converting the hydrogen required for a basic cooking at 1.16g, this is 0.0457 kWh of energy. However, it should be noted that for a complete cooking process involving food, the cooking duration may be longer thus the cooker hydrogen consumption will be higher.

Parameter	Measurements
Start temperature	25°C
Start time	15:33:00
Stop time	15:55:00
Duration to boiling	22 minutes 0 seconds
Stop temperature	102°C
Flow rate (H ₂)	10.9 NI/min

Table 23. Results of hydrogen cooking measurements

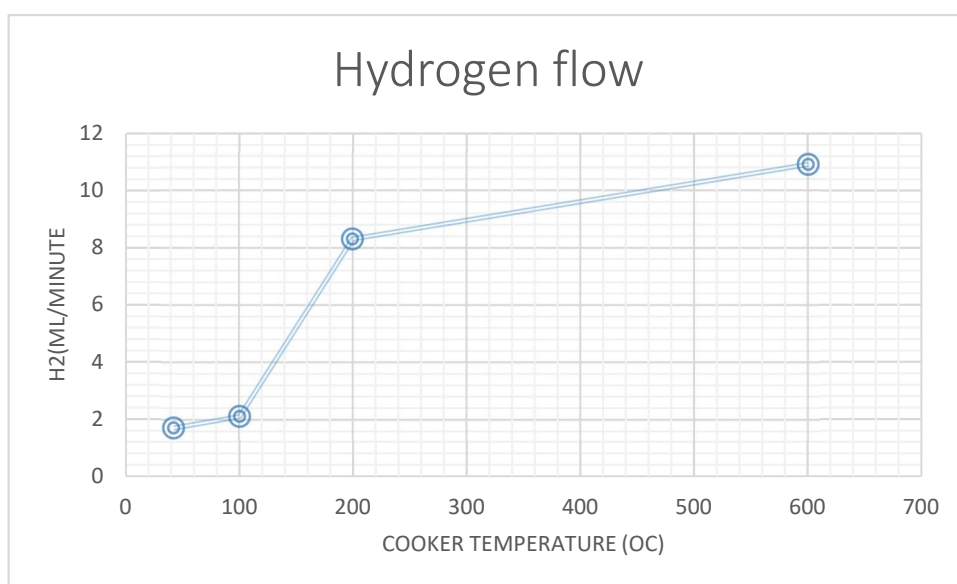


Figure 81. Hydrogen flow rate vs cooker temperature.

5.3.9 Modelling the Hydrogen Cooker

Currently, there are few reported works on the use of hydrogen as an alternative fuel for cooking. In this research, a model for hydrogen cooking has been developed. This considers the amount of wood fuel consumed by residential homes in the developing countries to meet cooking demand. It has been estimated that more than 90% of the rural population in the developing economy relies on fuelwood and charcoal for cooking [60]. Cooking with biomass or wood fuel is dangerous to health, therefore, there is need to develop an efficient way of cooking. The idea is to feed the cooker with hydrogen that could be generated by the electrolyser as follows;

$$H_{cooker} = m_{H_2} \text{ (kg/h)} * 3600 * HHV \text{ (MJ/kg)} * 0.0802 * (1/3.6) * (0.70) \quad (\text{Equation 52})$$

Where; m_{H_2} (kg/h) = mass of hydrogen produced by electrolyser

H_{cooker} = Hydrogen cooker

HHV = higher heating value of hydrogen

To compute the cooking demand, the tool uses the following illustration;

$$Demand = Fuel_{type} * CV_{fuel} * Fuel_{eff}. \quad (Equation 53)$$

Where CV_{fuel} = calorific value of the fuel, and $Fuel_{eff}$ = fuel efficiency.

However, as the H_2 cooking facility provides three options for a combination of two or three fuel types, the tool sums and divides accordingly by the number of fuel type selected to obtain the average cooking load. The control algorithm developed for the hydrogen delivery is that when power from H_2 -genset is not enough to cover the load demand, the user has the choice to decide whether to use the available hydrogen for cooking.

5.4 Control Strategies

When designing a renewable energy system, it is important that suitable and optimal control strategies are adopted, especially a system that integrates an electrolyser for hydrogen production.

Hydrogen controls: It has been noted that electrolysers, especially the alkaline type, has low operation threshold and only operate down to about 20% of their maximum rated power [61]. This means that an intermittent source of power like solar PV and wind can have a damaging effect on the electrolyser if its control strategy is not properly managed. For this reason, an appropriate control strategy was developed and integrated into the software tool in order to ensure that all excess energy produced is utilised to generate hydrogen. For instance, in developing countries of Sub-Saharan Africa there are little month to month variations in day length [62], except for the wet season when markedly low insolation values are experienced. Sizing a RES to accommodate this rainy period implies that for most of the year the system will be oversized, and this is where the utilization of hydrogen comes to the fore. However, a control strategy which ensures

that weather variations are well-managed needs to be adopted. In this study, the control strategy adopted allows the electrolyser switching flexibility from minimum to the electrolyser rated capacity. Though in this mode, it is likely that some losses will be incurred because of an intermittent electrolyser switching (on/off) process involved, however, the best practice is to ensure that alkaline electrolysers operate at the optimum level, by operating them at 20% of their rated power. This power threshold issue does not apply to PEM electrolyser. However, in the developed software tool, the user has the choice on how the generated hydrogen will be utilised and this is based on constraints imposed in the tool. Importantly there is also provision for switching hydrogen use from cooking to electricity generation depending on the user-defined loading patterns. The control strategies are as follows;

If $PV_{power} > P_{load}$ and Battery =100% full, then the surplus will be sent to electrolyser using the following equation;

$$P_{surplus} = P_{pv} - P_{load} - P_{batt} \quad (\text{Equation 54})$$

Also, if $H_2 - \text{genset} < P_{load}$ the software tool checks whether the available hydrogen is enough to meet cooking requirements. Based on the result obtained after the assessment, it will suggest to the user to use hydrogen for cooking or leave the hydrogen in the storage to accumulate. Hydrogen stored or left will accumulate for use during the wet season. Based on individual discretion, this algorithm makes the tool handle two controls simultaneously, both seasonal storage and dynamic use of hydrogen. **Figure 82** depicts the hydrogen decision control screen and its message display.

SOHYSIMO

PV Sizing | Input data | General data | Cost Evaluations | Energy Assessment | **Cooking Decision on Hydrogen Use**

Help

Click To Decide

ENTER DAILY COOKING DEMAND DATA (7 - Days)

	1	2	3	4	5	6	7
FIREWOOD (kg)							
CHARCOAL (kg)							
KEROSENE (L)							

OK

Click To Accept Data

Calculate

SELECT FUEL TYPE

FIREWOOD

CHARCOAL

KEROSENE

VISUALIZE DAILY H2-COOKING GRAPHS

JAN	JUL
FEB	AUG
MAR	SEP
APR	OCT
MAY	NOV
JUNE	DEC

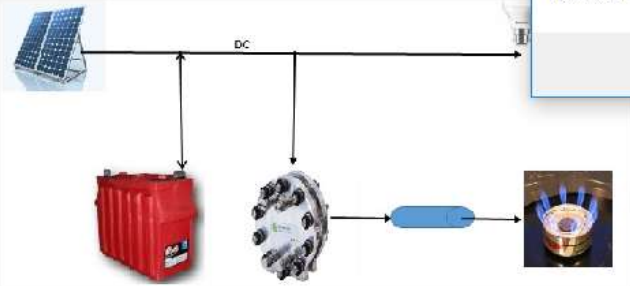
PLOT 365 DAYS H2-COOKER

PLOT 365 DAYS COOKER VS DEMAND

HAVE COOKING DEMAND DATA??

Import EXPORT RESULTS

Average Daily H2 Cooker



SOHYSIMO

H2_Genset Power Not Enough To Cover The Load Demand; Check If You Can Use Hydrogen for Cooking Demand

OK

Figure 82. Hydrogen cooking decision control in SOHYSIMO.

PV power dispatch strategy: The following control algorithm controls the whole process of PV power delivery in the tool; two dispatch strategies were implemented to run synchronously, namely load following and cycle charging. In load following, if the PV is not able to meet the load, the battery will make up the shortfall. In cycle charging, the solar PV will charge the battery after meeting the load.

```

IF PVpower < load power, PVpower + PBatt - Load => Load following
Else
IF PVpower > Load, PVpower - Load = PBatt => Cycle charging
Else
IF PVpower > Load & PBatt = 100%, PVpower - Load - PBatt => Surplus PV power
End If...

```

To calculate the unmet load, the following equation was used:

$$\% \text{ unmet load} = \left\{ \frac{\text{Total unmet load} \left(\frac{\text{kWh}}{\text{yr}} \right)}{\text{Total annual electric load} \left(\frac{\text{kWh}}{\text{yr}} \right)} \right\} \times 100 \quad (\text{Equation 55})$$

The control codes implemented in the tool for resource data utilization is as follows;

```

If CheckBox1.Value = True And TextBox369.Value = "" Then

```

```

    Range("G2:G8761" & LR).Formula = "=D2 * E2 * F2" 'COMPUTE PV POWER WITHOUT
MODIFIED IMPORTED HOURLY DATA (0.78 is assumed for % Loss due to dirt, shading etc)

```

```

    ElseIf CheckBox1.Value = True And TextBox369.Value = True Then

```

```

    Range("G2:G8761" & LR).Formula = "=BM2 * E2 * F2" 'COMPUTE PV POWER WITH
MODIFIED IMPORTED HOURLY DATA (0.78 is assumed % Loss due to dirt, shading etc)

```

```

    ElseIf CheckBox2.Value = True And TextBox369.Value = "" Then

```

```

    Range("G2:G8761" & LR).Formula = "=AP2 * E2 * F2" 'COMPUTE PV POWER WITH
SIMULATED HOURLY DATA

```

This is shown in **Figure 83** as it displays the warning alert to the user, as a reminder to select either imported or modelled data before the simulation can proceed. The software uses TextBox object of the VBA Userform for data entry, and therefore a control was implemented to ensure that all boxes are completed before the simulation

will run and to ensure the smooth simulation with the tool. If any box is left empty an error message like the one shown in **Figure 84** will be displayed.

SOHYSIMO

PV Sizing | Input data | General data | Cost Evaluations | Energy Assessment | Cooking Decision on Hydrogen Use

SYSTEM REQUIRMENTS

Enter DC Voltage (V)

Enter Depth of Discharge (%)

Enter PV Derate Factor (%)

OK

COMPONENTS

Use Imported Solar Data

Use Simulated Solar Data

Simulate H2-GENSET Power

Simulate ELECTROLYSER

Start Simulation

Enter Size of Solar Panels (kW)

Enter Battery Size (Ah)

Enter Size of Electrolyser (kW)

HAVE ELECTROLYSER PARAMETERS??

Power Consumption Parameters

A (kW/kg/h) B (kW/kg/h)

OK

Efficiency (%)

ENTER GENSET PARAMETERS

Enter H2-Genset Size (kW)

H2-GENSET CONSUMPTION

A B

OK

Click To Accept Entries

EXPORT **HELP**

Export Simulation Result **Help**

PLOT GRAPHS

Plot Simulated Irradiation

Plot Imported Irradiation

Plot Sys Monthly Av. Power

Plot Annual Totals

Plot Monthly Average PV

Plot Daily H2 prod (kg/day)

SELECT HOURLY GRAPHS BY COMPONENT

OK

VISUALIZE HOURLY PV SYSTEM GRAPH PER MONTH

JAN	JUL
FEB	AUG
MAR	SEP
APR	OCT
MAY	NOV
JUNE	DEC

SOHYSIMO

Please Select One Hourly Solar Option!

OK

Figure 83. General data page of SOHYSIMO showing the data selection message alert.

SOHYSIMO

PV Sizing | Input data | General data | Cost Evaluations | Energy Assessment | Cooking Decision on Hydrogen Use

ENTER 24 - HOURS LOAD DATA (W)

	1	2	3	4	5	6	7	8	9	10	11	12	13	14	15	16	17	18	19	20	21	22	23	24
LOAD 1																								
LOAD 2																								
LOAD 3																								
LOAD 4																								
LOAD 5																								

Click to Accept Load Data

Help

DISPLAY TOTAL DAILY LOAD DEMAND

Click Here - Total (kWh/day)

SOHYSIMO

Empty Box Detected! Please check Your Load Data.

OK

START

Click on 'START' or 'SAVE SIMULATION DATA' buttons unless you want to simulate Irradiation

Import kWh/m²/day

Modified Irrad at Tilt kWh/m²/day

HAVE HOURLY SOLAR IRRADIATION DATA ??

Import Load kWh/day

HAVE HOURLY LOAD DATA??

SAVE SIMULATION DATA kWh/m²/day

Enter PV Tilt Angle

OK

Figure 84. Input user interface page of SOHYSIMO showing an error reminder for a missing input data.

5.5 Analysis and Study of an Existing Off-grid Renewable Energy System – The Isle of Eigg

A proper feasibility study helps in providing a knowledge base during the design phase of a renewable energy system [63]. In this **chapter**, analysis of a successful existing renewable power system is presented, the power performance characteristics of the renewable electricity system using raw data obtained from the system is presented. This is particularly important to this research because; 1) it is a remote area power access, 2) the system is totally off-grid and today the inhabitants are enjoying electricity in the same way as people on the mainland. A simulation of the solar photovoltaic performance was done using the SOHYSIMO software tool. The simulation results obtained from SOHYSIMO were compared to the actual power performance characteristics of the solar PV at Isle of Eigg, and the associated analysis used to provide a validation for the model.

5.5.1 The Electrification of Eigg –a Brief History

The Isle of Eigg is an island approximately 10 miles off the West coast of Scotland, which since 1997 has been owned by the Eigg residents Association - Eigg Heritage Trust which purchased the island from the owners. As at the time there was no existing electricity network on the island, and it was not connected to the mainland electricity grid due to primarily due to cost and environmental factors. The electricity situation at Isle of Eigg was such that the inhabitants depended mostly on individual diesel generators for their electricity needs. Following acquisition by the Trust the community decided to install its own electricity supply system which took advantage of the renewable energy resources available on the island, and funding sources such as the European Regional Development Fund and the Big Lottery fund. On 1st February 2008, the RE electricity supply system was formally commissioned, and this provided distributed electricity for the first time to all residents and businesses on the island [64]. **Figure 85** is a map of Isle of Eigg that shows the layout of the Eigg electricity. The capacity and load demand of the scheme is an order of magnitude greater than the single dwelling scenario considered elsewhere, and this introduces additional complexities and matching supply to demand at all times. The main thrust of the following is to explore the performance of the PV farm on Eigg,

and to compare this with the modelled outputs from SOHYSIMO. On Eigg the PV is embedded within a system which is ac frequency controlled. Inverters are employed to manage the system and the decision-making process can lead to distortions in the performance figures of all of the renewables contributors. This will be discussed shortly, and then a justification made for using PV data from a particular temporal period to attempt the validation.



Figure 85. Map of Isle of Eigg showing the sites of the renewable electricity installations [65].

The electricity supply system is entirely self-contained and comprises generation, distribution and supply systems. Generation comprises of a mixture of hydro, wind and PV with a back-up battery/diesel generating set arrangement. Distribution is through underground cabling, and supply is by pre-payment meter. It is thought that the Eigg scheme was the first in the world to incorporate three distinct renewables sources in a distributed system. **Table 24** shows all power system components at Eigg and their installed capacities and **Figure 86** shows the Eigg electricity network system.

RE component	Capacity
Big Hydro	100kW
Small Hydro	12kW (2 x 6kW)
Solar PV	53.9 kWp
Wind	24kW
Diesel generator	(nominal) 2 x 80kW
Battery	(nominal) 4 x 48V 2242 Ah (C10)

Table 24. Power generators at Eigg [64].

All renewable generators are interconnected to an isolated medium voltage distribution network and coupled to a control system where they are managed through a system of inverters and distributed to consumers via the island-wide high voltage (3.3kV) grid. During the winter period, the renewable sources usually generate more power than the island can consume, largely due to the influence of the 100kW hydro scheme at Laig. Any excess power is used to charge the battery via the inverters. To keep the frequency within acceptable limits a series of controlled switches activates 12 x 3kW space heaters at the Community Hall, the Pier Centre and the churches. These are sequentially switched in to the system to accommodate over supply by means of frequency triggers. The behaviour of grid frequency in renewable energy electricity network system is used to determine the balance between system demand and total renewable energy generation. The grid frequency tells when the demand goes higher than generation. In the UK, the grid frequency is controlled to be within limits of +/- 0.5Hz, Control is achieved by accurately matching supply to demand. The off-grid system on Eigg uses this frequency feature to control the various system elements. As RES move up in scale (installed capacity and demand, as with Eigg), it becomes increasingly necessary to adopt more sophisticated control approaches.

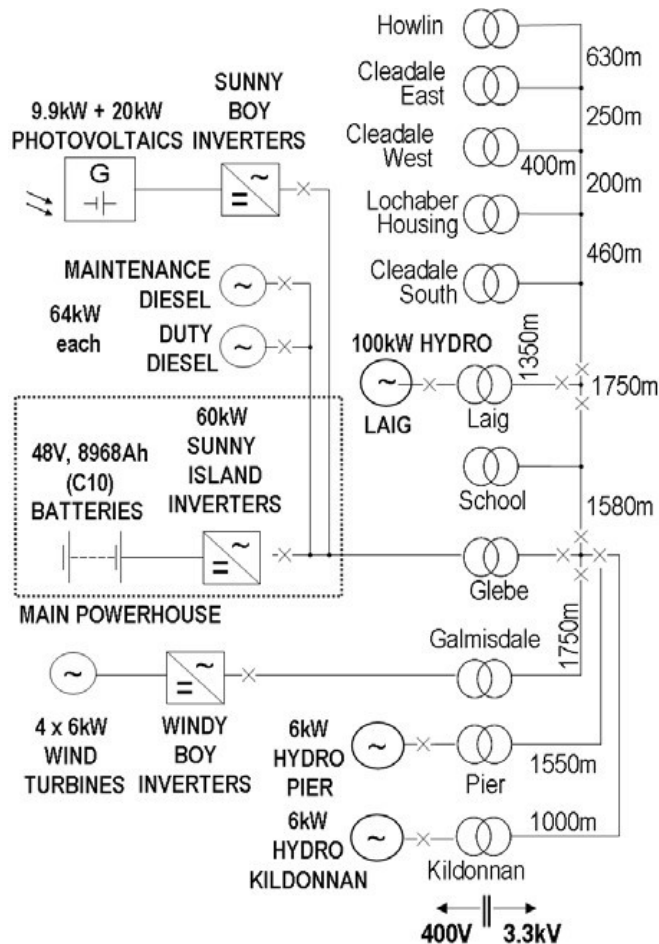


Figure 86. Isle of Eigg Renewable AC micro-grid Electricity network schematic [66].

As already noted, the grid frequency, is an important factor that needed good analysis, thus, to highlight the effects of frequency control in an AC micro-grid system, the following sections presents detailed analysis of series of actual events recorded at Eigg.

5.6 Evaluation of Power Performance Characteristics of Eigg PV

An energy monitoring system (data acquisition system) was installed by Kinetic Traction Systems on October 2014 to log data in seconds (1s) to characterize the electric power system. Power generation data from the generators (hydro, solar, wind and diesel generator) was obtained using high speed Hioki PW3360 data loggers (see **Figure 87**). The system power generation data was recorded from 11th October 2014 – 28th March 2015. Also, power generation data was downloaded from the SMA Sunny portal website

[67] which records and displays the performance characteristic of the Eigg Electric averaged at 5 minutes intervals (mean).

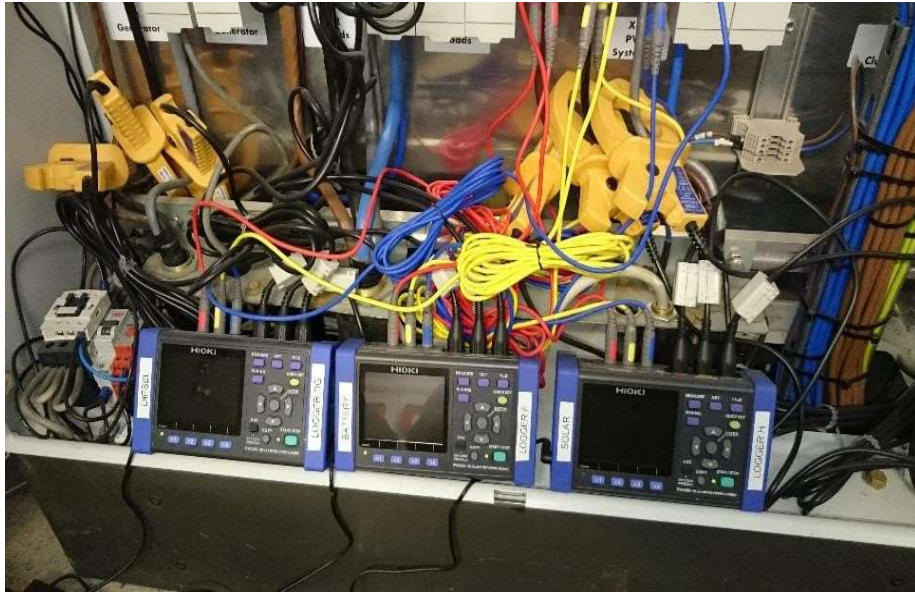


Figure 87. Hioki PW3360 data loggers connected at Eigg electric system for data acquisition.

For this research, only the solar photovoltaic data was analysed, in order to validate the accuracy of the output results of the model simulated, using the tool developed in this research. A three-day solar power generation dataset recorded in 5-minute intervals from 6th – 8th June 2016 was downloaded from the SMA Sunny Portal for the first analysis. This was synthesized and plotted as shown in **Figure 88**.

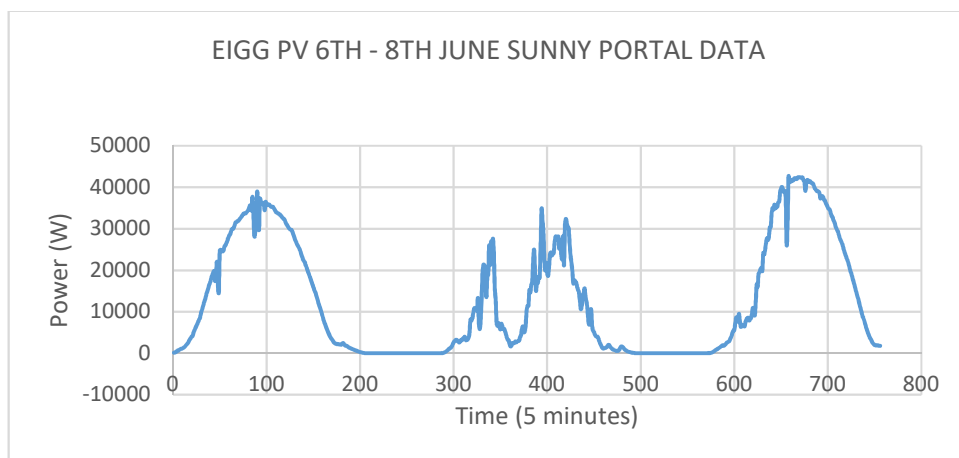


Figure 88. Three days of output power of the 53kW Eigg PV measured in 5mins interval from 6th – 8th June 2014. Data obtained from SMA Sunny Portal data loggers [67].

Data selection for this first analysis was based on the days (summer) on which the solar PV performed close to its optimum capacity over the period recorded. This period was chosen because the system frequency did not rise at any time to the point where PV would be curtailed. For system stability, the frequency control system offered as a standard within the SMA Sunny Boy PV inverters [66] usually curtails the PV output linearly anytime it generates above the frequency limit, which was stated to lie between 51Hz and 52Hz [66]. As shown in **Figure 89**, at approximately 43 kW, there was a rise in grid frequency from 50Hz to about 51.2Hz and consequently a drastic feathering of PV generation ensued. As already mentioned, this is an important complexity in a frequency controlled AC micro – grid electricity system, as injections from a variable power source (RES) in solar PV usually results to this frequency deviations, especially if the system is on a low electrical load. As this control is normally imposed in order to protect the battery from overcharging.

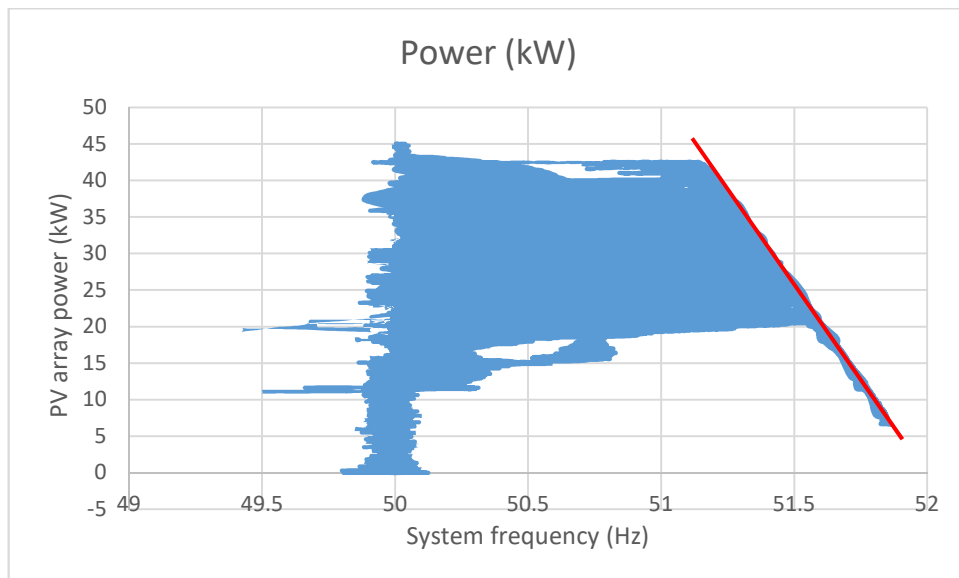


Figure 89. Limitations of grid frequency on solar PV generation at Eigg.

However, to obtain a direct comparison, with the model data, the data from 6th – 8th June 2014 was synthesised into hourly average range (5 x 12) by selecting, summing and averaging every 12 range in order to obtain a 24 – hour data, this was plotted as shown in **Figure 90**.

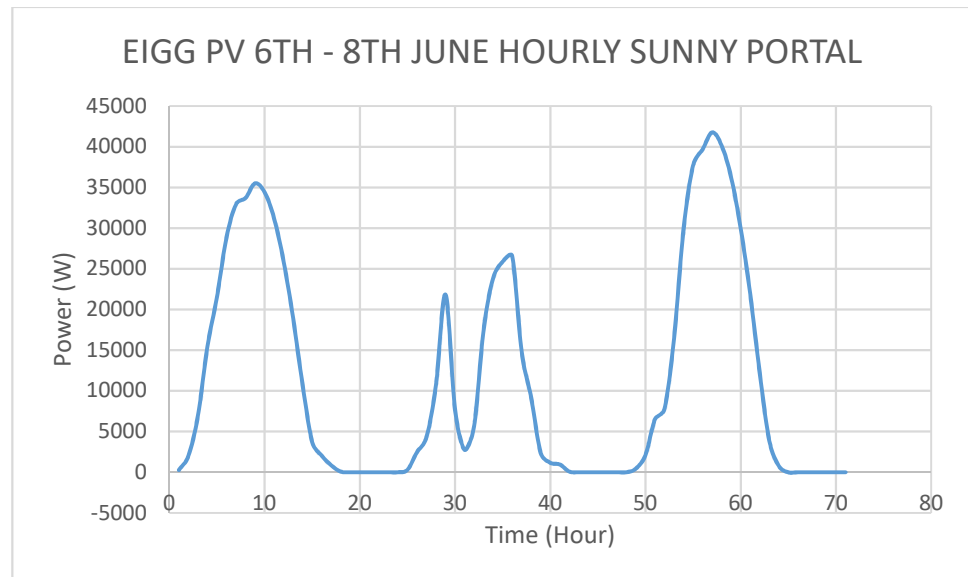


Figure 90. Output power of the 53kW Eigg PV measured in 5mins interval from 6th – 8th June 2016 converted to hourly values.

From **Figure 90**, it can be observed that the PV power performance on the 8th June peaked at 41.7 kW, while the other two days (6th and 7th June) analysed show some shortfall. This proved the effects of intermittency of solar radiation on solar power production. For instance, the PV power had fluctuated steadily on 7th June, but on 6th June it had maintained a steady power production. It also demonstrates a possibility that PV can be harnessed to perform at its optimum capacity, if it is installed at a location where it receives steady uninterrupted solar irradiation. However, to better understand the impacts of low solar irradiation and fluctuations on PV power productions, data set for the period of 24th February – 25th February 2015 (winter) was selected from the data recorded in seconds using HIOKI data loggers by Kinetic Traction Systems. This range of data was selected because it represented the period on which the PV power production was at its lowest within the duration the data was recorded. **Figure 91** depicts the PV output power captured at 1s intervals for the period of 24th – 25th February 2015.

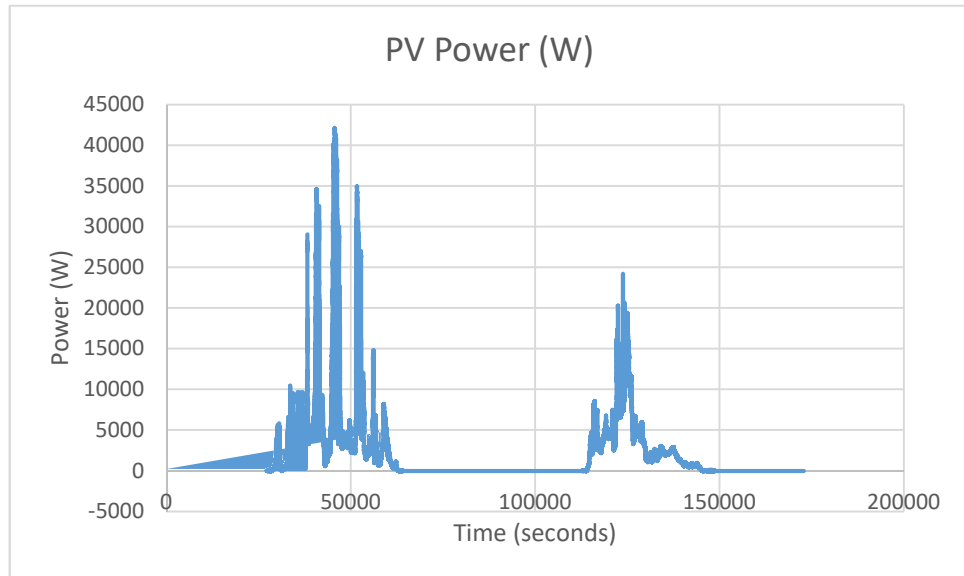


Figure 91. Output power of the 53kW Eigg PV measured in seconds interval from 24th – 25th February 2015 obtained from Hioki data loggers.

From the graph, the PV power production fluctuated periodically, as it peaked at around 42 kW but went flat to 2.3 kW within a short time frame on the 24th February 2015. On the next day, the 25th of February, the PV output power declined but there was a bit consistency unlike the previous day. The maximum output power recorded was 23 kW, but with minimal fluctuations, coupled with the fact that the data was recorded in seconds. To transform this to some more visible hourly power productions, the same smoothing process as described in the previous analysis was followed. **Figure 92** shows a plot of the hourly power generation by the 53 kW PV at Eigg recorded from 24th – 25th February 2015.

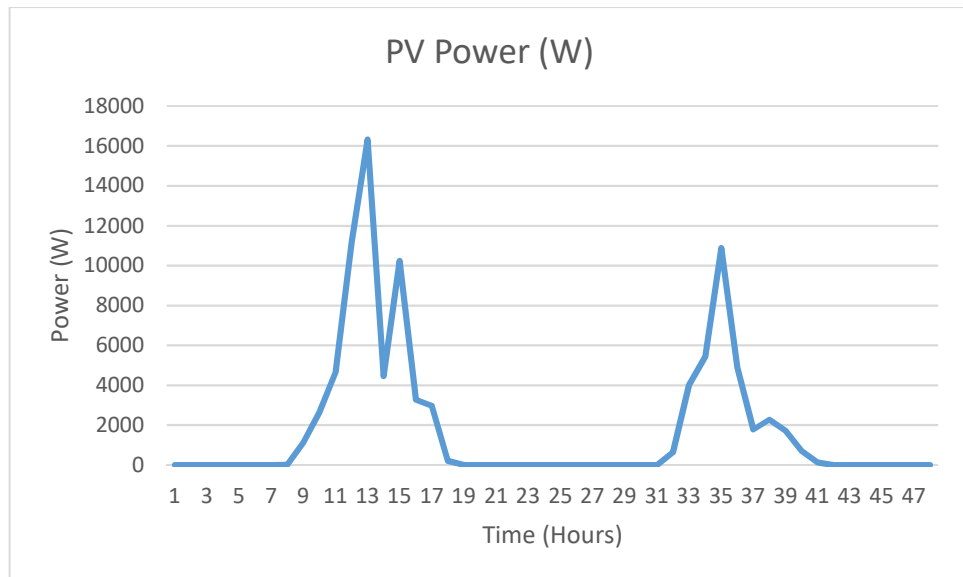


Figure 92. Output power of the 53kW Eigg PV measured from 24th – 25th February obtained from SMA Hioki data loggers converted to hourly values.

From the graph, a streamlined trend of the PV power output can be seen. On the first day (24th February 2015), the PV power peaked at 16.3 kW while it reached 10 kW on the second day (25th February 2015). However, based on 53 kW rated capacity of the PV, it shows a 31% and 19% maximum power rating on the consecutive days analysed. This highlights one of the problems of intermittency in solar PV and the seasonality, and thus supports the importance of employing good control strategies in its power dispatch, especially when it is connected to an electrolyser for hydrogen production. Some sources investigated [68] have suggested that the high frequency of voltage and current set point changes across electrolyser stacks and the power conditioning devices, induced by intermittent power availability and renewable power source characteristics, can lead to early degradation and failure in electrolysers. More research work is required on this subject.

5.6.1 Analysis and Simulation of Power Production Characteristics of 53kW Solar PV at Eigg.

In **section 4.12**, data collected from a solar PV system installed in Kuje Abuja Nigeria was presented, however, this was done just to show the possibility of harnessing decent amount of energy from a PV system in Nigeria. Therefore, data obtained from Isle of Eigg PV system, which is more comprehensive was used to validate the software tool developed by the author of this thesis. The tool is versatile and it can be used to size any PV system in anywhere in the world. To validate the accuracy of the software tool developed in this research, the power performance characteristics of the 53-kW solar PV array installed at Isle of Eigg was obtained with the use of data logging devices, and this has been presented in **section 5.6**. It was found that the variations of solar irradiation at Eigg may have contributed to the erratic power performances of the PV array. However, in this section, a simulation of the 53 kW PV array was done using the software tool developed in this research.

5.6.2 Solar Energy at Eigg

The data sets used for the two graphs of **Figure 90** and **Figure 92** showing the output power of the 53-kW solar PV array was combined and replotted as shown in **Figure 93**. This was done to mimic the rainy season and dry season of Nigeria. The first two days are representative of a rainy day with general low solar energy, while the 3rd and 4th days represent typical varying cloudy day. The 5th day represent a dry sunny day, close to typical tropical weather condition.

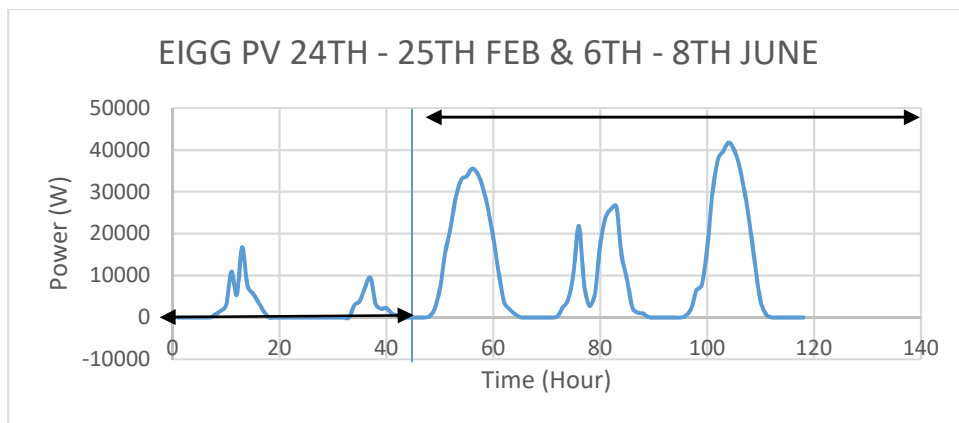


Figure 93. Combination of output power for the 53kW Eigg PV measured from 24th – 25th 2015 February and 6th – 8th June 2016.

It is important that hourly solar insolation of the selected location or site is determined before a simulation of a solar power system is carried out. The software tool developed in this research provides two options for input of solar irradiation data; it can either be imported or simulated. Basically, the imported data may be a measured solar irradiation data. To obtain a simulated dataset an input of the geographical coordinates (latitude and longitude) of the site are required. There was no measured irradiation data available for the location (Isle of Eigg) as at the time of this research. Therefore, an hourly irradiation data was obtained from an external source, Meteornorm.

“Meteornorm is a comprehensive meteorological reference. It gives you access to a catalogue of meteorological data for solar applications and system design at any desired location in the world. It is based on more than 25 years of experience in the development of meteorological databases for energy applications.” [69]

The choice of Meteornorm was based on the wide acceptance of its data for this kind of application. The coordinates (56.8937° N, 6.1533° W) of Eigg was entered into the software and it automatically generated a daily average of solar irradiation data in kWh/m²/day. This was converted to hourly data by utilising the hourly conversion model in Meteornorm and exported to text file using the export data facility in Meteornorm.

“Meteornorm calculates hourly values of all parameters using a stochastic model. The resulting time series correspond to typical years used for system design” [69].

Figure 94 is the general page of SOHYSIMO showing the imported hourly solar irradiation as obtained from Meteornorm. This was used to simulate the PV power productions at Isle of Eigg. The next section presents the simulation of the PV power characteristics.

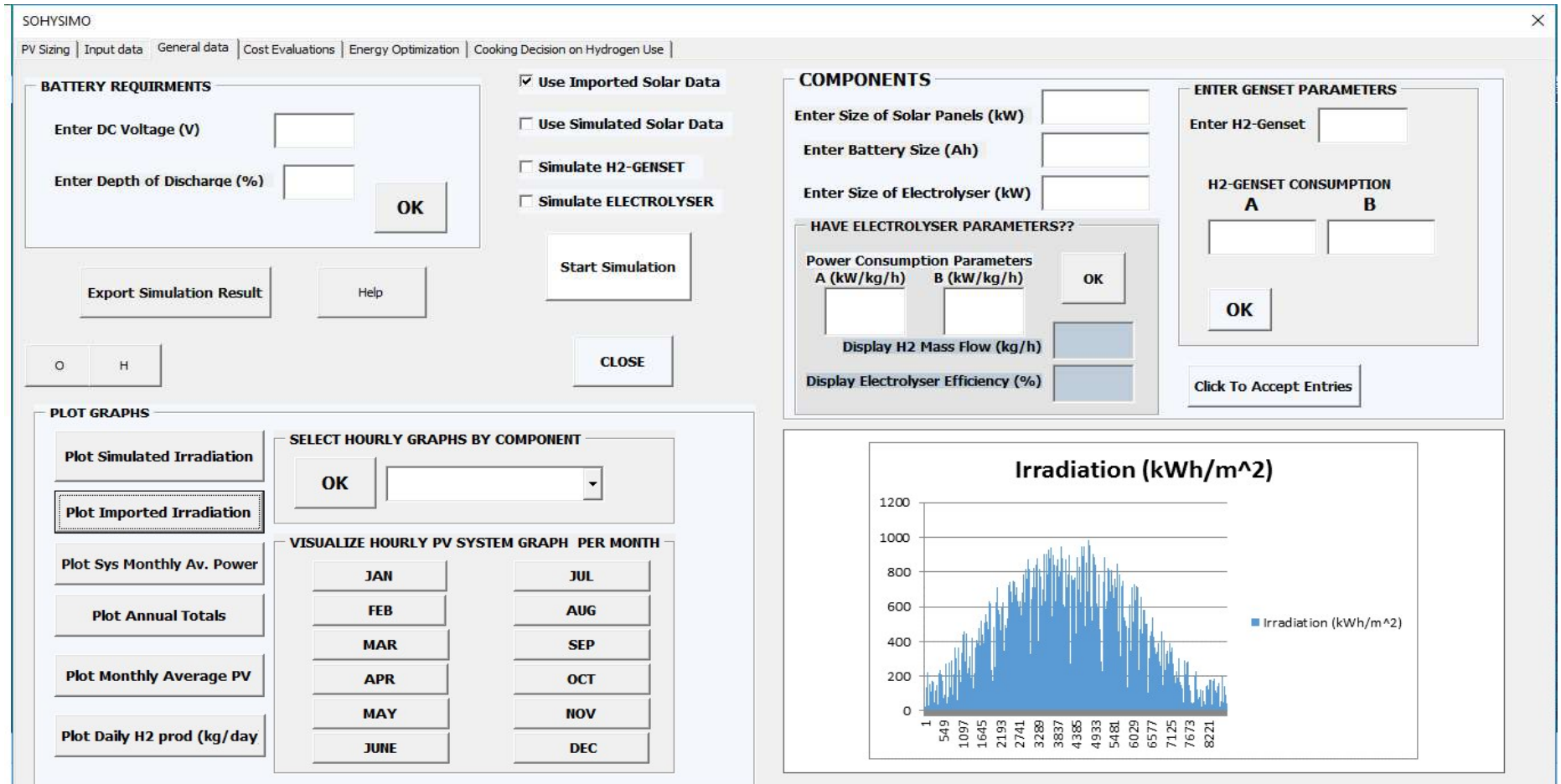


Figure 94. General page of SOHYSIMO showing a plot of Eigg irradiation data.

5.6.3 Simulation of Output Power of 53kW PV at Eigg with SOHYSIMO

Firstly, to carry out the simulation, the following input parameters was entered into the software tool.

- Rating of the solar panels = 53 kW
- Size of electrolyser = 25 kW (not compulsory)
- PV De-rate factor 78%
- PV tilt angle 35 degrees
- Battery size = 9500Ah
- DC voltage = 48V
- Battery depth of discharge = 60%

Thus, the annual hourly power productions of the 53-kW solar PV were simulated using SOHYSIMO. **Figure 95** show the simulation results of the hourly (8760) annual power productions as determined from the model.

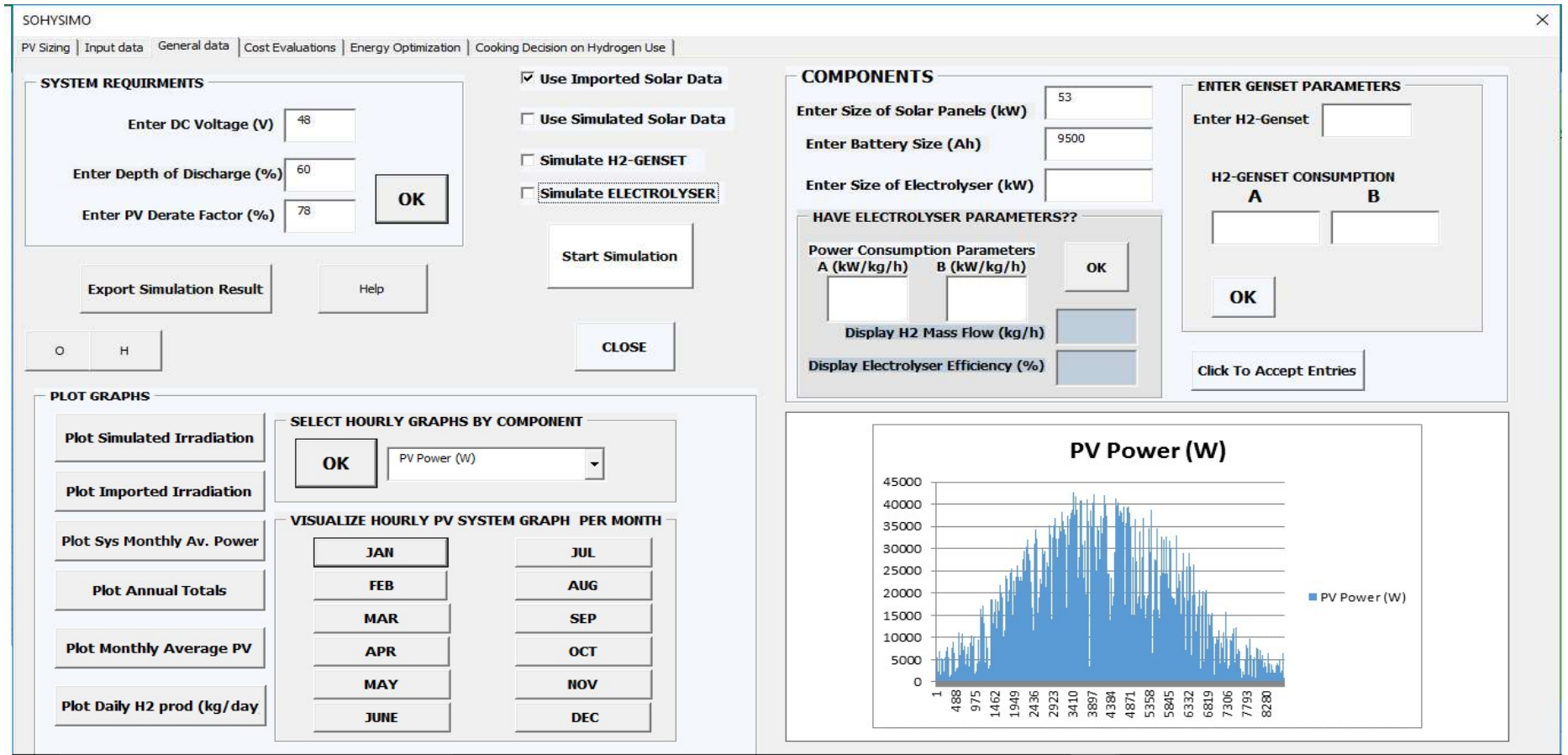


Figure 95. Simulation page showing the results of the 53kW PV output power computation.

The annual hourly data representing 24th February – 25th February was obtained from the simulation, and exported to an Excel sheet, and a data range from 24th – 25th February was selected. This was superimposed to the measured data range of **Figure 92** and plotted. **Figure 96** shows the SOHYSIMO simulated data as superimposed on Eigg recorded data (24th – 25th February 2015) for comparison.

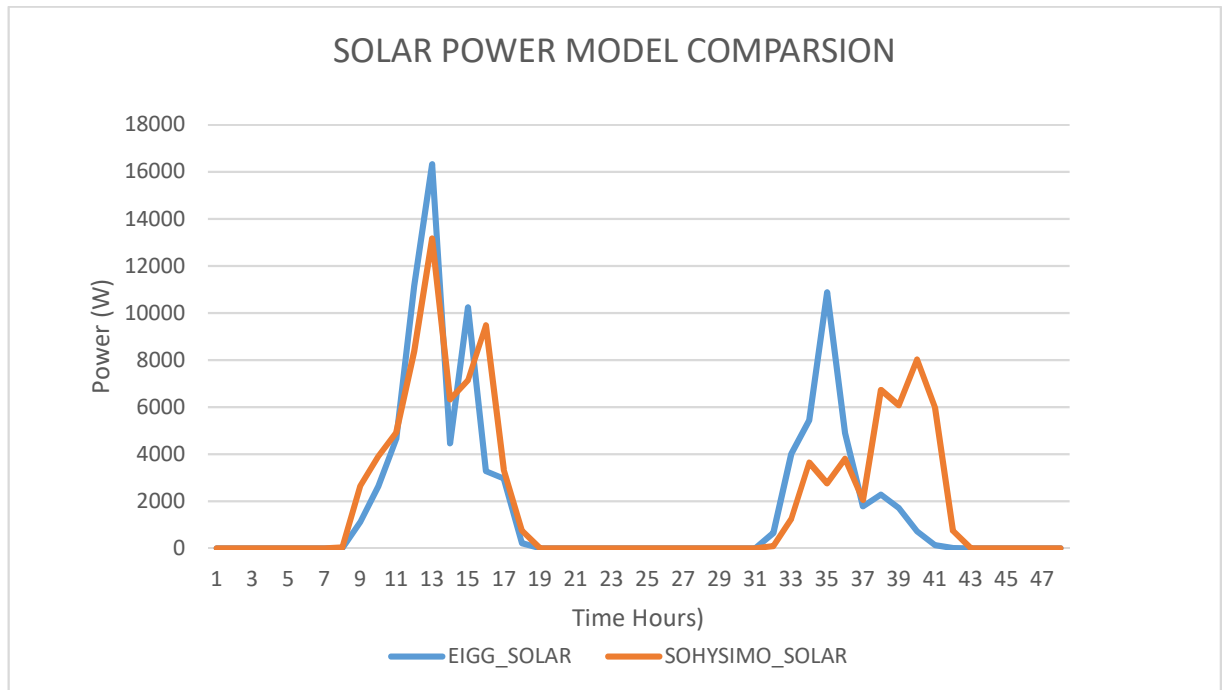


Figure 96. 24th – 25th February selected data from SOHYSIMO simulation results superimposed on Eigg measured data obtained from sunny portal.

Interestingly, it can be seen that the measured power generation data and the simulated data show close similarity in terms of trend. To appreciate this, a calculation was made using both data sets (SOHYSIMO and Eigg) to obtain the energy generated by each within this period. It was found that, on the first day SOHYSIMO model produced a 2.5 kWh of energy while Eigg data show 2.4 kWh. Also, the second day showed 1.7 kWh for SOHYSIMO and 1.4 kWh for Eigg data. These integrations show good agreement of the data on a daily scale, despite the hourly mismatches, some of which may be due to the way Meteoronorm define values as already noted in **section 5.6.2**. Given the degree of system autonomy associated with battery storage this agreement is sufficient to validate the accuracy of the developed model, and shows its capacity to simulate a complex system like Eigg electric with reasonable confidence. A second modelling of the solar PV

for 6th to 8th of June was carried out. A comparison of actual and predicted outputs is presented in **Figure 97**.

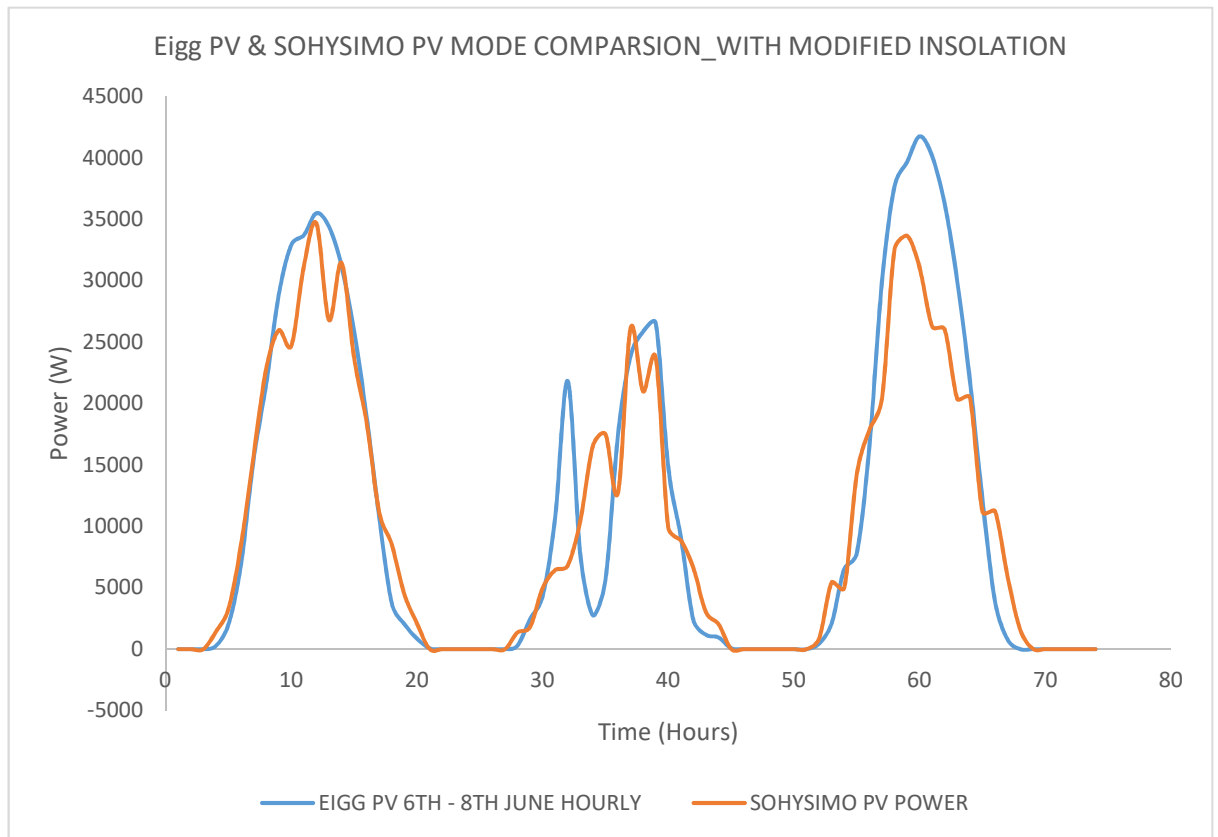


Figure 97. 6th – 8th June SOHYSIMO simulation results superimposed on Eigg measured data obtained from 6th – 8th June.

From **Figure 97** it can be seen that the peak power produced by the SOHYSIMO PV model showed excellent agreement with Eigg PV produced power on 6th and 7th of June. On the 8th of June, with a maximum difference in the data of about 20%. The likely cause of this variation is explained in the latter part of this **section**. However, it can be deduced that there may be a slight over-estimation in the downloaded solar irradiation data, and this proves the advantage of obtaining raw irradiation data from the selected site and to carry out this kind of comparative analysis. This confirms the points already highlighted about fine details in **Figure 91**. Oversizing or undersizing issues in renewable energy systems modelling and simulation has been a subject of interest over the last decades. Past Studies, describe different sizing methods to overcome this issue of oversizing the RE system components [70][71][72]. In addition, matching a load demand which ultimately varies at different time intervals of the day with power productions of

non-dispatchable power source is inherently a very challenging system design issue. Daily summed energy values are more critical than the hourly data, provided that the system has integrated storage. **Figure 98** compares the daily energy production from SOHYSIMO model and Eigg data. These are points which make the idea of integrating an energy storage system, especially those that can be optimised for long term storage an attractor for enhancing energy security.

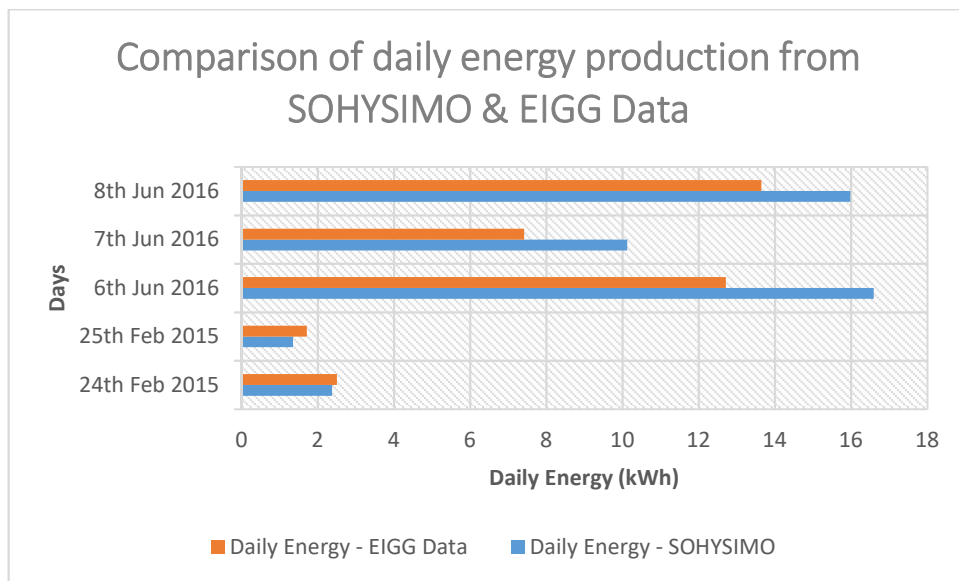


Figure 98. Comparison of SOHYSIMO energy results with Eigg real energy production data.

On Eigg during the winter period the renewable sources usually generate more power than the island can consume. This is primarily because of the normally high load factor of the 100kW Laig hydro in this period. In times of over supply the frequency of the system tends to rise above the default 50Hz. The system inverters are programmed to respond to frequency changes through a switching sequence which activates 12 x 3 kW space heaters in a cascading manner at the Community Hall, the Pier Centre and the churches. If the frequency continues to rise above 51Hz the wind turbines and PV are gradually feathered out of the system. Above 51.5 Hz the hydro power is reduced by deflecting water from the tailrace away from the turbine. When demand outstrips supply (from the renewable generators) the battery stack provides the balance, and the system maintains a 50Hz frequency. If the battery state of charge (SOC) falls below 60% a standby diesel generator switches in to the system providing approximately 50kW

extra power. This provides the required system balancing and charges the batteries. When the battery SOC rises above 80% the generator switches off and the system reverts to its mix of renewables and batteries to maintain the supply. In times of prolonged system stress (typically when there has been a very dry spell and the hydro is low) this process of charging and discharging the batteries and switching in and out of the diesel generator can be cyclical over many days.

Of particular importance here is the use of the invertors to progressively reduce the system input from the PV in times of over-supply. Care was taken in the collection of the PV data highlighted in figures 121 and 123 to ensure (by checking system frequency) that on the dates chosen there were no curtailments to the PV supply. A one year PV power generation data from the SMA Sunny Portal for the period of January 2014 – December 2014 is summarised in **Figure 99 and Figure 100**. From the graphs, a strong variation in monthly PV power production across the year is observed. This is as expected. For a typical grid connected system it would be expected that the PV would provide measurable power even on the darkest winter day. Looking at the power graphs, it can be seen that there are periods in March, October and December where the PV output looks artificially low. These periods coincide with the over-supply scenario described above. It can also be observed in the data that the peak value recorded for the year was 48kW (once in May and twice in June). This suggests that the PV system as configured may be approximately 90% efficient.

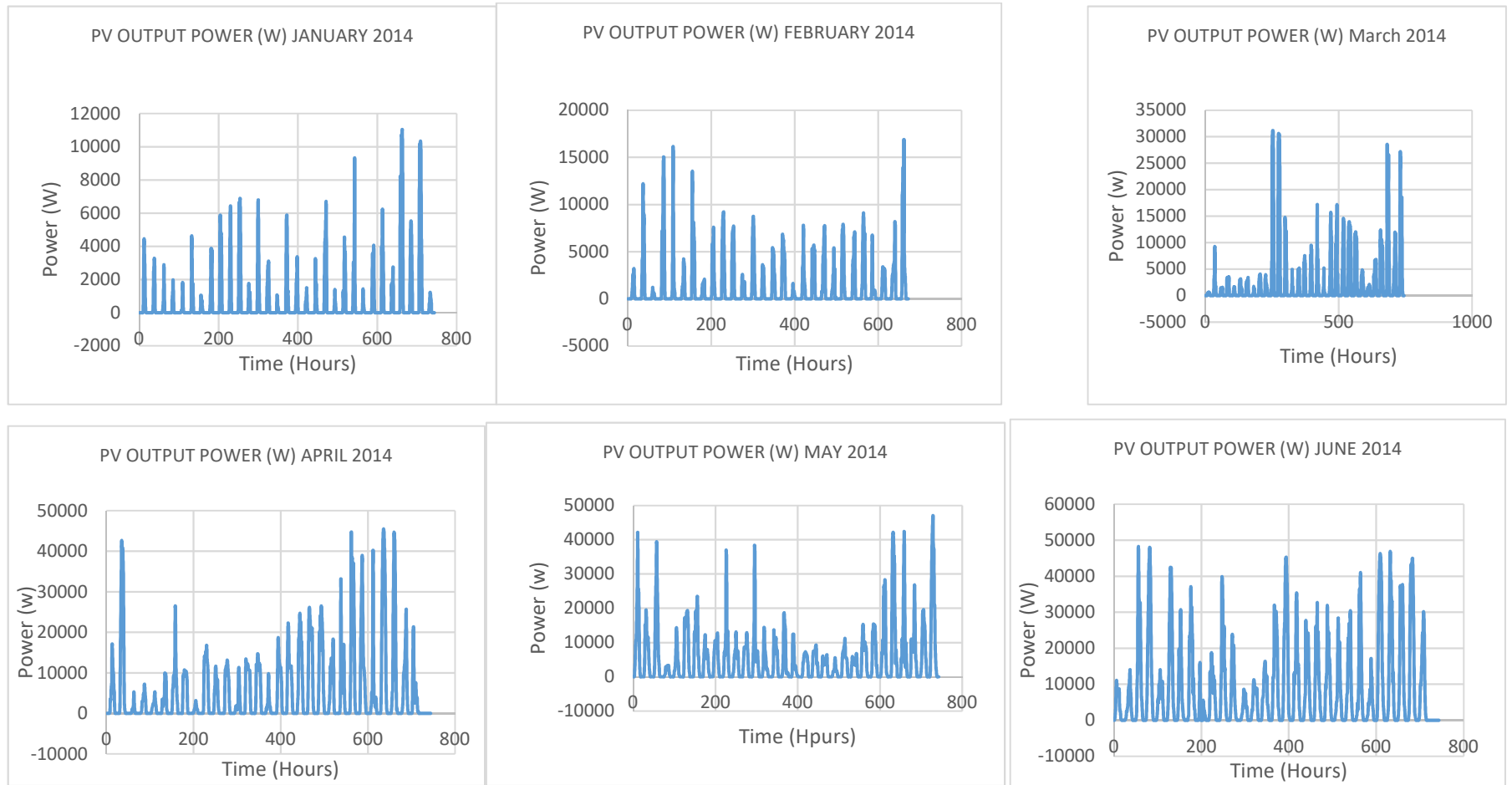


Figure 99. Plot of monthly - hourly output of Eigg 53KW PV for 2014 [67].

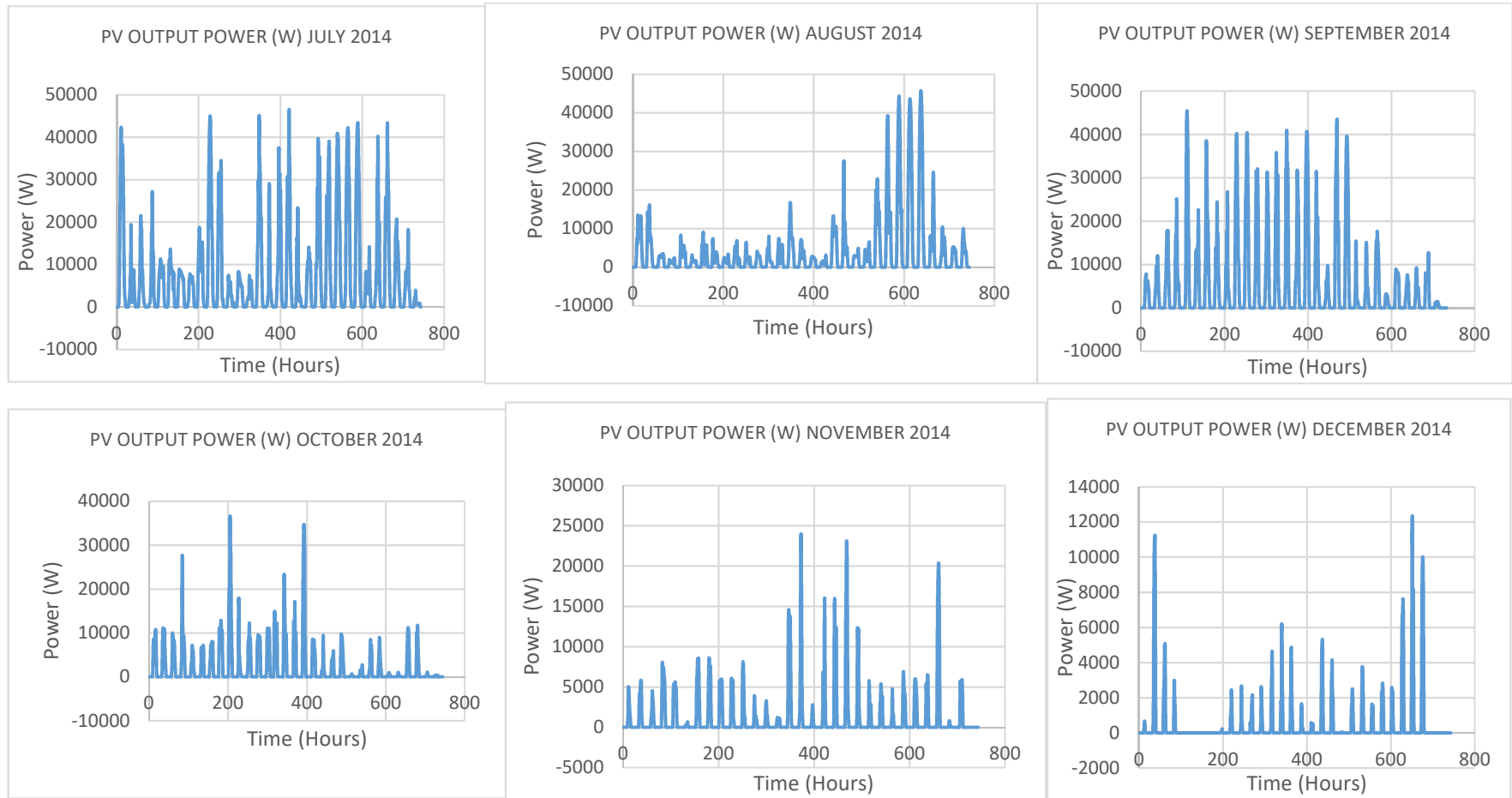


Figure 100. Plot of monthly - hourly output of Eigg 53KW PV for 2014 [67].

The SMA data-logging WebBox implemented in the Isle of Eigg system has provided an annual comparison mechanism which makes it easier to visualize the system's annual energy yield. **Table 25** lists the monthly and annual energy yields from the solar PV. The upward trend in annual outputs seen in the final column represents additional capacity integrated in two stages, taking the system from 10kW to 31kW to 53kW over a five-year period.

Total Yield (kWh)														
Year	January	February	March	April	May	June	July	August	September	October	November	December	Total	
2007													112	112
2008	143.91	377.28	748.34	1200.2	1491.1	1128.3	681.26	673.52	685.66	505.34	174.82	140.55	7950.22	
2009	86.03	2441.85	442.14	591.38	3295.9	1478	1256.5	304.77	381.27	305.89	155.09	200.47	10939.24	
2010	293.01	481.39	753.94	1105.4	1457.5	1357.4	976.97	1156.8	768.34	578.67	319.71	251.59	9500.7	
2011	214.04	344.45	525.38	1067.8	1143.1	1311	1448.1	972.34	570.43	276.09	234.83	59.15	8166.61	
2012	140.32	202.17	592.74	3996.4	4917.9	4252.9	3623.4	3094.6	1731.01	1627.3	519.6	417.03	25115.39	
2013	470.26	1328.64	2845.2	3812.6	3436.4	3999.9	4635.6	3199.6	2478.81	1969	568.54	313.11	29057.72	
2014	528.12	937.93	2051.3	4119.9	4172.4	6480.8	5750.9	2918.3	4239.61	1899.4	1039.88	434.7	34573.09	
2015	638.8	1166.69	2236.7	5117.5	4721.4	3544.5	3555.3	3145	4191.7	2326.2	605.61	391.86	31641.28	
TOTAL													157056.2	

Table 25. The Annual Energy Yield by the Eigg 53kW solar PV [67].

The PV system losses due to curtailment can be estimated on an annual basis by comparing the simulated outputs from SOHYSIMO with the data shown in table 26. **Figure 101** shows the comparison of monthly energy productions during 2014. From the graph, a significant mismatch between the two plots can be seen, with the modelled data consistently producing higher values than the generated monthly outputs, especially over the spring and summer periods. However, an opposite scenario can be observed in winter period as the PV at Eigg produced higher values than the modelled data. These can be attributed to the solar irradiation data used in this simulation. A measured irradiation data obtained from the site would give better results.

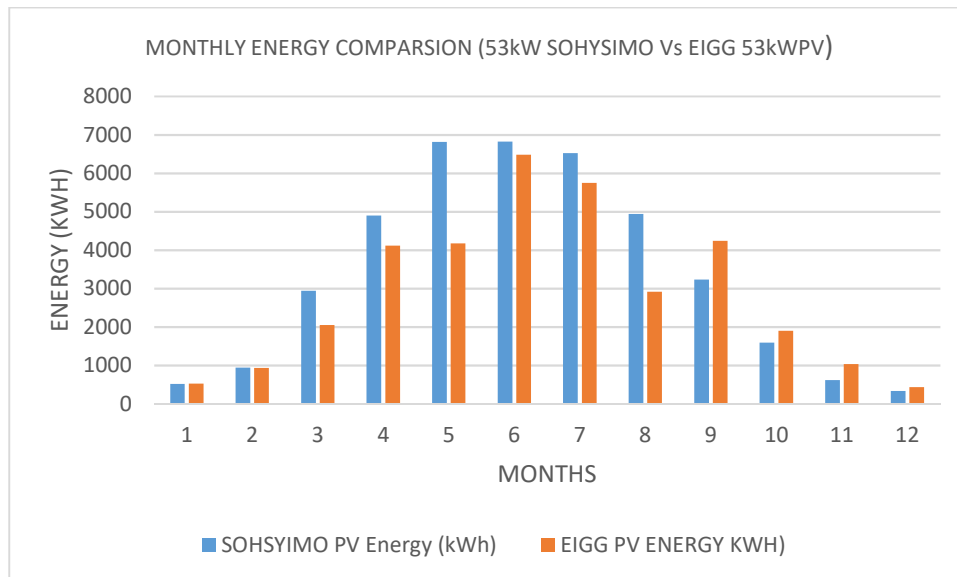


Figure 101. Monthly (2014) energy comparison of SOHYSIMO simulation results with Eigg data.

The total annual energy yield of the 53kW PV simulated using SOHYSIMO was 45,418kWh, but the metered generation was recorded as 34,573kWh. This gives a 24% difference and is representative of the total system losses. Earlier it was observed that the electrical/electronic losses appeared to be of the order 10%. This suggests strongly that the remainder of the losses are attributable to reduced generation at high system frequencies.

5.6.4 Comparison and Validation of SOHYSIMO Model Simulation with HOMER and iHOGA

In renewable energy system design and modelling, there is a basic requirement that results obtained from a new model or prototype developed be validated with existing standard models. In this thesis, the outputs from SOHYSIMO software tool are compared with two existing prominent software models, in order to draw a standardised validation of the developed tool. In **section 5.1.1** of this thesis, various software tools that are capable of simulating hydrogen system were reviewed. In that section, it was noted that HOMER and iHOGA presents a distinction among all other tools mentioned, as the models that are capable of simulating a hydrogen storage system, whereby the produced hydrogen can be used in some electrical energy generating devices (H2-

genset, fuel cell etc), For this reason the HOMER and iHOGA software presents an appropriate pathway for this kind of validation.

Validation 1

A representation of Isle of Eigg electric system was setup in HOMER and a simulation was carried out. In the simulation process, the aim was to determine the output power and annual energy yield of 53kW solar PV in HOMER. With this simple criterion, a full economic analysis was unnecessary, and therefore the cost components were assumed to be zero. To proceed in the simulation, a 53kW PV at 78% de-rate factor was entered into the sizing search space, the PV slope angle was neglected and the solar irradiation obtained from Meeonorm was imported into HOMER as shown in **Figure 102**. A load of 1.2kWh/day was assumed, and twelve 4V 7.6kWh Rolls/Surrette 4KS25P batteries was selected. The tiny load demand was selected simply in order to investigate the behaviour when considerable power is available to the electrolyser. This was configured in 12 string size with 5 parallel strings of 60 batteries totalling 456kWh nominal capacity at 48V at 60% DoD, thus partially mimicking the Eigg system. **Figure 103** shows the HOMER simulation user interface highlighting the electric power characteristics of the simulated PV system, and **Figure 104** shows the battery characteristics.

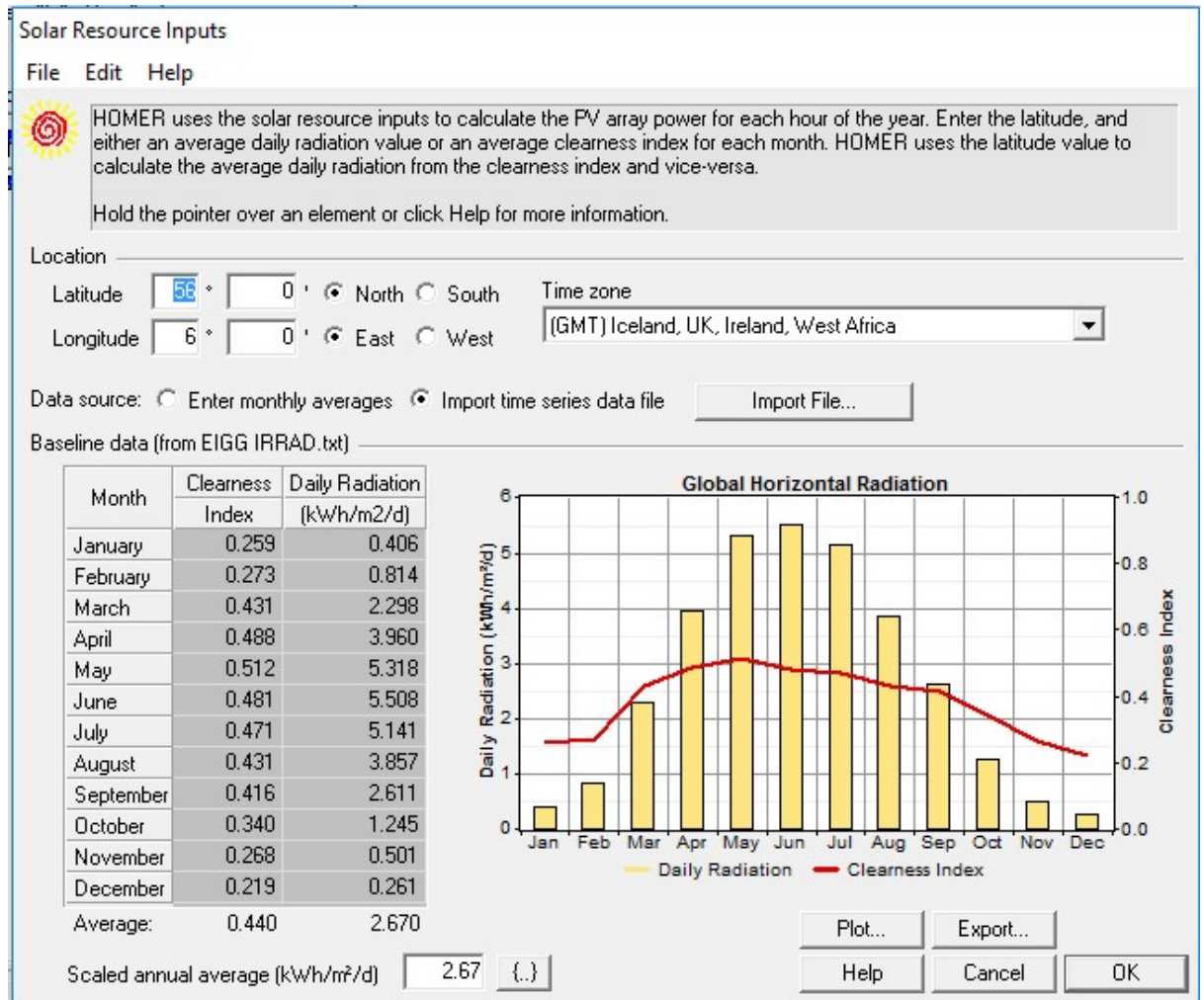


Figure 102. HOMER simulation user interface showing the simulated power characteristics of the 53KW PV.

From the inputs provided the simulated annual energy production of the PV was 40,276kWh/yr with a daily average at 127kWh/day. The match-loading energy delivered by the battery was 260kWh/yr. **Table 26** lists the simulation results obtained from HOMER.

Parameter	Value	Units
Rated capacity	53	kW
Mean output	127	kWh/d
Annual PV production	40276	kWh/yr
Excess energy	1233	kWh
Energy available for electrolyser	38557	kWh
Minimum output	0	kW
Maximum output	36	kW
Hours of operation	4381	hr/yr
Total DC load	442	kWh/yr
Battery Nominal capacity	456	kWh
Battery autonomy	3618	hours
Battery usable capacity	182	kWh
Energy delivered to battery	304	kWh
Energy out of battery	260	kWh

Table 26. HOMER simulation results.

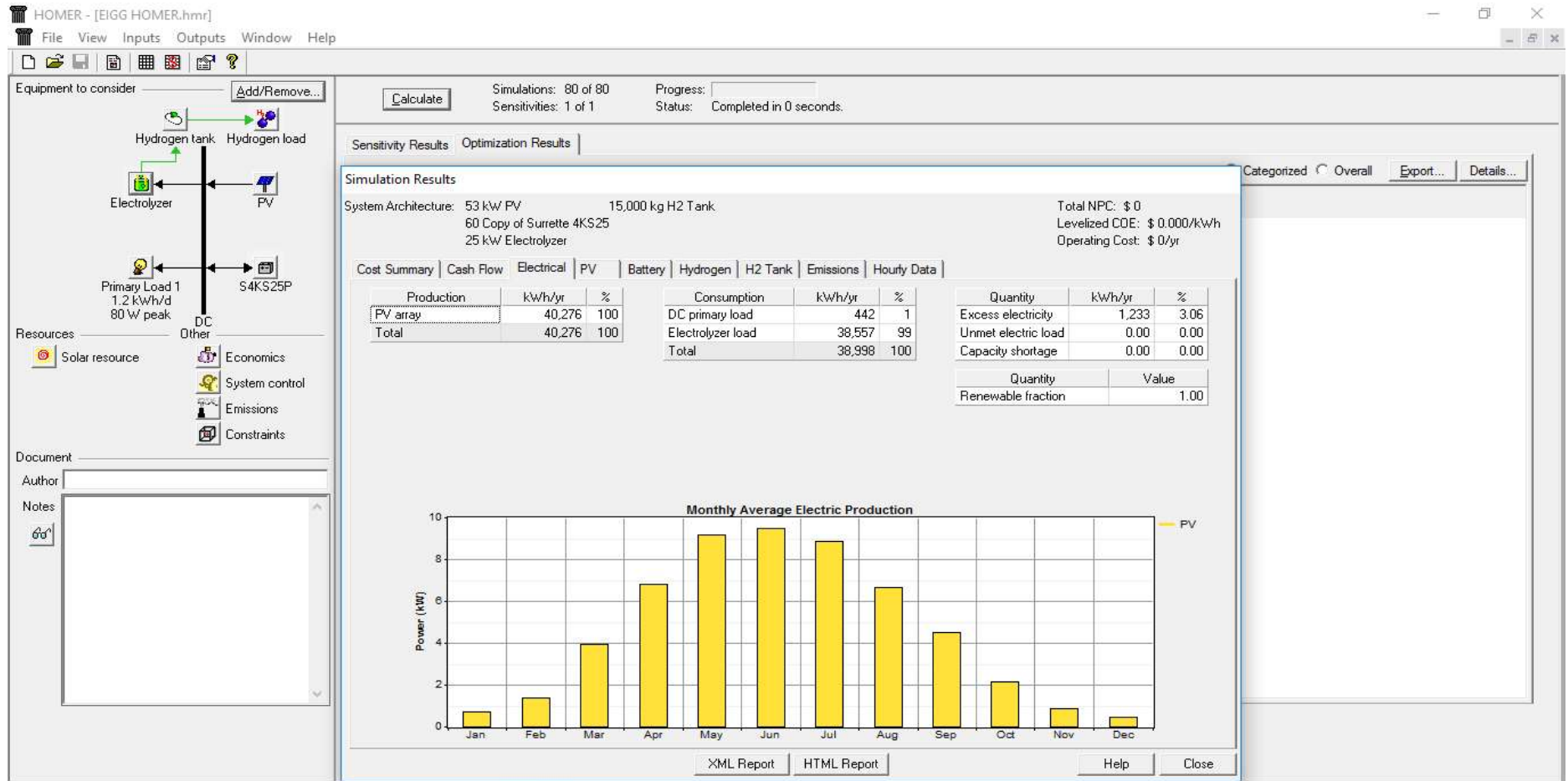


Figure 103. HOMER simulation user interface showing the simulated power characteristics of the 53KW PV.

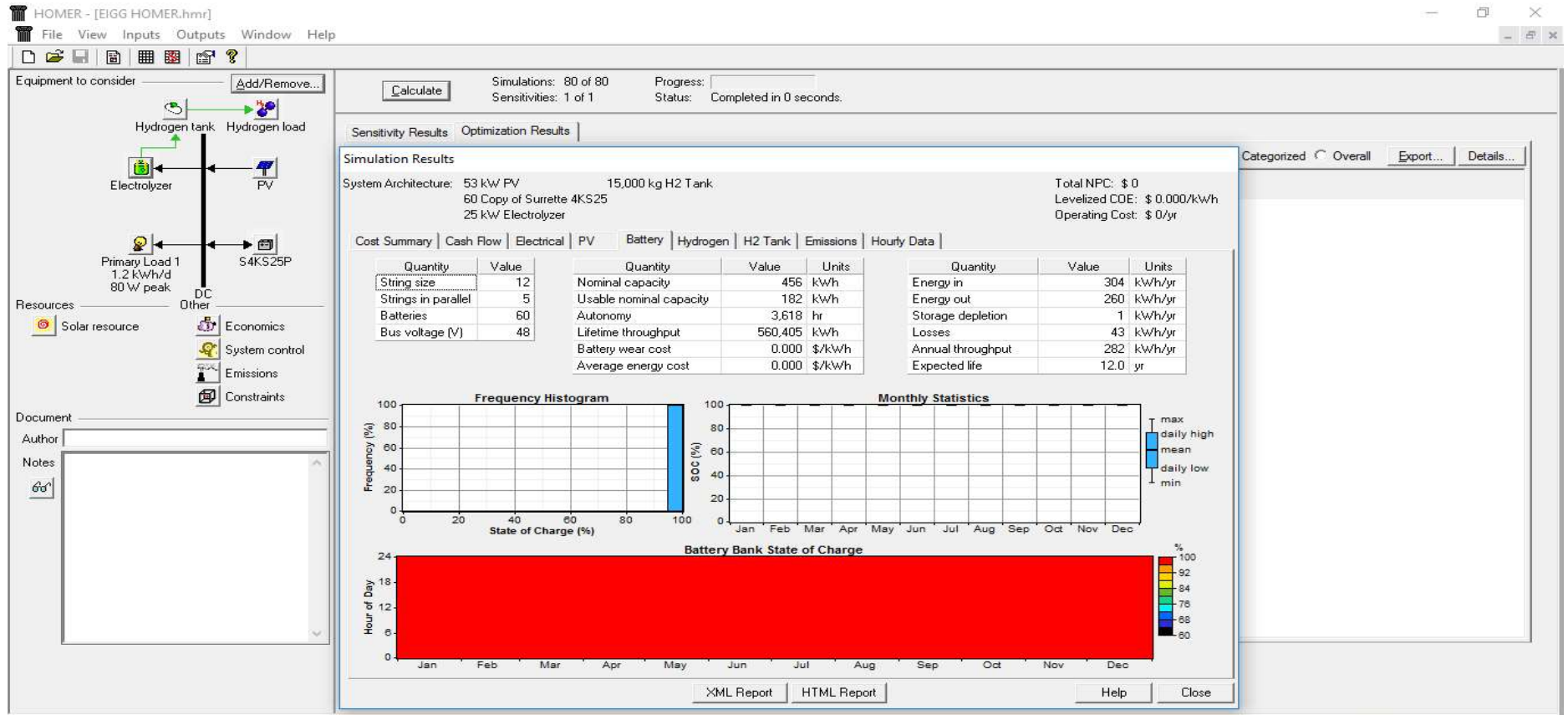


Figure 104. Battery performance characteristics in HOMER, showing that they maintain a full state of charge throughout the year. The batteries are just included in the system to allow the simulation to take place.

Next, a second simulation using the same input parameters was run using SOHYSIMO. **Figure 105** depicts the SOHYSIMO input interface where the load and irradiation parameters were imported for simulation, with the hourly load profile displayed graphically. **Figure 106** shows the main simulation interface with the PV monthly average power production results displayed in graph. **Table 27** list the simulation results obtained from SOHYSIMO. The annual energy production was 40287 kWh, with an excess of 1222kWh after providing 311kWh to charge the battery stack, while also supplying about 180kWh to the load and leaving 38,585kWh available to be utilised in an electrolyser if available.

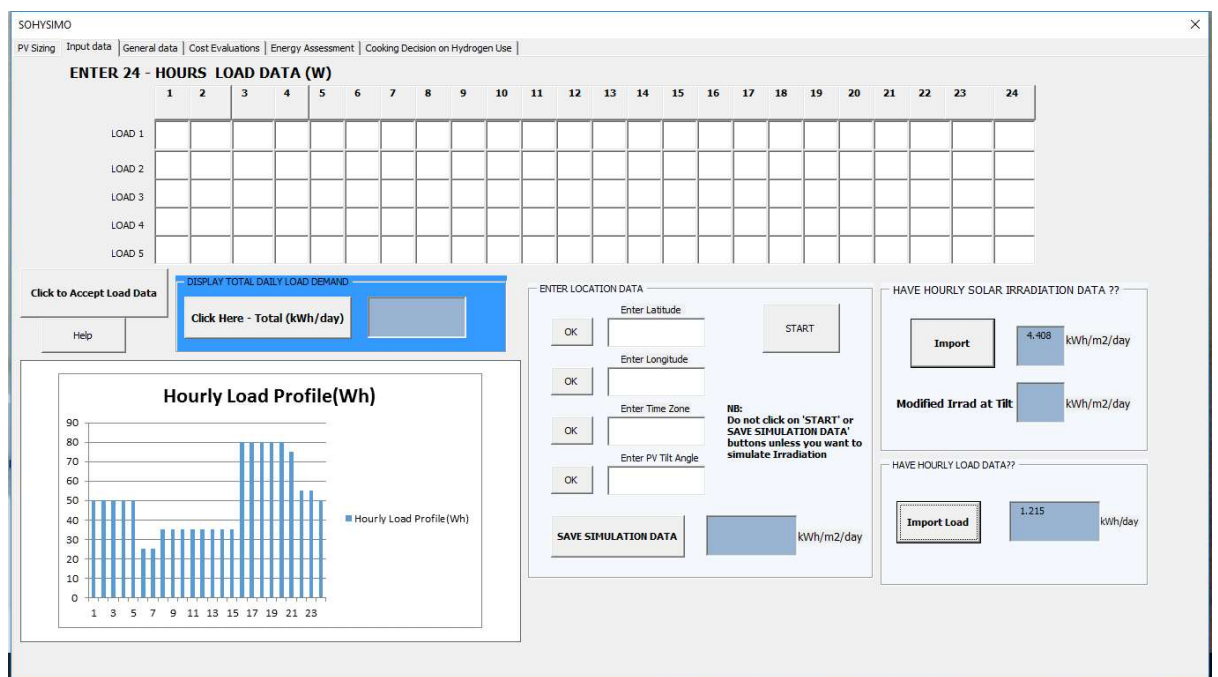


Figure 105. Input data page showing the imported load profile.

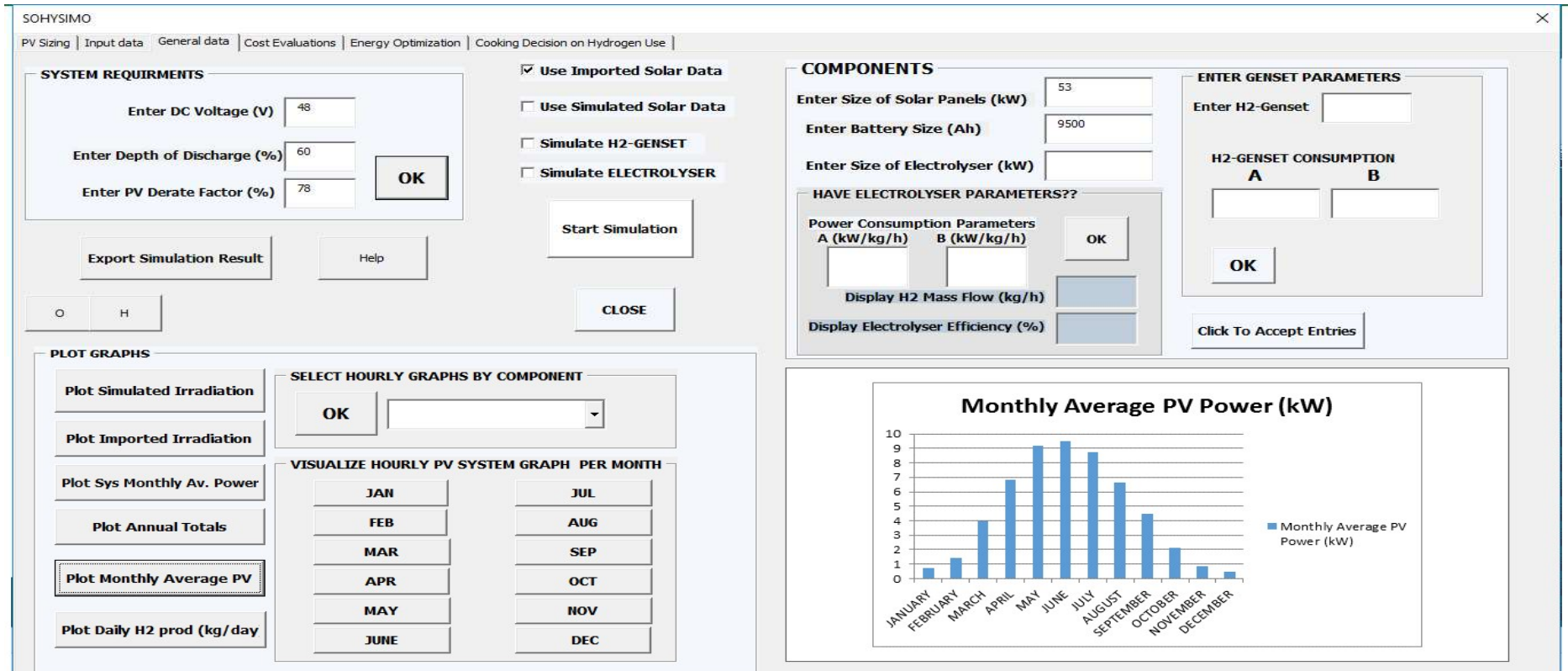


Figure 106. Main simulation page of SOHYSIMO showing the monthly average power.

Parameter	Value	Units
Rated capacity	53	kW
Annual PV production	40287	kWh/yr
Excess energy	1222	kWh
PV hours of operation	4562	hours
Total DC load	442	kWh/yr
Battery nominal capacity	456	kWh
Battery usable capacity	182	kWh
Battery hours of operation	4198	hours
Battery autonomy hours	3618	hours
Battery Energy in	311	kWh
Battery Energy out	255	kWh
Energy available for electrolyser	38585	kWh/yr
Suggested days of autonomy	1.7	days
Suggested battery size	53.6	Ah @50%DoD 48V
Suggested electrolyser size	35.9	kW
Unmet electric load	0	%
Suggested PV size	0.508	kW

Table 27. SOHYSIMO simulation results.

From the main simulation page, the monthly peak average power was 9.2kW and this was observed in the summer month of June. However, SOHYSIMO contains a facility where energy assessments can be run to obtain a suggested optimum size for the system components (battery, DoD and PV). **Figure 107** depicts the SOHYSIMO energy assessment page displaying the simulation results obtained.

SOHYSIMO

PV Sizing | Input data | General data | Cost Evaluations | Energy Assessment | Cooking Decision on Hydrogen Use

ENTER OPTIMISATION PARAMETERS

Enter Battery voltage(V)

Enter PV Carbon Factor (kgCO₂e/kWh)

Enter Firewood Carbon Factor (kgCO₂e/kWh)

Select Battery Depth of Discharge

DISPLAY SYSTEM RESULTS

CARBON SAVINGS

PV Carbon Savings (kg)

H2-Cooker Carbon Savings (kg)

BATTERY

Battery Nominal Capacity (Wh)

Battery Usable Capacity (Wh)

Autonomy (Hours)

SUGGESTED BATTERY SIZE

Battery Size (Ah)

Usable capacity (Ah)

Autonomy (Hours)

Safe Autonomy (Days)

Battery Hours of Operation

Energy Out of Battery (kWh/Yr)

Energy Into the Battery (kWh/Yr)

PHOTOVOLTAIC

SUGGESTED PV CAPACITY

PV Size (kW)

PV annual Yield (kWh/yr)

PV Hours of Operation

LOAD

Total Load (kWh/yr)

Energy Sent Electrolyser (kWh/Yr)

Unmet Electric Load (%)

Excess Energy (kWh)

HYDROGEN

Total Hydrogen Production (kg/yr)

Suggested Electrolyser Size (W)

Figure 107. SOHYSIMO Optimisation results of the 53KW PV.

In order to compare SOHYSIMO results with HOMER results, **Table 26** and **Table 27** was merged to produce **Table 28**. The results indicate an existence of good agreement between the two models. Clearly, in all the parameters considered in the simulation, the difference between the two models is insignificant. The PV output in HOMER was 40276kWh/yr while that of SOHYSIMO was 40287kWh/yr, when both are compared it shows a mere 11.9kWh/yr difference. Similarly, the energy available from the 53kW PV for electrolyser utilisation was 38585kWh/yr in SOHYSIMO, while in HOMER the PV produced about 38557kWh/yr, when compared, this is just 28kWh/yr difference. This can be attributed to different modelling algorithms used in the SOHYSIMO model, as compared to HOMER. However, the excess energy realised after serving the battery and load was 1222kWh/yr in SOHYSIMO, this was just close to that seen in HOMER with a difference of 11kWh/yr, as the results from HOMER showed about 1233kWh/yr.

Parameter	SOHYSIMO	HOMER
Rated capacity (kW)	53	53
Annual PV production (kWh/Yr)	40287	40276
Excess energy (kWh/Yr)	1222	1233
PV hours of operation (hours)	4562	4381
Total DC load (kWh/Yr)	442	442
Battery nominal capacity (kWh/Yr)	456	456
Battery usable capacity (kWh/Yr)	182	182
Battery hours of operation (hours)	4198	N/A
Battery autonomy (hours)	3618	3618
Battery Energy in (kWh/Yr)	311	304
Battery Energy out (kWh/Yr)	255	260
Energy available for electrolyser (kWh)	38585	38557
Suggested days of autonomy (hours)	1.7	N/A
Suggested battery size (Ah)	53.6	N/A
Suggested electrolyser size (kW)	35.9	N/A
Unmet electric load (%)	0	0
Suggested PV size (kW)	0.508	N/A

Table 28. Comparison of HOMER simulation results with SOHYSIMO results.

Validation 2

A second comparison using the iHOGA software tool was used with same the components, sizes and system profile as previously. **Figure 108** shows the solar irradiation in iHOGA.

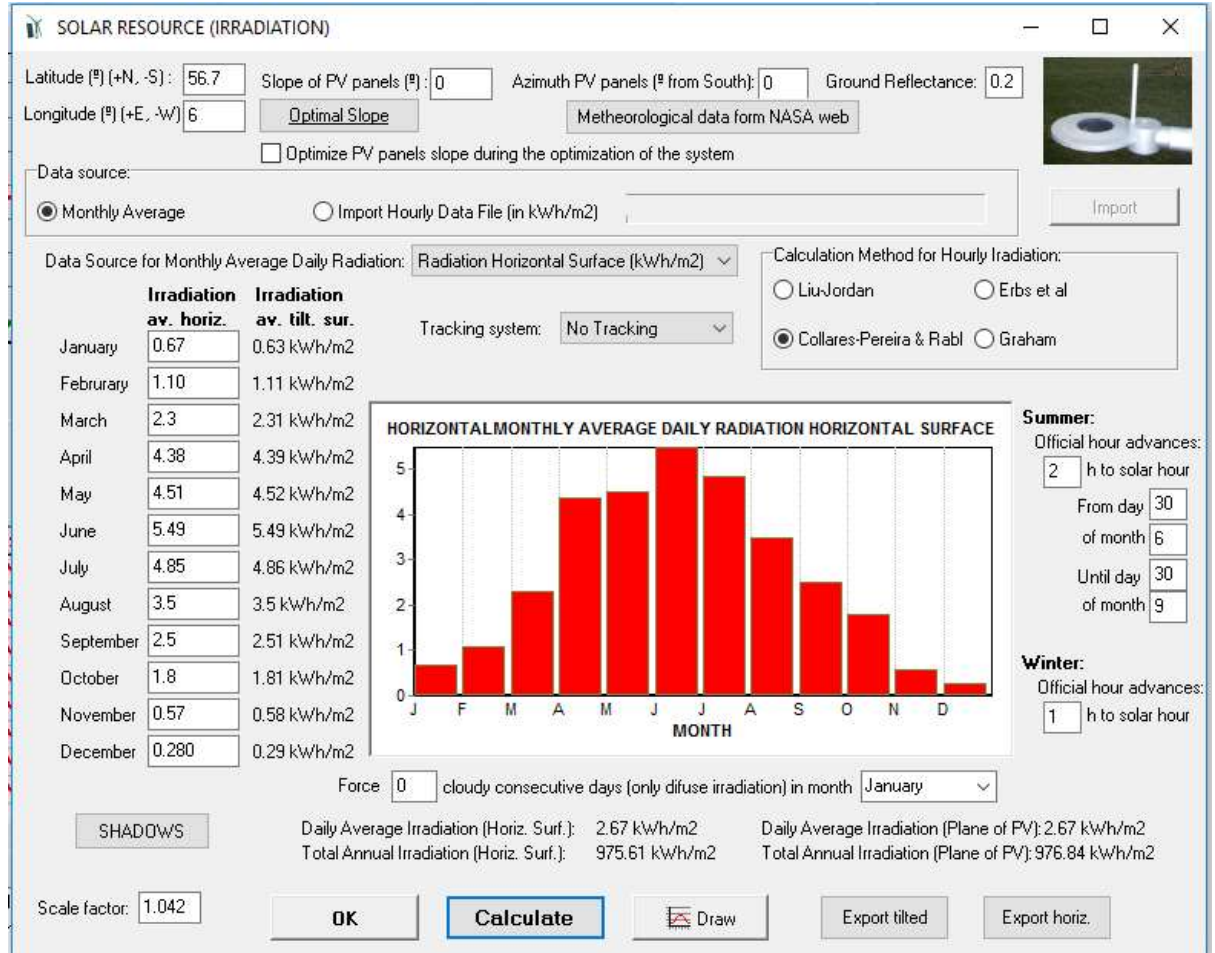


Figure 108. iHOGA simulation user interface showing the imported irradiation data.

Figure 109 shows the simulation results from iHOGA. The annual PV production was 40,269 kWh/year with excess of 37,252 kWh/year. **Table 29** compares the simulation results from iHOGA and SOHSYIMO.

Parameter	SOHYSIMO	iHOGA
Rated capacity (kW)	53	53
Annual PV production (kWh/yr)	40288	40269
PV hours of operation (Hours)	4562	N/A
Total DC load (kWh/yr)	441	441
Battery nominal capacity (kWh/yr)	456	456
Battery usable capacity (kWh/yr)	182	N/A
Battery energy out	255	216
Excess energy (kWh/yr)	38585	37252
Unmet electric load (kWh)	0	0
Suggested PV size (kW)	0.508	N/A*

*N/A = Not available

Table 29. Comparison of iHOGA simulation results with SOHYSIMO results.

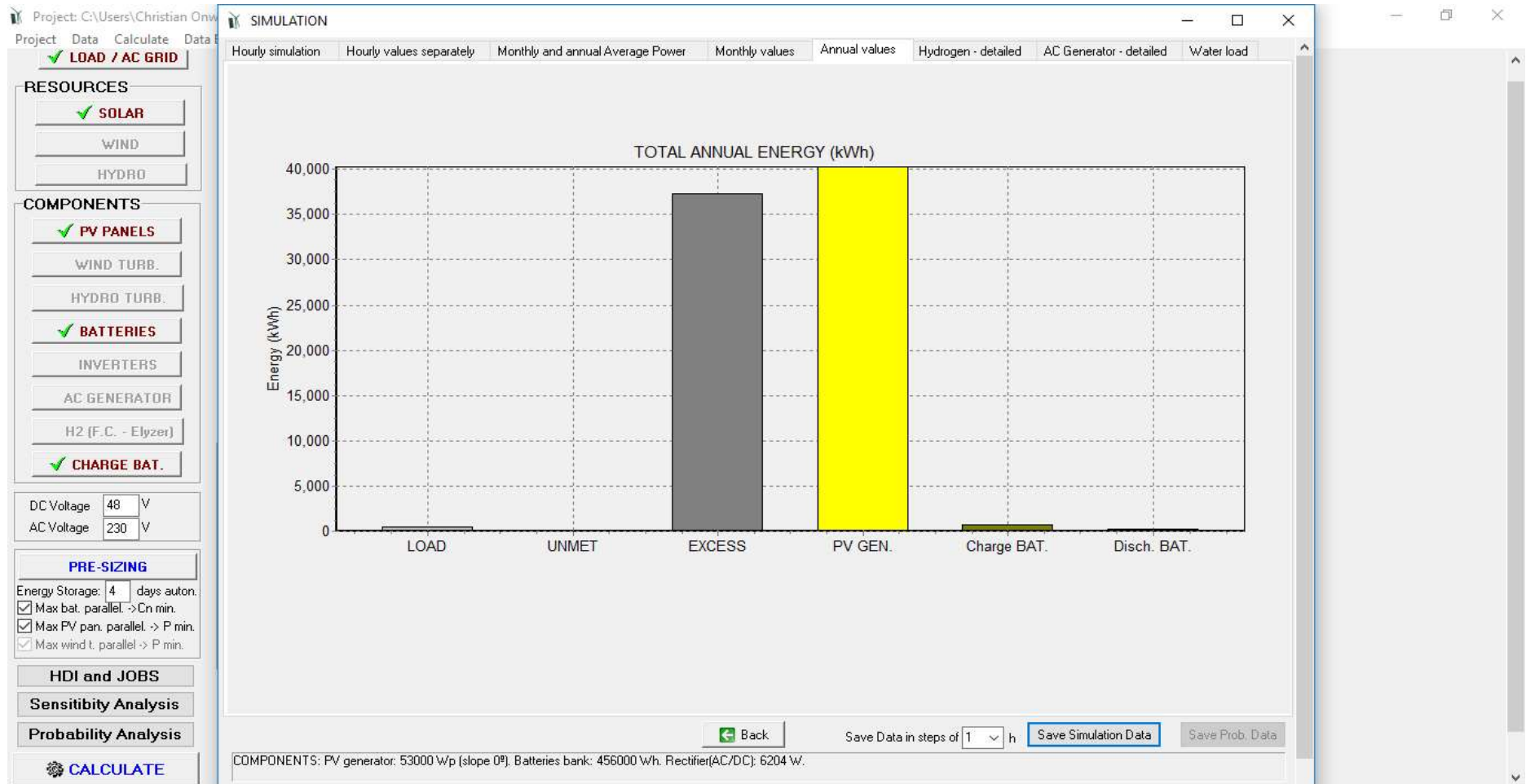


Figure 109. Simulation user interface showing the simulated power characteristics of the 53KW PV. The large excess production value is simply a consequence of the low load model adopted.

5.7 Summary

Table 30 draws together the simulation results for the three software models.

Parameter	SOHYSIMO	iHOGA	HOMER
Rated capacity (kW)	53	53	53
Annual PV production (kWh/yr)	40288	40269	40276
PV hours of operation (Hours)	4562	NA	4381
Total DC load (kWh/yr)	442	441	442
Battery nominal capacity (kWh/yr)	456	456	456
Battery usable capacity (kWh/yr)	182	NA	182
Battery energy out	255	216	260
Excess energy (kWh/yr)	38585	37252	38557
Unmet electric load (kWh)	0	0	0
Optimised PV size (kW)	0.510	NA	NA

Table 30. Comparison of HOMER and iHOGA simulation results with SOHYSIMO results.

The excellent agreement observed across the models provides the necessary validation of the solar modelling and battery elements of the SOHYSIMO software. The agreement of HOMER and SOHYSIMO with regard to excess energy available is important and allows some confidence in the next stages of modelling where hydrogen production is of interest. The agreement between the simulated data and the data obtained from an existing system in Eigg, has demonstrated the capacity of the developed tool.

5.7 Testing and Assessment of Off-grid Solar-Hydrogen Storage System.

The previous sections describe the development of a new software tool for the modelling and simulation of solar – hydrogen power system. As a standard, it is required that a new software tool be validated by comparing its simulation results with the results obtained from an accepted and widely used model. The tools' simulation accuracy of PV output power, which is the key component of the system was validated by comparing

its results with results from HOMER and iHOGA software models. Also, it was compared with the actual measured values and these shows good agreement with the SOHYSIMO simulated results, with some varying values which was suspected to be due to some constraints imposed on the system. In the next section, the studies for validation of the complete solar – hydrogen production model is presented.

5.7.1 Comparison of SOHYSIMO Hydrogen Model with HOMER.

To complete the testing and validation process of the software model developed in this research, a solar – hydrogen production system was simulated in HOMER, with the same component specifications as used in the solar output power simulation presented in **section 5.6.3**

Validation 3

However, in this simulation process the PV panel slope was adjusted to 35 degrees for optimum power production, and an electrolyser component was also included for hydrogen production to complete the model. The overall sizes of the components used in the simulation are 25kW electrolyser with 1000kg H₂ storage tank, 53kW solar PV at 78% de-rate factor, 456kWh battery capacity and 1.2kWh/day load demand, with all the cost components set to zero. In HOMER, for solar – hydrogen production system simulation to proceed, it requires the addition of a hydrogen load. Therefore, a 0kW hydrogen load was added to the system component. The hydrogen load was set zero because the aim at this stage was solely to produce hydrogen with the excess energy generated by the 53kW solar array. Meanwhile, it should be noted that for electrolyser modelling in HOMER a user should enter a pre-defined efficiency value. This is different when compared to the efficiency process in SOHYSIMO tool as described in **section 5.3.3**. A 75% efficiency was entered to reflect the efficiency depicted in SOHYSIMO. The simulation was run in HOMER and **Figure 110** shows the screenshot of the HOMER hydrogen simulation result. The total hydrogen produced by the 25kW electrolyser in HOMER was 778kg/year. The monthly average hydrogen production peaked at 3.9kg/day in the month of May, the lowest monthly average H₂ produced over the year was in December at 0.18kg/day. To compare these with SOHYSIMO, the same system components as used in this HOMER simulation were inputted into the SOHYSIMO tool.

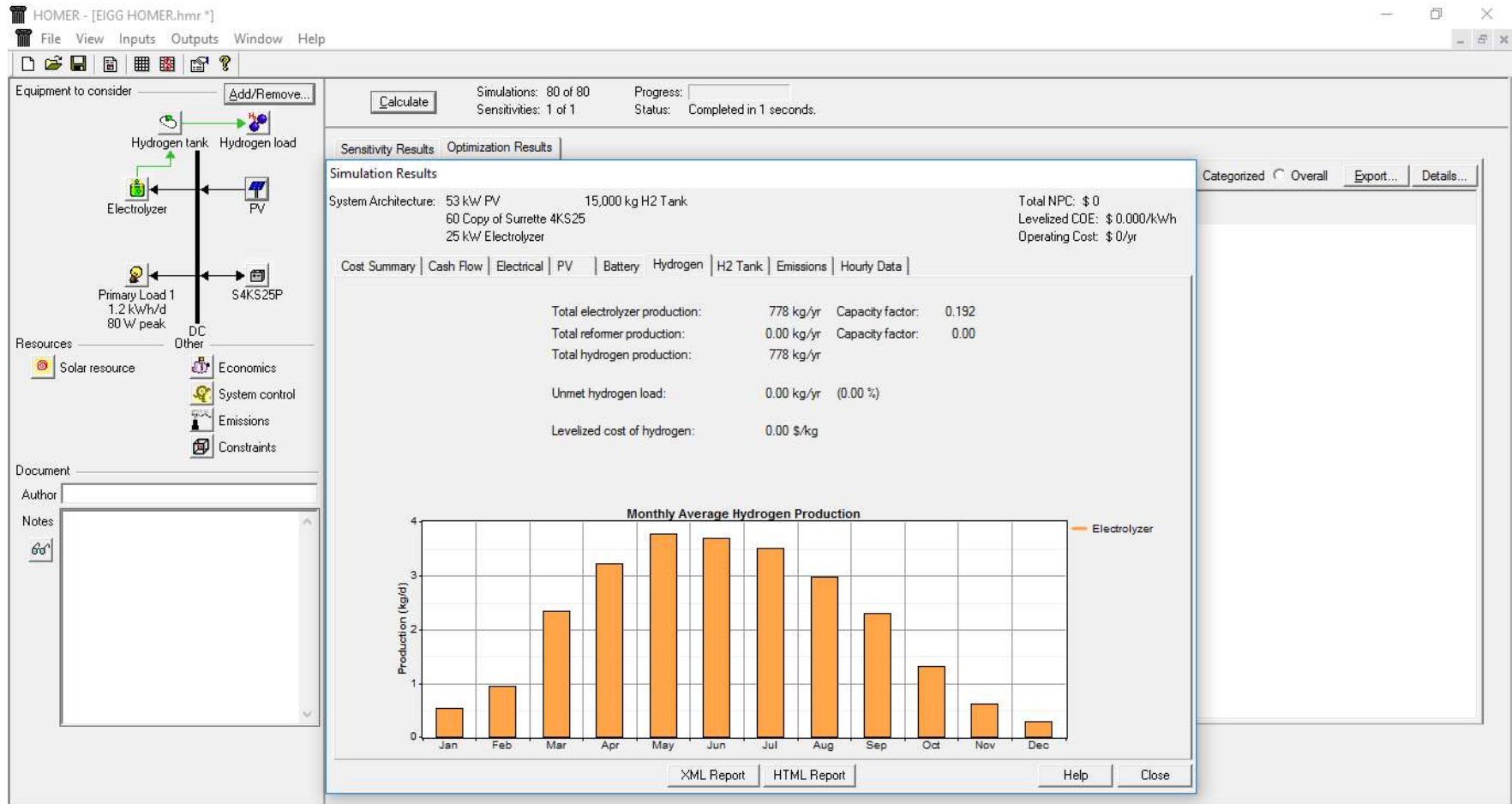


Figure 110. HOMER simulation user interface showing the hydrogen productions of the 25kW electrolyser.

The cost components were again set to zero. **Figure 111** is a screenshot of the SOHYSIMO simulation interface showing the monthly average hydrogen production in kilograms per day (kg/day). The monthly hydrogen production peaked at 4.93kg/day in May followed by 4.86kg/day in June, and declined to a minimum 0.24kg/day in December. **Table 31** summarises the hydrogen simulation results of SOHYSIMO and HOMER for comparison. The important outputs from each model (highlighted in red) show excellent agreement. From this and previous results, we can now infer that SOHYSIMO is an appropriate tool for this kind of modelling. Importantly, because it is seen to generate output values in close agreement with an established model we can now use it with some confidence to develop the SOHYSIMO model into the realm of thermal energy modelling in the form of hydrogen cooking.

Parameter	SOHYSIMO	HOMER
Rated capacity (kW)	53	53
Annual PV production (kWh/yr)	47723	46727
PV hours of operation (Hours)	4602	4381
Total DC load (kWh/yr)	443	442
Battery nominal capacity (kWh/yr)	456	456
Battery usable capacity (kWh/yr)	182	182
Battery energy out (kWh/yr)	255	260
Energy at electrolyser (kWh/yr)	43883	41764
Hydrogen production (kg/yr)	805	778
Unmet electric load (kWh)	0	0

Table 31. Comparison of HOMER hydrogen (25kW electrolyser) simulation results with SOHYSIMO results.

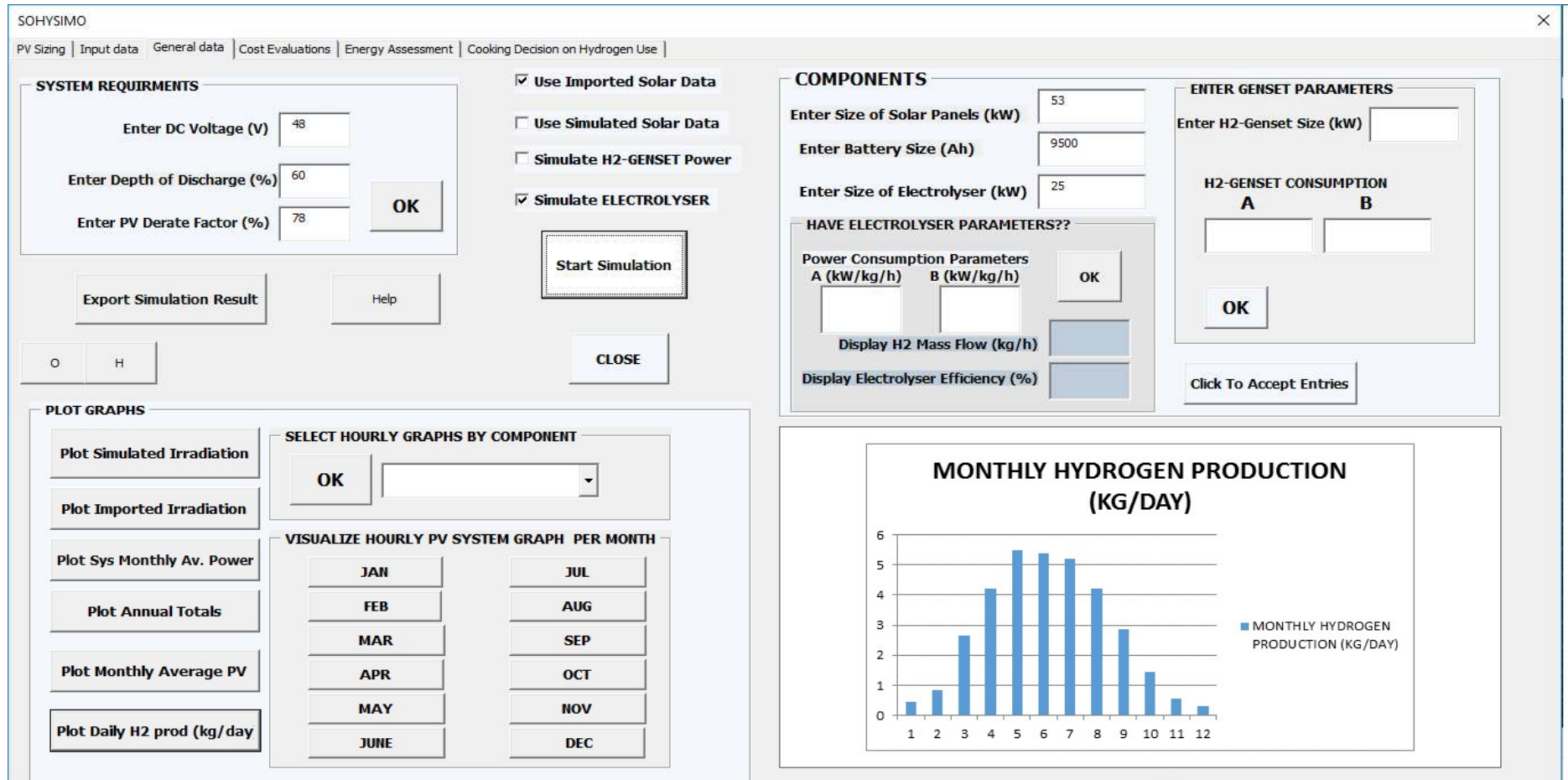


Figure 111. SOHYSIMO simulation user interface showing the monthly hydrogen productions of the 25kW electrolyser.

5. References

1. HYDROGEMS; Online available at <http://www.energyplan.eu/hydrogems/> accessed March 2017.
2. UniSyD3; online available at <http://www.energyplan.eu/unisyd3-0/> accessed March 2017.
3. Sinha, S. and Chandel, S.S., 2014. Review of software tools for hybrid renewable energy systems. *Renewable and Sustainable Energy Reviews*,32, pp.192-205.
4. Uzunoglu, M., Onar, O.C. and Alam, M.S., 2009. Modeling, control and simulation of a PV/FC/UC based hybrid power generation system for stand-alone applications. *Renewable Energy*, 34(3), pp.509-520.
5. Bernal-Agustín, J.L. and Dufo-López, R., 2009. Simulation and optimization of stand-alone hybrid renewable energy systems. *Renewable and Sustainable Energy Reviews*, 13(8), pp.2111-2118.
6. Boyd, S. and Vandenberghe, L., 2004. *Convex optimization*. Cambridge university press.
7. Professional photovoltaic softwares to download; online available at <http://photovoltaic-software.com/professional.php> accessed on 11/02/2016.
8. Online available at http://www.homerenergy.com/version_history.html accessed on 03/03/2017.
9. Online available at <http://hoga-renewable.es.tl/> accessed on 03/03/2017
10. iHOGA Version 2.2 User Manual R. Dufo-López (23 May 2014) Online available at http://personal.unizar.es/rdufo/images/ihoga/User_Manual.pdf accessed 08/03/2017.
11. Mitchell, M., 1998. An introduction to genetic algorithms. MIT press.
12. Gopalakrishnan, K., Khaitan, S.K. and Kalogirou, S. eds., 2011. Soft computing in green and renewable energy systems (Vol. 269). Springer.

13. Online available at [https://msdn.microsoft.com/en-us/library/office/ee814737\(v=office.14\).aspx](https://msdn.microsoft.com/en-us/library/office/ee814737(v=office.14).aspx) accessed on 25/01/2017.
14. Ali, M.M.E. and Salih, S.K., 2013. A visual basic-based tool for design of stand-alone solar power systems. *Energy Procedia*, 36, pp.1255-1264.
15. Vladimir Á.Č., and Suchanek, J., 2014. Expert system for design of off-grid renewable energy sources. *University review*, Vol. 8, No. 3-4, p. 38-44.
16. Kuo, Y.C., Liu, L.J., Tung, W.H., Huang, Y.M. and Ho, S.H., 2012, June. Smart Integrated Circuit and System Design for Renewable Energy Applications. In *Computer, Consumer and Control (IS3C), 2012 International Symposium on* (pp. 377-380). IEEE.
17. Mhalas, A., Kassem, M., Crosbie, T. and Dawood, N., 2013. A visual energy performance assessment and decision support tool for dwellings. *Visualization in Engineering*, 1(1), p.1.
18. Online available at <http://www.mpri.lsu.edu/textbook/Chapter6-b.htm#generalized>; accessed On 31/08/2017.
19. Yeniay, O., 2005. A comparative study on optimization methods for the constrained nonlinear programming problems. *Mathematical Problems in Engineering*, 2005(2), pp.165-173.
20. Kao, C., 1998. Performance of several nonlinear programming software packages on microcomputers. *Computers & operations research*, 25(10), pp.807-816.
21. Online available at <http://www.iue.tuwien.ac.at/phd/binder/node80.html> accessed on 31/8/2017.
22. Bourg, D.M., 2006. *Excel Scientific and Engineering Cookbook: Adding Excel to Your Analysis Arsenal*. " O'Reilly Media, Inc."
23. Zhou, W., Lou, C., Li, Z., Lu, L. and Yang, H., 2010. Current status of research on optimum sizing of stand-alone hybrid solar–wind power generation systems. *Applied Energy*, 87(2), pp.380-389.
24. Chadid, R., 1997. Unit sizing and control of hybrid wind-solar power system. *IEEE Transactions on Energy Conversion*, 12(1), pp.79-85.

25. Koutroulis, E., Kalaitzakis, K. and Voulgaris, N.C., 2001. Development of a microcontroller-based, photovoltaic maximum power point tracking control system. *Power Electronics, IEEE Transactions on*, 16(1), pp.46-54.
26. Kellogg WD, Nehrir MH, Venkataramanan G, Gerez V. Generation unit sizing and cost analysis for stand-alone wind, photovoltaic, and hybrid wind/PV systems. *Energy conversion, IEEE transactions on*. 1998 Mar;13(1):70-5.
27. Diaf, S., Diaf, D., Belhamel, M., Haddadi, M. and Louche, A., 2007. A methodology for optimal sizing of autonomous hybrid PV/wind system. *Energy Policy*, 35(11), pp.5708-5718.
28. Skoplaki, E. and Palyvos, J.A., 2009. On the temperature dependence of photovoltaic module electrical performance: A review of efficiency/power correlations. *Solar energy*, 83(5), pp.614-624.
29. Messenger, Roger A., and Jerry Ventre. *Photovoltaic systems engineering*. CRC press, 2010.
30. Šúri, M. and Hofierka, J., 2004. A new GIS-based solar radiation model and its application to photovoltaic assessments. *Transactions in GIS*, 8(2), pp.175-190.
31. Wong, L.T. and Chow, W.K., 2001. Solar radiation model. *Applied Energy*, 69(3), pp.191-224.
32. Gueymard, C.A., 2008. REST2: High-performance solar radiation model for cloudless-sky irradiance, illuminance, and photosynthetically active radiation—Validation with a benchmark dataset. *Solar Energy*, 82(3), pp.272-285.
33. Jimoh, D.D.J.M.A., 2009. Modelling of cloudless solar radiation for PV module performance analysis. *Journal of Electrical Engineering*, 60(4), pp.192-197.
34. Online available at <https://www.esrl.noaa.gov/gmd/grad/solcalc/> accessed on 30/07/2016.
35. Greg Pelletier. A solar position and radiation calculator for Microsoft Excel/VBA. online available at <http://www.ecy.wa.gov/programs/eap/models.html>, accessed on 30/07/2016.

36. Online available at http://www.solideas.com/pdf/SOLAR12_12113_final.pdf accessed on 30/12/2016.
37. Battery University, online available at [http://batteryuniversity.com/learn/archive/whats the best battery](http://batteryuniversity.com/learn/archive/whats_the_best_battery) accessed on 01/12/2016.
38. Nair, N.K.C. and Garimella, N., 2010. Battery energy storage systems: Assessment for small-scale renewable energy integration. *Energy and Buildings*, 42(11), pp.2124-2130.
39. Castañeda, M., Fernández, L.M., Sánchez, H., Cano, A. and Jurado, F., 2012, March. Sizing methods for stand-alone hybrid systems based on renewable energies and hydrogen. In *Electrotechnical Conference (MELECON), 2012 16th IEEE Mediterranean* (pp. 832-835). IEEE.
40. Kaviani, A.K., Riahy, G.H. and Kouhsari, S.M., 2009. Optimal design of a reliable hydrogen-based stand-alone wind/PV generating system, considering component outages. *Renewable Energy*, 34(11), pp.2380-2390.
41. Rajeshwar, K., McConnell, R. and Licht, S., 2008. *Solar hydrogen generation. Toward a renewable energy future*. Springer: New York.
42. Harrison, K. and Levene, J.I., 2008. Electrolysis of water. In *Solar Hydrogen Generation* (pp. 41-63). Springer New York.
43. Bunea, G.E., Wilson, K.E., Meydbray, Y., Campbell, M.P. and De Ceuster, D.M., 2006, May. Low light performance of mono-crystalline silicon solar cells. In *Photovoltaic Energy Conversion, Conference Record of the 2006 IEEE 4th World Conference on* (Vol. 2, pp. 1312-1314). IEEE.
44. Sankir, M. and Sankir, N.D. eds., 2017. *Hydrogen Production Technologies*. John Wiley & Sons.
45. Online available at <http://www.spiritofmaat.com/archive/watercar/h2ocar2.htm> accessed on 22/11/2016.
46. Ulleberg, Ø., Nakken, T. and Ete, A., 2010. The wind/hydrogen demonstration system at Utsira in Norway: Evaluation of system performance using operational data and

- updated hydrogen energy system modelling tools. *International Journal of Hydrogen Energy*, 35(5), pp.1841-1852.
47. Yamegueu, D., Azoumah, Y., Py, X. and Zongo, N., 2011. Experimental study of electricity generation by Solar PV/diesel hybrid systems without battery storage for off-grid areas. *Renewable Energy*, 36(6), pp.1780-1787.
48. Online available at <http://www.telegraph.co.uk/news/2016/04/09/uk-homes-could-be-heated-by-hydrogen-under-plan-to-tackle-global/> accessed on 9/12/2016
49. Topriska, E., Kolokotroni, M., Dehouche, Z. and Wilson, E., 2015. Solar hydrogen system for cooking applications: Experimental and numerical study. *Renewable Energy*, 83, pp.717-728.
50. Yilanci, A., Dincer, I. and Ozturk, H.K., 2009. A review on solar-hydrogen/fuel cell hybrid energy systems for stationary applications. *Progress in Energy and Combustion Science*, 35(3), pp.231-244.
51. Barbir, F., 2005. PEM electrolysis for production of hydrogen from renewable energy sources. *Solar energy*, 78(5), pp.661-669.
52. Fumey, B., Stoller, S., Fricker, R., Weber, R., Dorer, V. and Vogt, U.F., 2016. Development of a novel cooking stove based on catalytic hydrogen combustion. *International Journal of Hydrogen Energy*, 41(18), pp.7494-7499.
53. Fumey, B., Stoller, S., Fricker, R., Weber, R., Dorer, V. and Vogt, U.F., 2016. Development of a novel cooking stove based on catalytic hydrogen combustion. *International Journal of Hydrogen Energy*, 41(18), pp.7494-7499.
54. Winkler-Goldstein, R. and Rastetter, A., 2013. Power to gas: the final breakthrough for the hydrogen economy?. *Green*, 3(1), pp.69-78
55. Parkin, David., 2016. National grid. The future of gas: Supply of renewable gas.
56. Online available at <http://thenationonlineng.net/evil-kerosene-firewood> accessed on 10/12/2016.
57. Online available at <http://news.trust.org/item/20140530183509-63ekg/> accessed on 10/12/2016.

58. Watkins, T., Arroyo, P., Perry, R., Wang, R., Arriaga, O., Fleming, M., O'Day, C., Stone, I., Sekerak, J., Mast, D. and Hayes, N., 2017. Insulated Solar Electric Cooking—Tomorrow's healthy affordable stoves?. *Development Engineering*, 2, pp.47-52.
59. Leahy, S.B., 2004. Active flow control of lab-scale solid polymer electrolyte fuel cells (Doctoral dissertation, Georgia Institute of Technology).
60. IEA 2006; energy for cooking in developing countries.
61. Ulleberg, Ø., 2004. The importance of control strategies in PV–hydrogen systems. *Solar Energy*, 76(1), pp.323-329.
62. McEvoy, A., Markvart, T., Castañer, L., Markvart, T. and Castaner, L. eds., 2003. Practical handbook of photovoltaics: fundamentals and applications. Elsevier.
63. Twidell, John, and Anthony D. Weir. *Renewable energy resources*. Taylor & Francis, 2006.
64. The Isle of Eigg; Online available at http://www.isleofeigg.net/eigg_electric.html accessed on 30/12/2016].
65. Online available at <http://www.businessforscotland.co.uk/7-lessons-from-the-isle-of-eigg-for-an-independent-scotland/> accessed on 08/08/2016
66. Kemsley, R.H., McGarley, P., Wade, S. and Thim, F., 2011, September. Making small high-penetration renewable energy systems work—Scottish Island experience. In *Renewable Power Generation (RPG 2011)*, IET Conference on (pp. 1-7). IET
67. SMA Sunny portal; Online available at <https://www.sunnyportal.com/Templates/DefaultPage.aspx> accessed on 27/01/2016
68. Godula-Jopek, A., 2015. Hydrogen Production: By Electrolysis. John Wiley & Sons
69. Meteonorm: Online available at <http://www.meteonorm.com/en/features> accessed on 08/08/2016.
70. Celik, A.N., 2003. Techno-economic analysis of autonomous PV-wind hybrid energy systems using different sizing methods. *Energy Conversion and Management*, 44(12), pp.1951-1968

71. Türkay, B.E. and Telli, A.Y., 2011. Economic analysis of standalone and grid connected hybrid energy systems. *Renewable energy*, 36(7), pp.1931-1943.
72. Bhandari, B., Poudel, S.R., Lee, K.T. and Ahn, S.H., 2014. Mathematical modeling of hybrid renewable energy system: A review on small hydro-solar-wind power generation. *international journal of precision engineering and manufacturing-green technology*, 1(2), pp.157-173.

6.0 Evaluation and Assessment of Solar – Hydrogen system in a Nigerian Rural Area

6.1 Introduction

In Nigeria, more than 50% of the population live in the rural areas. Most of them are farmers who produce the food crops that sustain the country. They depend on biomass-wood and agricultural wastes for heating and cooking, and kerosene lamps, candles and dry cell batteries for lighting, all due to the lack of basic electrical facilities. Over-dependence on the traditional sources of energy have great implications on the health conditions of this rural populace. In 2016, The World Health Organisation estimates that over 4 million premature deaths per year are attributable to the use of inefficient cooking fuels in the low income rural households of the developing countries [1]. This is a 62.5% increase in 10 years when compared to the previous estimates of 2006 [2]. This means that continued use of solid fuels for cooking in these rural households may lead to 10 million premature deaths by 2030.

This affects mostly women whose duty is to fetch firewood for the cooking; they may be exposed to insect bites and suffer respiratory problems associated with prolonged indoor cooking. Providing them with a better source of cooking will go a long way in changing their quality of life. According to records, about 65% of total electricity generated in Nigeria is consumed by domestic households [3]. The main source of energy for cooking in rural area is firewood, with a small quantity of kerosene also used for lighting. In a typical Nigerian village the women need to walk on average about 6.5km to fetch firewood for cooking [4]. Non-cooking energy consumption among rural households in Nigeria are mostly for lighting and entertainment devices such as radio/ cassette players only. These are mostly powered with batteries.

A recent study suggests that for a family of 9 the average daily cooking gas requirement is 2.7m^3 at STP (0.24kWh) [5]. However, the use of gas for cooking is mostly confined to the cities, as it involves high transport costs and is too expensive for the majority of rural dwellers.

This chapter considers the future opportunities available in providing energy access to the Nigerian remote villages through uptake of solar energy systems which incorporate clean hydrogen cooking facilities.

6.1.1 Overview

Stand-alone off grid electricity has many possible configurations depending on climate, resource availability, geographical and economic factors. In Nigeria, solar energy is by far the most abundant resource, and is a relatively cost-effective and robust solution to energy provision in previously unserved areas. The addition of a hydrogen storage capability offers exciting possibilities to enhance energy security and/or provide opportunities for clean low carbon cooking. This chapter presents a modelled study utilising a hybrid solar –hydrogen system to provide both electrical and (thermal) cooking loads to a selected typical village in Nigeria.

6.2: Okenkwu Village Electrification

Okenkwu-Ebunwana village in Afikpo South LGA of Ebonyi state [6][7], south-eastern Nigeria has been considered for the purpose of evaluating the simulation tool developed in this research. The tool was used in the assessment of a stand-alone energy access for this rural area which would satisfy typical electrical loading. Various factors were considered including the distance of the village from the nearest grid point, the closeness of the houses, the energy requirement per household, the number of houses, the cost implications and relevant environmental factors.

6.2.1 Site Specifications

Okenkwu is located at latitude 5°58'N and longitude 7°52'E. Its total population is about 1,200 with 171 households. The FG of Nigeria in their bid to extend electric power access to the remote areas of the country have earmarked US\$251,294.50 (88 million Naira at 350/1USD) for the electrification (grid connection) project [8]. This corresponds to about US\$10,000/km for a 25km distance. The village terrain is notable for its hilly and near inaccessible nature, has a low mean altitude of about 107m above sea level, and average annual rainfall of about 198cm [9]. It is a tropical monsoon climate exposed to daily long hours (about 10 hours) of

sunshine for most of the year and receives on average $5.08\text{kWh/m}^2/\text{day}$ of solar irradiation, which is excellent for solar power utilization. There are seasonal variations of weather conditions across the country. There are two seasons experienced in Nigeria. The rainy season occurs between April and August in the south, while in the North the start of the rainy season is delayed till June [10]. The rainy seasons in southern Nigeria are characterised by cloudy weather conditions, which reduces the amount of solar radiation. A long dry season which lasts for about 6 months is experienced September – March. During this period, the weather is sunny and dry. Hydro-electric power is mostly suited for regions where there is a good water resource all year round and therefore it is not suited for this location. A study at a location close to this selected site estimates its annual mean wind speed at about 5.42m/s , but this is highly skewed by the short rainy season, with average speeds in the dry season of 3m/s [10]. This makes it unsuitable for wind power, which requires start-up wind speeds of greater than this value, and average wind speeds above 6m/s to produce meaningful power.

With regard to solar potential obtained via NASA, **Figure 112** shows the average monthly solar irradiation at Okenkwu village assuming a 10° - tilt angle.

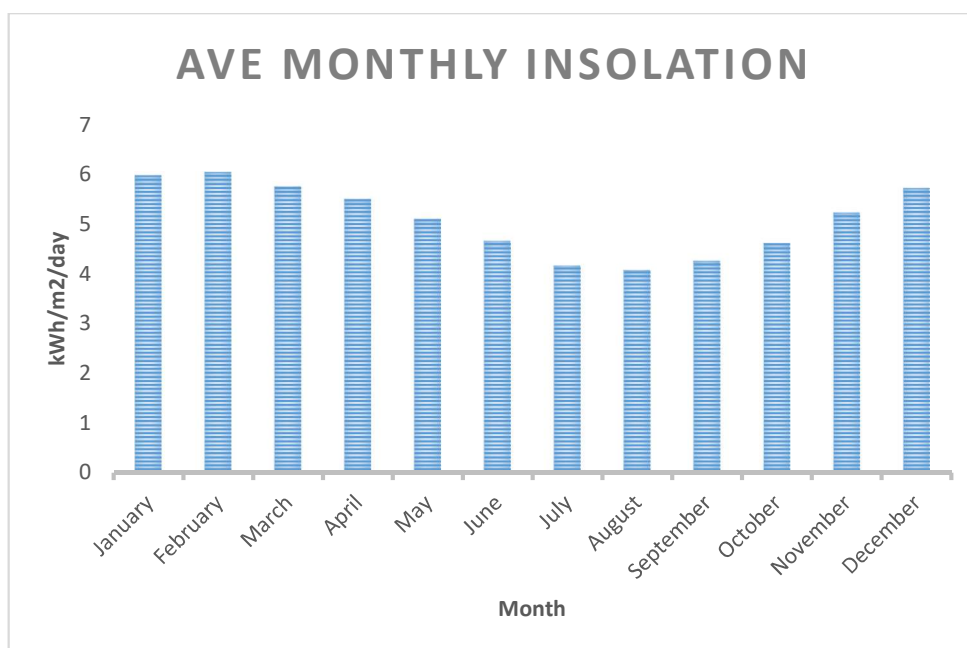


Figure 112. Average monthly solar irradiation at horizontal surface, adjusted for 10-degree tilt.

6.2.2 Okenkwu Load Profile Model

A load demand model has been generated in order to determine the appropriate sizing of the photovoltaic panels, storage battery and other auxiliary components that will be used in the design process. It was assumed that some appliances like lighting and radio set will be operational 11 hours of the day, while TV will be used for 6 hours mostly in the evening times.

Table 32 lists the load characteristics by appliance.

<u>Appliance</u>	<u>Number in use</u>	<u>Rate Power (W)</u>	<u>Total Power (W)</u>	<u>Hours of use</u>	<u>Energy (Wh/day)</u>
LED Lighting	6	15	90	11	990
Radio set	1	25	25	11	275
Television	1	35	35	6	210
Table fan	3	20	60	8	480
Phone	3	10	30	8	240
Total	12	105	200	44	2,195

Table 32. Load profile showing the daily power requirements for a household.

All power ratings of appliances used in this study are based on a consumption table provided in [11]. **Figure 113** shows the load demand; the maximum demand was 125W and for simplicity the assumption made was that this remained constant throughout the year. It must be remarked that the activities of a village community are fairly repetitive on a daily basis, so this assumption is reasonable. Future versions of SOHYSIMO could easily be adapted to accommodate more load variability. This entails that deferred load will be included in the future version. Under the daily loading profiled in **Table 32** the electrical demand is 2.195kWh/day, and the annual load is 800kWh. **Figure 114** shows the SOHYSIMO user interface for simulation data inputs such as solar irradiation and load.

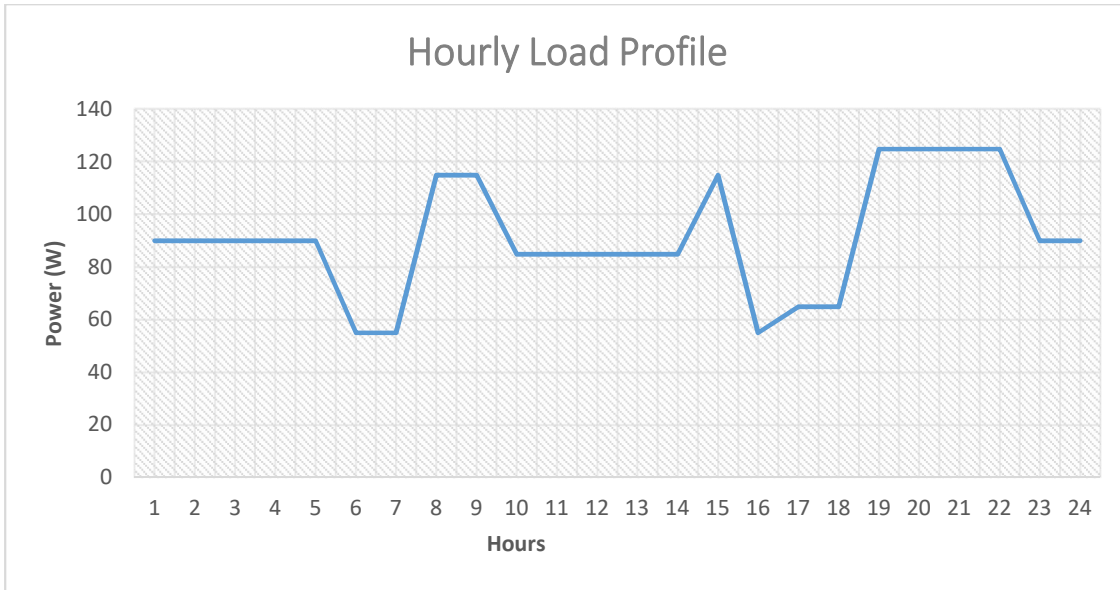


Figure 113. Daily load demand profile for a household in Okenkwo village.

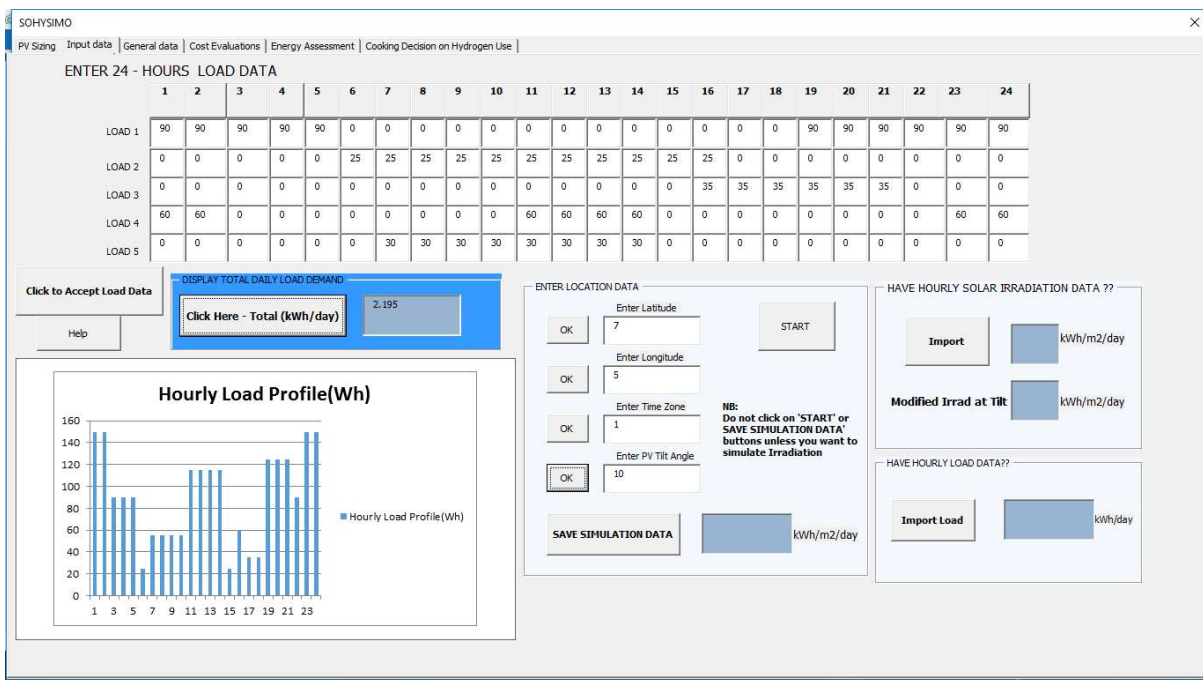


Figure 114. SOHYSIMO user interface showing the input data for load demand, site data and tilt angle entered for simulation, and the graphical view of the load demand.

6.2.3 Component Sizing

In the sizing process, the prime criteria are that the selected components must provide sufficient power to cover the expected load demand. The energy assessment facility in the SOHYSIMO tool ensures that the appropriate and optimised sizing configuration is obtained. However, the pre-sizing of the system components was done to determine the initial inputs needed to be entered into the simulation tool. The selected PV component should produce at least 2195 Wh/day on favourable weather conditions to ensure that electricity demand is met as desired. Therefore, a 1 kW solar array and 200 Ah batteries and 400 W electrolyser was selected. These components sizes are a marker, and will change after optimisation. The appropriate sizes obtained after assessment will be selected. The final stage of the sizing process is to evaluate an estimate of power capacity of the proposed electrolyser. This is an important stage of the sizing process, to achieve the best suitable size for the system, the electrolyser can be sized to minimise cost by ensuring that production of hydrogen is optimal for the purpose needed (electrical additional storage or cooking). The issue of cost is a big factor in the adoption of hydrogen as an energy carrier, but with growing penetration of renewable energy sources the issues associated with cost will soon be addressed as system optimisation and energy efficiency become increasingly important. Electrolyser size selection is mostly based on the maximum power that the PV system can deliver to it. As a starting point, here a 400W electrolyser was chosen to ensure that every excess power that the PV will produce after satisfying the load demand and charging the battery was utilised to generate hydrogen. **Table 33** lists the initial sizes of the components used to simulate the solar-hydrogen system. It should be noted that these are not the final sizes as the energy assessment algorithm will generate the optimum final sizing selections.

Component	Capacity
Solar PV	1 kW
Battery	200 Ah
Electrolyser	0.4kW
Voltage	48V

Table 33. Components sizes.

6.2.4 Simulation Results 1

These data were input into SOHYSIMO and the simulation was run. **Figure 115** shows the user interface, as it displays the monthly hydrogen production after a click on the 'plot daily H2 production' button.

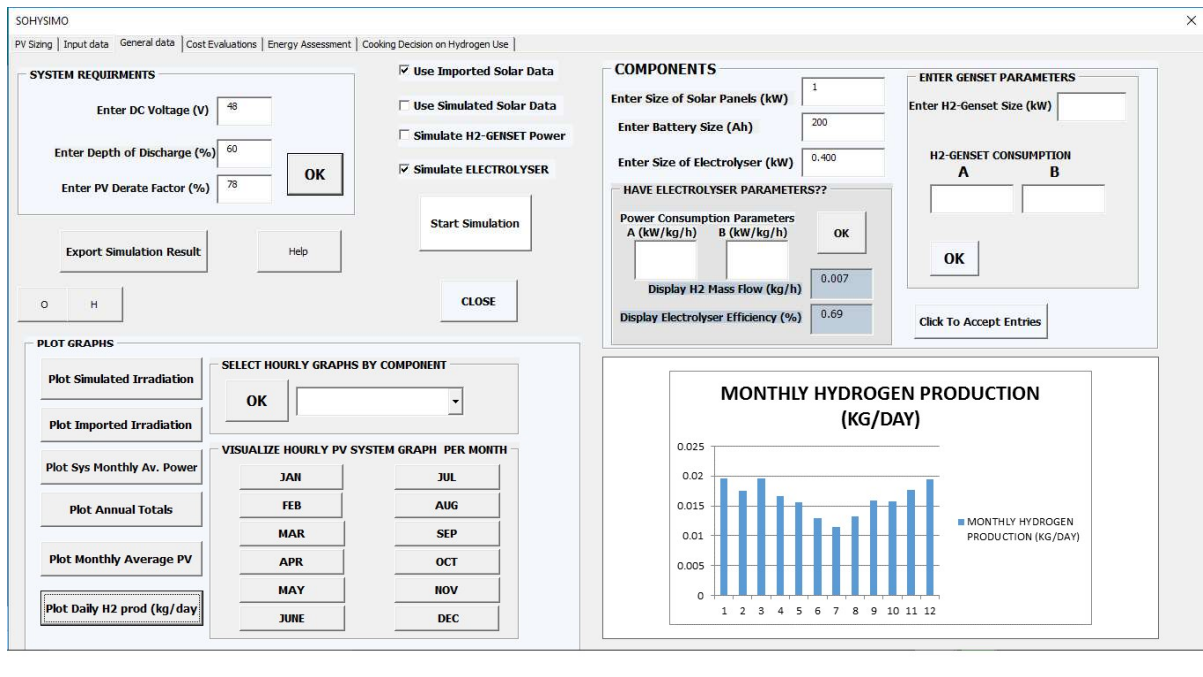


Figure 115. General data page user interface of SOHYSIMO showing the monthly hydrogen production.

To visualize more clearly the energy performance of individual components of the system, the simulation data was exported in excel file and plotted. **Figure 116** shows the hourly PV performance of the 1 kW PV array. There were continuous fluctuations in the PV power productions over the year, this is more visible in the middle of the year, which is a well-known period of low solar irradiation in Nigeria. The 1 kW PV array achieved an upper limit of about 900 W just few times, and that accounts for about 10% drop (from 1000 W) in output power, which inherently is a special issue in solar photovoltaics. PV system suffers from losses due to efficiency, basically, about 10% of energy is lost in the energy production process.

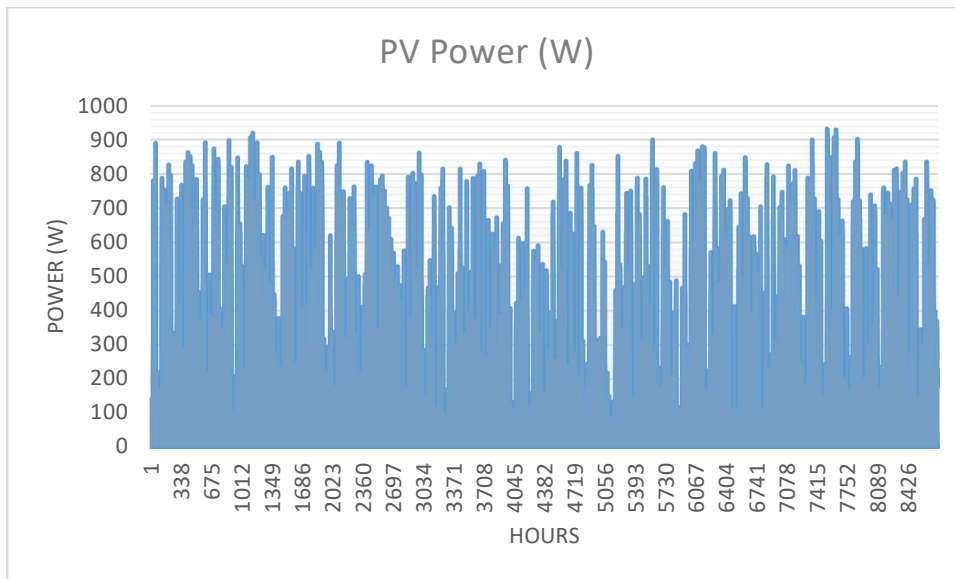


Figure 116. Hourly output power of 1 kW PV.

Figure 117 shows the system annual performance; the annual energy yield of the solar PV was 1300 kWh/year, the load demand was 802 kWh/year, and the energy delivered to the load by the PV was 338 kWh/yr. The system was designed such that if the available energy from the PV exceeds the load demand, it utilises the overflow to charge the battery and when the battery attains full state of charge the surplus will be delivered to the electrolyser to generate hydrogen. With this scheme about 561 kWh/yr was used to charge the battery and a total of 391 kWh was utilised in the electrolyser. Since the energy delivered to the battery was larger than that discharged from it, this means that they system is sustainable, it is unsustainable to discharge the battery to its lowest capacity. The simulation indicated that the electrolyser would produce 5.12 kg/yr of hydrogen and this is equal to 202 kWh/yr of energy, since 1kg of hydrogen = 39.4kWh. The hourly hydrogen production was also plotted for clarity; **Figure 118** shows the hydrogen generated over the year period simulated. The hydrogen produced peaked at 4.2 g/h with visible spread of variations and fluctuations which are linked to both the solar irradiation levels and to the load profile.

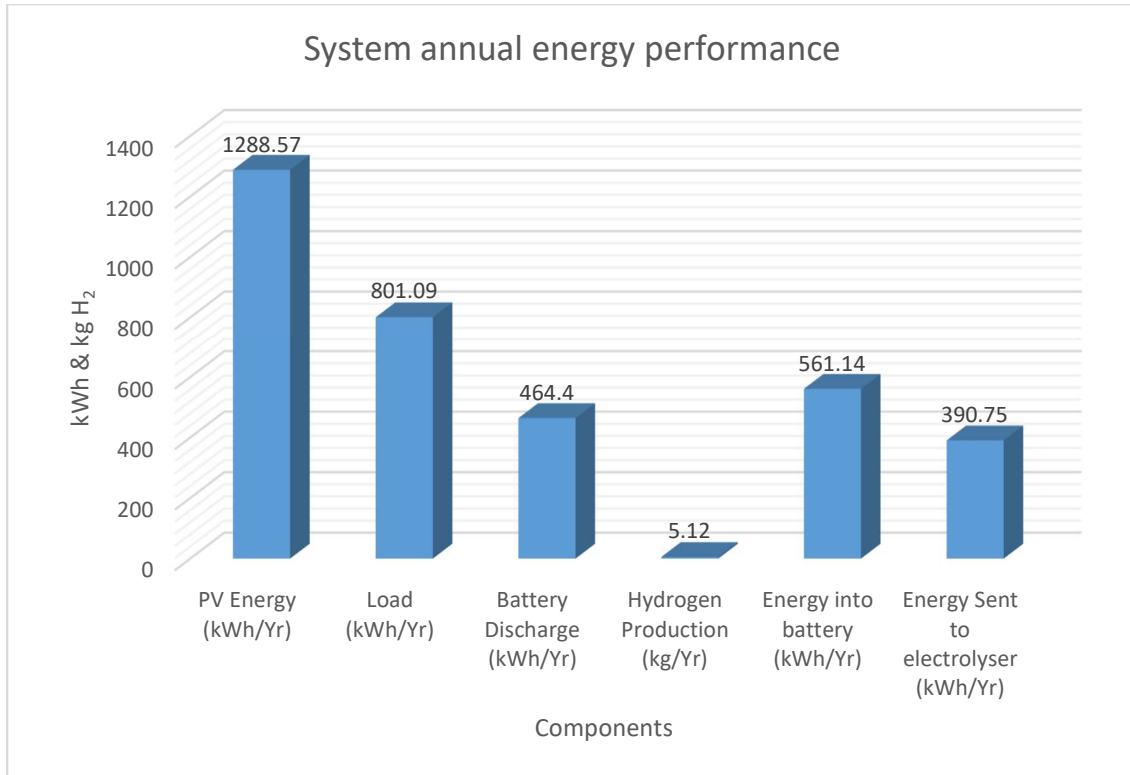


Figure 117. System annual performance.

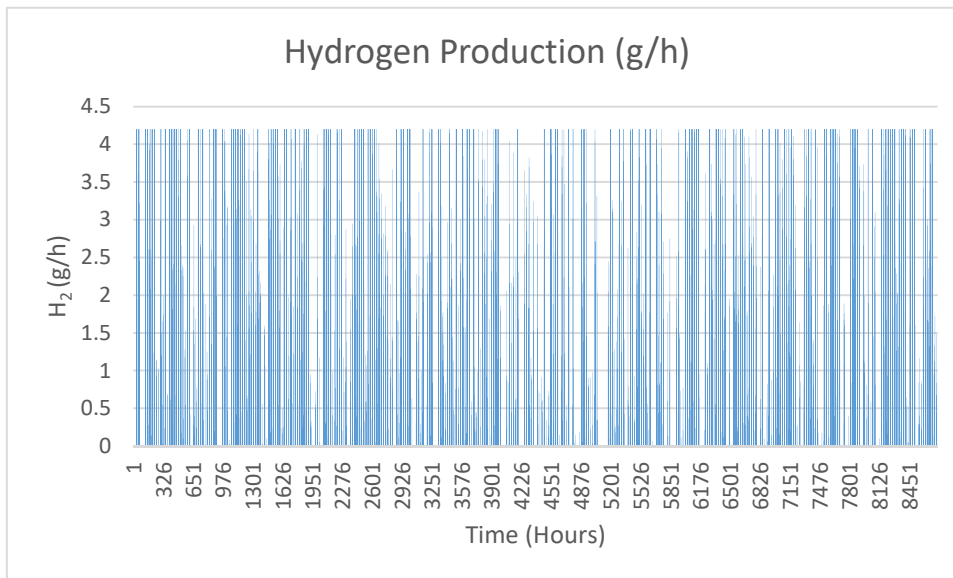


Figure 118. Hourly hydrogen production.

The monthly system performance was plotted as shown in **Figure 119**; the PV output had peaked at about 0.16kW in January, February, March and December, a decline in output was

seen beginning from the month of April which basically is the start of the rainy season in Nigeria, in the month of July the PV output was at the lowest level, depicting the period of heavy and frequent rain as normally experienced in Nigeria, a period marked by poor insolation and the battery was discharged accordingly to cushion its effects on the load demand. This also has an implication on the electrolyser hydrogen production as a decline was observed in June at 14.1 g in June and July at 12.4g. In contrast, the hydrogen produced had peaked at 21.2 g/day and 21.2 g/day in the months of January and December respectively, these are among the months with clear weather conditions in Nigeria, apart from dust due to harmattan. The generation of hydrogen largely depends on the amount of input power to the electrolyser, the higher the input the higher the hydrogen that is generated. The next sections describe how this hydrogen can be utilised to proffer a solution to domestic cooking needs of the rural household explained in this paper.

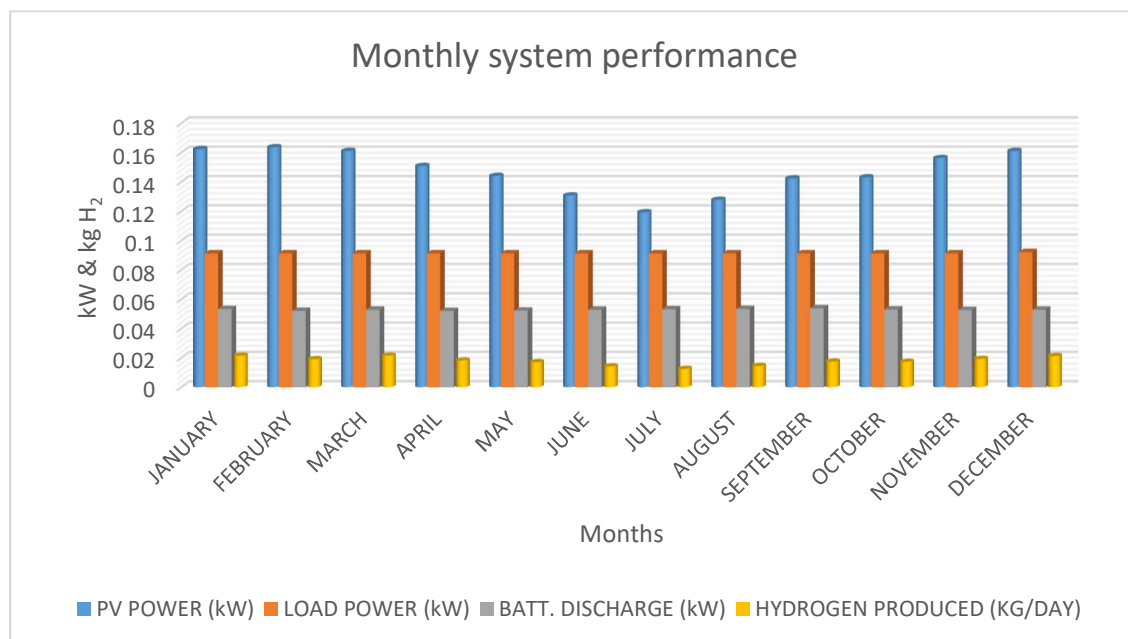


Figure 119. Monthly average system performance.

6.3 Energy Assessment and Evaluations

As explained in **section 5.2.2** the energy assessment was done to obtain the appropriate sizes of the RE energy system. In the process, the system voltage (48V), battery depth of discharge and carbon factors were entered into the tool to compute the optimal sizes. However, **Table 34** compares the initial guess sizes with sizes suggested by SOHYSIMO. There was a slight oversizing in all the system components, it was only the PV capacity that seemingly close values; mere 7.9% difference was obtained. The sizes obtained were 929W PV, 820W electrolyser (SOHYSIMO suggests electrolyser size based on the peak surplus output of the selected PV) and 114.3Ah @ 48V battery. The suggested PV size was rather close to the size of the PV array described in **chapter 4**. Thus, this gives an idea of the desired capacity size of the PV that will be selected. In electrolyser, the choice will be made between either selecting the size suggested by the tool or downsize it based on costs. It should be noted that the tool also provides a facility whereby a user can select battery depth of discharge based on design priorities. Battery depth of discharge is an important factor to consider, in the design process of an off-grid energy system. This has been explained in detailed format in **chapter 5**. However, **Figure 120** shows a screenshot of the SOHYSIMO energy assessment interface, the allowable depth of discharge obtained for the 114.3Ah@48V battery capacity was 50%, any value higher than this means the battery could struggle which may lead to battery depletion. This gives a 36 – hours autonomy. Some safe autonomy days was also calculated, this was based on the computing the number of days the solar PV will be operational as described in **section 5.3.2**, and it gives a 2 day of autonomy.

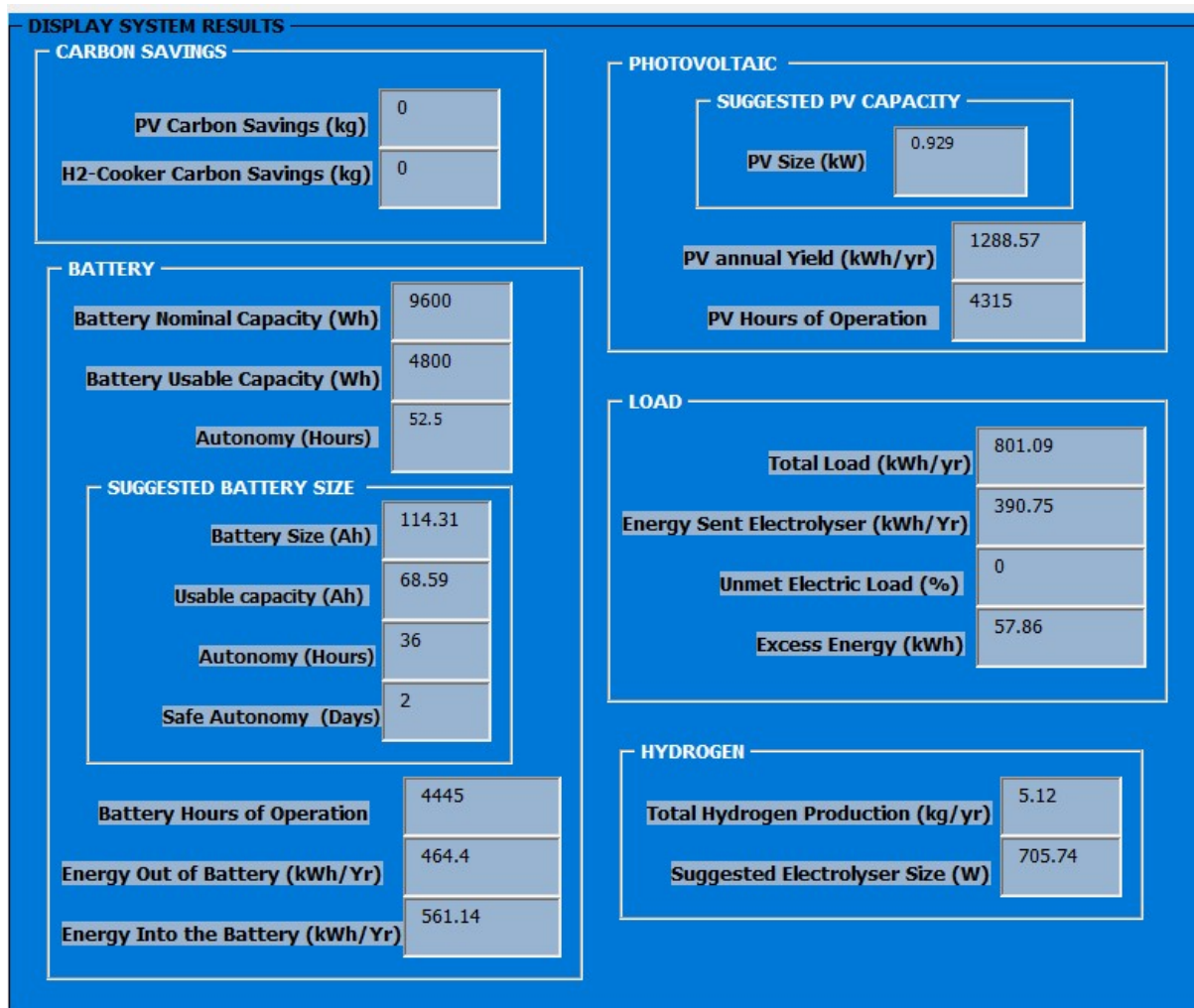


Figure 120. Simulation result showing the energy assessments.

Components	Sizes by manual inspection	Sizes by assessment
Solar PV	1000 W	929 W
Battery	200 Ah@48V (60% DoD)	114.31 Ah@48V (50% DoD)
Electrolyser	400 W	706 W

Table 34. Comparison of component sizes to be selected based on initial inputs.

6.3.1 Off-grid Energy System for the Rural Household in Okenkwu Village

The importance of proper sizing in renewable energy systems has been highlighted in some detail in **chapter 5** of this thesis, and this cannot be overemphasised. The previous simulations have provided credence to this fact. In this section, the selected appropriate sizes of solar PV, battery storage, and electrolyser obtained was used to run another simulation, all other system components (load demand, system voltage) were not changed during simulation. **Table 35 lists** the component sizes to be used in the next simulation.

COMPONENTS	Suggested Sizes	Selected Sizes
Solar PV	929 W	930 W
Battery	114 Ah@48V (50% DoD)	100 Ah@48V (50% DoD)
Electrolyser	705 W	400 W

Table 35. Selected component sizes.

6.3.2 Simulation Results 2

The selected sizes (930 W PV, 100Ah@48V battery, and 400W electrolyser) from the one suggested by the tool were entered into SOHYSIMO, and a simulation was run. **Figure 121** depicts a plot of the system performance over a year period simulated. The annual PV yield was 1198 kWh/year, and the amount of energy sent to the electrolyser was 309 kWh/year, this energy was utilised in the electrolyser and it produced 4.61 kg/year of hydrogen. When this is compared to the annual hydrogen production (5.12 kg/year) obtained in the previous simulation with system components derived by manual inspection, there is a 10% difference equating to 0.51 kg/year. The specifications and simulation results are summarised as follows;

Battery nominal capacity = 4.8 kWh

Battery usable capacity = 2.4kWh

Energy delivered to battery = 556 kWh/yr

Energy delivered to load = 334 kWh/yr

Energy out of battery = 467 kWh/yr

PV hours of operation = 4289 hours

Battery hours of operation = 4471 hours.

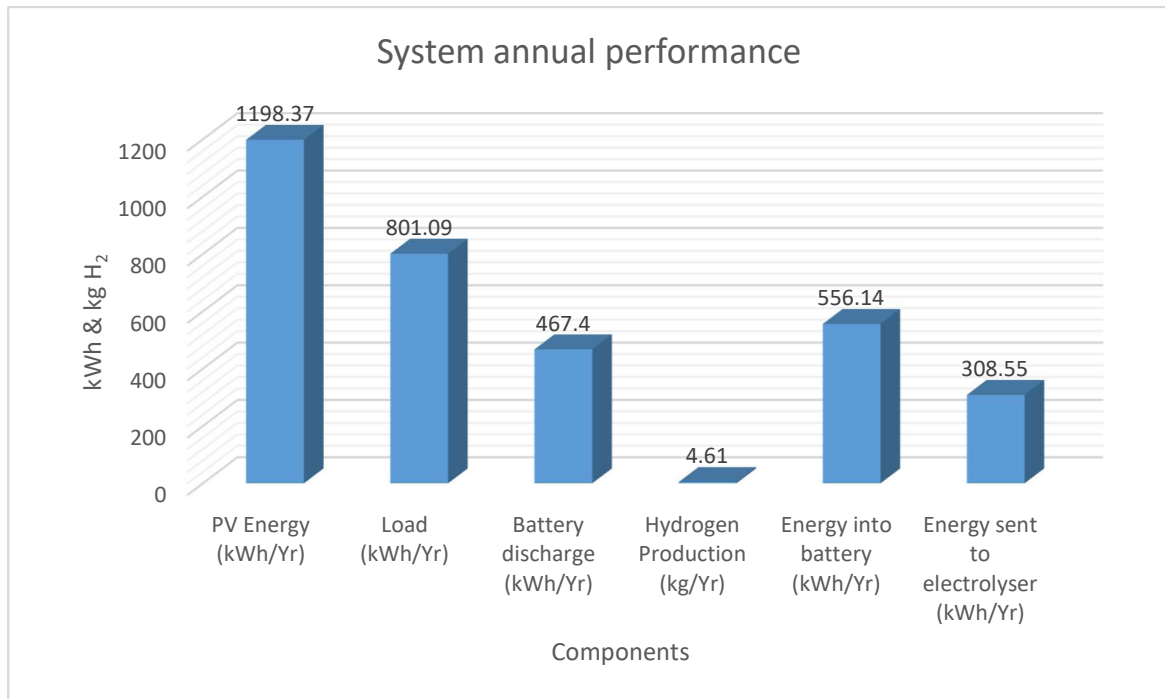


Figure 121 . A plot of the system performance over a year period simulated.

However, in view of the hydrogen production two opportunities will be sought. The prices per kW of solar PV and electrolyser will be compared, whether it will be more economical utilising the system configuration obtained through manual inspection or to select the system configuration obtained through sizing assessments. As already highlighted in **section 6.3.2** of this thesis, electrolysers are expensive devices presently at 1000\$/kW. However, it is hoped that in future the economies of scale and technological advancements in its manufacturing will bring down the costs. On the other hand, current advancements in solar PV manufacturing and production has led to the plummeting prices seen its costs per Wp in recent years. Selection of the electrolyser component will be based on this. To obtain a clear view of the system performance characteristics over the year, the simulation result was exported to an excel sheet via the '**Export Simulation Results**' facility in **SOHYSIMO**. **Figure**

122 shows the hourly power production of the 930W PV array over a year period. Expectedly, the variations inherent in solar PV power due to the intermittency in solar irradiations can be clearly seen. The PV performance showed some dip in its outputs between the second and third quarter of the year, corresponding to the rainy season, with a few peaks at around 880W in the last quarter of the year.

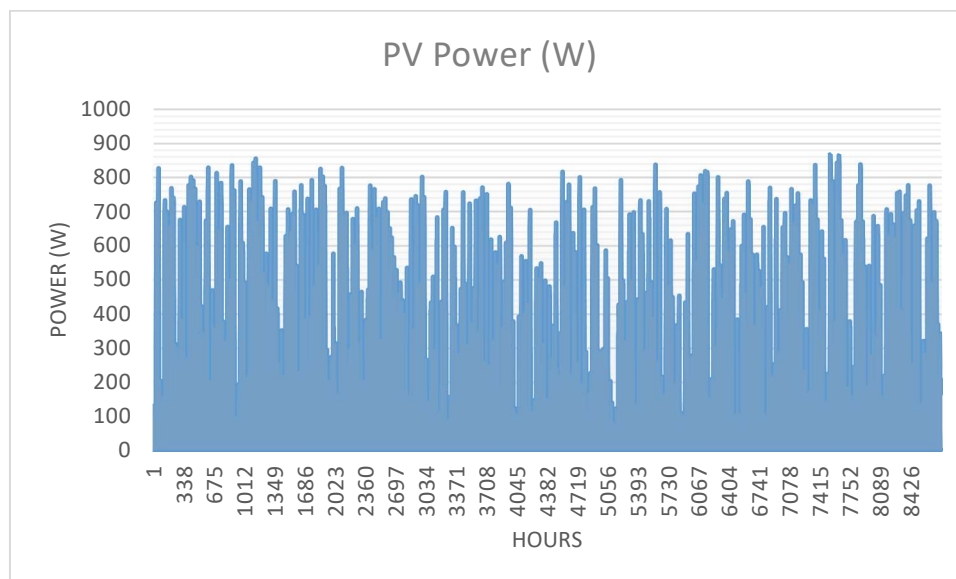


Figure 122. Hourly power production of the 930W PV array over a year period.

To obtain the hydrogen production figures, the data set representing the electrolyser hydrogen outputs was selected and plotted as shown in **Figure 123**. The hydrogen production peaked at around 4.2 g/h over the year period. However, to visualise the system monthly performance, the data set representing this was selected and plotted as shown in **Figure 124**. The PV power peaked at 0.15kW in December. The lowest was seen in July at 0.11kW, it can be noted that this dip in output power has an implication on the electrolyser, as the amount of energy delivered to the electrolyser is directly proportional to the amount of hydrogen it produces, which in turn depends on PV output. This can be observed by the corresponding drop in hydrogen, lowest at 11 g/day seen in the month of July compared to 19 g/day of January and December, with the other months exhibiting the same general relationships. From the experimental investigation presented in **chapter 5**, it was found that 1.16g was the amount of hydrogen required for a basic cooking process. Now, for an electrolyser that produces on average at 15g/day, this will be enough to satisfy a daily domestic cooking demand as we shall see later.

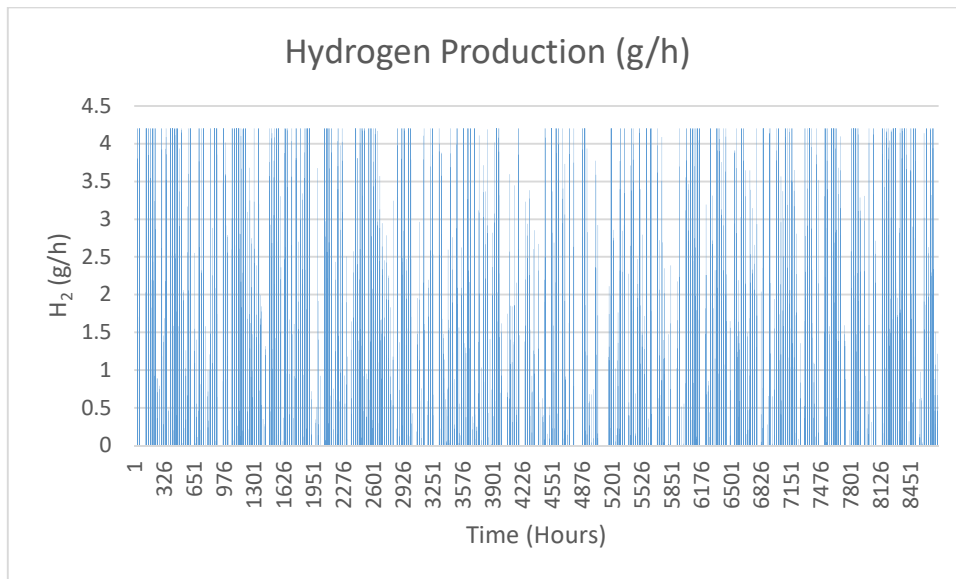


Figure 123. Hourly hydrogen productions of 400W electrolyser has produced over a year period.

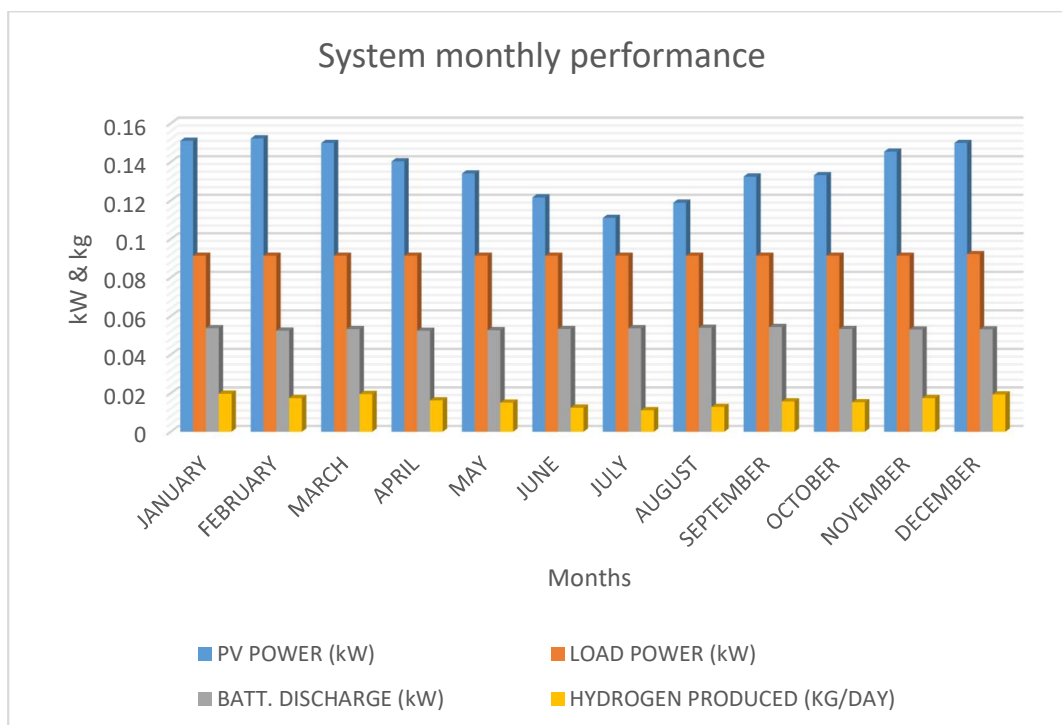


Figure 124. System monthly performance.

However, to appreciate the impact of a larger electrolyser on hydrogen, the 706 W electrolyser suggested by SOHYSIMO was used with a 1 kW PV to run a third simulation and the results is shown in **Figure 125**. The benefits of a larger electrolyser were obvious, as the 706 W electrolyser produced 6 kg/yr (236 kWh/Yr of energy) of hydrogen which is some

0.88 kg/yr more when compared to the amount of hydrogen produced by the 400 W electrolyser. However, in this arrangement, per economic consideration, it is not viable to invest on a 706 W electrolyser just because it can generate more hydrogen, even though this ensured that no energy was left unutilised (the annual excess energy was 0.01 kWh/yr).

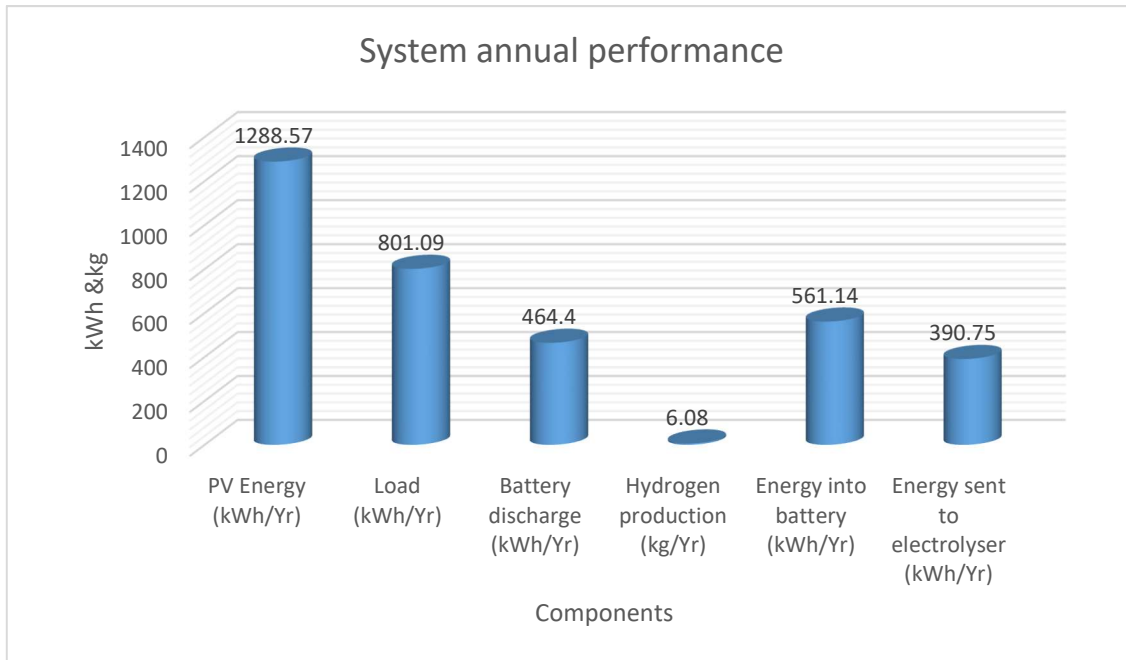


Figure 125. System annual performance showing 6 kg/Yr of hydrogen produced by the 706 W electrolyser.

6.4 Energy Optimisation

The previous sections describe the sizes obtained through energy assessment. The developed tool also has an energy optimisation facility and this enhances the versatility and flexibility of the tool. In this section, the optimal sizing that can supply the household's electric load and cooking load profile considered in this study is presented. In the process, the selected components (PV and battery) must provide sufficient energy to cover both demands as desired, at minimal costs. **Table 36** lists the cost specifications used in the optimisation process.

COMPONENTS	CAPITAL COSTS (\$)	O & M COSTS (\$/yr)	REPLACEMENT COSTS (\$)
Solar PV	3236	0	3236
Battery	1640	16.40	1640
Electrolyser	550	6	550

Table 36. System component costs used in the energy optimisation.

After optimisation, the sizes obtained were 1.53kW PV, 0.4kW electrolyser and 3.7kWh battery, the allowable depth of discharge obtained was 50%. **Table 37** lists the sizes obtained. **Figure 126** is the optimised components of the system in SOHYSIMO.

Components	Sizes
Solar PV	1.53kW
Battery	3.7kWh (50% DoD)
Electrolyser	0.4kW

Table 37. Optimised component sizes.

OPTIMISATION RESULTS								
#	PV (kW)	Batt. (kWh)	Elec. (kW)	Init. Cap. Cost (\$)	O&M (\$/Yr)	Total NPC (\$)	CH ₂ (\$/kg)	LCOE (\$/kWh)
1	1	9.6	0	4876	123	6639	0	0.5
2	1	9.6	0.4313	5427	140.4	7758.4	99.4	0.6
3	1.53	3.7	0	5592.87	80.2348	6347.95	0	0.5
4	1.53	3.7	0.43	6143.87	91.5851	6835.27	102.2	0.7

Figure 126. Hydrogen cooking optimisation results, showing the component configurations that fully satisfies both electric load and the cooking demand.

To obtain a clear view of the system performance characteristics over the year, the simulation result was exported to an excel sheet via the ‘**Export Simulation Results**’ facility in **SOHYSIMO**. The system annual performance is shown in **Figure 127**, the energy from PV was 1924 kWh, the annual load demand was 801.1kWh and the battery discharged total of 450.9 kWh to cover part of this demand while the rest was supplied by PV. The PV delivered total of 607.2 kWh to recharge the battery, and 591.6 kWh surplus energy was sent to electrolyser for hydrogen production.

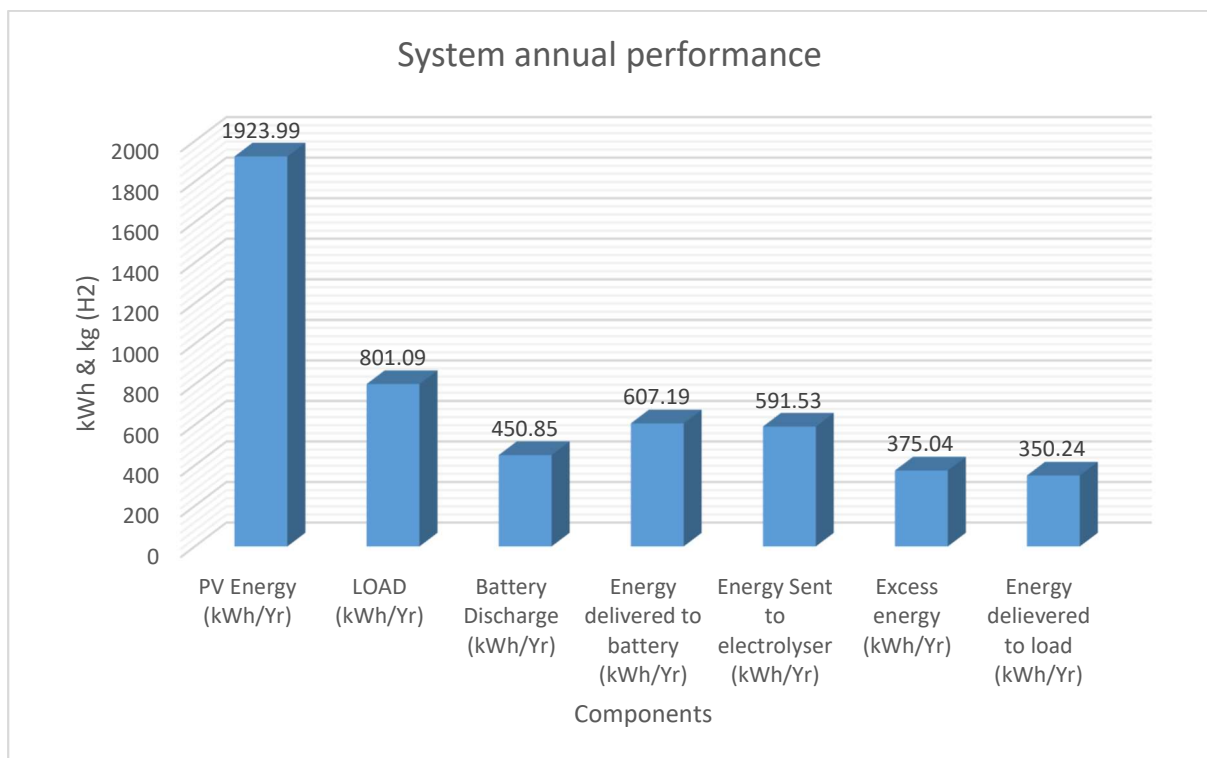


Figure 127. A plot of the system performance over a year period simulated.

Figure 128 shows the hourly power production of the 1.53 kW PV array over a year period, expectedly, the variations inherent in solar PV power due to the intermittency in solar irradiations can be clearly seen. The PV performance showed some dip in its outputs between the second and third quarter of the year, with a few peaks at around 1.4 kW in the last quarter of the year.

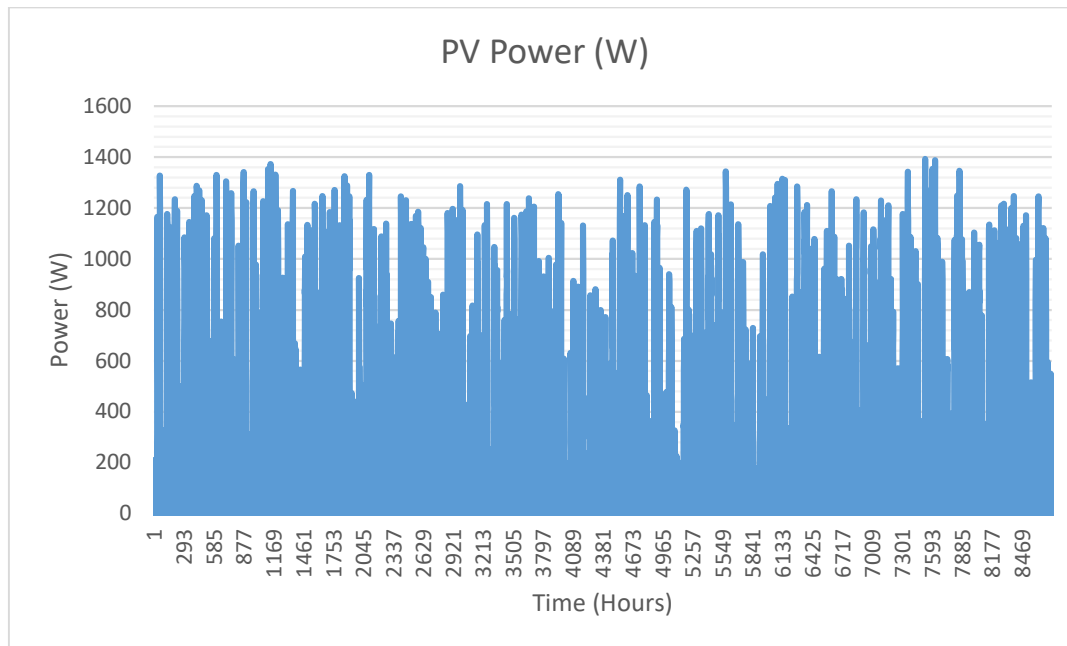


Figure 128. Hourly power production of the 1.53kW PV array over a year period.

To obtain the hydrogen production value, the data set representing the stored hydrogen outputs was selected and this is plotted as shown in **Figure 129**. Over the year period, the total stored hydrogen was 11 kg. However, to visualise the system monthly performance, data set representing this was selected and plotted as shown in **Figure 130**. The average monthly PV power peaked at 0.16kW in January, February and December. The lowest was seen in July at 0.12kW. This is accompanied by a corresponding drop in hydrogen production, as expected. The lowest figure at 8.9g/day is observed of July compared to 24g/day, 22g/day and 24g/day of January, February and December respectively.

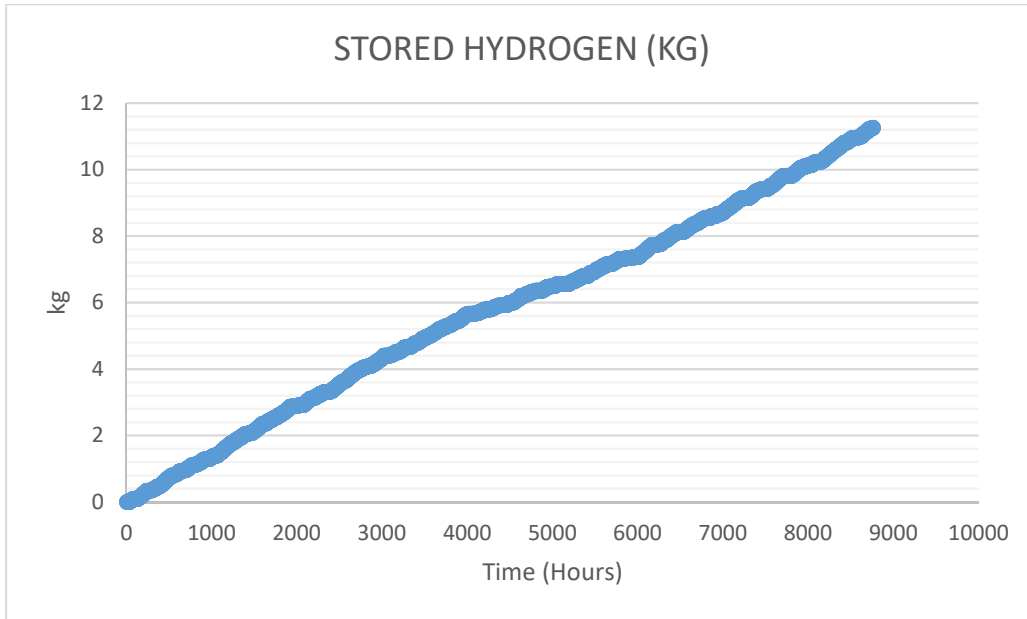


Figure 129. Hourly hydrogen productions of 400W electrolyser over a year period.

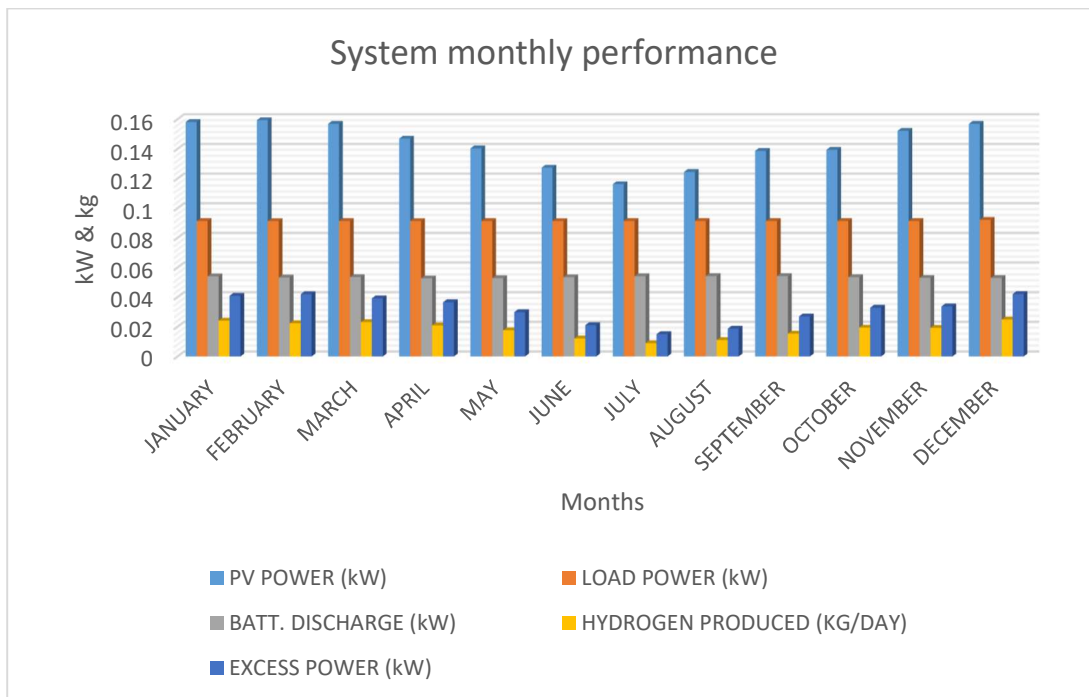


Figure 130. System monthly performance.

6.4.1 Summary

It has been shown in the last two simulations (simulation 1 and simulation 2) the appropriate configurations that may serve the load demand of 2.195kWh/day for a family house in Okenkwu village. This also presented an opportunity that some amount of hydrogen could be realised, with the excess energy available to be utilised for enhanced energy access. SOHYSIMO has sized the system and showed that a 930W PV will be required based on its customised architecture (SOHYSIMO selects the best system configurations that may serve the load demand over a year period, with enhanced model of days of autonomy), 100Ah battery @ 48V, and a 930W PV array. The selected configuration that satisfies the electric load was 930W PV array, 400W electrolyser and 100Ah@48V (50% DoD) battery storage, this gives around 30 hours autonomy. The tool has also suggested a 2 day (48 hours) safe autonomy based on the selected configurations. However, optimisation has also shown that the system can be balanced with minimal sizes based on costs. Though, the difference between the optimal sizes and the sizes obtained by assessments is quite significant. However, with the optimal sizes, the higher PV Capacity will guarantee more hydrogen production, which provides an opportunity to satisfy both cooking and electric load. To appreciate this the optimal sizes (1.53 kW PV, 0.4 kW electrolyser and 3.7 kWh batteries) were used for further analysis.

6.5 Designing the Off-grid Household Energy Access with Solar Home System

In previous sections, the components sizes for optimal system configuration of the solar home system that could supply a modest loading of 2.195kWh/day for the rural household in Okenkwu village was determined and presented. It is desired that the system selected would generate at least 2.2 kWh/day, which was the output productions obtained from a real PV array presented in earlier in this thesis. However, when compared to the sizes described in **section 4.12 of chapter 4**, the obtained PV optimal size is 14% bigger than the size the actual installed PV system but the optimal battery size is 29% less.

The following sections presents, the complete design process which includes;

- 1 determination of the optimal series – parallel configuration of solar PV array
- 2 battery storage system
- 3 computation of hydrogen cooking system
- 4 cost calculations
- 5 the expansion of the system to cover all households in the Okenkwu village.

6.5.1 Determination of Series – Parallel Configuration of the Solar PV System

For modelling purposes, an Panasonic HIT 240 W monocrystalline solar PV module [12] has been selected. This is because the high efficient power performance characteristics of this solar PV module. According to the manufacturers, this PV module produce the highest output on cloudy days at 21.6% cell conversion efficiency [12]. This would mean that for irradiance level of 1 kW/m², each square meter of this Panasonic PV module area would generate 220 W, and this can be an advantage for the rainy season in Nigeria. **Table 38** lists all parameters extracted from this Panasonic HIT 240W solar PV module for this work. The detailed electrical characteristics of the module can be found in **appendix 2**.

Rated Power (Pmax)	240 W
Maximum Power Voltage (Vpm)	43.7 V
Maximum Power Current (Ipm)	5.51 A
Open Circuit Voltage (Voc)	52.4 V
Short Circuit Current (Isc)	5.85 A
Temperature Coefficient (Voc)	-0.126% V/ °C
Temperature Coefficient (Isc)	1.76mA/ °C
Temperature Coefficient (Pmax)	-0.30% V/ °C
NOCT	48.3°C)
Module efficiency	19%
Cell Efficiency	21.6 %
Maximum System (DC) Voltage	600 V
Module Area	1.26 m ²

Table 38. List of electrical properties of 85 W Ameresco solar module used in this study [12].

To obtain the series – parallel configuration of the solar PV, the following calculations was done;

$$\text{Number of PV module in series} = \frac{\text{System voltage}}{\text{Voltage of 1-s module}} \quad (\text{Equation 56})$$

Where; system voltage = 48 V

Voltage of 1 – solar module = 43.7 V

Therefore;

$$\text{Number of PV module in series} = \frac{48}{43.7} = 1.09 \cong 1 \text{ modules}$$

PV parallel connection can be obtained as follows;

$$PV \text{ design power} = V_m \times N_{ms} \times I_r \times N_{mp} \quad (\text{Equation 57})$$

where;

V_m = voltage of 1 – solar module, N_{ms} = No. of series PV modules, I_r = PV rated current, N_{mp} = no. of parallel PV modules

Therefore, making the no. of parallel PV modules the subject of formula, we obtain that

$$\text{No. of parallel PV modules} = \frac{PV \text{ design power}}{\% \text{ losses} \times V_m \times N_{ms} \times I_r} \quad (\text{Equation 58})$$

$$\text{Number of parallel PV modules} = \frac{1530 \text{ W}}{0.85 \times 43.7 \text{ V} \times 1 \times 5.51} = 7.48 \cong 8 \text{ modules}$$

Therefore, the PV array comprises 1 module of 240 W PV in series with 8 240 W PV parallel strings.

Battery: To obtain the desired capacity characteristics batteries can be connected in a series – parallel formation. When two batteries are connected in series their output voltage will be doubled while the Amp hour capacity remains the same. This means adding voltages of both batteries. However, a parallel connection increases the batteries capacity while keeping their voltage the same. A similar procedure as in solar PV array was followed to determine the optimum battery connections. The 3.7kWh battery storage capacity obtained via optimisation was adopted. First, the 12V 70Ah deep cycle AGM battery used in the power monitoring and testing presented in **chapter 4** of this thesis will be selected. In this process, the 12V 70 Ah batteries will be configured to obtain a 3.7kWh capacity. However, to determine the parallel battery connection the following calculations was done;

Parameters to be considered included = **48V battery @ 80 Ah (3.84 kWh battery size).**

Hence, since 12V battery @ 80Ah was selected, **4 batteries** will need to be connected in series to obtain a 48V DC bus. To determine the parallel connection, the system battery currents was utilised as follows;

$$\text{Number of battery parallel strings} = \frac{\text{System Battery Ah}}{\text{Design Battery Ah}} \quad (\text{Equation 59})$$

$$\text{Number of battery parallel strings} = \frac{\text{System Battery Ah}}{\text{Design Battery Ah}} = \frac{80}{70} = 1.1 \cong 1 \text{ parallel strings.}$$

6.5.2 Obtaining the Cooking Demand

"We are like tenant farmers chopping down the fence around our house for fuel, when we should be using Nature's inexhaustible energy sources – sun, wind and tide. I'd put my money on the sun and solar energy. What a source of power! I hope we don't have to wait until oil and coal run out before we tackle that." - Thomas Edison, 1931.

That is a quote by Thomas Edison from more than eight decades ago and today we are still chopping down the fences and forests around us for fuel. It is high time we started doing this in a different way.

In Nigeria, as of 2013, it has been reported that the annual firewood consumption is about 266 million kg [13] This translates to about 1.49 kg per capita per day considering the present 180 million Nigeria population. This can be converted to a charcoal consumption figure by multiplying with the conversion factor of 1kg of firewood to charcoal, which falls between 0.1kg – 0.3kg [14]. In this study, a 0.25 kg factor was used, and this gives a 0.37 kg charcoal per capita per day. It was suggested that the household kerosene consumption in Nigeria as of 2006 was about 0.398l/day [15]. For this study, this was converted by multiplying with a factor of 1.05 to reflect the percent increase in cooking demand in Nigeria, and gives a 0.418l kerosene consumption per day per household.

In the process, it was assumed that the cooking demand increases twice a week per fuel type selected and remains constant on a weekly basis throughout the year. And the selection of fuel type for the simulations will be based on firewood and/or kerosene. Most rural dwellers use only two fuel types; they may use firewood for cooking and kerosene for either lighting or cooking. These all depends on the level of income in the household. Those who income level fall below \$1/day may prefer to use the kerosene only for lighting because of the costs, and rely totally on freely foraged firewood for cooking. Some villagers also use charcoal for cooking, but this is a relatively limited case. **Table 39 lists** the summary of daily cooking demand per household in Nigeria rural area used in the current study.

Fuel type	Energy content	Demand per head	Demand per household
Firewood(kg)	16 MJ/kg [14]	1.49 kg	10.43kg
Kerosene (l)	25.7 MJ/l [14]	0.0597l	0.418l
Charcoal (kg)	30 MJ/kg [14]	0.37 kg	2.59kg

Table 39. Estimated daily cooking demand for a typical rural household in Nigeria.

To simulate the hydrogen system these cooking demand data were entered into **SOHYSIMO** ‘cooking decision on hydrogen use’ page to compute the hydrogen energy requirements that would cover these cooking demands per year for a rural household specified in this study (Okenkwu village). The hydrogen produced in **simulation results 2** will be utilised in the hydrogen cooker to meet the domestic cooking demand of the rural household. After entering the data in SOHYSIMO a simulation was run, **Figure 131** is a SOHYIMO user interface showing the selected fuel types and the data entered; also, a plot of H₂-Cooker energy vs cooking demand. After computation, the daily energy demand available from the hydrogen cooker was 1.3 kWh/day, while the daily average cooking demand was 1.4 kWh/day. However, to present in clarity, a detailed analysis of the hydrogen cooking simulations, a data exporting facility available in the tool was utilised. Plotting the H₂-cooker versus cooking demand gives an indication of whether the hydrogen cooking demand was met, and this alerts the household to days which the hydrogen cooker will be available for use. The algorithm does this in such a way that any point along the H₂-cooker curve that falls below the cooking

demand curve denotes that energy in the hydrogen cooker is not enough to meet cooking demand on that day. This is a cumulative calculation taking into account the stored hydrogen. **Figure 132a and Figure 132b** depicts an annual cycle of daily supply and demand, split into monthly segments.

SOHYSIMO

PV Sizing | Input data | General data | Cost Evaluations | Energy Assessment | Cooking Decision on Hydrogen Use | Energy Optimisation

Help

ENTER DAILY COOKING DEMAND DATA (7 - Days)

	1	2	3	4	5	6	7
FIREWOOD (kg)	10.43	20.86	10.43	10.43	10.43	20.86	10.43
CHARCOAL (kg)							
KEROSENE (L)	0.418	0.836	0.418	0.418	0.418	0.418	0.836

OK

Click To Accept Data

Calculate

SELECT FUEL TYPE

FIREWOOD

CHARCOAL

KEROSENE

VISUALIZE DAILY H2-COOKING GRAPHS

JAN JUL

FEB AUG

MAR SEP

APR OCT

MAY NOV

JUNE DEC

PLOT 365 DAYS H2-COOKER

PLOT 365 DAYS COOKER VS DEMAND

HAVE COOKING DEMAND DATA??

Import 1.4 kWh/Day EXPORT RESULTS Average Daily H2 Cooker 1.3 kWh/d

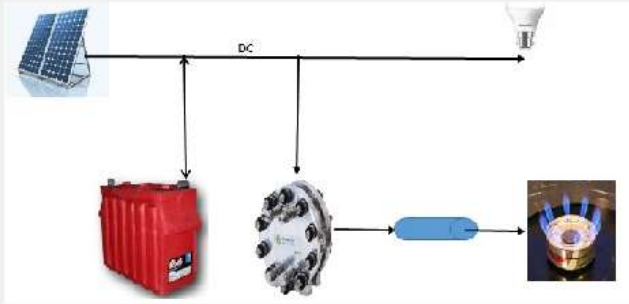
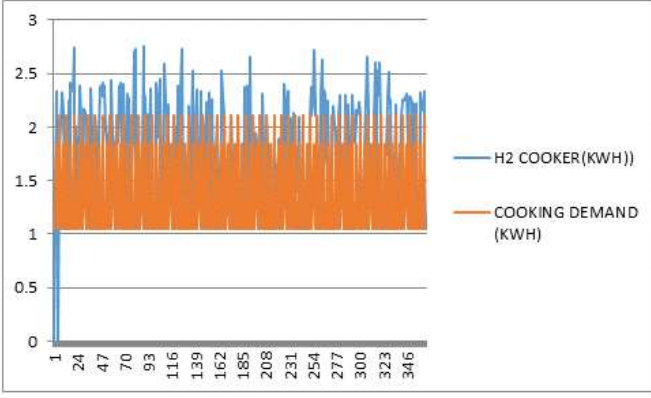



Figure 131. SOHYIMO user interface showing the selected fuel types and results.

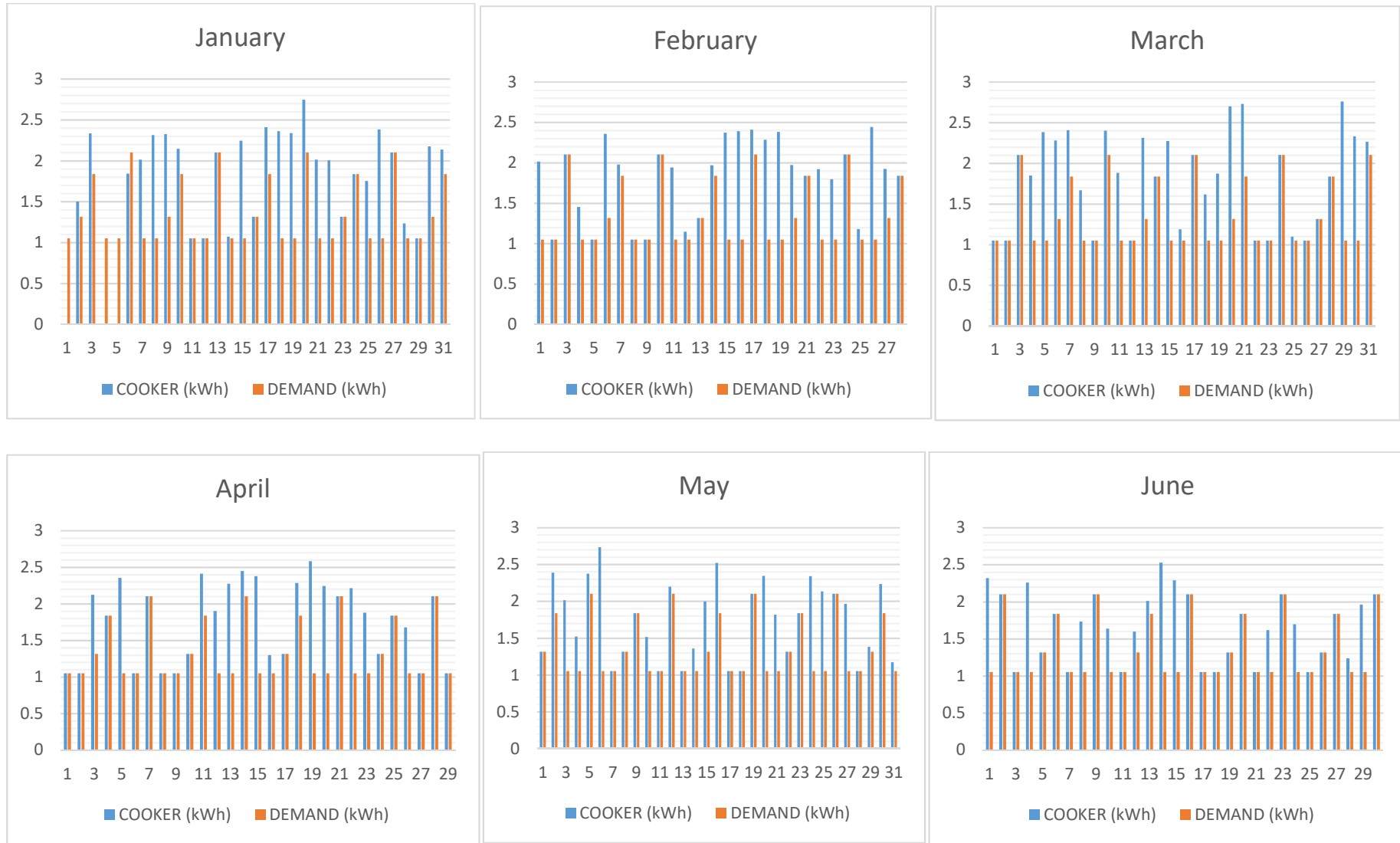


Figure 132a. Monthly cooking simulation results, Jan -Jun

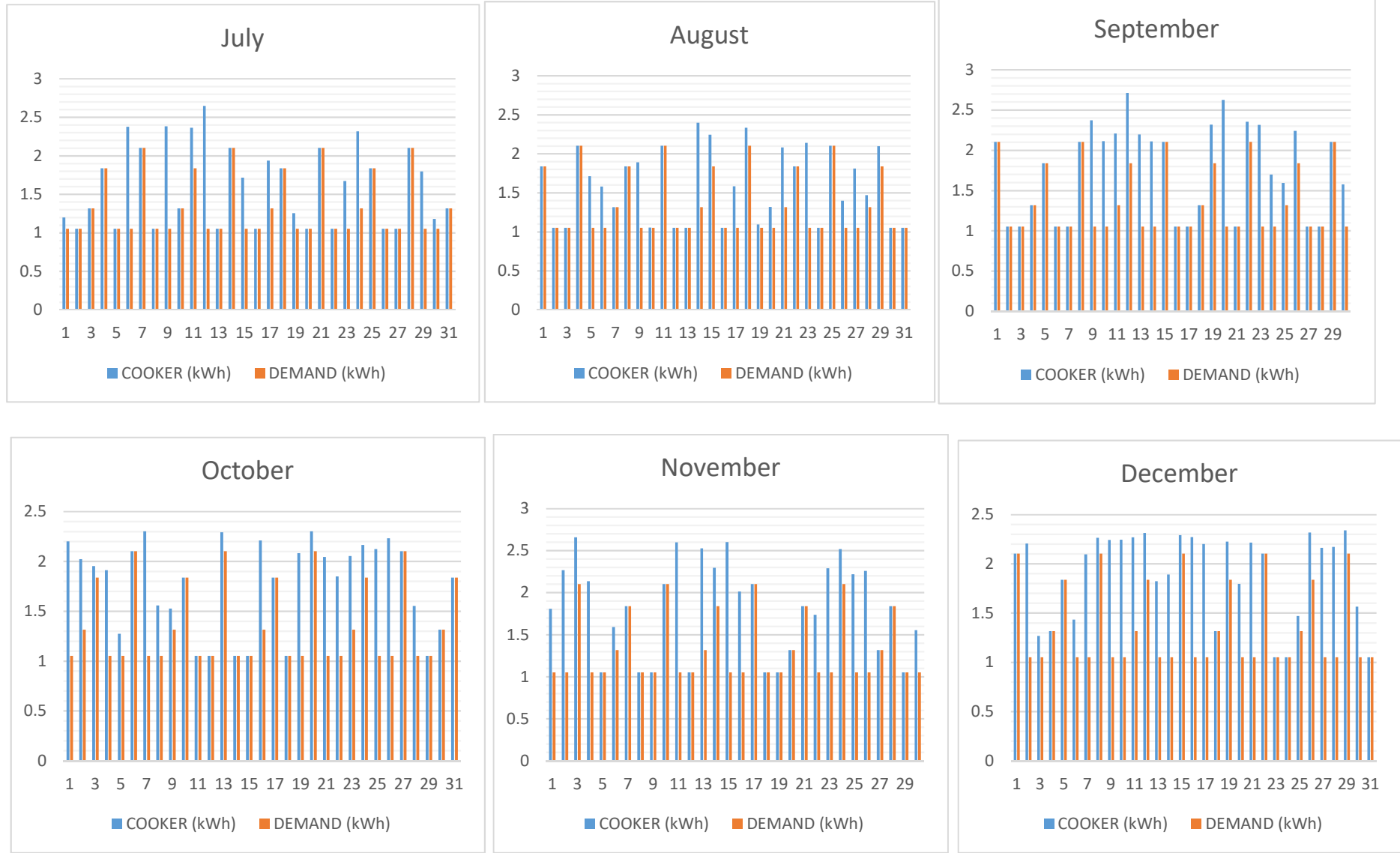


Figure 132b. Monthly cooking simulation results, Jul-Dec.

There are variations in the days in which the hydrogen cooker was available, all months from January to December analysed has shown that there are days in which energy in the hydrogen cooker declined, and thus could not meet the cooking demand for 3 - days, and this occurred in January which basically is because the simulation started with an empty tank. In other months, the H₂-cooker was available to serve the cooking demand. For example, in November – December the H₂-cooker was available with some surplus. This can be attributed to the clear weather conditions of this period, as it is a period called harmattan in Nigeria, when there is always a zero chance of rain. This also coincided with the Christmas season, when the need for cooking is almost doubled per household especially the Nigerian Christian families. The shortages of energy supply seen in the H₂ – cooker in January may be addressed by increasing either the size of the electrolyser or the size of solar panel. However, this opens a question of cost. As already stated, electrolysers are expensive, but a system that gave only 3 days short of supply is worth considering. Therefore, when this is factored in, the choice would be to increase the size of solar PV. The next **sections** give an insight into this. It should be remembered that these simulations are based around a system designed to satisfy an electrical load, and that H₂ production is as a result of the excess PV power available in the dry season. Satisfaction of the cooking load requires adjustments to the load profile and hence resizing of either the PV or electrolyser, or both.

6.5.3 Cost Evaluations

In every renewable energy based project, the system capital costs (CAPEX) and the resulting operation and maintenance (O & M) cost are paramount. Power productions from the renewable energy sources (Wind Turbine, Solar PV, Hydro etc) are totally dependent on weather and atmospheric conditions. This dependency constitutes a major difficulty in designing, planning, modelling, and implementation of any renewable energy based project. Energy investors and consumers are much more concerned with the cost implications as it relates to the inherent intermittency of the power productions from these energy sources, and this makes the optimal reduction of cost of implementing RE-based projects very important. Tremendous progress has been made thus far in the cost reductions of a range of renewable power generation technologies. Presently, among all the renewable energy sources, wind power is one of the most cost competitive source of electrical energy available,

at USD 0.05/kWh without financial incentives, compared to conventional power sources at around USD 0.045/kWh [16].

Moreover, the plummeting costs of solar photovoltaics as already highlighted in **chapter 3** is another important factor in the advance of RES. The declines in installed costs for these renewable energy technologies have made the total installed costs per kW of these RE sources close to or lower than fossil fuel technologies (with the exception of low-cost gas-fired plants) and this, advanced by considerable incentives, has allowed a rapid penetration of the electricity markets worldwide [16]. Islands and remote communities are usually located where connection to the electricity mainland grid is prohibitively expensive. Hence, their reliance on diesel generators for solving their energy problems. Diesel generators are not only expensive to run (high OPEX costs) but also are dirty and noisy, and they emit greenhouse gases.

Energy solutions UK [17] have carried out a test study to obtain the practical cost per kWh of diesel operated off-grid power system. According to their report the system was comprised of a 6kW diesel generator and 24V 700Ah battery bank. They ran a series of tests with the system. In their results, they found that the cost of running a diesel generator without renewables is high at £0.372/kWh with the diesel generator consuming about 0.49 litres per kilowatt – hour. They have suggested that the inclusion of a renewable source such as solar would bring the cost per kWh down to £0.09 (an exchange rate of £1 = \$1.48 in 2014 was used) and even more with increased capacity of the solar PV.

6.6 Obtaining Costs of Individual System Components

As already mentioned, prior to project implementation it is desirable that the project costs be determined per components to ascertain the costs distributions and contributions of each of the system components. This may help in providing a cost structure that shows the economical contributions of the individual components. To do this a detailed cost analysis of each of the components (solar PV, electrolyser, batteries) is of utmost importance.

6.6.1 Cost of Photovoltaic Panels

The costs of solar photovoltaic modules are specified in dollars per watt peak of capacity (US\$/Wp). As of 2016, the average installed cost of a residential solar power stood at approximately US\$3 per watt peak [18]. This represents a halving of installed costs of PV since 2010. The costs of energy production from the renewable technologies such as solar PV, wind and hydro have been compared with that of energy from fossil fuel in chapter 3 (**section 3.3.7**) of this thesis. In this study, the cost of the solar module used was obtained based on US\$3/Wp of 2016, if this multiplied by the selected PV array capacity (1530 W), it gives US\$4590, the US\$3/Wp includes installation costs. But according to sources, the cost of a Panasonic 240 W PV module is £192 [19], this is equivalent to US\$ 251 at £1 = \$1.31 in 2017. Therefore, if we assume that the balance of system is 60% the installed cost, this gives an extra \$150 per module, which brings the total cost to \$401 per module.

6.6.2 Battery Costs

A report in 2015 suggests that installed battery costs are around US\$300/kWh [20]. It has been estimated that with rapid scale up of production by several battery manufacturing companies, and perhaps new technologies, a dramatic battery cost reduction will be expected soon. In this study, battery costs specifications used was obtained from the manufacturer's market catalogue, based on the configurations selected in this design as stated in **section 6.3.2**. The selected battery configuration was 80Ah @ 12V, and a total of 4 batteries will be connected at a cost of \$154 per battery [21].

6.6.3 Cost of the Electrolyser

Currently, at \$1000/kW installed, electrolysers are the most expensive component of a renewable hydrogen system. But with economy of scale and technological advances it seems reasonable to expect significant cost reductions in these devices. In this study, this present cost of \$1000 per kilowatt has been adopted. The total cost was calculated by multiplying this by the selected electrolyser size ($0.400 \times 1000 = \text{US\$}400$). **Table 40** lists the cost specification of each individual system components used in this study and costs of its auxiliaries (DC-DC converters, charge controller).

Components	Number	Cost per module/piece (US\$)	Total (U\$)
Solar module	8	401	3,208
Battery	4	154	616
Electrolyser	1	400	400
DC-DC converter	1	151	151
Charge controller	1	446	446
Totals		1,552	4,821

Table 40. Components costs.

The average total LCOE can be determined by dividing the total expenditures over the lifetime of the project, by the total amount of energy the system produced. Levelised cost of energy is one of the most important factors used to evaluate the fiscal performance of renewable energy systems. However, levelised cost of energy (LCOE) refers to the average cost of electricity production per kWh over the life of the installed system, allowing for discounting over time. To calculate the cost performances of the individual system components, the total cost of each (which includes CAPEX, OPEX and any other ancillary costs) will be multiplied by a capital recovery factor (CRF), which is defined as the ratio of a constant annuity to the present value of receiving that annuity for a given length of time [22]. It was assumed that operating and maintenance cost of PV was zero percent of capital cost, while 1% was allocated for electrolyser and battery at a 5% return rate (interest rate). The PV life time was assumed at 25 years, while electrolyser and battery lifetime was 20 years (alkaline electrolyser) and 10 years respectively. **SOHYSIMO** simulates these parameters and determines the LCOE. It also calculates the different parameters which will determine the system's NPC throughout its useful lifecycle. **Table 41** lists the summary of all cost component used in the simulation.

COMPONENTS	CAPITAL COSTS (\$)	O & M COSTS (\$/yr)	Auxiliaries (\$)	REPLACEMENT COSTS (\$)
Solar PV	3208	0	446	0
Battery	616	6.2	0	616
Electrolyser	400	4	151	400

Table 41. Summary of costs components used in the simulation.

These numbers were entered into the **SOHYSIMO** cost evaluation facility. In the process, the net present cost (NPC) and Levelised energy cost (LCOE) in US\$/kWh can be determined

Figure 133 shows the screenshot of the calculated costs of the system. These costs are listed in **Table 42** for clarity.

SOHYSIMO

PV Sizing | Input data | General data | Cost Evaluations | Energy Assessment | Cooking Decision on Hydrogen Use | Energy Optimisation

ALL COST COMPONENTS MUST BE SPECIFIED IN US DOLLARS

ENTER PV COST COMPONENTS

Enter PV Cap Cost: 3208 Enter Project Lifetime: 25

Enter PV O&M Cost: 0 Enter Return Rate: 0.05

Enter PV Replacement Cost: 0

OK

PV AUXILIARIES ??

Enter Cost of Auxilliary Comp: 446

Help

START

ENTER ELECTROLYSER COST COMPONENTS

Enter Electrolyser Cap Cost: 400

Enter Electrolyser O&M Cost: 0

Enter Elec Replacement Cost: 400

Enter Elect Lifetime: 20

ELECTROLYSER AUXILIARIES

Enter DC-DC Converter Cost: 151

OK

ENTER BATTERY COST COMPONENTS

Enter Battery Cap Cost: 616

Enter Battery O&M Cost: 6.2

Enter Batt Replacement Cost: 616

Enter Project Lifetime: 10

OK

DISPLAY COSTS

Net Present Cost (\$)	5542.4
Project Initial Cost (\$)	4821
LCOE (\$/kWh)	0.419
PV Only (\$/kWh)	0.135
H2 (\$/kg)	47.121
PV with Battery Only (\$/kWh)	0.165

Figure 133. Cost Evaluation.

Component	Cost specification
Cost of Hydrogen (US\$/kg)	47.12
Cost for PV system with battery (US\$/kWh)	0.17
Cost for PV only (US\$/kWh)	0.14
LCOE (US\$/kWh)	0.42
Project initial costs (US\$)	4821
NPC (US\$)	5542

Table 42. Calculated system costs.

With this system, the calculated LCOE was US\$0.42/kWh, and the NPC was US\$5,542. It should be stated here that one of the motivations for this study is identifying suitable system configurations and integrations which can increase the energy capture that may lead to a future reduction in the unit cost of energy delivered. However, to say this once again, electrolysers are still relatively expensive. The cost of a renewable power system is partly defended based on the life cycle of the complete system, including the type of energy system it is replacing, and the remoteness of the location.

Any initiative done to improve the lifetime of electrolysers may help in reducing the levelised cost of the system. There are wide variations on reported works on the lifetime of electrolysers. As at 2013, the lifetime of an electrolyser was quoted in the range between 20 – 30 years for alkaline type and 10 – 20 years for PEM electrolysers [23]. However, with future improvements as reported which may lead to reduced electrode degradations, a stability in the lifetime of this device may be achieved [24]. To assess the sensitivities of electrolyser lifetime on the life-cycle cost of this system, another simulation was set up and a 25-year electrolyser lifetime was assumed. In the process, all other cost components remained the same. The simulation was run and this reduced the levelised cost of energy to US\$0.33/kWh. The results are summarised in **Table 43**. This represents a 30% cost reduction when compared to the previous scenario and demonstrates the sensitivity of the unit energy cost to changes in electrolyser lifetime.

Component	Cost specification
Cost of Hydrogen (\$/kg)	43.4
Cost for PV system with battery (\$/kWh)	0.17
Cost for PV only (\$/kWh)	0.14
LCOE (\$/kWh)	0.33
NPC (\$)	5222
Capital cost (\$)	4821

Table 43. Calculated costs at 25 years' electrolyser lifetime.

This did not only reduce the LCOE, the NPC was also reduced from US\$5542 to US\$5222. Converting these costs from US dollars to its Naira equivalent (the Nigerian currency) at US\$1 = N350 exchange rate in 2016, we obtain as follows;

$$\text{LCOE (1)} = \text{N147/kWh}$$

$$\text{LCOE (2)} = \text{N116/kWh}$$

$$\text{COE (PV – battery)} = \text{N49/kWh}$$

$$\text{Capital cost} = \text{N1.69 million}$$

Per sources investigated, and as of 2016, the cost of electricity in Nigeria was around US \$0.07/kWh (N27/kWh at exchange rate of US\$1 = N350 in 2016) [25]. Recognising the decline in the value of the Naira over the past 2 years, and comparing this to the presumed value of Naira in 2014 at US\$1 = N165 in 2014 [26] this gives US\$0.16/kWh, and means, a 58% increase which indicates how low the purchasing power of Naira has become at present. It could be argued that based on the current situation, a PV – hydrogen project in a remote location of Nigeria, is expensive, but the externalities (emission, terrain, deaths) should be considered.

6.6.4 The Impacts of a Hydrogen Cooker on Domestic Energy Costs

As explained in **section 6.5.3** the current per capita daily firewood consumption in Nigeria is 1.49 kg. An average household of 7 people would thus consume approximately 10.43 kg/day. It can be recalled that there is a correlation between the income level and social status of households and

the type of fuel they use. However, for kerosene consumption, a 0.418 litre/day was assumed based on future costs projections. The simplest measure used to assess the financial viability of a renewable energy project is by comparing the savings the owner will make with avoiding a unit cost of other energy options, for example; kerosene, battery or conventional sources. To assess the cost implications of these fuels, data regarding this was obtained from the National Bureau of Statistics (NBS) [27]. According to NBS, in 2016 the average pump price of kerosene in Nigeria was N293 per litre (US\$0.84/litre, at US\$1 = N350 exchange rate).

A variation in prices across the 36 states of the country was noted. For example, in Ebonyi state the price of kerosene was stated at N302.28/litre (US\$0.86/litre, at US\$1 = N350 in 2016). For the cost of firewood, in this study, it was assumed that villagers can source firewood from the forests at no cost. However, this only applies to rural areas on which this study was based. Ideally, those who live in the urban areas will need to buy firewood from the market, mostly sold by the villagers who make a living out of firewood trading. The price of kerosene stated here would only favour those who live in the cities, as villagers may need to pay more for the same commodity due to the remoteness of the location. Transportation costs may also be added by the kerosene suppliers. This paralleled and uneven fuel cost may constitute some of the reasons the villagers resort to fetching firewood from the forests to meet their cooking needs, thereby increasing the consequences of deforestation. To determine the impacts the use of hydrogen cooker will have in future if it is introduced as a source of fuel for domestic cooking in the Nigerian rural areas, the following analysis was made;

The cost of PV – hydrogen energy simulated in this design = US\$0.42/kWh

The cost of kerosene = US\$0.86/litre

Therefore, with consideration to the quantity of kerosene which may be consumed per day (0.418 litres, doubles every week), and figuring out how many times it may be used in a week (7 times). However, a data input section of the hydrogen cooking page of SOHYSIMO tool was cropped to illustrate the number of times and quantity of kerosene used per week. This is depicted in **Figure 134**.

	1	2	3	4	5	6	7
FIREWOOD (kg)	10.43	10.43	20.86	10.43	10.43	10.43	20.86
CHARCOAL (kg)							
KEROSENE (L)	0.418	0.836	0.418	0.418	0.836	0.418	0.418

Figure 134. Screenshot of daily cooking demand at Okenkwu village.

The total kerosene consumption per week was 3.8 litres. Taking the mean value, it gives 0.54 litre per day. Hence, multiplying this by the cost per litre of kerosene (US\$0.86/l), we obtain that US\$0.46 (N161, at US\$1 = N350) will be spent daily on kerosene. This represents the kerosene pump price. Usually, the rural dwellers buy the kerosene at 3-4 times the pump price. This brings the amount they may spend on kerosene to US\$1.84 (N644) per day. In the rural areas, dry cell batteries are mostly used as source of lighting and listening to radio. However, popular brands of dry cell batteries in Nigeria villages are Tiger Head and Flash, costing around US\$0.34 (N120) for two. The estimated average battery lifespan is 1 week depending on use. In this study, it was assumed that each household may consume about 30 batteries per month or 1 battery per day. If this cost is distributed accordingly; we obtain US\$0.037 (N12.95) per day. Basically, if the use of dry cell batteries is included in the domestic energy cost calculations, it means US\$1.89 (N660) will be the amount spent on energy by each household per day or US\$689.85 (N241,447.5) per annum in the rural area of Nigeria. These costs calculations are extended across the project lifetime, compared and presented in **Table 44**. And the cost savings of US\$11,704 (N4.1million) is clearly visible, added to the life the savings from indoor pollutions. This calculation, although somewhat crude, highlights the fact that although RE energy solutions are generally considered relatively expensive this is only true in terms of the CAPEX. The zero-fuel cost (and hence very low OPEX) is sometimes not fully considered in the decision-making process. With fossil-based fuel prices on a steep and long-term upward trend RES will become increasingly attractive.

Component	Cost (US\$)/household	Years
PV - Hydrogen	5542	25
Traditional energy	17,246	25

Table 44. Extended projects costs over the lifetime.

6.6.5 Energising the Entire Village

As mentioned in **section 6.2** the village under study is made up of 171 households, assuming all the households are provided with solar – hydrogen system, the cost implications will be compared in this section. It has been estimated that, grid connection of a rural area may cost around US\$10,000/km (3.5 million Naira) per kilometre for a medium voltage line [28]. In contrast, other authors have suggested a cost of \$20,000/km [29]. However, it should be noted that the amounts quoted here are based on assumptions, as the authors did not consider other factors such as topography of the location (for example, mountainous areas as in the case of the location considered in this study). Experience elsewhere is in support of this. A report published by the National Rural Electric Cooperative Association (NRECA) and the USAID, on a rural electrification project in Bolivia (Tomoyo) [30] suggested that connecting a village of 200 population located at 6.4 km distance to a national grid point would amount cost around US\$12,700. However, the cost varies by location and decreases with distance from the grid point. The full list of cost breakdown of this project is presented in **Table 45**. According to USAID, this work was presented as a guide for rural electrification projects.

Villages	km	Phases	Users	KWh	kW	Staking	Feeder	Distribution	Total Cost	US\$/User
Molle Molle (ambos)	6.4	1	200	6,000	25	\$4,723	\$28,160	\$94,000	\$126,883	\$634
Sorojchi	2.7	1	105	3,150	14	\$2,240	\$11,880	\$49,350	\$63,470	\$604
Yoroqa	2.5	1	98	2,940	13	\$2,084	\$11,000	\$46,060	\$59,144	\$604
Tomoyo	4.2	1	114	3,420	15	\$2,893	\$18,480	\$53,580	\$74,953	\$657
Llatapata	2	1	50	1,500	7	\$1,326	\$8,800	\$23,500	\$33,626	\$673
Isluco	2	1	30	900	5	\$1,086	\$8,800	\$14,100	\$23,986	\$800
Jiroja	1	1	60	1,800	8	\$1,083	\$4,400	\$28,200	\$33,683	\$561
Kasapata	3	1	50	1,500	7	\$1,689	\$13,200	\$23,500	\$38,389	\$768
Sorocoto	3.5	1	160	4,800	20	\$3,191	\$15,400	\$75,200	\$93,791	\$586
Soroscopa	1	1	60	1,800	8	\$1,083	\$4,400	\$28,200	\$33,683	\$561
	28.3	10	927	27,810	121	\$21,397	\$124,520	\$435,690	\$581,607	\$627

Table 45. Grid connection costs for rural electrification in Bolivia [30].

As an illustration consider a village that is 25km away from the grid terminal point and with 1200 populations (171 households), then an approximate cost can be deduced as follows;

$$200 \text{ users at } 6.4 \text{ km} = \text{US\$}127,000$$

$$171 \text{ users at } 25\text{km} = \left[\frac{200}{171} \right] * \left[\frac{25}{6.4} \right] * [127000] = \text{US\$}580,000$$

This gives US\$3,390 (N1.18 million) per household. It should be noted that this does not include the cost of road clearing, house connection and un-factored costs associated with the inaccessible

topography of this location. A study has suggested that an additional spend of around US\$7,000/km will be required to cover these costs [31]. Therefore, when this amount is shared among the households, it gives US\$40.9 per household. Including this to the other costs stated above, the cost will rise to about US\$3,400 per household. However, if the initial capital cost of the solar – hydrogen system designed in this study (US\$4,821 for a household) is compared with the estimated grid connection costs, and the entire village was to be provided with this system, it means some US\$824,391 will be required. Based on this (admittedly simplified) scenario, implementation of this type of a system at this location will be expensive, and this opens two opportunities as follows;

- 1) The need to model a customised system whereby the income level of each household will be put into consideration
- 2) To model and analyse a possible use of a connected hydrogen-micro-grid system
- 3) The need to verify if this could be economically feasible in other locations

These are presented in the next chapter.

6. References

1. Online available at <http://www.who.int/mediacentre/factsheets/fs292/en/> accessed on [10/01/2017](#).
2. IEA World energy outlook 2006.
3. Osueke, C.O. and Ezugwu, C.A.K., 2011. Study of Nigeria Energy resources and its consumption. International Journal of Scientific & Engineering Research, 2(12), pp.121-130.
4. Garba, B., 2011. Renewable Energy for Rural Industrialization and Development in Nigeria: Energy Commission of Nigeria.
5. Adeoti, O., Ilori, M.O., Oyebisi, T.O. and Adekoya, L.O., 2000. Engineering design and economic evaluation of a family-sized biogas project in Nigeria. Technovation, 20(2), pp.103-108.
6. Extension of electricity to Okenkwu Eburnwana in Afikpo South LGA of Ebonyi state; online available at; <http://www.tracka.ng/issues/view/268> accessed on 10/11/2016.
7. Social control system - role of traditional associations in of Edda; online available at <http://www.doublegist.com/social-control-system-role-traditional-associations-edda/> accessed on 10/02/2017.
8. Invitation for tender at rural electrification agency; online available at <http://tenders.nigeriang.com/federal-government-tenders-in-nigeria/invitation-to-tender-at-rural-electrification-agency-2/13275/> accessed on 10/01/2017.
9. Online available at <http://www.doublegist.com/road-construction-edda-topography-problems/> accessed on 10/11/2016.
10. Online available at <http://www.vanguardngr.com/2013/02/climate-climate-change-the-dry-and-wet-seasons-in-west-africa-2/> accessed on 10/01/2017.

11. Online available at <http://www.absak.com/library/power-consumption-table> accessed on 10/12/2016.
12. Online available at https://midsummerenergy.co.uk/pdfs/panasonic_240W_data_sheet.pdf accessed on 10/12/2016.
13. Online available at <http://www.premiumtimesng.com/news/137723-nigerians-use-266-million-kg-of-firewood-daily-senator-saraki.html> accessed on 10/12/16.
14. Sepp, S., 2014. Multiple-household Fuel Use: A Balanced Choice Between Firewood, Charcoal and LPG: BMZ, Federal Ministry for Economic Cooperation and Development.
15. Anozie, A.N., Bakare, A.R., Sonibare, J.A. and Oyebisi, T.O., 2007. Evaluation of cooking energy cost, efficiency, impact on air pollution and policy in Nigeria. *Energy*, 32(7), pp.1283-1290.
16. International Renewable Energy Agency (IRENA) January 2015 "Renewable Power Generation costs in 2014 - 2015".
17. Online available at http://www.energy-solutions.co.uk/pdf/off-grid/off_grid_system_fuel_usage_tests_updated.pdf accessed on 12/12/2016.
18. Global trends in renewable energy investments 2016: Bloomberg new energy finance report, online available at http://fs-unep-centre.org/sites/default/files/publications/globaltrendsinrenewableenergyinvestment2016_lowres_0.pdf accessed on 22/12/2016.
19. Online available at <http://www.buypvdirect.co.uk/Panasonic%20PAN-240%20HIT> accessed on 01/09/2017.
20. Online available at <http://arstechnica.co.uk/science/2015/07/electric-vehicle-batteries-are-getting-cheaper-much-faster-than-we-expected/> accessed on 10/11/2016.
21. Online available at <https://www.walmart.com/ip/12V-80Ah-AGM-Deep-Cycle-Battery-for-RENOGY-PV-SOLAR-PANELS/140778764http://www.maplin.co.uk/p/12v-100aah0solar-battery-135br> accessed on 22/06/2017.

22. Online available at http://www.nrel.gov/analysis/tech_lcoe_documentation.html accessed on 22/12/2016
23. Carmo, M., Fritz, D.L., Mergel, J. and Stolten, D., 2013. A comprehensive review on PEM water electrolysis. *International journal of hydrogen energy*, 38(12), pp.4901-4934.
24. Symes, D., Al-Duri, B., Bujalski, W. and Dhir, A., 2015. Cost-effective design of the alkaline electrolyser for enhanced electrochemical performance and reduced electrode degradation. *International Journal of Low-Carbon Technologies*, 10(4), pp.452-459.
25. Online available at <http://www.vanguardngr.com/2016/02/how-45-electricity-tariff-hike-will-affect-you/> accessed on 15/12/2016.
26. Oladokun, V.O. and Asemota, O.C., 2015. Unit cost of electricity in Nigeria: A cost model for captive diesel powered generating system. *Renewable and Sustainable Energy Reviews*, 52, pp.35-40.
27. Online available at <http://www.nigerianstat.gov.ng/report/464> accessed on 10/12/2016.
28. Bonnet, D., 2014. *Clean Electricity from Photovoltaics*.
29. Foley, G., 1995. Photovoltaic applications in rural areas of the developing world (Vol. 304). World Bank Publications.
30. NRECA, Guides for Electric Cooperative Development and Rural Electrification.
31. Feltenstein, A. and Shah, A., 2000. Reducing the cost of grid extension for rural electrification

7.0 Assessment of Solar – Hydrogen Micro-Grid System for Remote Energy Access

In chapter 6, the possibility of utilising a solar-hydrogen system (in form of Solar – Home Systems) to provide energy access to each household in rural areas, was evaluated, assessed and presented. The analysis was done and some critical questions concerning the feasibility of the process were noted. In this section, an emerging power network system in DC Micro – Grid will be assessed to determine its suitability in providing energy access to unserved remote areas, and particularly, the villages that are not connected to the national grid at about 10km distance from the grid connection point. It is assumed that the villagers will be using energy efficient DC appliances.

7.1 DC Micro-Grid an Overview

A small scale (usually < 500kW) stand-alone DC power system network with advanced capabilities which controls its own power generation, transmission, distribution and consumption for improved operational performance, is referred to as DC micro grid. This kind of system has been around in a very basic form for more than a century. In the early 1880s, Thomas Edison (the American famous inventor) predicted that future electricity networks would be based around the DC Micro grid. A fierce technological battle, termed 'the war of currents' took place between Edison, who was a leading proponent of DC, and Nikola Tesla and George Westinghouse who were proponents of AC (alternating current) electricity. Edison proposed a system of small local power plants in form of a DC micro - grid that would power individual neighbourhoods or city sections [1][2]. Largely due to voltage limitations at the time, requiring power plants to be located within 1.6km to the consumer, Edison lost the fight and the AC power generation dominated. The rest, they say, is history.

In recent years, widespread adoption and utilisation of renewable technologies has made it much more appealing for the world to turn to DC micro grid. In recent decades, there has been a tremendous increase in interest in utilisation of abundant solar resources for electricity generation. Solar photovoltaic is a DC power source, and designing a power system which makes it easy for it to be connected or integrated directly to the network, without any intermediary power conversion processes, will effectively enhance its power harnessing capability. The current national grid power network infrastructure supports an AC micro grid system, thus to connect solar PV to the network, a DC – AC converter is a sine qua non. The AC mains frequency employed is either 50 Hz, or 60 Hz, and the voltage 110-120 V rms or 220-240 V rms per phase, depending upon country.

One of the problems that has historically contributed to the acceptance of AC over DC was the difficulty in transforming a DC voltage, since the straightforward application of wound components (transformers) is not possible. However, over the past decades, due to confluence of several technological advances, tremendous progress and remarkable success has been made in the power electronics industry in the development of DC power converters [3][4]. Essentially, this success, coupled with the increasing penetration of DC loads (such as personal computers, phones TV, radio, LED lighting...) and the advent of renewable technologies, especially, solar photovoltaics, has led to a resurgent interest in DC micro – grid systems. **Figure 135** shows a typical schematic representation of a DC micro – grid comprised of a solar photovoltaic array and battery storage. Four residential houses with low power consuming DC appliances are connected to a common DC bus. The system network can also be integrated with supervisory controllers to optimise the energy utilisation, such that the PV will charge the battery in the day time after satisfying the DC load demand of the household, while the battery will be configured to provide power to cover night time demand.

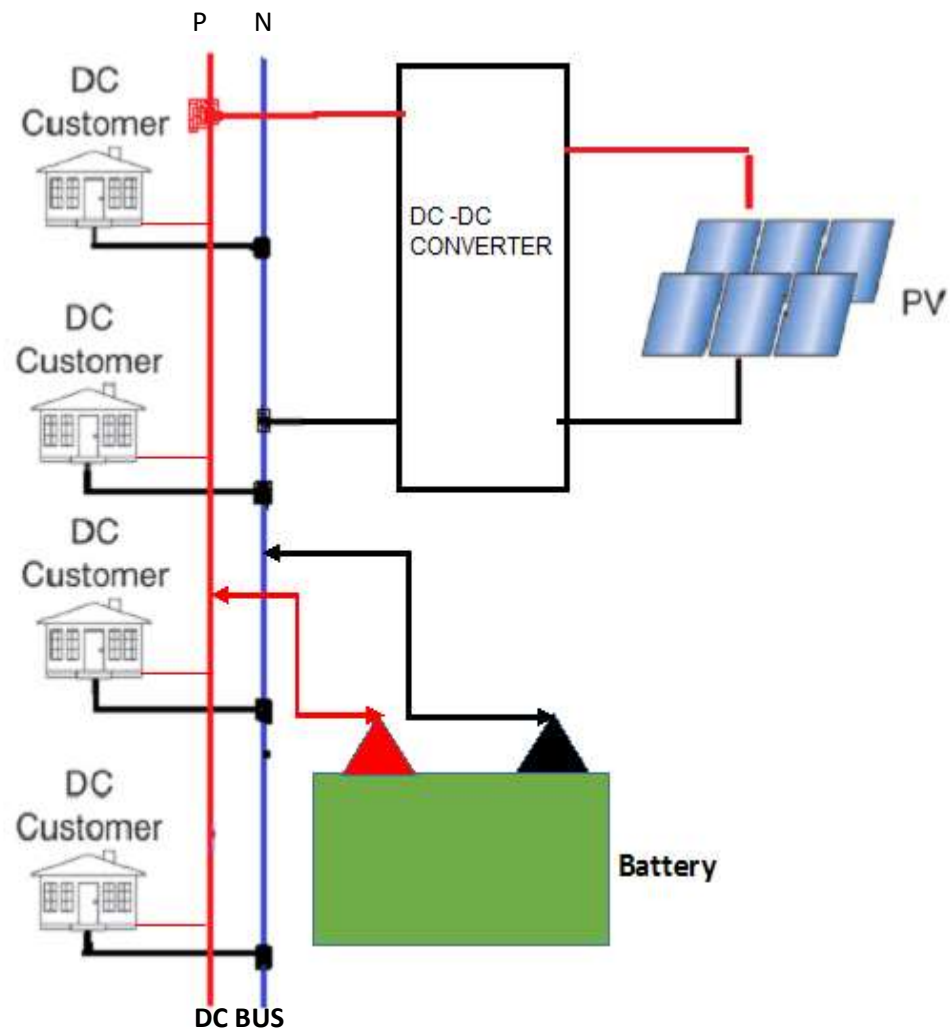


Figure 135. Schematic representation of solar – battery DC micro – grid system.

In the past decade, DC micro – grids have been demonstrated on various scales. The first was introduced in 2002 [5], and since then there has been continued interest in this topology [6][7]. Elsayed et al [8] presented a review of recent progress.

They found many advantages of utilising a DC micro grid over AC to provide energy access to the residential and commercial buildings, including but not limited to the following;

- ✓ Reduced power losses
- ✓ High efficiency
- ✓ Low cost
- ✓ Easy implementation
- ✓ Safety
- ✓ Reduction in electromagnetic fields
- ✓ Power quality improvement
- ✓ The possibility in which power systems can easily be built by directly-connected batteries.

However, some limitations and challenges facing the application of DC micro – systems in renewable energy technologies has been documented. A major challenge concerns development of appropriate protection systems for DC micro – grids due to lack of standards, guidelines and practical experience [9]. However, the recent popularisation of DC consuming devices and the opportunities of utilising the alternative energy technologies, in providing electricity to regions of the world that lack access to it, has inspired interests in the development and deployments of standards that may lead to the rapid adoption of low voltage direct current (LVDC) grid [10].

7.1.1 DC Micro – Grid for Rural Energy Access

The penetration of renewable technologies has offered an opportunity for researchers to reconsider the use of DC micro – grid for distribution and transmission of electric power. The use of a DC micro – grid removes the frequency component or reactive power flow control issues identified in the Eigg AC micro – grid described in **chapter 5**. However, the influence of renewable generators on the AC micro – grid frequency depends on the proportion that renewable generation capacity accounts for, relative to the total installed capacity of the power system [11]. Ideally, most household appliances are DC consuming devices, and with a DC micro-grid, the wall socket in the building will provide a DC source. This overcomes the hurdle of rectification, and by appropriate design of appliances minimises DC-DC conversion stages, and thereby improves the energy consumption efficiency of these devices. For a typical village in Nigeria, the energy

requirements are mostly based on these devices, and providing them an electricity access using a power network that matches this is actively worth considering. Therefore, considering the plan by the Federal Government of Nigeria to increase energy access in Nigeria with an integration of renewables, as already highlighted in chapter 2, clearly, there is no plan by the FGN to utilise a DC micro – grid to provide power access to the rural dwellers. Perhaps, this may be because, DC micro – grid is a re-emerging power network idea, and the conception may not have occurred to the analysts who made the proposal at the time. Here, we lift these restrictions, and consider a DC micro – grid system that consist of a solar photovoltaic power source, hydrogen system and battery storage system. DC micro – grid architecture has been identified as a suitable option for rural electrification in developing countries [12].

In **chapter 6**, a study on utilising solar home system to energise the selected village was presented. However, from the simulations, for economic and technical reasons the following was noted;

- To model and analyse a possible use of a connected hydrogen-micro-grid system
- The need to verify if this system may be more feasible in other locations.

7.1.2 Why DC micro – Grid?

DC micro – grid was adopted based on the reasons already highlighted in **section 7.1**, including the line frequency problems observed in Isle of Eigg electricity network as discussed in **chapter 5**. To demonstrate the reasons behind this choice, as an example **Figure 136** [13] is a picture of an existing DC – Micro grid electricity system implemented at Xiamen University China in 2012. The system is operational today, and according to Zhang et al [13], the system consists of a roof mounted 150 kW PV array, a 220 Ah 336V lead acid battery storage system, and a 160kW AC/DC back up unit. These are connected to a 380V DC bus and a 1.6 kW Nextek converter, was also integrated to convert the 380V DC input to 16 channels 24V DC input suitable to power a 100W LED load. The micro – grid DC loads consist of a 20 kW LED lighting system (which has both 24V DC and 380V DC inputs), 30 kW DC air-conditioner and a 40kW electric car charging station. For different loading they tested, DC micro – grid achieved about 93% efficiency compared to 77% efficiency of the AC micro – grid [14]. This is about 16% increase in system efficiency, which may be largely due to the elimination of multiple power conversion stages (DC – AC, AC – DC) involved

in a PV micro – grid system that provides power to some DC consuming devices. This DC micro – grid system may be used as a typical demonstration of the future possibility of having a low voltage DC distribution system for residential applications in place of an equivalent AC system. This system can be adapted to a village or community scale as already proposed in [15].



Figure 136. Campus building at Xiamen University, China, showing the roof top installation of 150 kW PV array for DC micro – grid [13].

However, a renewable– hydrogen DC micro – grid system with variable energy sources, such as solar photovoltaic systems mostly requires system auxiliary devices that will be carefully designed to obtain an optimum power performance when used with the PV system. Ideally, the power produced by renewable generators, particularly solar generators, can be used by various electricity consumers. One of the main problems associated with renewable energy systems is their fluctuating output depending upon weather conditions and the day/night cycle in the case of PV. To be sustainable the hybrid renewable energy system need to be designed to accommodate fluctuations. In renewable power system, matching power generation with load demand is critical at the early stage of the design process. Batteries are frequently used as energy storage in periods of over-generation, supplying this stored energy during periods of under-generation.

Ultimately, for the solar photovoltaic system to be able to charge a directly-connected battery, its output voltage must be at least equal to the battery voltage, which makes the PV operating voltage dependent on the battery and vice versa. However, considering the intermittency inherent in the PV system, optimal power transfer is required at all times. To meet the load demand, in most cases a device is integrated between the solar PV system and the load to decouple the voltage at the load from the voltage at the solar PV system. This process enables efficient power flow from the source to the load. The electronic device used in this adaptation purpose is called DC – DC converter. The following **sections** will discuss the application of DC – DC converter in solar PV applications.

7.2 DC – DC converter.

The conversion of one dc input voltage source to either high or low output voltage is made possible with DC – DC converter. The 4 major components used in DC – DC design are Switches – such as Metal – oxide semiconductor field effect transistors (MOSFETs), Bipolar Junction transistors (BJTs), or Insulated gate bipolar transistors (IGBTs), inductor, capacitor, and freewheeling diode. In some applications, the diode may be replaced with an additional switch. Basically, inductors are used in the DC – DC converter circuit as an energy storage device. The inductor stores energy during the charging period denoted by t_{on} and discharges energy to the load during the off-time t_{off} . The switches (MOSFETs, IGBTs, BJTs) can be turned on and off when control signals (typically pulse width modulated) are applied to their control terminals [16]. It is possible to operate these switches at high frequencies to reduce filtering requirements. Ideally, capacitors are mostly used to filter off any ripple in the output DC voltage.

These devices are still evolving, and new devices are being investigated, such that it is expected that in future, switches with high power ratings and faster speeds may emerge. However, in current designs, based on desired application, MOSFETs are given higher preference over other switches due to their fast switching speeds. There are two distinct operation modes that are usually adopted when designing a DC – DC converter. They include; discontinuous mode and continuous mode. The discontinuous mode defines the operation time when the energy stored in the inductor is discharged to the load via the output capacitor before initiating a new charge

period, the reverse process is the case in terms of continuous mode. It has been found that coupling a DC – DC converter to a PV system enhances its energy harnessing [17].

In ideal world, all direct power, and energy or circuit converters would be 100% efficient, but realistically there is no direct converter that ever work without a loss. However, with carefully selected components, a good DC – DC converter would achieve at least 95% conversion efficiency [18]. Based on component configuration, DC – DC converters are classified under 5 broad topologies; buck – converter, boost – converter, buck – boost converter, fly-back converter and charge pump converter [18]. The buck and the boost converter topologies are relevant to this research. These are described in detail and their operation simulated in **Appendix 7E – 7F**. It may also be possible to utilise these converters to facilitate a multi-bus system in terms of 12V, 24V, and 48V for household appliances that are rated (nameplate rating) with these various ranges of voltages. However, according to Emerge Alliance standard for occupied spaces [19], and as presented by Backhaus et al [20], for lighting and other low – power devices, a 24V final distribution system is preferable. This is because of safety and protection measures as specified by the National Electric Code (NEC) [21].

7.3 Modelling and Simulation of a DC – DC Micro – Grid Power System for Remote Area Energy Access.

This section describes a micro – grid model utilising a solar –hydrogen system to supply power to a remote village in Nigeria. Design of a renewable power system begins with a detailed study of the energy requirement of the location of interest. However, the load model already developed in **chapter 6** was adopted. In the process, a software tool developed by the author was used to carry out a year-round simulation in order to analyse the energy characteristics of the location, and determine the feasibility of providing a low-cost low carbon energy supply system to the village. Meanwhile, since a central power system in DC micro - grid is considered, the PV array capacity and battery storage size was obtained based on the total energy requirement of the entire village.

7.3.1 Sizing the DC – Micro – Grid Components

A similar procedure to that used in **chapter 6** was followed to obtain the capacity of the system components. The load demand calculated was 2.2kWh per day for each household and the village is made up of 171 households. This serves as a baseline data on which the sizing capacities of the key components of the rural DC micro – grid energy system will be obtained. This means that 376.2kWh is the total energy requirement for the whole village per day.

7.3.2 Load Demand Model for Okenkwu

Over the past decade, there has been a growing research interest in load profile modelling [22][23][24][25]. In these models, various different modelling approaches have been presented. One of the difficulties an energy profile modeller may encounter is the high variability of energy demand. However, Reiss and White [26] have made efforts to address this problem. It is almost impossible to predict the daily energy consumption of each individual household, which covers, particularly, a whole village or community. Conventionally, a load model for multiple households can be obtained by estimating the demand of one household, and then extending this to represent the total load demand for the whole village considered. Adoeti, Oyewole and Adegboyega [27] investigated the energy requirements of families in a rural area of Nigeria. Their study sampled 4 villages consisting of up to 200 households in the Southwestern Nigeria. They found that their daily electricity requirement varied from 1.583kWh/day for villages with access to grid electricity supply to 2.324kWh/day for villages without grid access. This study is particularly important to the current research as the data were based on a rigorous survey using direct interviews and questionnaires, and matches the energy requirements considered in this thesis.

Ideally, energy price and income level is key in evaluation and estimation of average household demand for energy, as it is a major determinant of the appliances a consumer can possess. Load demand is strongly coupled to behavioural characteristics of consumers and the relative income level of the household. Good practice in the early energy design process is to interactively carry out individual household load assessment for the whole village in consideration of some socio-economic factors. To demonstrate the dependency of income on the capability of the individual household to own a kind of appliance, and the relative correlation between education or social

status of the household and the behavioural characteristics towards use of the domestic appliances. In the rural setting, variables such as occupation, social behaviour and level of education in the household need to be examined to obtain a reasonable load profile. The current load model, considers a typical load demand for a village consisting of 171 families for a single day, by taking a load demand for one household and multiplying it by 171. The load profile for each day throughout the year was considered to be identical. **Table 46** lists the load demand considered for the Okenkwu village DC micro – grid design.

Appliance	Number in use/171 HH	Total Number in use/171 HH	Rated Power (W)	Total Power (W)	Hours of use	Energy (Wh/day)
LED Lighting	6 x 171	1026	15	15390	11	169290
Radio set	1 x 171	171	25	4275	11	47025
Television	1 x 171	171	35	5985	6	35910
Table fan	3 x 171	513	20	10260	8	82080
Phone	3 x 171	513	10	5130	8	41040
Total		2394	105	41040		375345

HH= Household.

Table 46. Village energy demand data.

These data were entered into SOHYSIMO for simulation, **Figure 137** depicts the load model and **Figure 138** shows the load profile model in SOHYSIMO

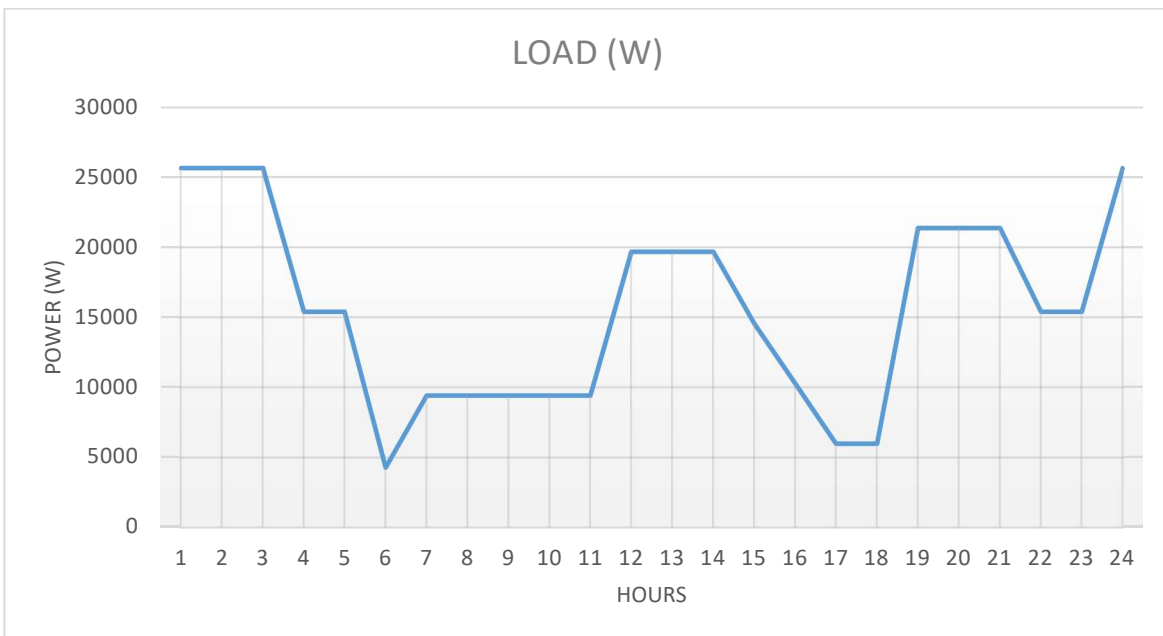


Figure 137. Load profile for Okenkwu village micro – grid system.

Other factors that should be considered are the energy requirement for relevant basic amenities such as community health centre, schools etc. The village considered in this study have just a few of these amenities. Thus, here we assume this additional load may be neglected. A recent study in Sri Lanka suggests that about 270kWh/day per village was the energy requirement for a village consisting of 150 households in a rural electrification project that has been implemented [28]. It follows that a solar PV array generating at least 375.35kWh per day is required. As a first estimate therefore, the following components were selected:

- 400kW PV array
- 844kWh (380V 2222Ah), a 2222Ah 2V battery bank to be connected as 190 string size in series and 1 in parallel
- 50kW electrolyser.

The excess energy generated from the solar resource will be utilised by the electrolyser to produce hydrogen, which the households will use in hydrogen cooker to meet their cooking needs. The amount of solar irradiation received in this selected location has already been analysed in previous **chapters**.

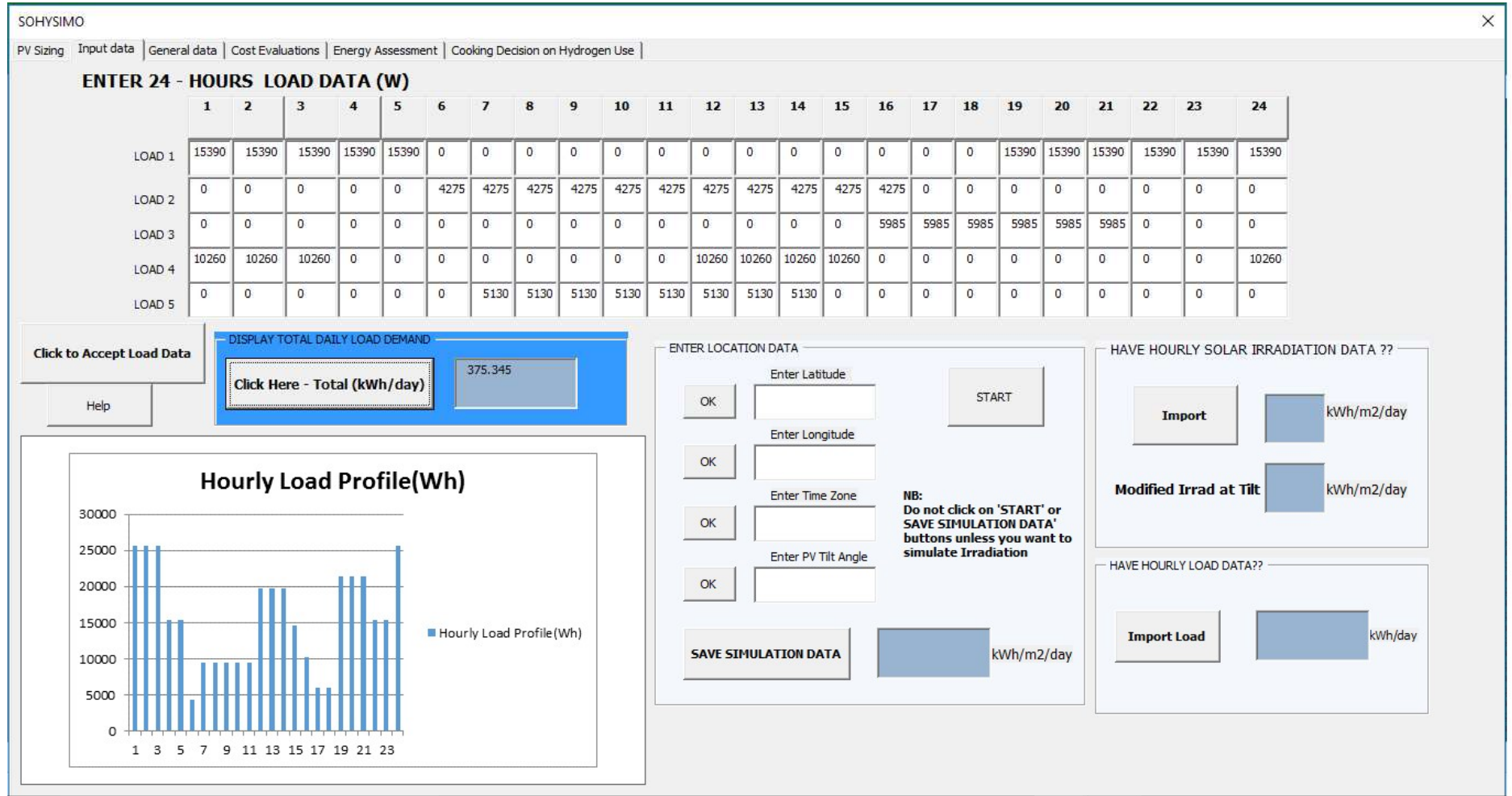


Figure 138. SOHYSIMO user interface showing the modelled load profile.

These data were entered in SOHYSIMO and simulation was run and **Table 47** lists the results obtained from the simulation.

Parameter	Value	Units
PV rated capacity	400	kW
Annual PV production	502,018	kWh/yr
PV hours of operation	4745	hours
Energy sent to load	53,000	kWh
Total DC load	136,975	kWh/yr
Excess energy	225,717	kWh/yr
Battery nominal capacity	844.36	kWh
Battery usable capacity	422.2	kWh
Battery hours of operation	4015	hours
Battery autonomy hours	27	hours
Battery Energy in	115,611	kWh
Battery Energy out	84,501	kWh
Energy available for electrolyser	108,215	kWh/yr
Suggested days of autonomy	1.8	days
Hydrogen produced	2,005	Kg/yr
Unmet electric load	0	%
Suggested PV size	411	kW

Table 47. Micro-grid simulation results.

From the results, over one year simulated, the PV generated energy 502,018 kWh, which is enough to serve the 137,000 kWh annual DC load, and charge the battery. When the PV output power exceeds the load and the battery is at its full state of charge, the excess was utilised in the electrolyser for hydrogen production. The electrolyser produced a total of 2,005 kg/year of hydrogen. On average, this corresponds to 5.5 kg/day. The distribution system (storage) described by Gardiner et al [29] is considered. As explained in **chapter 3**, hydrogen can be stored as a

compressed gas under pressure. However, theoretically it has been shown that using a pressurised electrolyser it may be possible to store hydrogen at elevated pressure and thereby eliminating the requirement for compressor and reducing the storage capacity required [30]. This has the potential to lower the unit cost of electricity and investment cost [31]. To compute the storage capacity, we consider the daily hydrogen demand and the quantity of hydrogen produced per day. This will be shown later.

7.4 Connected Hydrogen Cooking System

In the previous section, we have simulated a solar - hydrogen production system for the case study village. In this section, a system where the hydrogen will be utilised effectively and efficiently is discussed. The scope of this study is limited to 400kW solar PV and 50kW electrolyser as used in this simulation, and the cost implications are considered with reference to future component cost projections, the interest is to model an energy efficient system that can provide the selected village with an instant energy access.

7.4.1 Connected Hydrogen

The idea of connected hydrogen is to develop a system whereby a central electrolyser will be used to generate hydrogen, and the generated hydrogen will be distributed to all household via a hydrogen interconnected pipeline. This kind of system has been demonstrated in various scales over the past decade [33][29]. Gardiner et al [29], have described the first ever prototype and existing implementation of connected hydrogen scheme in a typical village of New Zealand. This has been operational since 2007 and consists of 5.5 kW solar – wind power system, a 400W electrolyser which produces 0.37kg/day (equivalent to 14.58 kWh/day) with storage volume of 1.5m³/day at 3bar [33]. The system was described as a stand – alone wind – hydrogen electrolysis, which was piped 2 kilometres to a farming community used to meet the hot water and cooking needs of the community. On a village scale, Lolland hydrogen community in

Denmark is an example [34]. This has an underground hydrogen distribution grid that connects directly to the houses in the community and provides power via fuel cell and heating via micro – central heat pump to the households. In this study, a village has been selected for assessment to determine the feasibility of implementing this kind of stand – alone connected hydrogen scheme. This is based on the obvious complexity in connecting the stated village to the national grid, and a possible means of providing the residents who rely mostly on firewood for cooking, with an efficient cooking option in hydrogen – cooking. This is not limited to the village considered in this study only, as it is just a representative of a prototype for adoption in several other areas in Nigeria.

7.4.2 Cooking Demand

In **chapter 6**, a cooking load for typical household in a Nigeria village has been calculated and presented. In this section, the calculated cooking load will be used to serve as representative for all the 171 households in the village. This was done by taking one household cooking demand and interpolating these 171 times. Ideally, it is difficult to predict the consumptions of various households and to model the varying characteristics of electrical load and cooking load, however, this variation was not taken into consideration in this current design. This is one of the problems encountered by engineers in modelling an energy system accurately. But it is useful in the early stages of energy system design, particularly, a renewable energy system to conduct this type of analytical feasibility study. Therefore, **Figure 139** depicts the daily cooking load data considered in the current design, as it was entered in SOHYSIMO. In the process, it was assumed that cooking demand for firewood and kerosene doubles in a week.

ENTER DAILY COOKING DEMAND DATA (7 - Days)							
	1	2	3	4	5	6	7
FIREWOOD (kg)	1783	3567	1783	1783	1783	3567	1783
CHARCOAL (kg)							
KEROSENE (L)	71	71	71	142	71	71	142

Figure 139. Cooking demand data.

7.4.3 Simulation Results

The data were entered and simulation was run, the average daily cooking load simulated was 231 kWh/day, and the daily average energy available from the cooker was 240 kWh/day. This averages at 1.35 kWh/day per household, but the cooking demand for each household is 1.4 kWh/day, which gives an excess of 0.05 kWh/day. **Figure 140** is a plot showing the energy available from the hydrogen cooker vs cooking demand. Cooker energy exceeded demand over the one year simulated, the energy from the cooker peaked at 408 kWh/day and the cooking load peaked at 313 kWh/day. There are days in which the cooker energy available surpassed demand, these can be stored energy for future use as shown. As previously explained, the excess energy available from the cooker (with respect to cooking demand per household) will be used to determine the hydrogen storage size while considering the cooker efficiency (70%). To determine the size of the storage system (or container/tank) required in cubic meter as previously explained, we start by converting kilogram hydrogen to cubic meter of hydrogen thus;

$$1 \text{ kg H}_2 = 11.13 \text{ m}^3 \text{ (gas at s.t.p) [35].}$$

$489 \text{ kg H}_2 = 11.13 \text{ m}^3/1 \text{ kg} \times 489 \text{ kg} = 5,443 \text{ m}^3$ to cover the whole year. Therefore, if this is stored at 30 bar pressure, perhaps with a pressurised electrolyser, it follows that the size of storage volume required is 181 m^3 . To compare this system to 2850 m^3 (largest size) hydrogen storage installed in HARI in West Beacon farm Leicester UK

discussed in **chapter 5**, at a low pressure (s.t.p) the storage volume obtained here is almost twice larger. Now, if the storage type and 137 bar pressure used in HARI is assumed, then, the storage volume will reduce to 40 m³. However, for this storage requirement, there are cost implications involved [36].

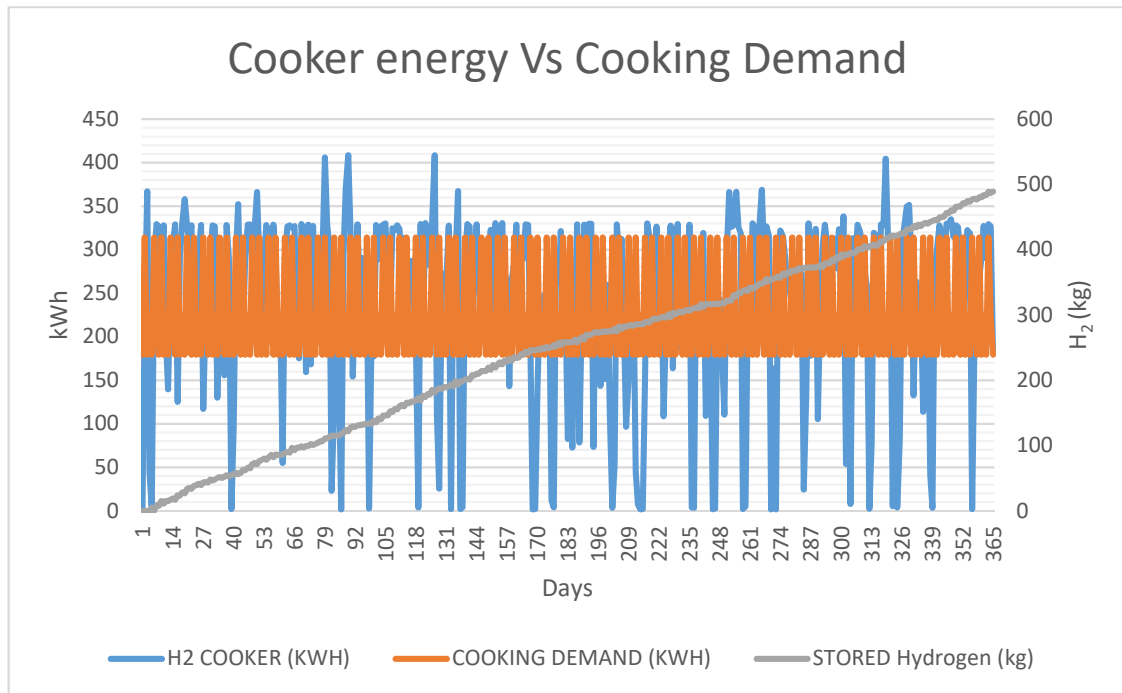


Figure 140. Graph of hydrogen cooker vs cooking demand.

Fortunately, SOHYSIMO has an algorithm which facilitates accumulation of unused hydrogen – energy content, this was utilised to determine the number of days in a month the cooker can provide 100 percent service and the days in which it declines. **Figure 141** shows the hydrogen cooker monthly performance per energy availability over the course of the year simulated. The cooker could not meet the cooking load for only 2 – day for January and 1 – day in December, while between July – September a 12 – days of cooker unavailability was found. This can be attributed to the months of rainy season as we head towards July, a period marked by poor solar PV operations. In other months, the cooker is supplied with enough energy to cover all days of cooking activities.

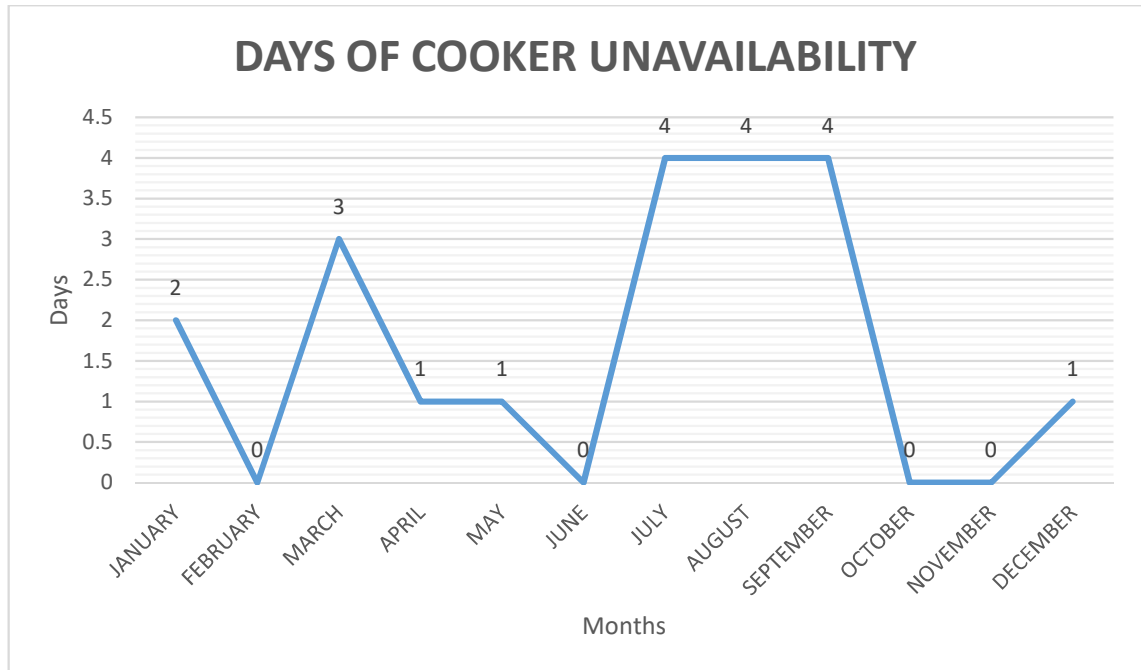


Figure 141. Hydrogen cooker days of energy unavailability.

7.4.4 Network architecture of the connected hydrogen village

Figure 142 shows a schematic representation of the solar – hydrogen DC micro grid network considered in this study for a clear illustration. A DC – DC boost converter will be implemented to step – up the solar PV voltage to 380V (in **Appendix 7E – K** a DC – DC converter has been simulated using Matlab/Simulink software), and act as maximum power point tracker to ensure optimum utilisation of the output power from the PV. This will be stepped down using cheap DC – DC bulk converter at the demand side. All residential homes will be connected to a common DC – bus, and control system ensures that energy from the PV is used to charge the battery and the battery will be discharged in the events when PV becomes un-operational, for example night time periods. At full battery state of charge, the control system will divert the excess PV output to electrolyser for hydrogen production. Produced hydrogen will be stored in a hydrogen pipe, and distributed to all interconnected residential homes, for cooking.

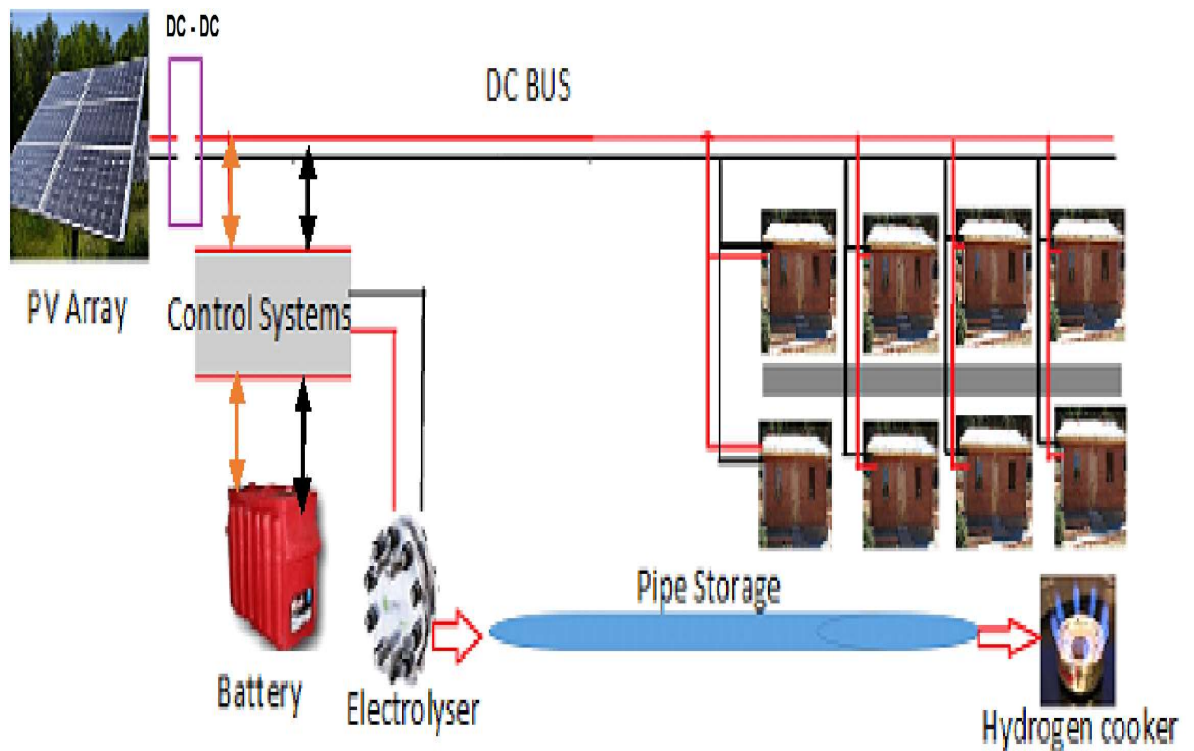


Figure 142. DC micro – grid network for interconnected hydrogen village.

Each home will be implemented with a hydrogen connection point for H₂-cooker. It was stated that hydrogen distribution pipeline has been constructed since the late 1930s [37], and the pipelines have generally operated at less than 68.9 bar with no safety concerns. In Europe, the existing hydrogen network is estimated at 1600 km while 900 km transmission pipelines exist in North America [38]. However, it can be stated that these are steel pipes which has the disadvantage of high cost. It has been estimated that a length of 80 km would cost about \$237,000/km [39]. The pipeline distribution system adopted in this research is the low-cost polymer fuel pipeline implemented in a community in New Zealand [29][40], though the cost of this pipeline was not stated, but according to them the total cost of the project was lower than the cost of grid connection in New Zealand at \$30,000/km (USD21,900/km) [41]. Therefore, for this study, distribution pipeline is assumed at \$20,000/km and a 2km length. **Table 48** lists the component costs used in the calculation. The PV cost was

assumed at \$1000/kW, all cost assumptions include balance of system (BOS). For electrolyser, future cost projections at \$435/kW was used at 15 years lifetime, based on the assumptions that the cost drops 43% from the current \$1000/kW as previously mentioned.

COMPONENTS	CAPITAL COSTS (\$)	O & M COSTS (\$/yr)	REPLACEMENT COSTS (\$)
Solar PV	400,000	0	0
Battery	150,000	150	150,000
Electrolyser	21,750	217	21,750
Pipe storage	40,000	0	0

Table 48. Summary of costs components used in the simulation.

Figure 143 shows the estimated costs of the connected solar hydrogen village. It was found that the project initial cost was \$ 612,300 and the Levelised Cost of Energy (LCOE) was \$0.26/kWh and the Net Present Cost (NPC) was \$ 718,525. The cost per kilogram of hydrogen produced by the electrolyser was \$6.95. In 2016, it was estimated that the cost per kilogram of hydrogen produced using solar generation was €6.65/kg [42] this is equivalent to \$7.6/kg at 1 Euro = 1.14 US dollar in 2017. This is slightly higher (8.6%) than the cost per kilogram H₂ (\$6.95/kg) obtained from this simulation, because of the future cost reductions as mentioned earlier. The initial project cost obtained for micro grid is 25.7% lower than the cost obtained in **chapter 6** at \$824,391, this is because different cost factors are considered (to reflect the cost variations in centralised distributed energy system as compared to individual stand – alone system) in the two scenarios. In the first scenario, the present cost of components and materials was considered, while the second scenario (connected hydrogen village) is based on assumptions for future cost projections. However, it should be noted that these costs calculations are based assumptions, as costs for real applications of a DC micro – grid that integrates hydrogen may differ, considering other technical factors it may involve.

DISPLAY COSTS	
Net Present Cost (\$)	718525
Project Initial Cost (\$)	612300
LCOE (\$/kWh)	0.255
PV Only (\$/kWh)	0.057
H2 (\$/kg)	6.95
PV with Battery Only (\$/kWh)	0.084

Figure 143. SOHYSIMO cost evaluation display showing the costs for the hydrogen village project.

7.5 Hydrogen Safety

As previously explained, hydrogen like other flammable fuels for example Liquefied Petroleum Gas (LPG) and gasoline has safety hazards associated with them. All that is required is just to handle these fuels with safety precautions and guidelines. However, the following are lists of hydrogen safety concerns;

- Wide flammability range (4% - 75% in air), this means that hydrogen is combustible at a very low ignition. However, at a low concentration, the energy required to initiate combustion is high similar to LPG and gasoline [36]. Hydrogen detection sensors can be used to control this.
- Hydrogen is an odourless and colourless gas, and this pose two potential risks as (i) it cannot be detected by human senses, hydrogen detection sensors can be implemented to help detect leaks (ii) it is nearly invisible when it burns in air.

7.5.1 Energising the Nation

Assuming, this same energy system is populated across the country, and the selecting villages at a significant distance to the grid from various local government areas. As presented in **chapter 2**, states with highest percentage of household without grid access across the six geopolitical zones in Nigeria has been selected, and given in **Table 49**. In chapter six, a village in Ebonyi state has been used as a case study, and if more villages are selected and the same energy system is implemented, this will reduce the number of villages with no grid access, and it will improve the percentage of total grid access in the state.

Geo-political zones	State	% without access
South East	Ebonyi State	60.7
South South	Bayelsa State	47.3
South West	Ondo State	33.7
North East	Taraba State	88.8
North Central	Benue	77.9
North West	Zamfara State	70.6

Table 49. Selection of states in six geopolitical zones with highest number that lack grid access.

Same could be said for other states with similar electricity situation as listed. Rural dwellers are predominantly low-income earners and would not afford the cost of diesel, and providing them with energy access using solar energy system will enhance their quality of life. To develop an electrification plan, it is essential that the population or the number of household that lack grid access is studied. Estimates, by the National Population Commission (NPC) [43] based on the 2006 census suggests the total Nigeria population in 2016 is over 193 million. This is given in **Table 50**, and the six states (Ebonyi, Bayelsa, Ondo, Taraba, Benue, and Zamfara) which currently has the highest number of households without electricity supply from the mainland grid are highlighted in yellow.

POPULATION FORECASTS 2006 - 2016											
STATE	2006	2007	2008	2009	2010	2011	2012	2013	2014	2015	2016
ABIA	2,845,380	2,923,252	3,003,255	3,085,447	3,169,889	3,256,642	3,345,769	3,437,336	3,531,408	3,628,055	3,727,347
ADAMAWA	3,178,950	3,272,489	3,368,781	3,467,906	3,569,948	3,674,992	3,783,127	3,894,444	4,009,037	4,127,001	4,248,436
AKWA/IBOM	3,902,051	4,037,002	4,176,620	4,321,067	4,470,509	4,625,120	4,785,078	4,950,568	5,121,781	5,298,916	5,482,177
ANAMBRA	4,177,828	4,296,460	4,418,461	4,543,926	4,672,954	4,805,646	4,942,106	5,082,440	5,226,760	5,375,177	5,527,809
BAUCHI	4,653,066	4,813,990	4,980,480	5,152,728	5,330,933	5,515,302	5,706,046	5,903,388	6,107,554	6,318,781	6,537,314
BAYELSA	1,704,515	1,754,670	1,806,300	1,859,450	1,914,163	1,970,487	2,028,468	2,088,154	2,149,597	2,212,849	2,277,961
BENUE	4,253,641	4,383,184	4,516,671	4,654,225	4,795,967	4,942,026	5,092,533	5,247,624	5,404,238	5,572,118	5,741,815
BORNO	4,171,104	4,315,360	4,464,605	4,619,012	4,778,758	4,944,030	5,115,017	5,291,918	5,474,937	5,664,285	5,860,183
CROSS RIVER	2,892,988	2,978,113	3,065,743	3,155,951	3,248,814	3,344,409	3,442,816	3,544,120	3,648,404	3,755,757	3,866,269
DELTA	4,112,445	4,246,171	4,384,246	4,526,811	4,674,012	4,825,999	4,982,928	5,144,961	5,312,262	5,485,004	5,663,362
EBONYI	2,176,947	2,238,763	2,302,334	2,367,710	2,434,943	2,504,085	2,575,190	2,648,315	2,723,515	2,800,851	2,880,383
EDO	3,233,366	3,321,856	3,412,768	3,506,168	3,602,124	3,700,706	3,801,987	3,906,039	4,012,938	4,122,764	4,235,595
EKITI	2,398,957	2,474,489	2,552,400	2,632,764	2,715,657	2,801,161	2,889,357	2,980,330	3,074,167	3,170,959	3,270,798
ENUGU	3,267,837	3,367,357	3,469,909	3,575,583	3,684,476	3,796,685	3,912,311	4,031,459	4,154,235	4,280,750	4,411,119
GOMBE	2,365,040	2,441,945	2,521,351	2,603,339	2,687,993	2,775,400	2,865,649	2,958,833	3,055,047	3,154,389	3,256,962
IMO	3,927,563	4,055,278	4,187,145	4,323,301	4,463,884	4,609,038	4,758,912	4,913,660	5,073,440	5,238,416	5,408,756
JIGAWA	4,361,002	4,489,323	4,621,419	4,757,403	4,897,387	5,041,491	5,189,835	5,342,543	5,499,746	5,661,573	5,828,163
KADUNA	6,113,503	6,299,687	6,491,541	6,689,238	6,892,955	7,102,877	7,319,192	7,542,095	7,771,785	8,008,472	8,252,366
KANO	9,401,288	9,716,706	10,042,707	10,379,645	10,727,888	11,087,814	11,459,817	11,844,300	12,241,682	12,652,397	13,076,892
KATSINA	5,801,584	5,978,269	6,160,334	6,347,944	6,541,268	6,740,479	6,945,757	7,157,287	7,375,259	7,599,869	7,831,319
KEBBI	3,256,541	3,359,075	3,464,837	3,573,929	3,686,456	3,802,526	3,922,250	4,045,745	4,173,127	4,304,520	4,440,050
KOGI	3,314,043	3,414,971	3,518,972	3,626,141	3,736,573	3,850,369	3,967,630	4,088,462	4,212,974	4,341,279	4,473,490
KWARA	2,365,353	2,437,389	2,511,618	2,588,108	2,666,928	2,748,148	2,831,842	2,918,084	3,006,953	3,098,528	3,192,893
LAGOS	9,113,605	9,409,957	9,715,945	10,031,883	10,358,095	10,694,915	11,042,686	11,401,767	11,772,524	12,155,337	12,550,598
NASARAWA	1,869,377	1,926,308	1,984,973	2,045,424	2,107,717	2,171,906	2,238,051	2,306,209	2,376,444	2,448,817	2,523,395
NIGER	3,954,772	4,091,546	4,233,051	4,379,449	4,530,911	4,687,610	4,849,730	5,017,456	5,190,982	5,370,510	5,556,247
OGUN	3,751,140	3,876,993	4,007,068	4,141,507	4,280,457	4,424,069	4,572,499	4,725,908	4,884,465	5,048,342	5,217,716
ONDO	3,460,877	3,566,276	3,674,886	3,786,803	3,902,128	4,020,965	4,143,422	4,269,608	4,399,637	4,533,626	4,671,695
OSUN	3,416,959	3,528,070	3,642,794	3,761,249	3,883,555	4,009,839	4,140,228	4,274,858	4,413,866	4,557,394	4,705,589
OYO	5,580,894	5,773,907	5,973,595	6,180,190	6,393,929	6,615,061	6,843,840	7,080,532	7,325,409	7,578,755	7,840,864
PLATEAU	3,206,531	3,294,287	3,384,444	3,477,069	3,572,229	3,669,993	3,770,432	3,873,621	3,979,633	4,088,547	4,200,442
RIVERS	5,198,716	5,378,512	5,564,525	5,756,972	5,956,075	6,162,063	6,375,176	6,595,659	6,823,767	7,059,764	7,303,924
SOKOTO	3,702,676	3,815,439	3,931,637	4,051,373	4,174,756	4,301,896	4,432,908	4,567,910	4,707,024	4,850,374	4,998,090
TARABA	2,294,800	2,362,324	2,431,834	2,503,390	2,577,051	2,652,880	2,730,940	2,811,296	2,894,018	2,979,173	3,066,834
YOBE	2,321,339	2,404,024	2,489,655	2,578,336	2,670,175	2,765,286	2,863,785	2,965,792	3,071,433	3,180,836	3,294,137
ZAMFARA	3,278,873	3,385,494	3,495,582	3,609,249	3,726,613	3,847,793	3,972,914	4,102,103	4,235,493	4,373,221	4,515,427
FCT ABUJA	1,406,239	1,543,293	1,693,706	1,858,777	2,039,937	2,238,752	2,456,945	2,696,403	2,959,199	3,247,608	3,564,126
NIGERIA	140,431,790	144,998,281	149,713,264	154,581,566	159,608,173	164,798,232	170,157,060	175,690,143	181,403,148	187,301,926	193,392,517

Table 50. Population forecast 2006 -2016 [43].

From this data, it is evident that states with poor grid access are those with the smallest populations. From this data and assuming 7 persons per household, then the total number of households with no grid access in 2016 is estimated as follows:

- Ebonyi state: 249,770 households
- Bayelsa state: 153,925 households
- Ondo state: 224,908 households
- Taraba state: 389,049 households
- Benue state: 638,932 households
- Zamfara state: 455,413 households
- **Total = 2,111,997 Households**

However, as presented in **chapter 6**, if it is assumed that each village in a state comprised of 171 households, it means the total number of villages that will be provided with solar – hydrogen energy system can be estimated thus;

- Ebonyi state: 1460 villages
- Bayelsa state: 900 villages
- Ondo state: 1315 villages
- Taraba state: 2275 villages
- Benue state: 3736 villages
- Zamfara state: 2663 villages

The solar energy density in these six states is presented in **Appendix 3**, and it shows that tremendous opportunities is available if solar energy projects is implemented in those states. The Federal Government targets is to provide electricity access to 39.6 million people by 2020, however, in future adopting a renewable energy system as presented in this thesis will be a viable option.

Selecting these villages across the six states with 2.1million households and giving them energy access via solar will go a long way to improve their quality of life.

7.6 Environmental Impact Assessment of Solar – Hydrogen Cooking

As highlighted in previous sections, the climatic consequences of greenhouse gas (GHG) emissions into the atmosphere has been recognised. The two main components that make up ‘Solar – Hydrogen Cooking’ are solar PV and hydrogen gas produced using an electrolyser, and these are free from emission concerns as already noted. The use of an energy – inefficient and unsustainable cooking stoves in the low and middle income rural areas of the developing countries has gross effect on the health and wellbeing of the people. Cooking and lighting with kerosene and/or firewood emits substantial amount of carbon – dioxide (CO_2), carbon mono – oxide (CO), sulphur oxide (SO_2), Nitrous –oxide (N_2O) and methane (CH_4) into the atmosphere. Often, the combustions are done indoors without chimneys, however, exposure to pollutions caused by these fuels have been associated with a range of health hazards [44].

In addition, the use of firewood for cooking in the rural areas has been shown to have significant environmental impact. Firewood used for cooking in these rural households are usually sourced from the forests and the adverse effect of this practice is deforestation. Deforestation means the perpetual termination or destruction of indigenous forests woodlands for economic or social advantage of serving human wood needs. This has huge consequences on global carbon cycle, and may lead to soil erosion. Forests are good storage reserve for carbon, as they take up carbon – dioxide from the atmosphere and thereby reducing the CO_2 concentration in the atmosphere. It has been estimated that about one-third of all CO_2 released into the atmosphere today is caused by deforestation [45]. Deforestation leads to extinction of species e.g. the wildlife that live on forests as habitat for survival. According to sources investigated [46], in 1990 the average annual deforestation rate in Nigeria stood at

2.68%, this was stated to have increased to 3.67% by 2010 [46]. However, due to the lack of accurate database, the current deforestation situation in Nigeria cannot be ascertained. From these available data, it can be inferred that, on average, deforestation increases at the rate of 0.50% in every 10 years, and 0.05% every year. Therefore, by using these numbers it can be calculated that, in 2017, the average annual deforestation rate in Nigeria will be around 3.9%. The negative impacts of dependence on firewood for cooking is not limited to deforestation alone, as this is also associated with the emission of carbon – monoxide into the atmosphere [47]. A study in Nigeria, has suggested that using these fuels for cooking causes respiratory diseases, especially in the households in rural areas, who rely on wood fuel and kerosene for cooking [48].

7.6.1 Carbon Emission Reductions

Now, to compare the benefits of providing the rural households with a sustainable means of cooking; for example, a village consisting of 171 (7 -persons) households. This means that about 1,200 people will be saved from respiratory diseases (lungs). As previously stated, for kerosene consumption, each household would consume approximately 16 litres (equivalent to 3.5 gallons at 0.54 litre per day, by averaging the 7 – day cooking load) per month. According to reports, the CO₂ emission factor for kerosene burned is 2.61kg per litre [49]. Similarly, for other green – house gases e.g. N₂O and CH₄, the emission factors for kerosene are 0.0731kg/L and 0.0183kg/L respectively. GHG emissions is calculated as a product of the amount of fuel, its energy density and the emission factor. A study in Nigeria has shown that the firewood emission factors for GHG; CO, N₂O and SO₂ are 181.84g/kg, 44.7g/kg and 9.87g/kg respectively. To calculate the GHG emission savings from these unsustainable fuels, we consider the quantity of kerosene and firewood burned per household per village. In **section 7.4.2**, it was shown that the daily firewood and kerosene requirements for cooking in Okenkwu village are 1783 kg and 71L respectively, and these doubles per week. Therefore, the average daily firewood and kerosene consumption will be

2,293kg (16,048/7) and 91.3L (639/7) respectively. This translates to 68,790kg firewood and 2,739L kerosene per month or 836,945kg firewood and 33,690L kerosene per year. With the emission factors, we obtain the GHG emission savings from these fuels as follows:

Firewood

12,509kgCO/month or 152,156kgCO/year

3,075kgN₂O/month or 37,411kgN₂O/year

679kgSO₂/month or 8,260kgSO₂/year

Kerosene

200kgN₂O/month or 2,463kgN₂O/year

50kgCH₄/month or 617kgCH₄/year.

For over a 25 – years lifetime of the solar – hydrogen system, reduction in the use of kerosene and firewood will save;

Firewood: 3.8ktCO, 0.94ktN₂O, 0.22ktSO₂

Kerosene: 61,575kgN₂O, 15,425kgCH₄.

However, if the whole country is considered, based on the states with poor grid access as highlighted in **section 7.5.1**. The GHG emission reductions is shown in **Table 51**

States	Number of villages	Firewood (ktGHG)savings/year	Kerosene (ktGHG)savings/year
Ebonyi	1460	222.14CO, 54.6N ₂ O, 12.1SO ₂	3.59N ₂ O, 0.9CH ₄
Bayelsa	900	136.9CO, 33.7N ₂ O, 7.43SO ₂	2.24N ₂ O, 0.56CH ₄
Ondo	1315	200CO, 49.2N ₂ O, 10.8SO ₂	3.24N ₂ O, 0.81CH ₄
Taraba	2275	347CO, 85.11N ₂ O, 18.8SO ₂	5.6N ₂ O, 1.4CH ₄
Benue	3736	568.5CO, 139.8N ₂ O, 30.86SO ₂	9.2N ₂ O, 2.31CH ₄
Zamfara	2663	405.2CO, 99.6N ₂ O, 21.9SO ₂	6.56N ₂ O, 1.64CH ₄

Table 51. Estimated emission savings by selected states if supplied with solar – hydrogen energy system.

There is also an opportunity to attract free or subsidised solar – hydrogen projects to these rural areas through carbon trading via Carbon Development Mechanism (CDM). As defined by UNFCCC, CDM is a scheme whereby countries (countries listed as high emitters) with an emission-reduction commitment are saddled with the responsibility to implement emission reduction project in the developing countries [50]. Several implementations of such project are available in various scales in Nigeria [51].

7. References

1. DC microgrids and the virtues of local electricity, IEEE online available at <http://spectrum.ieee.org/green-tech/buildings/dc-microgrids-and-the-virtues-of-local-electricity> accessed on 10/01/2017.
2. Online available at <https://learn.sparkfun.com/tutorials/alternating-current-ac-vs-direct-current-dc> accessed on 10/01/2017.
3. Bose, B.K., 2009. Power electronics and motor drives recent progress and perspective. IEEE Transactions on Industrial Electronics, 56(2), pp.581-588.
4. Acha, E., Agelidis, V., Anaya, O. and Miller, T.J.E., 2001. Power electronic control in electrical systems. Elsevier.
5. Lasseter, R.H., 2002. Microgrids. In Power Engineering Society Winter Meeting, 2002. IEEE (Vol. 1, pp. 305-308). IEEE.
6. Ito, Y., Zhongqing, Y. and Akagi, H., 2004, August. DC microgrid based distribution power generation system. In Power Electronics and Motion Control Conference, 2004. IPEMC 2004. The 4th International (Vol. 3, pp. 1740-1745). IEEE.
7. Madduri, P.A., Poon, J., Rosa, J., Podolsky, M., Brewer, E. and Sanders, S., 2015, March. A scalable dc microgrid architecture for rural electrification in emerging regions. In 2015 IEEE Applied Power Electronics Conference and Exposition (APEC) (pp. 703-708). IEEE.
8. Elsayed, A.T., Mohamed, A.A. and Mohammed, O.A., 2015. DC microgrids and distribution systems: An overview. Electric Power Systems Research, 119, pp.407-417.
9. M. Sechilariu., F. Locment., 2016. Urban DC Microgrid 1st Edition Intelligent Control and Power Flow Optimization, Elsevier.
10. EMerge Contributes to 1st IEC LVDC Conference on Sustainable Electricity Access (2017); online available at <http://www.prweb.com/releases/2017/03/prweb14117613.htm> accessed on 09/07/2017.

11. Du, P., Baldick, R. and Tuohy, A. eds., 2017. Integration of Large Scale Renewable Energy into Bulk Power Systems: From Planning to Operation. Springer.
12. Zhang, F. Economic and market analysis of DC microgrid with photovoltaic; a case study from Xiamen University DC microgrid: online available at <http://microgrid-symposiums.org/wp-content/uploads/2015/09/10-Zhang-Economic-Market-Analysis-20150818.pdf> accessed on 08/072017.
13. Zhang, F., Meng, C., Yang, Y., Sun, C., Ji, C., Chen, Y., Wei, W., Qiu, H. and Yang, G., 2015, June. Advantages and challenges of DC microgrid for commercial building a case study from Xiamen university DC microgrid. In DC Microgrids (ICDCM), 2015 IEEE First International Conference on (pp. 355-358). IEEE.
14. APEC project database; Online available at <https://aimp2.apec.org/sites/PDB/Lists/Proposals/DispForm.aspx?ID=1864> accessed on 08/07/2017.
15. Mohan, N. and Undeland, T.M., 1995. Power electronics: converters, applications, and design. John Wiley & Sons.
16. Zhao, L. and Qian, J., 2006. DC-DC power conversions and system design considerations for battery operated system. In Texas Instrument Seminar. (May 2006). [Online]. Available: www. ti. com.
17. Microchip Portable Power Conversion Design Guide.
18. Rashid, M.H., 2010. Power electronics handbook: devices, circuits and applications. Academic press.
19. Emerge Alliance; online available at <http://www.emergealliance.org/Standards/OccupiedSpace/Overview.aspx> accessed on 09/07/2017.
20. Backhaus, S.N., Swift, G.W., Chatzivasileiadis, S., Tschudi, W., Glover, S., Starke, M., Wang, J., Yue, M. and Hammerstrom, D., 2015. *DC Microgrids Scoping Study. Estimate of Technical and Economic Benefits* (No. LA-UR--15-22097). Los Alamos National Lab.(LANL), Los Alamos, NM (United States).
21. Online available at http://www.esventura.com/manuals/sola_introNECclass2_rg.pdf.

22. Karabiber, A., Keles, C., Kaygusuz, A., Alagoz, B.B. and Akcin, M., Power Converters Modeling in Matlab/Simulink for Microgrid Simulations.
23. Alfares, H.K. and Nazeeruddin, M., 2002. Electric load forecasting: literature survey and classification of methods. *International Journal of Systems Science*, 33(1), pp.23-34.
24. Heshmati, A., 2012. Survey of models on demand, customer base-line and demand response and their relationships in the power market.
25. Balachandra, P. and Chandru, V., 1999. Modelling electricity demand with representative load curves. *Energy*, 24(3), pp.219-230.
26. Reiss, P.C. and White, M.W., 2005. Household electricity demand, revisited. *The Review of Economic Studies*, 72(3), pp.853-883
27. Adeoti, O., Oyewole, B.A. and Adegboyega, T.D., 2001. Solar photovoltaic-based home electrification system for rural development in Nigeria: domestic load assessment. *Renewable energy*, 24(1), pp.155-161.
28. Kolhe, M.L., Ranaweera, K.I.U. and Gunawardana, A.S., 2015. Techno-economic sizing of off-grid hybrid renewable energy system for rural electrification in Sri Lanka. *Sustainable Energy Technologies and Assessments*, 11, pp.53-64.
29. Gardiner, A.I., Pilbrow, E.N., Broome, S.R., McPherson, A.E., 2008. HYLINK – A renewable distributed energy application for hydrogen. 3rd International Solar Energy Society Conference – Asia Pacific Region (ISES-AP-08) Incorporating the 46th ANZSES Conference.
30. Saetre, T. ed., 2013. *Hydrogen Power: Theoretical and Engineering Solutions: Proceedings of the Hypothesis II Symposium Held in Grimstad, Norway, 18-22 August 1997*. Springer Science & Business Media.
31. Scott, K., 2017. *Sustainable and Green Electrochemical Science and Technology*. John Wiley & Sons.
32. Aki, H., Taniguchi, Y., Kondoh, J., Tamura, I., Kegasa, A., Ishikawa, Y., Yamamoto, S. and Sugimoto, I., 2008. The operation result of the demonstration of energy networks of electricity, heat, and hydrogen at an apartment building in 2007. *Proceedings of the 2008 ACEEE Summer Study on Energy Efficiency in Buildings*, pp.1-11
33. Online available at <http://www.hylink.co.nz/> accessed on 08/07/2017.

34. Nakajima, T. and Groult, H. eds., 2015. Advanced Fluoride-Based Materials for Energy Conversion. Elsevier.
35. Barthelemy, H., Weber, M. and Barbier, F., 2017. Hydrogen storage: Recent improvements and industrial perspectives. International Journal of Hydrogen Energy, 42(11), pp.7254-7262.
36. Online available at <https://h2tools.org/bestpractices/h2properties> accessed on 09/06/2017.
37. Barthelemy, H., Weber, M. and Barbier, F., 2017. Hydrogen storage: Recent improvements and industrial perspectives. International Journal of Hydrogen Energy, 42(11), pp.7254-7262.
38. Online available http://corridoreis.anl.gov/documents/docs/technical/APT_61012_EVS_TM_08_2.pdf accessed on 09/06/2017.
39. Léon, A. ed., 2008. Hydrogen technology: mobile and portable applications. Springer Science & Business Media.
40. Online available at <http://www.nrel.gov/docs/fy99osti/25106.pdf> accessed on 10/06/2017.
41. Online available at http://www.iphe.net/docs/Renew_H2_HYLINK.pdf accessed on 10/06/2017.
42. Nicoletti, G., Bruno, R., Arcuri, N. and Nicoletti, G., 2016. Real costs assessment of solar-hydrogen and some fossil fuels by means of a combustion analysis. Journal of Combustion, 2016.
43. Online available at <http://www.nigerianstat.gov.ng/> accessed on 09/04/2017.
44. Lam, N.L., Smith, K.R., Gauthier, A. and Bates, M.N., 2012. Kerosene: a review of household uses and their hazards in low-and middle-income countries. Journal of Toxicology and Environmental Health, Part B, 15(6), pp.396-432.
45. M.P Mishra (2009) ICSE environmental education, class x. S.Chand publishers New Delhi.
46. B. Garba (2010), Energy Commission of Nigeria. Renewable Energy for Rural Industrialization and Development in Nigeria.

47. Dary, O., Pineda, O. and Belizán, J.M., 1981. Carbon monoxide contamination in dwellings in poor rural areas of Guatemala. *Bulletin of Environmental Contamination and Toxicology*, 26(1), pp.24-30.
48. Adeniji, B.A., Ana, G.R.E.E., Adedokun, B.O. and Ige, O.I., 2015. Exposure to Emissions from Kerosene Cooking Stoves and the Pulmonary Health Status of Women in Olorunda Community, Ibadan, Nigeria. *Journal of Environmental Protection*, 6(05), p.435.
49. Schäfer, M., Kebir, N. and Philipp, D., 2013. *Micro Perspectives for Decentralized Energy Supply*. Universitätsverlag der TU Berlin.
50. Online available at http://unfccc.int/kyoto_protocol/mechanisms/clean_development_mechanism/items/2718.php. Accessed on 01/09/2017.
51. Online available at <http://climatechange.gov.ng/division/mitigation/cdm/registered-cdm-projects-in-nigeria/> accessed on 02/09/2017.
52. Online available at <http://www.ni.com/tutorial/14678/en/> accessed on 11/02/2017.
53. Online available at <http://www.powere.dynamictopway.com/dc7.htm> accessed on 17/03/2017.
54. Wang, D., Deng, Y., Wu, J. and He, X., 2008, November. ZVT interleaved boost converter with intrinsic voltage-doubler characteristic. In *Industrial Electronics, 2008. IECON 2008. 34th Annual Conference of IEEE* (pp. 2371-2377). IEEE.
55. [Matlab: online available at <https://uk.mathworks.com/help/physmod/sps/powersys/ref/mosfet.html;jsessionid=ed14e2c4cee78a5d9f8139616402> accessed on 10/02/2017.
56. Online available at https://uk.mathworks.com/help/physmod/sps/powersys/ref/idealswitch.html?s_tid=srchtitle accessed on 13/02/2017.
57. Online available at <https://uk.mathworks.com/help/physmod/sps/powersys/ug/simulating-with-continuous-integration-algorithms.html> accessed on 10/02/2017.

8.0 Conclusions and Recommendations for Future Work

8.1 Conclusions

It has been shown that there is a great opportunity in generating electricity from the renewable sources, especially when it is properly sized. It has also been shown that excess energy that will be generated can be made more useful and efficient if it is used to produce hydrogen, and the hydrogen produced be utilised for domestic cooking rather than increased storage. Solar – hydrogen energy system could be a viable option for the future, and this kind of scheme can be adopted for power access in those remote areas with no grid connection. Though this scheme is not limited to off-grid energy systems, it can still be integrated into an existing grid to boost energy harnessing. As an example, as it is a known fact that renewable power is an unpredictable energy source, integrating a hydrogen storage to a power source that has a fluctuating input in renewable energy sources, will enhance the productivity of the energy system. As the Federal Government of Nigeria has proposed to integrate renewable power sources e.g solar into the energy mix, however, it is advisable to include a portable energy storage system like hydrogen to effectively utilise the abundance solar resource. This study has shown that over-dimensioning of renewable energy system such as solar PV, which is advisable due to its variable nature, mostly results to an excess power, and a hydrogen storage system is particularly suitable for a location with little or no variation of day length, such as in Nigeria. Sequel to this, the rainy season has been found to have a little impact on the performance of the system.

This thesis has unearthed new innovative potentials for improving the off grid solar energy system and comprised of 7 chapters; **chapter 1** presented a concise introduction to the research, and gave insight into the questions addressed and the aim and objectives of the project. **Chapter 2** presented a comprehensive review of the energy situation in Nigeria, and chronicles the key indicators that makes energy access a

prerequisite for enhanced livelihood. It was found that currently, Nigeria is faced with huge energy challenges. This led to a review of some alternative means of providing instant energy access to the low – income communities, and presents the concentrations of various renewable energy resources available in the country. Nigeria is blessed with abundance renewable energy resources, which could be exploited for the benefit of those areas currently with no electricity access. Moreover, the irony is while the cost of fossil fuelled energy sources is increasing the cost per watt of renewable energy sources especially solar is decreasing. It has been justified why access to affordable energy is an entitlement for everyone. **Chapter 3** discussed state of the art energy storage system, and examined the opportunities available in each system, and based on this presents the storage system that matches the focus of this study. There are considerations based on suitability when it comes to making a choice on which energy storage system to utilise in renewable energy system applications, in future hydrogen will be particularly suitable for these systems as it can offer two pathway solutions in seasonal and short term.

However, hydrogen storage was adopted in this research for this reason and others. In **Chapter 4** the renewable energy data logging system designed and constructed by the author of this thesis was presented. The system installation and analysis of the real data obtained from the energy with storage system. From this, the internal resistance of the battery was determined based on the various system performances analysed. Also, the energy analysis of a data set obtained from a solar power system installed in Nigeria was presented. In **Chapter 5** a new software tool developed in this research was introduced, it started with the general overview of the model, and gave a comprehensive explanation on various aspects of the tool. Operating and maintenance cost is an important factor in every renewable energy based projects, a novel method for calculating this has been developed and incorporated into the model to obtain an optimal design of a solar PV-hydrogen project. A study of an existing renewable energy system was presented, and based on this, the validations of the software model was made. The developed tool contains a hydrogen cooking feature which is non-existent in other tools, it has been shown the importance of this for the developing countries,

especially the rural dwellers. The validations of this model using three different methods was shown to have effectively enhanced its simulation capability.

Chapter 6 described a case study where the developed tool was utilised to model a solar – hydrogen system for a typical village in Nigeria. It has been demonstrated that unlike other tools the developed tool goes beyond the realm of electrical load and includes a hydrogen cooking load facility, as an efficient means of utilising the hydrogen produced. Different system configurations were tested, and to fully satisfy both the electric load and cooking demand, an enhanced cooking optimisation facility in SOHYSIMO was utilised, to obtain the optimal configurations. A rural household in Nigeria has been used to evaluate the tool. It was found that 1.53 kW solar photovoltaic module, 0.4kW electrolyser and 3.7 kWh battery would be enough to provide steady 24-hour supply for a modest daily energy demand of 2.2 kWh. A prospect of harnessing an excess energy on clear weather conditions and utilising it to produce hydrogen has been achieved. In the results, the PV generated 1924 kWh/yr of energy and the 0.4 kW electrolyser produced a total of 11 kg/yr of hydrogen with excess energy realised. This was used in a H₂-cooker which produced an average of 1.35 kWh/day and covered the estimated 1.4 kWh/day cooking demand of the household over a year period simulated, with only 3 – days shortage. For Nigeria to achieve its 2030 energy target, it was shown that adopting this type of energy system is crucial especially for the inaccessible locations.

Though the cost may be higher at US\$824,391 per village, but when implemented the project will last for approximately 25 years. **Chapter 7** introduced a case study for utilising a DC – micro grid for energy access in a typical village in Nigeria. This is presented in this thesis as a notional case study for future consideration. However, as it is obvious that most domestic (household) appliances are inherently DC devices, however, it is also possible that other few AC dependent appliances may be connected to the power system using an individual DC - AC inverter. The hydrogen system considered in this thesis does not take into account detailed technical involvement of how the hydrogen will be stored, however, this is one of the challenges faced by the hydrogen economy. Metal hydride storage presents better future opportunity, but there is a problem of cost and availability of the storage materials. But as per this work, metal

hydride storage may not be a better option due to unavailability of heat source that is required in the desorption process, waste heat from fuel cell may be used for the hydrogen desorption process in systems that integrate fuel cell. A hydrogen pipeline was investigated, and it was found that for a connected hydrogen village based on storage pressure considerations, a 181 m³ or 40 m³ storage size will be required, the storage size was calculated based on the excess energy above the cooking demand, and the initial cost of the project was \$612,300 and the electrolyser produced hydrogen at \$6.95/kg. This research has proved that the developed software will be useful for renewable energy system designers interested in this kind of applications. Also, an energy system involving the H₂-genset was not simulated, but this has the capacity to increase energy utilisation in the household. Environmental impact analysis was done, through the sustainable energy supply system derived from the developed model. It was shown that significant GHG emission savings will be realised, by replacing the current unsustainable fuels like kerosene and firewood with a solar based hydrogen energy system is implemented in selected villages in the country.

8.2 Recommendations for Future Work

Points unearthed in this research for future study are as follows;

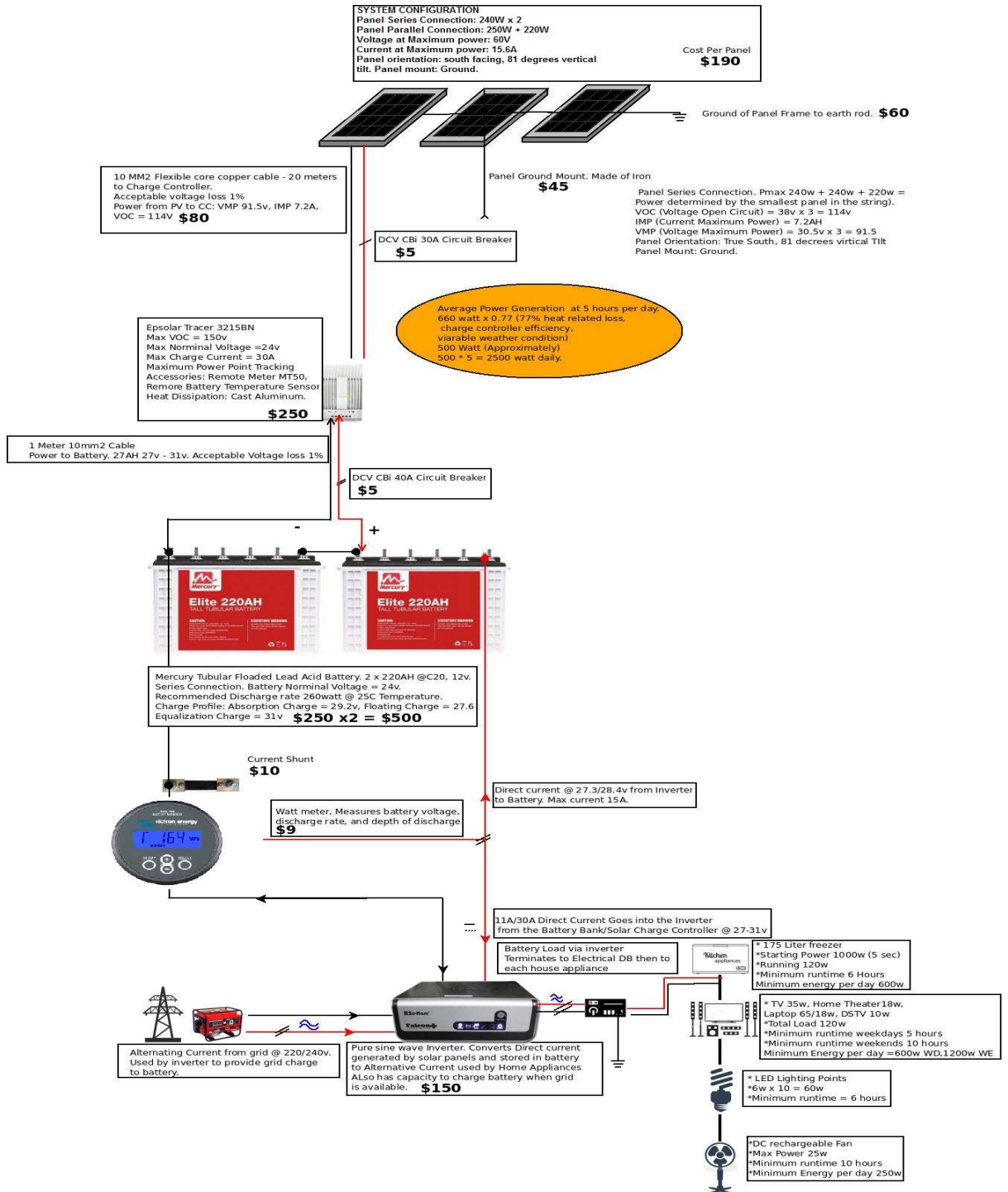
1. The cost of solar – hydrogen system is on high – side and this means that Government incentives is needed for its uptake.
2. The limitations of utilising software models for solar – hydrogen energy systems designs are the inherent variations and unpredictability of the solar resource, particularly the cloudy weather conditions.
3. It is important that solar - hydrogen demonstration prototypes which integrates a hydrogen cooking system be established, this is almost scarce now and needed to be addressed.
4. Hydrogen storage considered in this work did not include the miscellaneous cost implications and technicalities of the storage components of the system, this need to be improved in future studies.

5. DC micro-grid system is an emerging research subject, governments funding and support is needed to facilitate research demonstrations of DC micro – grid on various scales.
6. Research is needed to identify suitable odorants and colorants that will be added to hydrogen as currently done in the case of natural gas, so it can easily be detected by human senses, as well as being visible to human eye. This will help reduce the public apprehension on hydrogen and may eventually lead to its acceptability.

In future models, the simulation capability of the developed software tool may be enhanced by including one or more renewable energy source, e.g. wind, and the solar radiation model may also be improved by adding a facility that can enable a user to access irradiation data via the internet; e.g. the NASA real time solar data. Future versions of SOHYSIMO will address the need for more sophisticated load modelling on a village scale, and consider the trade-offs between component sizing and meeting of the cooking load in more depth.

APPENDIX

Appendix 1. Kuje Solar Project Schematic



Appendix 2: Panasonic HIT 240 W Photovoltaic module (VBHN240SA06) specifications

HIT Power 240S

Electrical Specifications

Model	HIT Power 240S or VBHN240SA06
Rated Power (P _{max}) ¹	240 W
Maximum Power Voltage (V _{pm})	43.7 V
Maximum Power Current (I _{pm})	5.51 A
Open Circuit Voltage (V _{oc})	52.4 V
Short Circuit Current (I _{sc})	5.85 A
Temperature Coefficient (P _{max})	-0.30%/°C
Temperature Coefficient (V _{oc})	-0.126 V/°C
Temperature Coefficient (I _{sc})	1.76 mA/°C
NOCT	118.9°F (48.3°C)
CEC PTC Rating	223.5 W
Cell Efficiency	21.6%
Module Efficiency	19.0%
Watts per Ft. ²	17.70 W
Maximum System Voltage	600 V
Series Fuse Rating	15 A
Warranted Tolerance (-/+)	-0% / +10%

Mechanical Specifications

Internal Bypass Diodes	3 Bypass Diodes
Module Area	13.56 Ft ² (1.26m ²)
Weight	33.1 Lbs. (15kg)
Dimensions LxWxH	62.2x31.4x1.4 in. (1580x798x35 mm)
Cable Length +Male-/Female	40.55/34.64 in. (1030/880 mm)
Cable Size / Type	No. 12 AWG / PV Cable
Connector Type ³	Multi-Contact [®] Type IV (MC4 [™])
Static Wind / Snow Load	50 PSF (2,400 Pa)
Pallet Dimensions LxWxH	63.2x32x.65 in. (1607x815x1650 mm)
Quantity per Pallet / Pallet Weight	40 pcs./1388.9 Lbs (630 kg)
Quantity per 40' Container	560 pcs.
Quantity per 20' Container	280 pcs.

Operating Conditions & Safety Ratings

Ambient Operating Temperature ²	-4°F to 115°F (-20°C to 46°C)
Hail Safety Impact Velocity	1" hailstone (25mm) at 52 mph (23m/s)
Fire Safety Classification	Class C
Safety & Rating Certifications	UL 1703, cUL, CEC
Limited Warranty	10 Years Workmanship, 20 Years Power Output

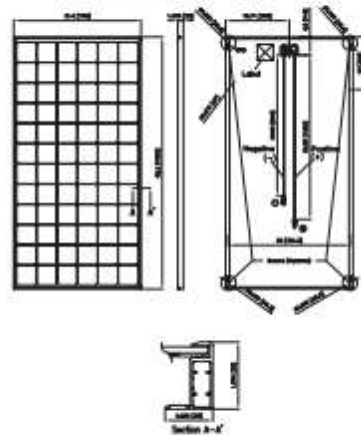
¹ STC: Cell temp. 25°C, AM 1.5, 1000W/m²

² Monthly average low and high of the installation site.

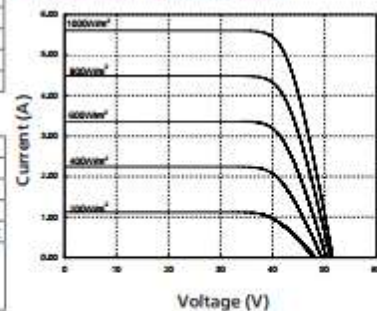
Note: Specifications and information above may change without notice.

³ Safety locking clip (PV-SSH4) is not supplied with the module.

Dimensions and Weight



Dependence on Irradiance



HIT is a registered trademark of Panasonic Group. The name "HIT" comes from "Heterojunction with intrinsic Thin-layer" which is an original technology of Panasonic Group.

Appendix 3: Daily Solar Resource at Zamfara, Ebonyi, Benue, Taraba, Ondo and Bayelsa

Days	Zamfara (W/m ²)	Ebonyi (W/m ²)	Benue (W/m ²)	Taraba (W/m ²)	Ondo (W/m ²)	Bayelsa (W/m ²)
1	1587.92	949.54	1200.6	931.69	931.69	780.03
2	5996.68	5971.34	6108.59	5964.07	5964.07	5756.77
3	7034.36	7494.31	7454.86	7447.12	7447.12	7476.29
4	2465.5	1565.76	1959.02	1529.17	1529.17	1276.84
5	2432.46	1511.26	1857.68	1501.13	1501.13	1270.73
6	7005.2	7492.75	7442.38	7442.59	7442.59	7493.44
7	6249.98	6411.4	6479.25	6388.12	6388.12	6281.37
8	6254.65	6443.74	6526.85	6390.93	6390.93	6302.81
9	6553.74	6763.78	6813.03	6742.71	6742.71	6646.03
10	6322.6	6537.83	6602.62	6482.92	6482.92	6425.65
11	4045.85	2882.92	3445.37	2866.78	2866.78	2398.5
12	3757.45	2526.17	3099.46	2478.91	2478.91	2086.6
13	6002.54	5911.59	6125.25	5853.91	5853.91	5619.68
14	4518.99	3862.7	4272.02	3832.24	3832.24	3414.11
15	6486.7	6696.14	6780.39	6629.06	6629.06	6559.51
16	3444.29	2508.95	3032.13	2433.86	2433.86	2037
17	6906	7298.97	7273.52	7256.92	7256.92	7282.22
18	7109.05	7478.09	7475.5	7430.11	7430.11	7427.54
19	6932.64	7323.38	7318.17	7258.59	7258.59	7287.07
20	7144.42	7580.05	7565.97	7505.02	7505.02	7548.15
21	5918.29	5663.32	5940.18	5616.62	5616.62	5303.35
22	6409.78	6538.62	6612.42	6502.03	6502.03	6399.76
23	4971.99	3663.72	4295.58	3667.85	3667.85	3093.75
24	5006.89	3326.67	4036.56	3323.61	3323.61	2771.15
25	5853.44	5571.23	5872.57	5506.1	5506.1	5205.77
26	7307.88	7667.15	7661.79	7620.76	7620.76	7615.24
27	3510.36	2249.84	2755.1	2251.7	2251.7	1866.38
28	5143.7	4136.1	4686.69	4132.08	4132.08	3550.85

29	4237.19	3006.15	3599.33	2997.06	2997.06	2480.98
30	6672.29	6781.22	6881.26	6734.18	6734.18	6635.41
31	5816.58	5556.24	5834.05	5486.97	5486.97	5217.99
32	6951.76	6869.42	6998.62	6870.63	6870.63	6751.49
33	3877.11	2279.54	2846.91	2363.7	2363.7	1903.43
34	5053.57	3485.84	4176.72	3526.55	3526.55	2980.87
35	5627.15	4925.37	5266.09	4958.35	4958.35	4635.97
36	5081.44	3432.75	4127.43	3480.8	3480.8	2938.67
37	7244.86	7413.34	7449.39	7359.94	7359.94	7401.57
38	6924.09	6660.36	6883.59	6661.57	6661.57	6457.62
39	1968.13	895.5	1145.11	901.88	901.88	780.07
40	4035.2	2122.29	2724.97	2163.88	2163.88	1782.99
41	6968.01	7100.79	7105.15	7070	7070	7132.21
42	6758.64	5769.3	6271.92	5836.88	5836.88	5319.46
43	5434.44	4101.81	4673.86	4179.7	4179.7	3628.9
44	4565.76	2356.31	2978.77	2419.97	2419.97	2015.74
45	6899.89	6471.83	6727.72	6500.72	6500.72	6228.22
46	7097.72	7139.74	7203.24	7102.43	7102.43	7120.5
47	7544.26	7780.9	7768.86	7719.45	7719.45	7828.91
48	7530.43	7754.02	7727.84	7713.26	7713.26	7815.92
49	6955.94	6083.48	6538.23	6150.43	6150.43	5658.13
50	7290.93	7382.54	7426.29	7320.68	7320.68	7373.33
51	6793.12	6348.54	6611	6349.86	6349.86	6117.18
52	5524.19	3903.91	4614.99	3947.99	3947.99	3360.27
53	6375.08	5020.07	5649.55	5089.66	5089.66	4485.06
54	6227.78	5228.04	5721.42	5249.83	5249.83	4794.55
55	6589.98	5770.58	6180.45	5806.97	5806.97	5395.4
56	5819.54	4090.52	4783.2	4198.17	4198.17	3571.83
57	7545.88	7076.78	7358.71	7103.17	7103.17	6797.68
58	6145.37	4791.12	5396.97	4869.01	4869.01	4284.32
59	4156.05	2365.24	3001.54	2441.41	2441.41	1924.46

60	5625.96	3765.65	4697.94	4008.52	4008.52	3500.62
61	3180.31	1638.27	2261.31	1719.17	1719.17	1487.67
62	7031.57	6731.88	6969.77	6778.14	6778.14	6672.9
63	6637.07	6016.08	6418.8	6106.04	6106.04	5887.06
64	6739.31	6289.29	6579.31	6367.12	6367.12	6212.95
65	7191.97	6755.21	7096.58	6802.39	6802.39	6637.39
66	7887.38	7832.04	7951.1	7838.58	7838.58	7811.32
67	6420.65	4628.8	5658.48	4795.16	4795.16	4281.03
68	4416.04	2415.42	3222.05	2570.83	2570.83	2217.89
69	7636.77	7514.96	7652.48	7529.37	7529.37	7487.48
70	6693.09	5850.69	6414.44	5915.9	5915.9	5637.7
71	4852.74	3000.08	3929.7	3176.3	3176.3	2715.5
72	7081.97	6502.11	6869.81	6583.49	6583.49	6384.96
73	5009.69	3260.45	4093.32	3490.39	3490.39	3011.44
74	7262.8	6846.74	7106.17	6906.73	6906.73	6761.46
75	5770.69	3992.39	4944.11	4187.6	4187.6	3675.24
76	7130.35	5936.66	6655.13	6096.08	6096.08	5665.37
77	6519.25	5306.05	6043.03	5424.35	5424.35	5017.68
78	7250.81	6310.91	6928.74	6382.16	6382.16	6051.22
79	7884.47	7663.69	7836.72	7675.45	7675.45	7603.82
80	7762.36	7538.02	7676.31	7575.45	7575.45	7501.42
81	5265.8	3205.26	4210.21	3362.21	3362.21	2899.04
82	3309.99	1636.49	2264.45	1726.94	1726.94	1482.28
83	4735.53	2659.56	3585.01	2853.42	2853.42	2401.57
84	5917.01	4117.94	5073.72	4273.32	4273.32	3790.56
85	4715.91	2615.14	3549.23	2797.39	2797.39	2353.51
86	1395.65	713.84	934.79	736.87	736.87	665.17
87	7945.92	7515.66	7764.23	7579.17	7579.17	7411.87
88	7943.17	7678.86	7819.7	7712.47	7712.47	7632.07
89	7655.92	7112.59	7420.66	7169.95	7169.95	6983.3
90	7185.21	6289.13	6783.22	6400.67	6400.67	6086.7

91	5049.2	2389.89	3166.45	2654.25	2654.25	2190.56
92	5960.49	3760.5	4625.52	4122.13	4122.13	3477.59
93	7358.9	6447.39	6822.92	6591.12	6591.12	6298.67
94	6259.6	4073.45	4877.18	4468.77	4468.77	3825.59
95	7179.32	6377.48	6650.39	6499	6499	6279.47
96	4798.19	2790.9	3492.92	3030.17	3030.17	2547.9
97	6415.83	4262.28	5141.37	4609.34	4609.34	3955.99
98	2613.54	978.06	1327.74	1109.19	1109.19	901.5
99	6471.03	3655.22	4654.34	4040.25	4040.25	3370.71
100	5713.1	3563.03	4396.76	3867.84	3867.84	3284.28
101	7715.07	7225.22	7333.43	7288.36	7288.36	7195.15
102	6854.32	5546.15	6044.45	5773.1	5773.1	5351.27
103	7508.8	6384.98	6836.26	6585.19	6585.19	6199.81
104	7402.28	6698.51	6925.98	6772.5	6772.5	6611.07
105	7663.22	7097.02	7259.24	7151.12	7151.12	7036.67
106	5978.7	3506.67	4392.94	3915.18	3915.18	3229.86
107	6413.33	4734.74	5349.01	5037.39	5037.39	4522.5
108	7842.02	7013.07	7301.89	7163.92	7163.92	6884.28
109	7655.73	6700.58	7068.02	6843.09	6843.09	6538.6
110	7307.39	6281.99	6640.11	6447.59	6447.59	6137.4
111	7662.47	5801.6	6575.19	6149.39	6149.39	5502.76
112	6996.39	5881.92	6279.83	6043.94	6043.94	5724.39
113	7178.44	5491.51	6146.17	5812.33	5812.33	5244.4
114	6260.42	3822.97	4733.9	4210.96	4210.96	3519.42
115	6764.82	4288.58	5239.39	4689.74	4689.74	3970.65
116	7272.46	4592.87	5603.77	5038.96	5038.96	4269.56
117	6126.72	3373.52	4352.25	3746.38	3746.38	3078.25
118	5918.1	3592.98	4447.29	3941.34	3941.34	3307.93
119	3319.53	1350.06	1768.6	1477.02	1477.02	1250.32
120	7477.32	6826.87	6978.37	6882.73	6882.73	6759.51
121	6283.66	2752.94	3373.08	3321.28	3321.28	2714.2

122	8205.54	7478.31	7677.79	7637.31	7637.31	7420.2
123	7633.94	6498.43	6763.07	6823.52	6823.52	6474.46
124	6557.62	3812.97	4427.21	4529.69	4529.69	3800.98
125	8434.95	7857.99	7984.07	7982.33	7982.33	7809.98
126	7989.11	7266.65	7429.01	7421.23	7421.23	7215.84
127	4596.74	1731.42	2102.84	2031.48	2031.48	1695.67
128	3996.4	1301.41	1685.78	1628.73	1628.73	1267.93
129	6321.78	3800.62	4423.8	4446.2	4446.2	3757.32
130	6578.52	4054.62	4726.17	4700.72	4700.72	3997.51
131	6251.77	2748.61	3389.43	3335.04	3335.04	2701.06
132	7494.45	5941.82	6414.69	6333.24	6333.24	5858.68
133	2839.1	835.15	1059.03	1014.71	1014.71	810.71
134	7710.1	4658.73	5495.49	5419.99	5419.99	4581.53
135	7255.63	5827.83	6172.84	6206.87	6206.87	5782.58
136	7680.38	6828.15	7058.28	6952.88	6952.88	6741.45
137	1869.68	891.99	981.55	950.58	950.58	873.82
138	4028.67	1344.79	1714.91	1634.18	1634.18	1303.78
139	6958.56	5257.28	5728.33	5672.78	5672.78	5182.83
140	7634.43	6200.67	6598.99	6582.79	6582.79	6129.35
141	6656.31	4079.93	4763.02	4753.56	4753.56	4017.21
142	6016.91	2558.66	3112.94	3140.74	3140.74	2533.77
143	6402.79	4031.7	4633.94	4644.96	4644.96	3979.02
144	7639.77	6698.99	6914.54	6892.19	6892.19	6629.69
145	6947.24	4878.14	5458.59	5412.66	5412.66	4802.9
146	5888.43	2521.59	3133.4	3129.11	3129.11	2483.46
147	7895.49	6632.37	6975.12	6967.62	6967.62	6560.77
148	6293.78	2739.26	3339.83	3324.25	3324.25	2697.87
149	7038.61	4050.66	4816.1	4755.76	4755.76	3978.45
150	8368.25	7129.43	7540.71	7471.08	7471.08	7031.98
151	6482.76	2934.92	3581.16	3546.02	3546.02	2887.41
152	7896.64	7117.34	7229.93	7218.04	7218.04	7063.48

153	7642.47	6004.35	6397.24	6433.24	6433.24	6064.88
154	5952.27	2291.3	2711.19	2830.26	2830.26	2384.19
155	7631.16	6634.42	6814.28	6791.87	6791.87	6594.81
156	6117.75	2293.34	2629.73	2759.58	2759.58	2384.75
157	7355.08	5109.46	5650.22	5740.34	5740.34	5225.82
158	5661.39	2160.32	2581.95	2778.32	2778.32	2283.36
159	7112.39	4681.83	5229.18	5370.52	5370.52	4821.88
160	7435.34	4338.29	4950.74	5186.71	5186.71	4521.54
161	7308.87	4748.2	5344.6	5454.96	5454.96	4880.73
162	5353.01	2251.69	2760.24	2933.63	2933.63	2398.01
163	7063.82	4104.5	4728.22	4908.89	4908.89	4267.22
164	7366.05	5623.42	5995.02	6080.83	6080.83	5680.14
165	8383.98	7774.15	7871.48	7807.29	7807.29	7682.66
166	7824.2	6857.42	7035.09	7013.28	7013.28	6809.51
167	6201.08	3001.77	3512.09	3771.42	3771.42	3167.94
168	1626.28	769.43	815.38	807.84	807.84	763.82
169	3503.49	838.06	1098.27	1199.33	1199.33	894.71
170	5946	2727.61	3295.51	3356.42	3356.42	2836.86
171	7549.38	4419.09	5040.12	5253.58	5253.58	4583.13
172	6118.43	2806.9	3334.66	3573.55	3573.55	2965.93
173	6685.03	4226.77	4692.06	4913.98	4913.98	4377.37
174	6604.74	2918.31	3407.46	3653.11	3653.11	3072.45
175	7360.09	5570.85	5987.33	6026.88	6026.88	5628.42
176	2991.82	755.46	906.19	935.33	935.33	783.46
177	3848.06	1210.44	1394.92	1462.73	1462.73	1245.65
178	6762.34	4232.74	4769.66	4917.84	4917.84	4369.57
179	6425.55	3758.98	4315.84	4434.23	4434.23	3895.47
180	6908.22	4982.98	5418.88	5429.5	5429.5	5034.13
181	6298.74	2550.67	3000.73	3192.76	3192.76	2680.18
182	5988.05	3245.9	4235.31	4095.39	4095.39	3613.3
183	3646.69	1045.63	1509.53	1402.08	1402.08	1177.68

184	5864.57	2642.14	3385.21	3313.55	3313.55	2919.18
185	3267.21	1304.84	1589.88	1554.37	1554.37	1408.7
186	5712.43	2374.22	3183.63	3077.76	3077.76	2655.81
187	7236.04	6200.8	6614.32	6589.25	6589.25	6331.21
188	4028.35	1354.74	1866.88	1708.92	1708.92	1486.43
189	5435.32	2538.58	3465.61	3338.61	3338.61	2875.93
190	8112.93	7793.69	7916.3	7927.05	7927.05	7782.57
191	6250.86	2894.8	3886.37	3786.33	3786.33	3267.67
192	7842.63	7029.3	7397.8	7355.78	7355.78	7124.24
193	8140.72	6723.3	7449.5	7346.78	7346.78	6982.84
194	3147.04	1349.13	1598.7	1552.15	1552.15	1427.03
195	7018.78	4575.35	5610.8	5457.21	5457.21	4967.23
196	6764.87	3840.14	4914.2	4795.24	4795.24	4257.94
197	4587.01	1754.95	2219.7	2186.51	2186.51	1929.47
198	7543.08	5168.05	6144.88	6048.84	6048.84	5560.1
199	4647.91	1747.18	2248.96	2144.44	2144.44	1901.13
200	6810.49	3858.62	4896.94	4695.07	4695.07	4217.4
201	4183.66	1436.74	1993.22	1857.9	1857.9	1589.75
202	2761.79	1019.57	1258.07	1220.73	1220.73	1098.8
203	3895.89	1408.16	1800.83	1728.87	1728.87	1538.16
204	7764.92	5559.59	6538.02	6406.65	6406.65	5933.71
205	7792.73	6715.27	7234.94	7190.4	7190.4	6909.95
206	6174.8	3205.12	4222.25	4105.37	4105.37	3601.1
207	5960.57	2526.01	3371.24	3205.06	3205.06	2806.59
208	4554.09	1650.9	2165.28	2076.78	2076.78	1824.87
209	5121.35	1978.51	2689.39	2519.97	2519.97	2192.95
210	7156.85	4564.14	5673.93	5509.2	5509.2	4996.87
211	5845.24	2688.89	3657.67	3426.02	3426.02	3002.23
212	3690.88	1268.89	1646.44	1581	1581	1394.69
213	2074.1	1252.74	1240.62	1146.21	1146.21	1076.86
214	1371.92	835.57	831.2	766.34	766.34	726.27

215	1417.91	895.54	890.72	824.42	824.42	784.54
216	6759.42	4518.89	4349.65	4000.64	4000.64	3629.9
217	8125.78	7700.49	7749.88	7681.82	7681.82	7545.88
218	6407.14	5028.63	4911.63	4608.26	4608.26	4225.28
219	5195.76	3214.04	3055.86	2748.12	2748.12	2414.98
220	5490.97	3972.71	3849.15	3560.12	3560.12	3220.75
221	7596.6	6586.12	6518.32	6250.32	6250.32	5890.89
222	5347.51	3693.91	3501.69	3316.64	3316.64	2944.13
223	7050.07	5939.05	5848.99	5593.14	5593.14	5230.71
224	2397.88	1492.09	1458.76	1385.04	1385.04	1313.68
225	5120.73	3175.52	3017.63	2718.61	2718.61	2414.07
226	7557.24	6790.38	6731.72	6604.89	6604.89	6325.43
227	7564.25	6825.09	6797.67	6598.29	6598.29	6340.19
228	4607.02	2622.93	2478.19	2223.1	2223.1	1970.98
229	6813.4	5178.05	4983.37	4681.07	4681.07	4248.18
230	7315.97	6831.96	6841.61	6727.76	6727.76	6596.97
231	5557.21	3624.26	3464.42	3154.27	3154.27	2848.15
232	5996.31	4198.61	4001.02	3687.22	3687.22	3294.54
233	8161.76	7765.81	7715.44	7747.91	7747.91	7591.23
234	4158.1	2389.65	2240.78	1997.53	1997.53	1752.94
235	7829.54	7187.23	7152.78	6924.97	6924.97	6679.39
236	2523.37	1350.49	1278.07	1204.54	1204.54	1095.44
237	2612.75	1312.75	1229.2	1143.46	1143.46	1024.56
238	7494.84	6895.04	6819.72	6751.59	6751.59	6536.7
239	6465.74	4582.21	4379.23	4033.88	4033.88	3659.92
240	6670.22	4944.2	4763.7	4388.41	4388.41	4031
241	6043.52	4891.06	4773.65	4482.73	4482.73	4165.84
242	3497.93	1944.01	1854.34	1691.11	1691.11	1550.28
243	4370.81	2623.02	2466.49	2233.73	2233.73	1984.52
244	5967.96	3035.65	3451.11	3116.5	3116.5	2870.73
245	1868.29	771.49	827.68	775.65	775.65	749.36

246	2973.35	851.14	966.08	883.68	883.68	812.82
247	6802.26	3729.52	4193.67	3795.83	3795.83	3540.97
248	6906.79	4748.24	5064.96	4872.07	4872.07	4620.69
249	5331.99	2068.86	2327.1	2117	2117	1974.1
250	4721.66	1747.2	1986.81	1772.12	1772.12	1660.67
251	8031.78	6720.48	6898.04	6828.34	6828.34	6651.94
252	7410.95	5686.81	5952.75	5786.65	5786.65	5579.02
253	7892.1	6007.68	6341.76	6089.63	6089.63	5860.14
254	8066.4	6900.52	7092.67	6960.65	6960.65	6817.76
255	7394.39	6171.5	6322.62	6245.17	6245.17	6111.49
256	7907.9	6729.49	6940.73	6752.36	6752.36	6634.18
257	8024.38	6695.91	6939.32	6746.34	6746.34	6592.69
258	2624	797.13	909.77	799.76	799.76	755.37
259	3808.37	1376.53	1537.39	1399.83	1399.83	1319.29
260	6971.99	4305.05	4707.76	4425.86	4425.86	4154.59
261	5876.36	2586.48	2933.1	2635.4	2635.4	2460.87
262	8116.98	7265.6	7413.8	7280.48	7280.48	7207.33
263	7363.14	5443.21	5780.38	5526.48	5526.48	5311.21
264	5161.01	2275.17	2574.57	2362.02	2362.02	2177.81
265	7880.23	7100.99	7208.84	7122.82	7122.82	7068.34
266	7506.81	6649.52	6730.53	6700.56	6700.56	6635.09
267	7196.49	4460.31	4906.32	4526.64	4526.64	4291.67
268	6678.95	4470.33	4811.52	4565.75	4565.75	4350.47
269	7229.66	5884.51	6093.19	5939.69	5939.69	5814.91
270	1822.13	719.01	767.5	728.9	728.9	704.7
271	5577.55	2814.25	3170.04	2901.02	2901.02	2690.26
272	1832.51	760.7	813.87	770.95	770.95	748.08
273	7221.28	6206.76	6347.49	6232.07	6232.07	6164.62
274	7099.12	5914.2	6218.83	6121.7	6121.7	5854.3
275	6503.8	4832.38	5267.75	5087.13	5087.13	4726.49
276	7451.63	6938.91	6998.1	7032.9	7032.9	6962.7

277	6829.92	5446.22	5800.41	5687.28	5687.28	5374.06
278	6383.97	4511.39	4963.56	4832.51	4832.51	4422.65
279	5630.42	3154.49	3688.9	3506.33	3506.33	3046.68
280	6723.24	5753.72	5958.13	5914.88	5914.88	5736.77
281	6921.65	4650.28	5226.15	5038.21	5038.21	4531.69
282	6173.07	4487.58	4912.89	4752.05	4752.05	4397.75
283	6534.49	5074.4	5400.85	5361.06	5361.06	5040.46
284	3155.92	986.68	1186.28	1103.02	1103.02	952.53
285	5535.57	2788.86	3296.06	3145.77	3145.77	2700.62
286	7496.77	7332.11	7349.13	7326.81	7326.81	7367.26
287	5335.74	2260.59	2686.24	2497.78	2497.78	2179.44
288	5619.57	2840.43	3337.41	3209.93	3209.93	2764.57
289	7206.29	6493.6	6698.11	6629.27	6629.27	6478.85
290	4186.78	1877.4	2225.23	2161.01	2161.01	1823.85
291	6256.4	3685.63	4244.92	4065.22	4065.22	3586.19
292	6698.76	5984.93	6178.39	6065.3	6065.3	5964.28
293	7071.6	6620.47	6713.1	6708.65	6708.65	6650.83
294	6115.13	4904.41	5208.19	5085.67	5085.67	4858.34
295	6647.74	5120.89	5519.28	5438.48	5438.48	5073.15
296	6825.29	6349.61	6460.05	6404.08	6404.08	6362.16
297	6507.24	5606.47	5837.4	5745.83	5745.83	5586.39
298	6297.98	5283.15	5525.52	5463.16	5463.16	5267.47
299	7241.34	6911.68	7006.98	6971.5	6971.5	6938.77
300	6230.01	4471.56	4899.36	4786.97	4786.97	4404.37
301	5926.18	4529.2	4903.23	4755.65	4755.65	4467.34
302	3989.15	1535.61	1832.23	1732.15	1732.15	1486.74
303	5354.64	2946.46	3459.4	3271.37	3271.37	2853.12
304	3531.17	1291.63	1528.54	1429.76	1429.76	1255.01
305	6810.52	6355.17	6764.59	6686.54	6686.54	6252.89
306	6657.46	6067.74	6478.59	6502.85	6502.85	5989.93
307	7658.42	7982.87	8025.9	8059.17	8059.17	8028.96

308	6702.27	5955.59	6489.57	6471.09	6471.09	5826.99
309	5216.3	3564.64	4389.41	4269.8	4269.8	3370.81
310	6418.64	5294.73	6004.24	5953.38	5953.38	5107.81
311	5746.56	3597.57	4639	4540.33	4540.33	3346.58
312	2932.21	1025.09	1495.77	1343.38	1343.38	933.55
313	4799.93	2232.19	3235.65	3011.41	3011.41	2025.71
314	7271.45	7376.37	7511.03	7558.22	7558.22	7396.71
315	6916.49	6772.72	7052.56	7026.17	7026.17	6731.6
316	5056.36	3051.05	3969.41	3908.53	3908.53	2845.26
317	7414.3	7823.38	7840.24	7875.89	7875.89	7888.02
318	7475.83	7905.94	7910.22	7958.6	7958.6	7973.63
319	6881.85	6925.23	7112.76	7106.43	7106.43	6928.84
320	6079.25	5072.43	5741	5666.74	5666.74	4899.54
321	6322.84	5462.1	6086.69	6021.36	6021.36	5301.12
322	3828.67	1500.13	2186.38	2018.7	2018.7	1373.6
323	5433.4	4058.19	4796.19	4766.45	4766.45	3877.25
324	3657.6	1444.8	2122.08	2011.01	2011.01	1323.04
325	4900.36	2122.69	2997.66	2881.06	2881.06	1964.7
326	6168.95	5783.23	6174.13	6087.63	6087.63	5702.01
327	7143.72	7523.51	7560.31	7598.44	7598.44	7585.73
328	7283.77	7746.51	7792.92	7750.43	7750.43	7788.1
329	6435.07	6195.25	6495.46	6514.34	6514.34	6164.78
330	6128.82	5464.46	5954	5960.69	5960.69	5364.24
331	4423.12	1943.9	2766.89	2688.56	2688.56	1800.98
332	6176.95	5149.16	5871.63	5801.67	5801.67	4964.36
333	4988.57	2403.35	3323.89	3257.95	3257.95	2240.63
334	5845.65	4879.98	5565.31	5397.8	5397.8	4696.3
335	3806.99	2308.22	2999.47	2321.46	2321.46	1870.13
336	6478.5	6289.81	6575.05	6239.59	6239.59	6014.34
337	5261.42	4348.86	4906.63	4347.33	4347.33	3888.22
338	3401.75	1742.9	2448.58	1750.18	1750.18	1348.81

339	3004.25	1385.59	1934.38	1396.12	1396.12	1120.53
340	6375.81	6323.05	6498.65	6303.89	6303.89	6175.94
341	6404.55	6030.76	6454.88	5956.46	5956.46	5631.36
342	6406.41	6520.23	6653.54	6453.69	6453.69	6419.52
343	6294.41	6336.31	6498.28	6280.9	6280.9	6213.15
344	6273.5	6222.54	6418.56	6184.35	6184.35	6055.23
345	6714.13	6891.23	6997.38	6836.23	6836.23	6808.71
346	6936.38	7225.29	7269.49	7177.24	7177.24	7199.17
347	5159.34	4399.23	4922.67	4347.28	4347.28	3979.97
348	6319.56	6036.37	6392.93	5983.43	5983.43	5703.68
349	6700.73	6981.16	7046.96	6908.02	6908.02	6939.96
350	6889.17	7093.65	7190.61	7041.06	7041.06	6996.26
351	6007.1	5812.67	6110.03	5732.37	5732.37	5564.5
352	4404.2	2686.07	3540.6	2682.79	2682.79	2159.33
353	6504.22	6288.67	6622.59	6229.74	6229.74	5967.84
354	6144.35	6130.78	6317.98	6078.22	6078.22	5991.16
355	6354.92	6394.2	6542.77	6350.59	6350.59	6277.36
356	1652.54	813.29	1003.91	791.63	791.63	750.8
357	4893.21	3694.73	4409.66	3674.03	3674.03	3157.01
358	4774.98	3006.23	3885.76	3016.75	3016.75	2468.28
359	5308.35	4543.83	5064.61	4511.26	4511.26	4115.24
360	6819.87	7125.45	7172.04	7061.78	7061.78	7101.14
361	5756	5313.85	5714.4	5262.4	5262.4	4986.57
362	6397.06	6521.96	6628.41	6480.87	6480.87	6438.11
363	6715.46	6917.7	7007.22	6862.48	6862.48	6848.43
364	5640.06	4453.4	5224.77	4425.13	4425.13	3862.43
365	5070.1	3315.94	4216.81	3331.65	3331.65	2745.17

Appendix 4: Specific global existing solar - hydrogen

		1	2	3	4	5	6	7	8	9
Project		Hunterston Hydrogen Ltd & Wind Hydrogen Ltd (proposed) (Pritchard, 2000)	Anglesey Wind & Energy Ltd (proposed) (Anglesey Wind, 2004)	Statkraft, (Dutton, 2002)	Mawson Station, (Dutton, 2002)	(Jacobson, Purcell, & Wermers, 2001)	(Ulleberg, 2003), PHEOBUS	Utsira (Norsk Hydro, ENERCON) (Norsk Hydro, 2004)	Pure Project (Unst Partnership & siGEN (Gazey & Macauley, 2004)	Econnect (Altener Programme, 2001)
Location		Ladyland Moor, West Kilbride.	Anglesey	Smola wind farm, Norway	Antartica	Reno, Nevada	Germany	Norway	Unst, Shetland.	England
Turbine		25MW (15 x 1.75MW)	3MW of wind turbines	Phase 1 40MW, Phase 2 110 MW	900kW Enercon turbines E30	3kW	--	2 600kW Enercon wind turbines	two 15 kW Proven wind turbines	20kW Gazelle wind turbine
PV		--	--	--	--	2kW	30kW	--	--	--
Battery		--	--	--	--	--	300kWh 220V	5kW flywheel.	--	--
Electrolyser	Rating	4MW electrolysis project	300kW hydrogen electrolysis plant	--	2KW electrolyser	5kW	26kW	48kW electrolyser	electrolyser	8kW, 48V PEM
	Pressure	--	--	--	--	--	7bar	10 Nm ³ /h	--	--
	Manufacturer	--	--	--	--	Stuart energy	--	Norsk Hydro Electrolyser s	--	--
Storage		600,000Nm ³ hydrogen per yr.	--	--	--	Hydrogen tank 100psi 80 ft3, psi to FC	120 bar 26.8m3 H ₂ 70 bar 20 m3 O ₂	5.5kW compressor with 2400 Nm ³ storage.	metal hydride bottle hydrogen storage	--
Fuel Cell	Type	Conventional internal combustion hydrogen generators	Plans to install a fuel cell for back-up power and grid support.	By 2007 excess wind energy will be used to generate hydrogen. Fuel cells will replace diesel generators.	--	--	--	hydrogen engine and fuel cell.	Plug Power hydrogen fuel cell system.	--
	Rating	up to 10MWe.	--	--	--	2kW	6kW	55kW engine 10kW FC	5 kW	6kW
	Manufacturer		--	--	--	Dais-Analytic	--	--	--	--
Comments		Plan for H ₂ plants and fuelling stations along electricity nets. Electrolysis plant "despatchable load" and hydrogen gensets "despatchable peaking plant".	Study of hydrogen energy storage as an alternative to grid reinforcement. Hydrogen and oxygen to be used in local fish farm.	Turbines supplying 80% of the station's energy needs.	Poor performance due to "one-off" design of electrolyser	30% depending on conditions	--	--	Power generated will supply five industrial units at Unst's Hagdale industrial estate	+ 40kVA synchronous compensator and 10kVA PF correction capacitor.

	9	10	11	12	13	14	15	16	
Project	Abbossou, Chahine, Hemeline et al. (2001) and Kolhe, Agbossou, Hamelin et al. -2003	Shatter et al., (2001)	Isherwood, Smith, Aceves et al. (2000)	Datta, Velayutham, & Goud (2002)	(Galli & Stefanoni, 1997)	(Vanhannen, Lund, & Tolonen, 1998)	(Mills & Al-Hallaj, 2004)	(Dutton, Bleijs, Dienhart et al., 2000)	
Location	Canada	Egypt	Alaska (hypothetical)	India	Rome Casaccia Research centre ENEA	Helsinki	Chicago	Rome Casaccia Research centre ENEA	
Turbine	10kW	--	70kW	--	--	--	12kW	5.2kW	
PV	1kW	2.24 kW	--	--	5.6kWp	--	6.5kWp	--	
Battery	42.24kWh	--	--	--	--	--	350Ah, 6Vdc per battery	330Ah	
Electrolyser	Rating	Alkaline 5kW, 65% to 71% without compression (5%)	--	--	--	Alkaline bipolar ALyser-0100 17 cell 29 Vdc 5kW	Alkaline then 30W SPEL 5 bar, prefer in future 100 - 200W,	5.76kW/8kW, 70%, idling power 25% rated	1kW pre but 2.25kW used, 50V,
	Pressure	7 bar, 1 N m ³ h ⁻¹	--	--	--	20 bar max	operating 5 - 10 bar	--	20 bar
	Manufacturer	Stuart	Stuart	--	--	Metkon-Alyser,	--	--	Hoerner System electrolyser
Storage	10 bar, 3.8m ³ = 125kWh and 207 bar (4.5 1 N m ³ h ⁻¹) 154 m ³ = 507kWh	3 bar tank	Low pressure compressed H ₂ storage. 4.1MPa, 600psi	--	Metal hydride tank based on automotive manuf HWT, Germany 18Nm ³ , 15bar + standard gas cylinders	Pressure Vessel, then metal hydride min 5bar - 10bar	Low pressure 0.6bar to 3kW compressor to 22m ³ high pressure tank	--	
Fuel Cell	Type	PEM	PEM	--	PEM	SPFC	PAFC / SPFC	PEM	commercial Otto engine.
	Rating	5kW, 19 - 35V > 45% when gen over 4kW.	Current density 400mA/cm ² , stack of 90 cells	--	500W, 12V,	22 - 30Vdc, max P 30psigH ₂	100W	1/2kW	8kW
	Manufacturer	Ballard	--	--	--	Ballard	--	NTT labs	--
Comments	--	--	--	--	--	30% round trip efficiency	--	--	

Appendix 5: Technoeconomic comparisons of ESS

ESS TECHNOLOGIES → DEFINING FEATURES ↓			Unit	1	2	3	4	5
				SUPERCONDUCTING MAGNETIC ENERGY STORAGE (SMES)	COMPRESSED AIR ENERGY STORAGE (CAES)	SMALL-SCALE COMPRESSED AIR ENERGY STORAGE (SSCAES)	FLYWHEELS ENERGY STORAGE SYSTEM (FESS)	HIDROGEN ENERGY STORAGE SYSTEM (HESS)
1.- COST	1.1	INITIAL CAPITAL COST / INVESTMENT PER KW	[\$/Kw]	300	425 - 1,250	517 & 1,950 - 2,150	300 - 2,200	1,100 - 2,600
	1.2	INITIAL CAPITAL COST / INVESTMENT PER kWh	[\$/kWh]	2,000 - 72,000	3 - 150	50 & 390 - 430	170 - 8,800	2 - 15
	1.3	BOP (Balance Of Plant): housing, environment control & electrical connection equipment	[\$/kWh]	1,500	50	40	9.60	-
	1.4	FIXED RUNNING COST (OPERATION + MAINTENANCE)	[\$/kWh]	8 - 26	1.42	3.77	1,000	2-15 €/kWh
	1.5	VARIABLE RUNNING COST (OPERATION + MAINTENANCE)	[\$/kWh]	0.5 - 2	0.01	0.27	0.4	1
2.- EFFICIENCY	2.1	ROUNDTrip EFFICIENCY (RTE)	[%]	80 - 95	64 - 80	50 - 57	80 - 95	34 - 42
3.- ELECTRICAL CAPACITY	3.1	POWER RATING	[MW]	0.001 - 100	20 - 500	3 - 100	0.1 - 20	0.0001 - 50
	3.2	ENERGY STORAGE CAPACITY	[MWh]	< 0.25	400 - 7,000	250	0.0052 - 5	0.00012 - 200
	3.3	POWER DENSITY	[W/kg]	-	-	-	11.9	-
	3.4	ENERGY MASS DENSITY	[Wh/kg]	10 - 75	3.2 - 5.5	-	5 - 100	100 - 1,000
4.- STORAGE / DISCHARGE BEHAVIOUR	4.1	SELF-DISCHARGE	[%]	10 - 15 %	0	-	1 - 3	-
	4.2	DEPTH OF DISCHARGE	[%]	~ 100	-	-	~ 100	-
	4.3	STORAGE TIME	-	-	-	-	-	Days - 1 Week
	4.4	RESPONSE TIME	-	~ 17 ms	Sec - Min	Sec - Min	< 4 ms	< 1/4 cycle
	4.5	DISCHARGE DURATION	-	1 s - 30 min	6 Hrs - Days	1 - 6 hrs	< 1 Hr	Min - Hrs
5.- LIFETIME	5.1	DISCHARGE CYCLES	[n ^o]	10,000 - 100,000	10,000 - 30,000	> 10,000	100,000 - 10,000,000	-
	5.2	LIFESPAN / LONGEVITY	[years]	20 - 40	30 - 40	30	20 - 30	2 - 20
6.- ENVIRONMENT	6.1	ENVIRONMENTAL HOSTILITY, POLLUTION, SAFETY		Magnetic field safety issue	Greenhouse emissions	Gas emissions, pressure vessels	Containment safety	Highly flammable
	6.2	GEOLOGICAL REQUIREMENTS		-	Medium (Underground site)	-	-	-
7.- STATE-OF-THE- ART	7.1	MATURITY		Mature	Mature	Demonstration	Commercial in Low-Speed. Pre- commercial in High-Speed.	Demonstration
8.- APPLICATIONS	8.1	SHORT TERM[a few seconds or minutes], LONG TERM[minutes or hours] or REAL-LONG TERM [many hours to days]]		Short-Term	Real Long-Term	-	Short-Term	Long-Term
	8.2	POWER APPLICATIONS ENERGY APPLICATIONS POWER & ENERGY APPLICATIONS BRIDGING APPLICATIONS						

ESS TECHNOLOGIES → DEFINING FEATURES ↓		Unit	6	7	9	10	11	
			PUMPED HYDRO- POWER ENERGY STORAGE (PHES)	THERMAL ENERGY STORAGE (TES)	FLOW BATTERIES ENERGY STORAGE (FBES)	SUPER-CAPACITORS ENERGY STORAGE (SCEs)	CHEMICAL STORAGE / BATTERIES ENERGY STORAGE (BESS)	
1.- COST	1.1	INITIAL CAPITAL COST / INVESTMENT PER KW	[\$/Kw]	500 - 4,300	-	1,200 - 2,000	300	-
	1.2	INITIAL CAPITAL COST / INVESTMENT PER KWh	[\$/kWh]	5 - 430	3,500 - 7,000	175 - 800	82,000	-
	1.3	BOP (Balance Of Plant): housing, environment control & electrical connection equipment	[\$/kWh]	Included	-	Included	10,000	85 - 4,800
	1.4	FIXED RUNNING COST (OPERATION + MAINTENANCE)	[\$/kWh]	3.8	-	-	5.55	-
	1.5	VARIABLE RUNNING COST (OPERATION + MAINTENANCE)	[\$/kWh]	0.38	-	-	0.5	-
2.- EFFICIENCY	2.1	ROUNDTrip EFFICIENCY (RTE)	[%]	65 - 87	< 60	60 - 88	95	60 - 90
3.- ELECTRICAL CAPACITY	3.1	POWER RATING	[MW]	0.00001 - 4,000	0.1 - 200	0.005 - 25	< 0.25	0.0001 - 50
	3.2	ENERGY STORAGE CAPACITY	[MWh]	0.0005 - 24,000	< 2,000	0.1 - 120	< 3	< 40
	3.3	POWER DENSITY	[W/kg]	-	-	-	800 - 2,000	-
	3.4	ENERGY MASS DENSITY	[Wh/kg]	0.5 - 1.5	-	-	-	-
4.- STORAGE / DISCHARGE BEHAVIOUR	4.1	SELF-DISCHARGE	[%]	Evaporation	-	Very Low	5 % per day	~ 1 - 5 %
	4.2	DEPTH OF DISCHARGE	[%]	-	-	~ 100	-	Limited
	4.3	STORAGE TIME	-	Hours - Months	-	-	-	-
	4.4	RESPONSE TIME	-	Sec - Min	-	< 1/4 cycle	< 1/4 cycle	~ 20 ms
	4.5	DISCHARGE DURATION	-	1 hr - Days	Hrs	2 - 20 Hrs	Sec - Min	Min - Hrs
5.- LIFETIME	5.1	DISCHARGE CYCLES	[n#]	20,000 - 50,000	-	1,000 - 13,000	10,000	-
	5.2	LIFESPAN / LONGEVITY	[years]	30 - 50	-	10 - 20	8 - 40	2 - 16
6.- ENVIRONMENT	6.1	ENVIRONMENTAL HOSTILITY, POLLUTION, SAFETY		Reservoir	-	Chemical handling and disposal	None	Chemical handling and disposal
	6.2	GEOLOGICAL REQUIREMENTS		Reservoir	-	Chemical disposal	None	Chemical disposal
7.- STATE-OF-THE- ART	7.1	MATURITY		Mature	Mature	VnRedox and Zn/Br Redox commercially viable	Commercial	-
8.- APPLICATIONS	8.1	SHORT TERM[a few seconds or minutes], LONG TERM[minutes or hours] or REAL-LONG TERM [many hours to days]		Real Long-Term	Long-Term	-	Short Term	Long-Term
	8.2	POWER APPLICATIONS ENERGY APPLICATIONS POWER & ENERGY APPLICATIONS BRIDGING APPLICATIONS						

Appendix 6. Empa visit tag



Appendix 7.

7A. The Isle of Eigg AC Micro – Grid Power Characteristics Analysis

An energy monitoring system (data acquisition system) was installed at Eigg on November 2013 by Kinetic Traction Systems to log data in one second intervals in order to characterize the electric power performance, in a plan to install a flywheel energy storage into the mix. Six Weeks power generation data from the generators (hydro, solar, wind and diesel generator) was obtained using five high speed Hioki data loggers. This represented a baseline data upon which the anticipated performance

characteristics of flywheel energy storage was designed, before the final installation in October 2014. The flywheel has the effect of smoothing abrupt changes in frequency, which are characteristic of such schemes. During the observation period, several power trips and reverse power events have been observed from the recorded data. If a power system is not properly optimized with an energy storage, a frequency distortion is mostly seen, the frequency deviates and follows the pattern of generation. According to the information we obtained from Eigg Electric system manager Eddie Scott, the Laig hydro tripped on the following dates

- 10/11/14
- 13/11/14
- 28/12/14
- 08/02/15
- 16/02/15
- 24/02/15
- 29/03/15

7B. Hydro Trip Event on 13 November 2014

To address this hydro-power trip issue and to utilise the excess energy that is mostly generated from the renewable energy sources, Kinetic Traction Systems installed a flywheel energy storage system into the Island RE generation mix to stabilise power generation and smooth out grid frequency deviations. This also has the benefit of reducing stresses on the battery system. **Figure A7 1** shows the power generation mix after the flywheel energy storage was installed. The graph shows the relevant (one second) traces observed around the trip event on 13th November 2014. From this the hydro power output fluctuated between around 30 kW – 40 kW before it tripped. From the graph, the frequency was maintained at 50 Hz dropping to 49 Hz when the hydro tripped. The red ring in the graph highlights this moment of fluctuations. This apparent noise in the data is attributable at least in part to the frequency of the data logging (1s). Also, observed on this trace are negative output powers recorded in both wind and solar PV.

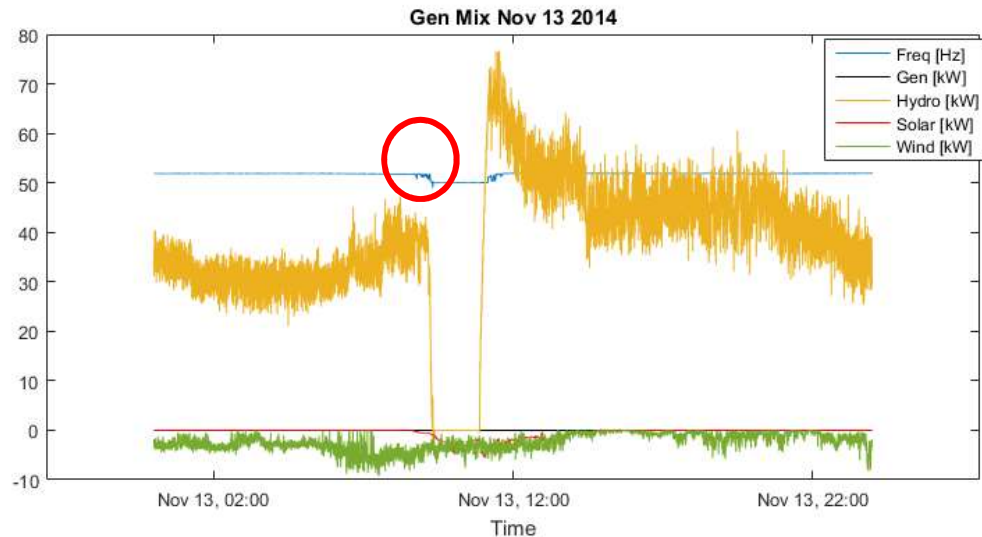


Figure A7 1. Power generation mix 13 November 2014.

To visualize clearly the reverse power events, the data was then synthesized, isolating and plotting the period when the hydro power tripped. **Figure A7 2** shows the hydro power output during the trip period. The batteries were at a full state of charge (about 93% of rated capacity) until 9 am when the hydropower system tripped. As shown in **Figure A7 3** battery discharged to compensate for the loss of power from the hydro, this can be explained further by the responses in the grid frequency.

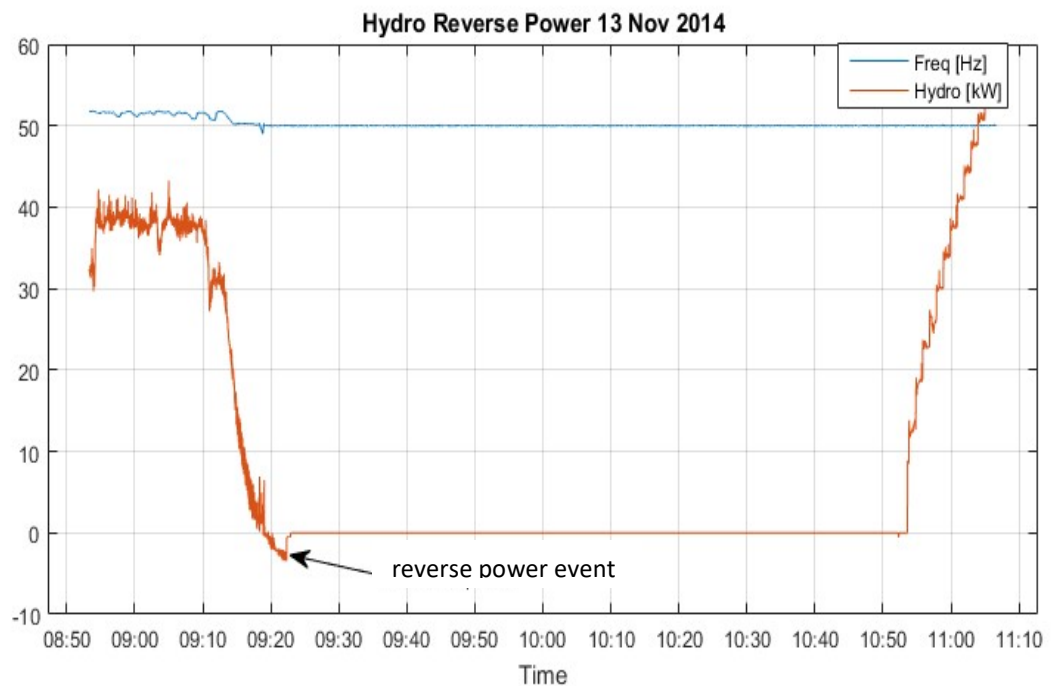


Figure A7 2. Hydro Power output and frequency between 9:00 – 11:00, 13 November 2014.

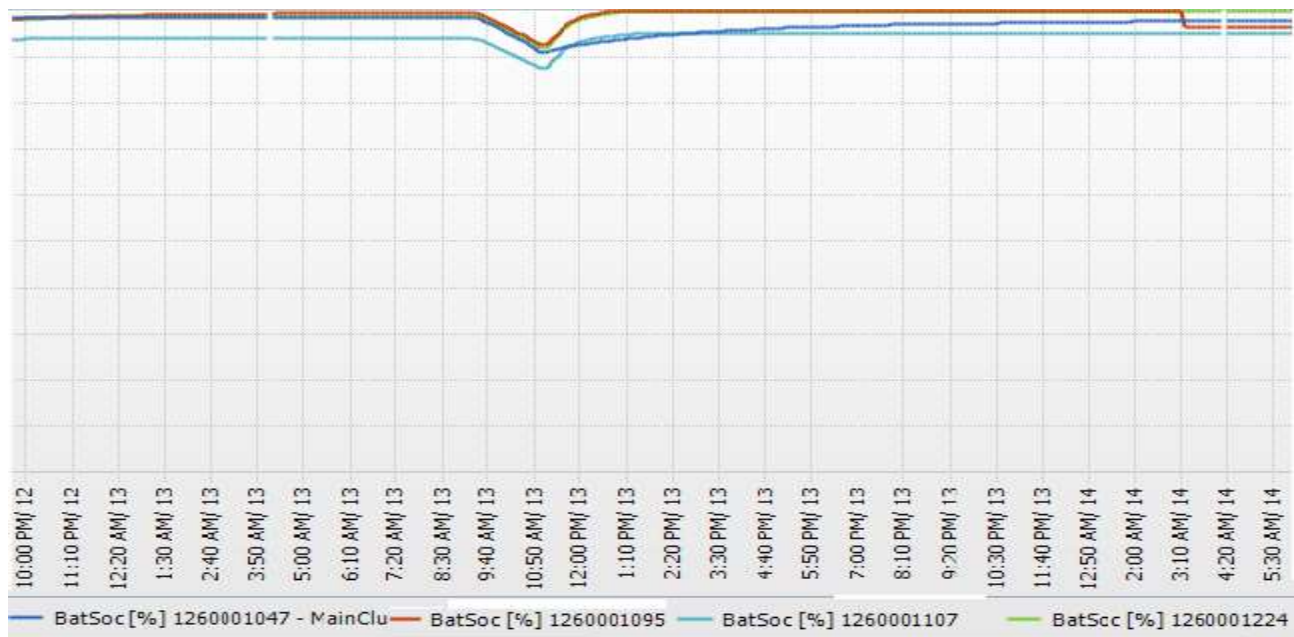


Figure A7 3. Battery SOC 13 November 2014 [67].

In **Figure A7 4** the grid frequency prior to the hydro trip was close to the upper limit of 52 Hz, which means that hydro generation dominated the supply (wind and PV are tapered out at these high frequencies). Immediately after the trip the frequency began to drop to 50Hz, thus any wind and PV available was switched back in, with the batteries supplying the demand shortfall. It can be seen from the frequency that it dropped to 50Hz when the hydro went off, and the frequency rose back to 52Hz when the hydro kicked in again at 11 am. The voltage shown with red trend line was maintained at 230V.

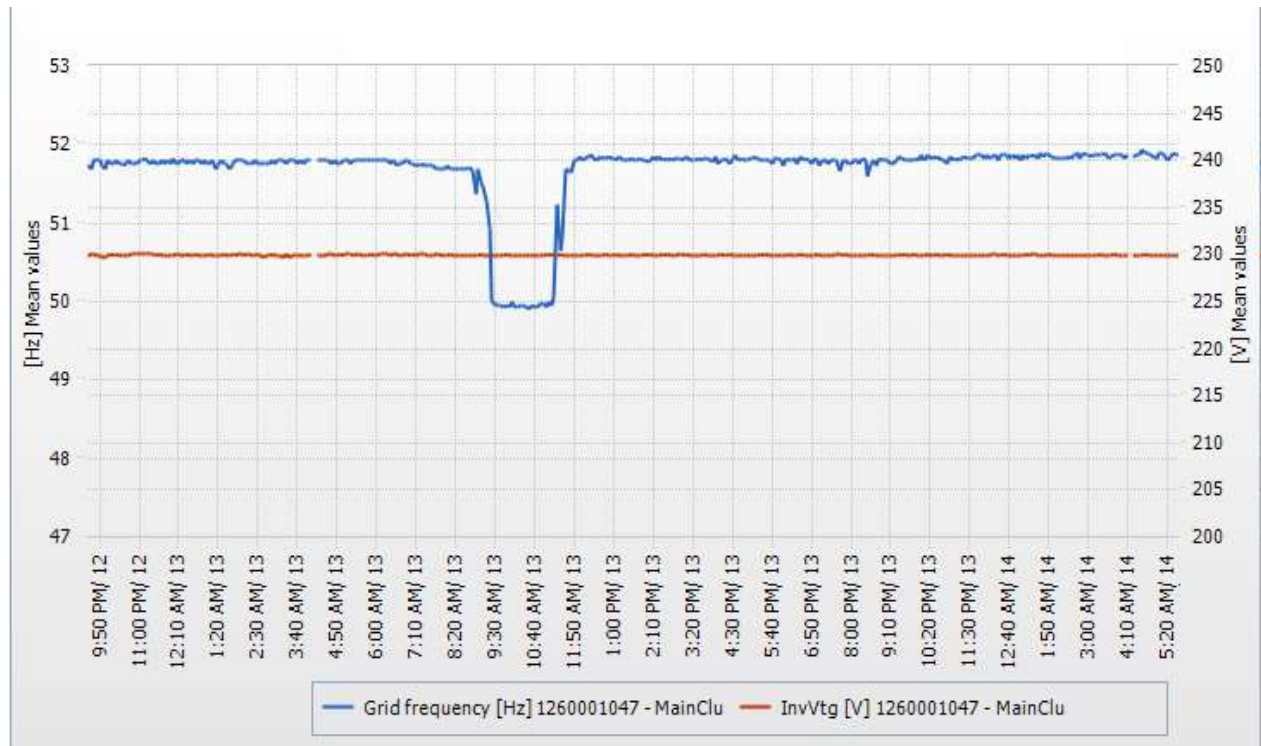


Figure A7 4. Voltage and grid frequency 13 November 2014 [67].

7C. Hydro Trip Event 13 Nov 2014 with Synchronised KT and SP Data

The power generation data recorded by kinetic Traction from Isle of Eigg hydro turbine system on 13th November 2014 has been synthesized, averaged at 15 minutes (mean) and plotted in order to obtain a clearer view of the system behaviour. Also, power generation data from hydro for the same period was downloaded from the SMA Sunny portal website [67], which records and displays the performance characteristic of the Eigg Electric averaged at 15 minutes intervals (mean) with solar and wind outputs synthesized to **positive values**, and compared to the graph from the Sunny Portal in order to obtain a criteria for further investigations on the cause of the negative readings. As shown in **Figure A7 5** the Sunny Portal graph was superimposed on that of Kinetic Traction.

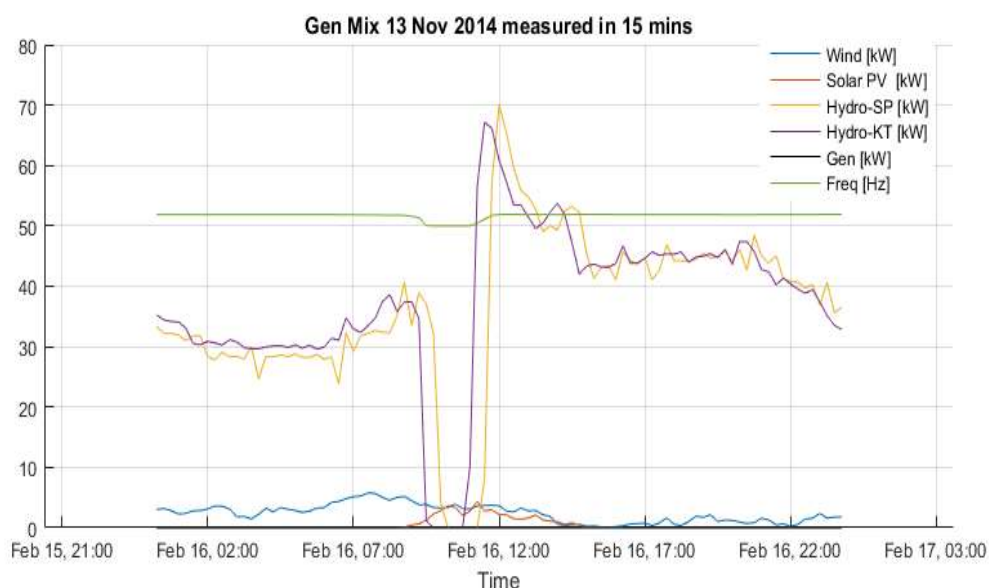


Figure A7 5. Power generation mix at Eigg on 13 Nov 2014 showing a superimposed graphs of Sunny Portal and Kinetic Traction data.

Interestingly, it can be seen that there is an unexplained temporal displacement of around 30 minutes between the two graphs, which becomes obvious within the period the hydro tripped (9AM – 10AM). However both graphs show close similarity in terms of trend. The observations here suggests that the Sunny Portal data was recorded based on average values. However, the 30 minutes gap between the two sets of data suggests that perhaps the timing mechanisms lack synchronisation. From this event a number of observations have been made, none of which give any apparent reason to explain why the hydro tripped. However, looking at the graph, one can see that the output power from wind generators to the system prior to the period the hydro tripped averaged at about 5kW.

Prior to the trip contributions to the total generated power from solar and wind would be expected to be relatively small due to the feature of the inverters which progressively tapers out their contributions at frequencies over 51 Hz. In this regime the island is powered predominantly by the hydros, which are seen to be delivering around 40kW. After the trip the expectation was that contributions from PV and wind would increase as the frequency drops. However, the average wind speed for this date (4.5m/s) obtained from a weather station on the Isle of Skye (the closest to the Isle of Eigg) indicates that there was no sufficient wind resource for the wind turbines to increase their contribution. During the trip period the shortfall in island power was predominantly provided by discharge of the batteries. Referring back to **Figure A7 4**, the

observed discharge rate of the batteries is consistent with the shortfall of renewable power in this period.

7D. Hydro Trip Event 16 February 2015

The raw power generation data recorded on 16th February 2015 was synthesized and is plotted as shown in **Figure A7 6**. From the graph it can be observed that solar and wind power outputs are all in negative range, as referred to earlier. Observing the hydro trip period (11AM – 5:30PM), the graph shows that neither the Laig hydro nor the diesel generator were operational during this 6 – hour period so demand was met from a combination of small hydro, wind, PV and batteries.

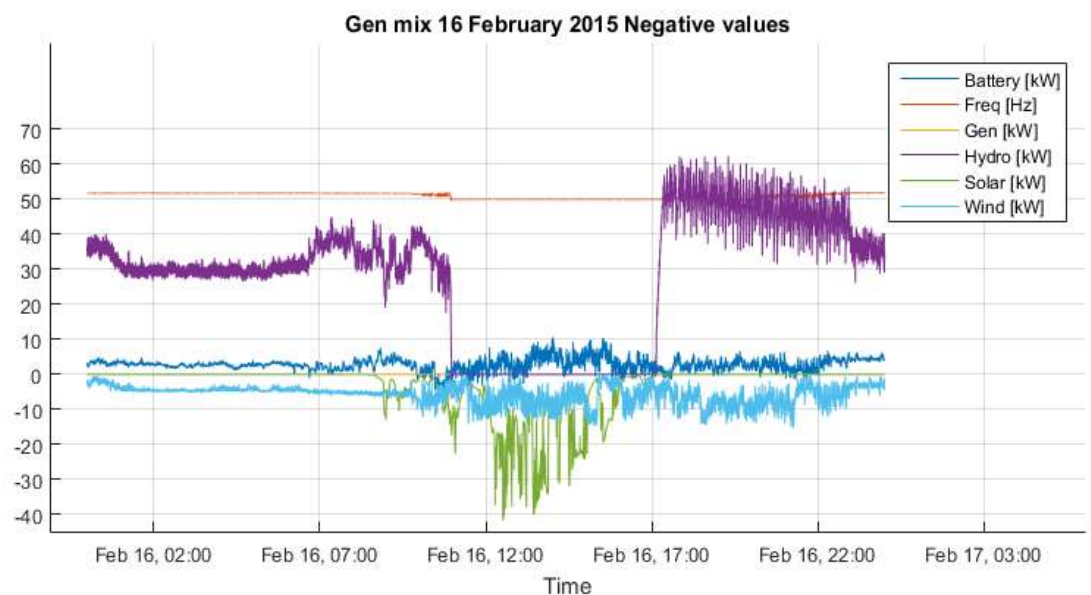


Figure A7 6. Power generation mix on 16 February 2015 showing the negative values for PV and wind.

This scenario suggest that solar PV and wind generators may be making some reasonable contributions within the period the hydro tripped, but the negative values may be as a result of artefacts. However, to analyse the power contributions by each component there is need to re-plot the graph in a more believable and viewable way. **Figure A7 7** shows the power generation plot with the solar and wind data synthesized to **positive values** (plotted in positive-reverse order). Concentration was based on

period when the hydropower system tripped, therefore the current graph covers only power generation from 11AM – 5:30PM, in order to stretch out a visible and detailed presentation of individual power contributions.

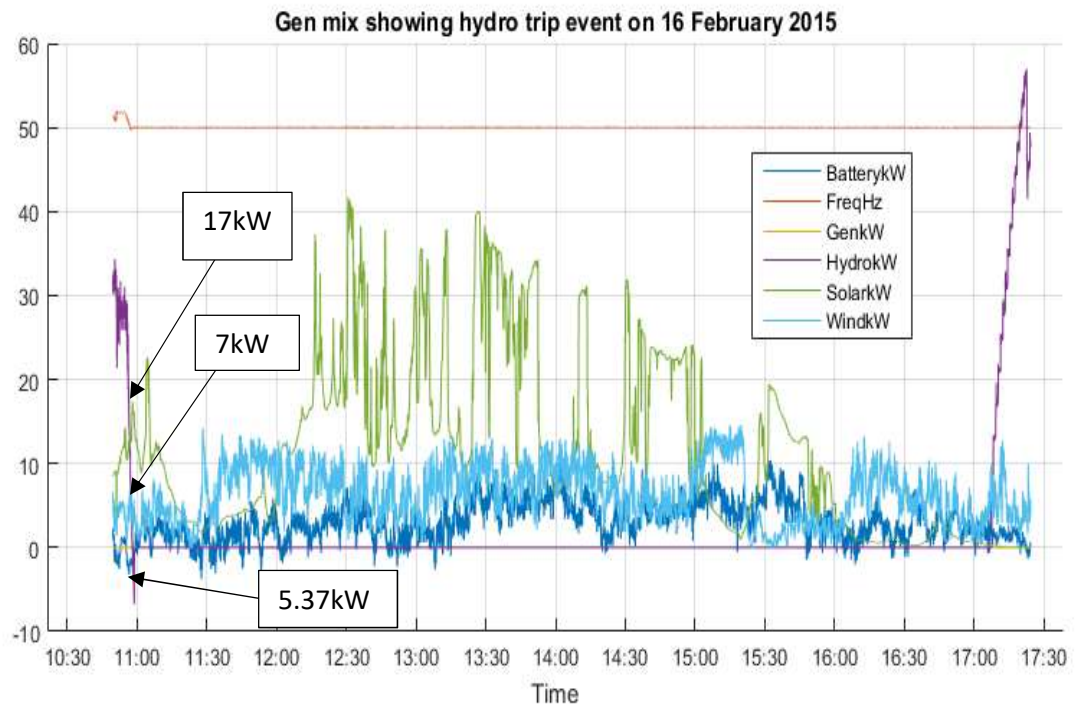


Figure A7 7. Power generatio mix at Isle of Eigg on 16 February 2015 at hydro trip period.

From the graph, hydro output power fluctuated between 30kW and 40kW, a situation which seems quiet a familiar occurrence (if compared to the 13th November 2014 events). Significantly, the hydro trip events always happen during the day time, a period when on average the total load demand at the Isle of Eigg may be around 30kW - 40kW. The synthesized solar and wind data (as shown in **Figure A7 8**) happen to show some interesting evidence. The total power generation prior to the period of hydro trip event was 59.37kW; 30kW of this came from the hydro power system and solar PV produced about 17kW with turbine generating about 7Kw, while the battery discharged 5.37kW (totalling 29.37kW, approx 30kW). It should be noted that the two 6kW small hydro may be adding some little amount of power to the mix during this trip period, this is not metered. This apparantly suggest that the load demand at Eigg varies between 30kW – 40kW depending on time of consumption. Probably, the steep decline in hydropower

output at this period which continued until it tripped was to balance the power demand at Eigg as a response to the incoming generation from other sources (solar and wind). The total power demand at Eigg during the period may have been met by the contributions from the solar and wind power sources while that from hydro backed off. This continued until about 5:30PM when the solar had stopped producing and wind power dipped, then the hydro kicked on again. It can therefore be inferred that RE power design at Eigg may be such that, hydro was electronically implemented to follow and monitor power generation pattern of all power sources and detect when other RE sources are not generating enough power to cope with demand. **Figure A7 9** shows a synchronised graph of Sunny Portal and Kintetic Traction Systems data. This was plotted in order to ensure a better understanding of this trip events and how it affects the Eigg electric system. The KT data was synthesized and averaged at 15 minutes to correspond to the SP data which was recorded at 15 minutes interval.

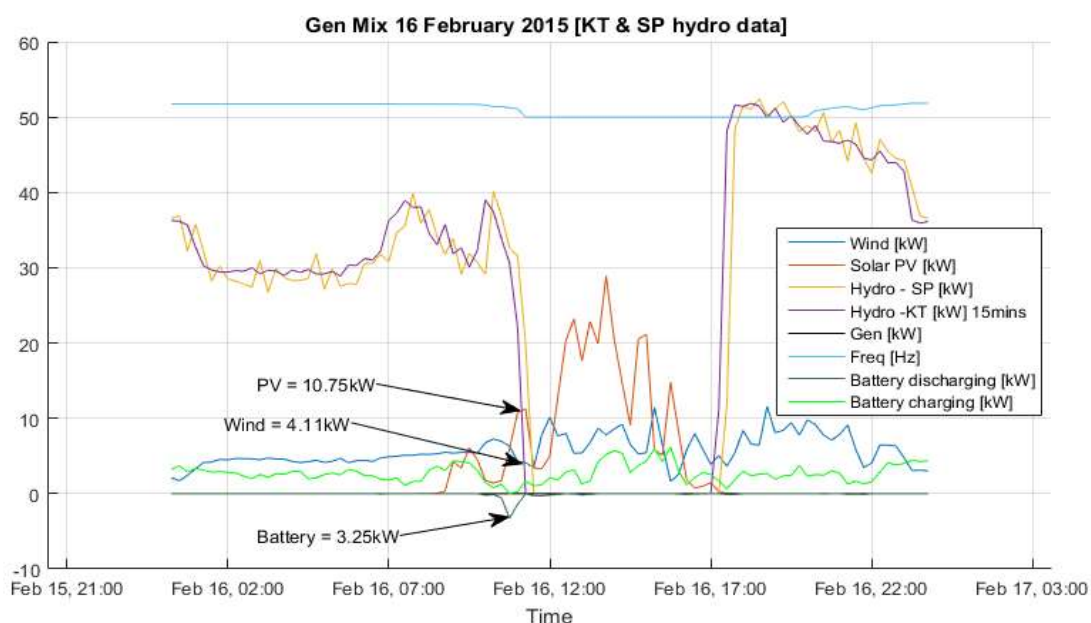


Figure A7 8. Power generation mix at Eigg on 16th February 2015 including a superimposed graph of Sunny Portal and Kinetic Traction hydro data.

From the graph it can be seen that there is a more defined correlation between the SP and KT plots. Comparing the gap as was seen before in the graph of **Figure A7 5** it is to some extent minimal on this plot, both SP and KT plots are more closely matched with 15 minutes gap. Clearly, from the graph the cause of hydro power trips can be

examined, looking at the output power conditions within the period it occurred. However, comparing this graph with that of **Figure A7 7** which was plotted using the raw KT data (recorded at 1s); one would notice a change in power outputs from the generators. This reflects the issues associated with averaging, and this suggests that KT data is more reliable in terms of getting the actual power performances at Eigg in real time. In conclusion, the observations are that the system frequency becomes unstable first, which causes the hydro to trip. As with the other events the pre-trip conditions appear benign, with batteries at or near full charge. However, for this research, only the PV component of Eigg electric system have been selected for further analysis.

The following **sections** will discuss the application of DC – DC converter in solar PV applications.

7E. Buck Converter

In buck converter mode, the output voltage is always less than the input voltage. Hence, it is mostly referred as step-down transformer. As shown in **Figure A7 9** the transistor switch **S** is connected in series with the dc input voltage and has the current in the inductor controlled by two switches **S** and **D** (MOSFET and Diode). The principle of the buck converter can be thought of as pulse width modulation (PWM) whereby the input voltage V_i is switched on for a specified time t_{on} to the output voltage V_o , and given a pulsed output voltage $V_o(t)$.

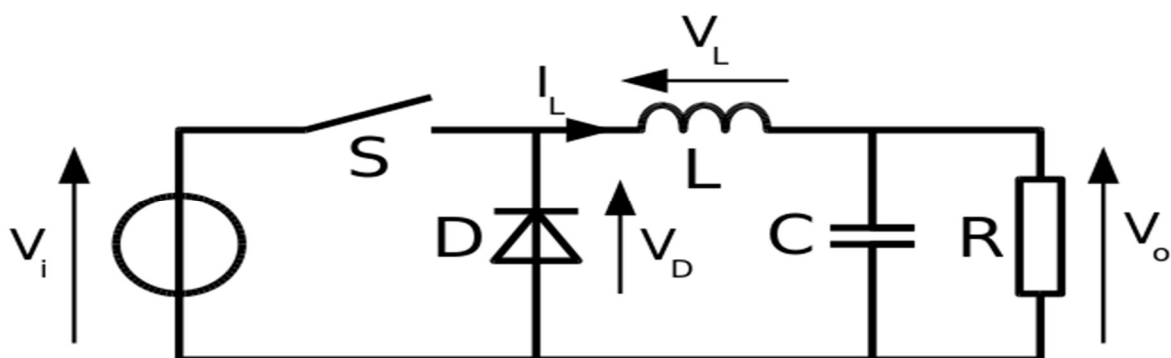


Figure A7 9. DC – DC buck converter [52].

The switch (**S**), controls the input voltage (V_i); when the switch is at off- state (when the switch is open) the current in the circuit is zero, and when the switch **S** is closed

(on-state) current will start to increase as it flows through the inductor, according to Lenz's law the inductor will produce an opposing voltage (V_L) (the arrow shows the direction of opposing voltage) across its terminals to counteract the changing current. In that process, the voltage across the load is reduced. Buck converter can be operated both in a continuous mode and discontinuous mode, at continuous mode the inductor current (I_L) never falls to zero during the cycle, the reverse is the case for discontinuous mode. However, for efficiency considerations, this research deals with the continuous operation mode of DC-DC converter, so any descriptions related to discontinuous mode is not dealt with. The pulse-width modulated (PWM) output under continuous conduction mode conditions is shown in **Figure A7 10**.

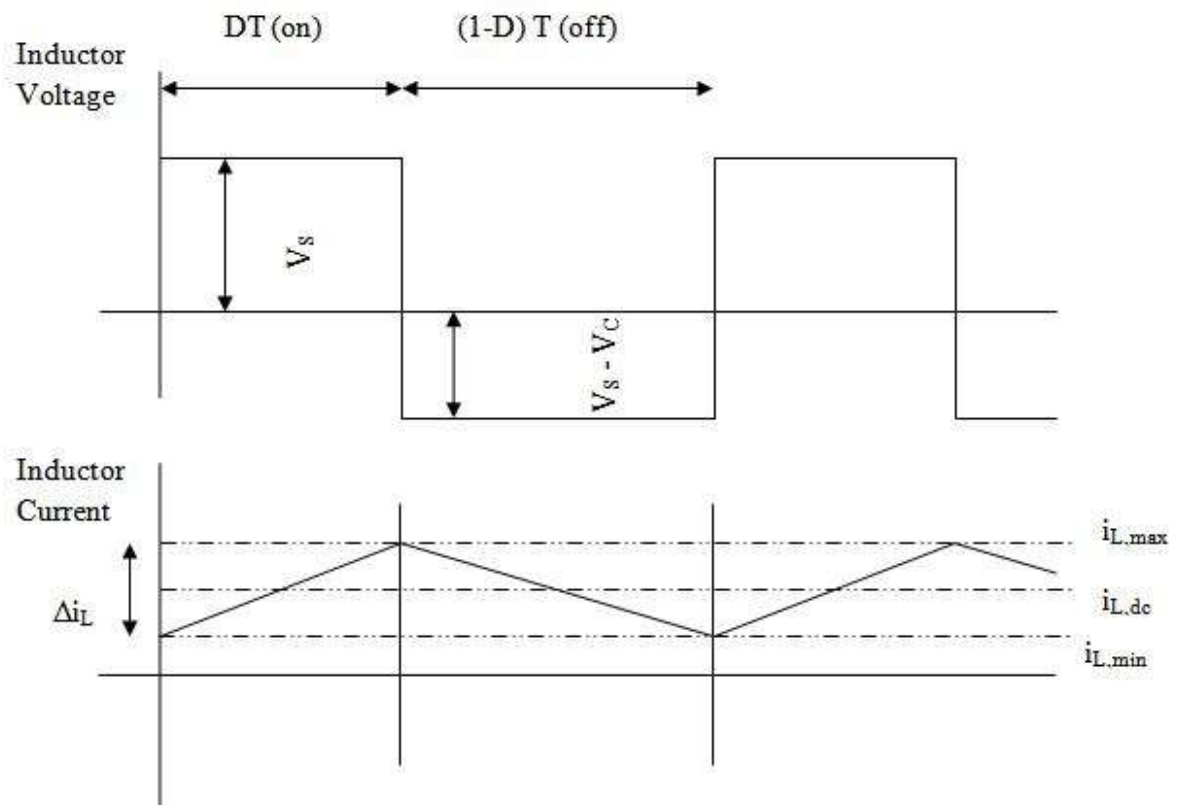


Figure A7 10. PWM output of DC – DC buck converter under continuous conduction mode [53].

The components of the buck converter can be determined using the following governing equation as follows;

When the switch (**S**) is closed; the voltage across the diode can be stated as V_D , then let

$$V_D = V_i \quad (\text{Equation 60})$$

It follows that voltage across the inductor can be given as;

$$V_L = V_D - V_o, \quad (\text{Equation 61})$$

hence

$$V_L = V_i - V_o \quad (\text{Equation 62})$$

And from induction law; $V_{L(t)} = L \cdot \frac{di}{dt}$ (Equation 63)

Therefore, at time t_{on} ; $\frac{di_L}{dt} = \frac{V_L}{L} = \left(\frac{V_i - V_o}{L} t_{on}\right)$ (Equation 64)

If an ideal diode is assumed $V_D = 0$, then;

$$\frac{di_L}{dt} = \frac{V_L}{L} = \left(\frac{-V_o}{L} t_{off}\right) \quad (\text{Equation 65})$$

As can be seen from **Figure A7 10**

$$t_{on} = DT \text{ and } t_{off} = (1 - D)T \quad (\text{Equation 66})$$

Then $\left(\frac{V_i - V_o}{L} t_{on}\right) = \left(\frac{-V_o}{L} t_{off}\right)$ (Equation 67)

$$(V_i - V_o) t_{on} = (-V_o) t_{off} \quad (\text{Equation 68})$$

Hence, Duty cycle (D) $= \frac{V_o}{V_i} \quad (V_o \leq V_i)$ (Equation 69)

7F. Boost Converter

The principle of operation in boost converter is based on producing a DC output voltage that will be larger in magnitude than the input DC voltage. This is achieved by controlling the signal driver duty cycle. The basic components that is normally used in the boost converter implementation are MOSFET (switch), diode, inductor and Capacitor. This is often necessary in low voltage power system applications such as RE generators. The difference between boost converter and buck converter lies in the position of the switching device and the diode, and hence their difference in outputs.

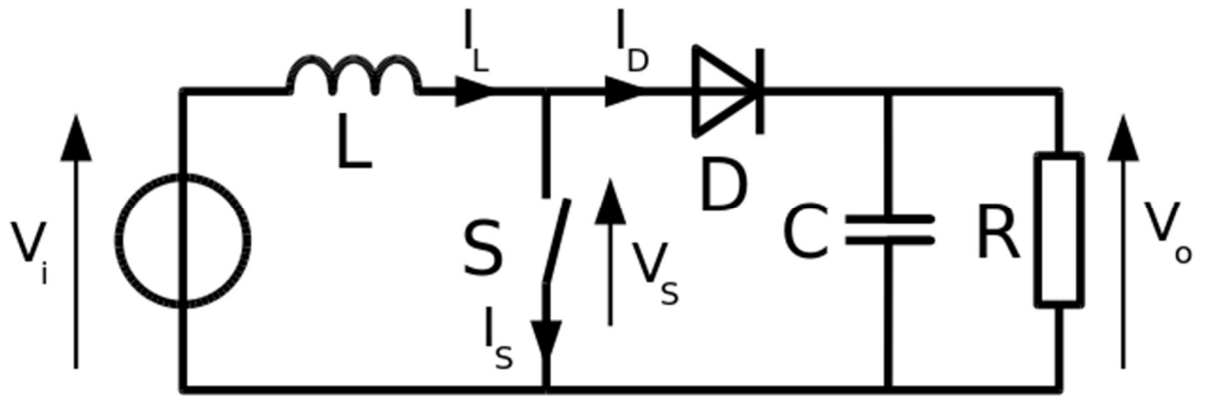


Figure A7 11. DC – DC boost converter [52].

In buck converter, the switch is placed in series with the dc input voltage and this interrupts the dc input voltage (PWM), but in boost converter it is rather placed in parallel and has the input voltage connected in series with the inductor. The boost converter stores energy forms the source (V_i) in the inductor (L) and delivers the stored energy to the load when the switch (S) is closed. The inductor stores energy in form of magnetic field. The magnitude of energy stored in the inductor is given by;

$$E = \frac{1}{2}LI^2 \quad (\text{Equation 70})$$

Where E = stored energy, L = inductor, I = current.

As shown in **Figure A7 11** when the switch (S) is closed current (I_L) flows through the inductor (L) and the switch, charging the inductor in the process, the inductor then maintains the current and not delivering it to the load (R) at first instance.

It follows that;

$$V_L = V_i \quad (\text{Equation 71})$$

Then the rate of change of current at time (t) can be given as follows;

$$\frac{di_L}{dt} = \frac{V_L}{L} = \left(\frac{V_i}{L} t_{on}\right) \quad (\text{Equation 72})$$

Then when the switched (S) is opened (t_{off}) the inductor drives the current through the load (R) via diode D , hence V_o can be assumed to be greater than V_i , the switch can be controlled by high frequency pulse width modulated (PWM) square wave. PWM is a

technique that can be used to deliver power to the load by sending sequential rectangular pulses based on a reference voltage. It follows that by increasing the pulse width the output voltage will be increased. However, the actual output voltage is a function of the duty cycle, the inductance, switching frequency and the output current.

Thus $V_o > V_i$

And voltage across the inductor => $V_L = V_i - V_o$ or $V_o = V_i - V_L$

Rate of change of current;

$$= \frac{di_L}{dt} = \frac{V_L}{L} = \left(\frac{V_i - V_o}{L} t_{off}\right) \quad (\text{Equation 73})$$

This can be transformed as $\left(\frac{V_i - V_o}{L} t_{off}\right) = \left(\frac{V_i}{L} t_{on}\right)$ (Equation 74)

Also $(V_i - V_o)(t_{off}) = (V_i)(t_{on})$ (Equation 75)

Then $V_o (t_{off}) = V_i (T)$ where $T =$ time period

The output voltage is thus

$$V_o = \frac{V_i(T)}{t_{off}} \quad (\text{Equation 76})$$

But $t_{off} = T - t_{on}$ (Equation 77)

So $V_o = \frac{V_i(T)}{T - t_{on}} = \left(\frac{1}{1-D}\right) V_i$ (Equation 78)

Where $D = \frac{t_{on}}{T}$

Hence, Duty cycle (D) $= \frac{V_i}{V_o}$ ($V_o > V_i$)

Figure A7 12 depicts a DC – DC boost converter waveforms

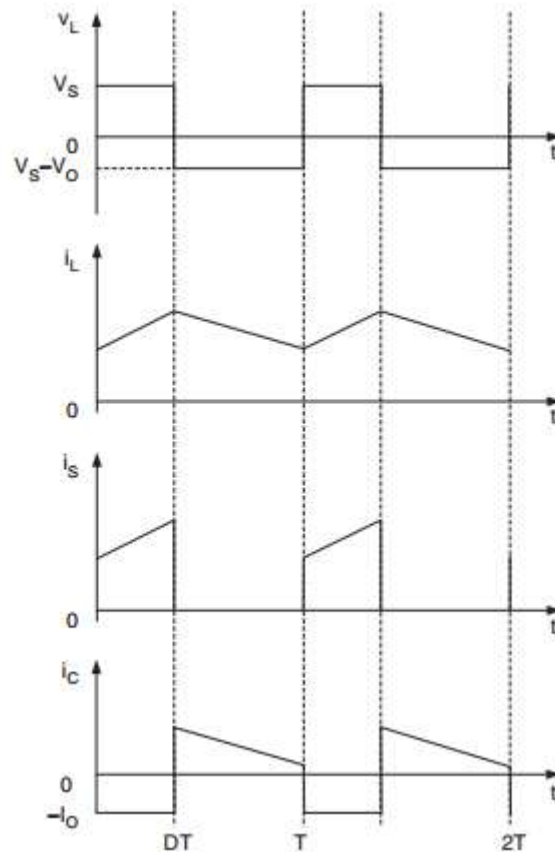


Figure A7 12. DC – DC boost converter waveforms [18].

7G. Component Selection

Ideally, the efficient interaction between the energy storage components (Inductor and capacitor) and the switch (MOSFETs) is key to smooth operation of power converters. For better power converter performance, it is important that the most appropriate components are selected. In boost converter application, it is recommended that an inductor of large value is used, while a lower value may be preferred for buck converter application. Boost filter capacitance can be selected based on equivalent series resistance (ESR). High ESR capacitors degrades performance efficiency, while a low ESR enhances efficiency. Specifically, the filter capacitors should be chosen depending on the required output voltage ripple and its ability to handle the required ripple current. Basically, the choice of capacitors is categorised based on the desired converter topology. Larger filter capacitors are required for DC – DC boost converters, while capacitors of smaller value could be utilised in DC – DC buck converter application.

For diodes, it is useful that a fast recovery diode that can handle a peak current and can block the required off state voltage stress is selected. It has also been recommended that snubber circuits be implemented across diodes used for switching circuits, to protect them from overvoltage spikes, which may arise during the reverse recovery process. This, could be achieved by connecting either a capacitor or resistor or both in parallel with the diode [18]. The switching devices are selected based on voltage requirements and switching frequency. At low voltages below 500V, MOSFETs are preferable [18]. The on-state resistance of the MOSFET, which determines the forward voltage drop across the device, can be quite significant, however, for a low voltage MOSFET, this varies between tens of milliohms, the reverse is the case for a high – voltage MOSFET [18]. A MOSFET with low on-state resistance should be selected. To better understand the importance, performance and operational principles of these devices, a model has been developed using the typical theoretical study as presented above.

7I. Design and Simulation of DC – DC Converter for Solar – Hydrogen Micro Grid System.

In the early stages of a solar – hydrogen DC micro – grid feasibility study, it is necessary that these DC – DC converters are designed to visualise their effects on DC grid power system network. In practical applications, these devices will need to be constructed or purchased. However, it has been recommended that software simulation tools could be used to obtain some comparable behavioural characteristics of these devices [18] [22]. In this study, a range of available simulation tools described in **chapter 5** was considered and Matlab/Simulink was adopted. A block diagram environment used for multi-domain simulation and Model-Based Design is called Simulink. This supports system-level design, simulation, automatic code generation, and continuous test and verification of embedded systems. Models are built by either clicking or dragging blocks from the Simulink browser window to Simulink editor. The tool is commonly used by researchers for virtual experiments and for new model prototyping. An interactive workspace in Matlab facilitates the exchange of data with other software tools for the comparative analysis of results obtained. This makes the tool a universal

one, as it allows evaluation of real data obtained through experimental measurements, in the simulation environment. In this research, a Simulink model of DC – DC converters was developed. The following sections describes the process adopted to obtain the values of the external components and simulation of the converters. All models described was used to investigate the performances of these devices on a DC micro – grid system.

7J. Modelling and Simulation of a DC – DC Boost Converter

As already explained, this study deals with only the continuous conduction mode (CCM) of operation, however, the following equation was used to obtain the component of the boost converter at CCM [18]. Low input DC voltages (e.g. 12V – 48V) that is commonly present in solar photovoltaic panels can be raised to as high as 400Vdc for a DC micro – grid application using a DC – DC boost converter.

Experimental investigations have shown that this process can be realised with the selection of appropriate devices [54]. Right component selection is key to obtaining a desired output voltage, as variation in any of these components may result to an increase or decrease of the output. In this design, the desired circuit parameters are; output voltage = 380Vdc while the input voltage = 48Vdc, the frequency = 5kHz and R (load) = 100 Ohm. From these the desired components values was calculated thus;

the duty cycle can be derived as;

$$\text{Duty cycle } (D) = 1 - \frac{V_i}{V_o} \quad (V_o > V_i) \quad (\text{Equation 79})$$

$$D = \frac{48}{380} = 0.13$$

$$\text{At } L > L_b \text{ (CCM)}$$

$$L_b = \frac{(1-D)^2 * DR}{2f} \quad (\text{Equation 80})$$

Where D = duty cycle, R = load, L_b = boundary inductor and f = frequency.

$$L_b = \frac{(1-0.13)^2 * 0.13 * 100}{2 * 5000} = 0.984mH \cong 1mH$$

The minimum value of filter capacitor (C_{min}) was obtained using the following equation;

$$C_{min} = \frac{DV_o}{V_r R f}$$

Where V_o = output voltage, V_r = input voltage ripple.

$$C_{min} = \frac{0.13 * 380}{48 * 100 * 5000} = 2.05\mu F$$

Table A7 1 lists the specifications deduced from the calculations to be used in the simulation.

Components	Values
Input voltage	48V
Output voltage	380V
Power Level	1.4kW
Inductor	1mH
Capacitor	2.05 μ F
Switching Frequency	5kHz
Load resistor	100 Ω
PWM period	200 μ s

Table A7 1. DC – DC boost converter Parameters.

Other components selected from the Simulink Tool-Box are, diode, pulse generator, pulse width modulation generator (PWM), a MOSFET switch, and the Ideal switch block. However, a 46.7V 329.9W PV panel was selected from the Simulink tool – box as a power source for this simulation the electrical characteristics of the PV is shown in **Figure A7 13**.

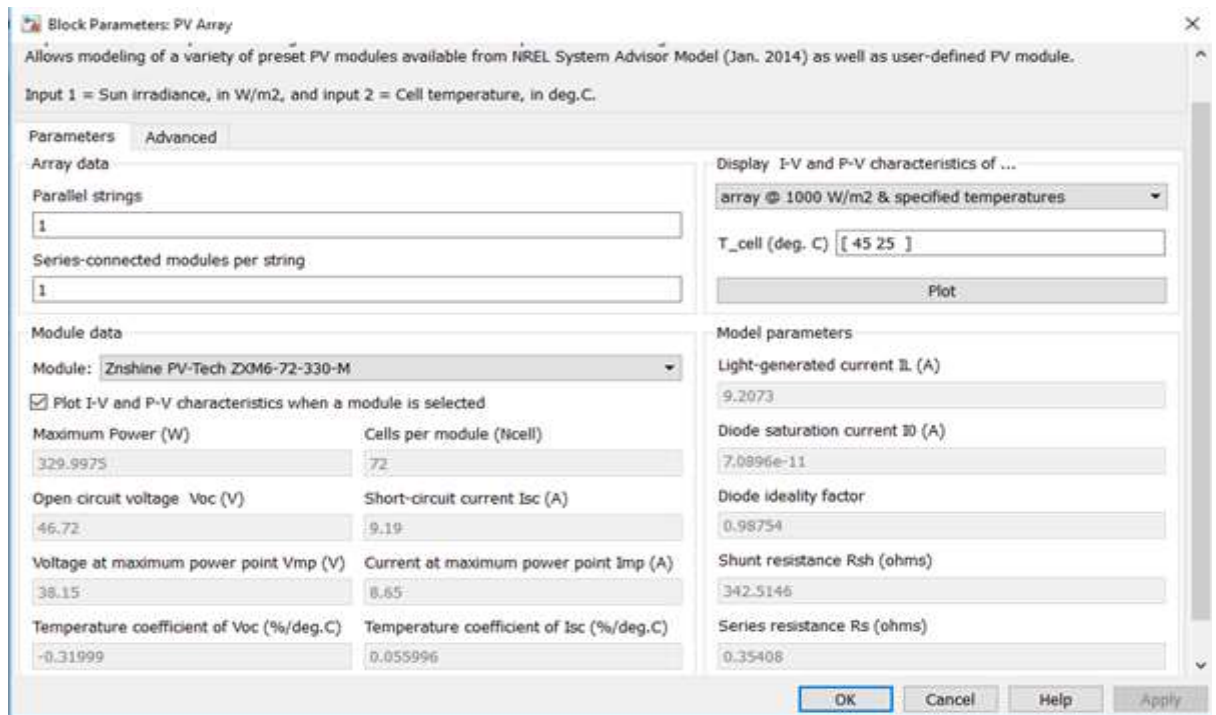


Figure A7 13. 329W PV module electrical characteristics.

These components were selected from the Simulation Tool-Box and implemented with the values obtained from the above calculations. It is however, worth it that a detailed description of the functionalities of the *Simulink ideal switch block* be presented, to fully understand how it was used and its functions in the DC – DC boost converter model. According to Matlab/Simulink, with an appropriate logic the ideal switch can be utilised to model switched devices. As shown in **Figure A7 14** the block is fully controlled by the gate signal (g), the switch can be turned on by applying a positive signal at the gate input. It can also be turned off when the applied gate signal falls to zero. There is also an internal resistance, which makes a series connection to the positive terminal when the switch is in a closed state. However, utilising the ON and OFF states of this device, it is possible that its functionality can be exploited to model a variable system component. This is the basics of how Simulink MOSFET switch was modelled. In **Figure A7 14** when the MOSFET is reverse biased and no gate signal is applied, an internal diode that is connected in parallel with the switch will turn on.

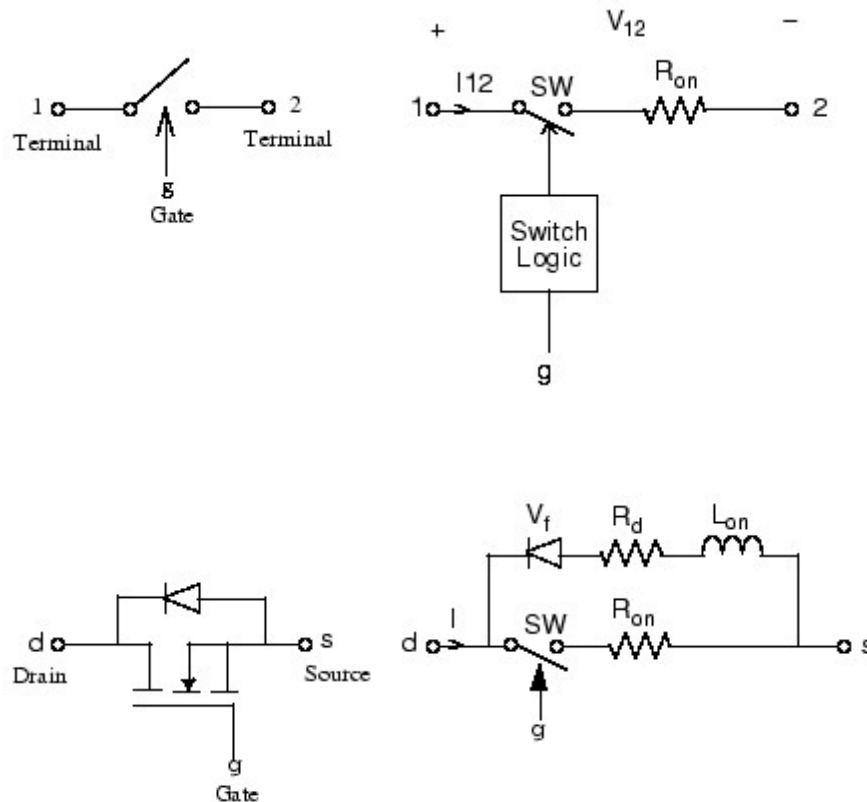


Figure A7 14. Simulink MOSFET switch [55].

Meanwhile, a variable load resistor was designed using the *MOSFET switch* and a 100 Ω resistor that was selected from the Tool – Box. In the process, the current that flows through the resistor will be varied by the input pulses from the PWM generator. In the process, the *MOSFET switch* block was connected in series with the resistor and in parallel to the output of the DC – DC converter. The gate signal of the switch connects with the output of the PWM generator. From Ohms law, current is directly proportional to voltage and inversely proportional to resistance. It follows that, in a linear circuit, an increase in voltage results to a corresponding increase in current, conversely, an increase in resistance will result to a decrease in current. The period (T) of the PWM generator which controls the resistor was set to 200 micro seconds and the pulse width adjusted to 1miliseconds. This varied the resistor value from 0.1 Ohm through 1kilo Ohm. In Simulink, to model a system that has power electronic devices, it has been recommended that the *ideal switching devices* parameter of the *powergui* solver block be enabled [57][56]. This ensures a fast simulation process. Therefore, the

ideal switching devices was enabled in the course of the simulation. **Figure A7 15** shows the modelled DC – DC boost converter.

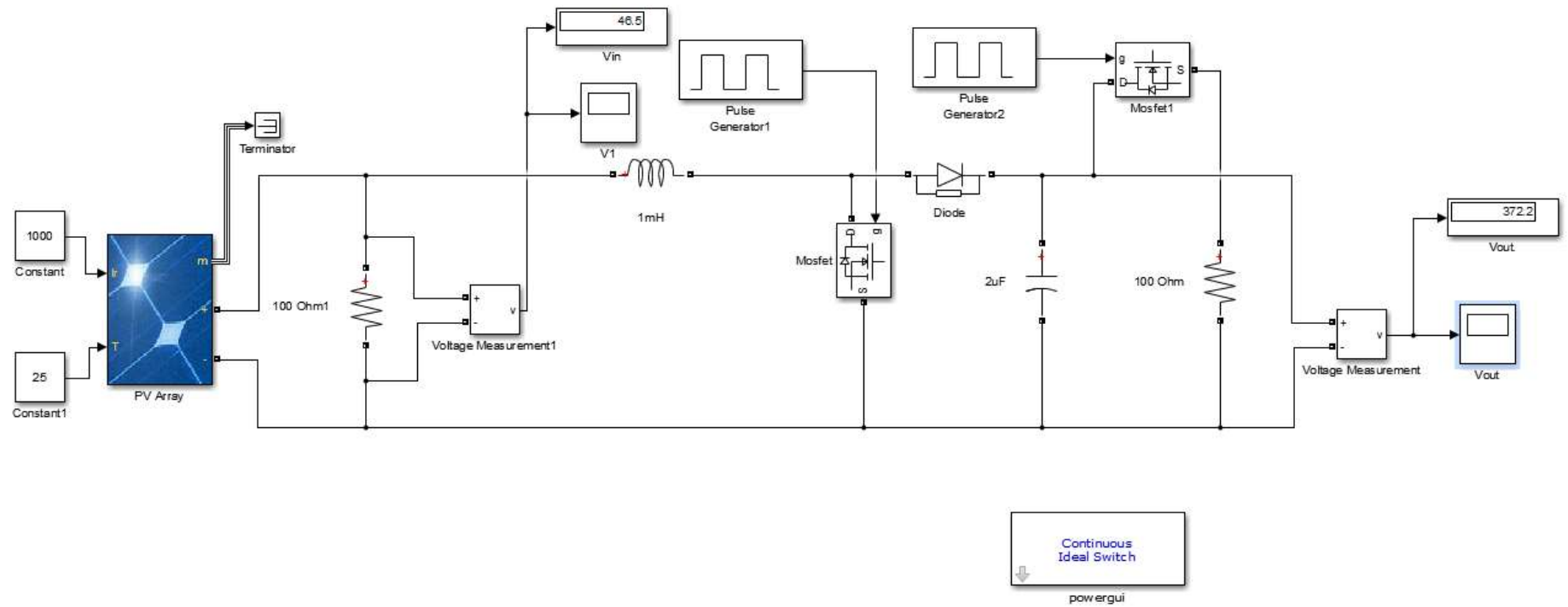


Figure A7 15. A Simulink model of DC – DC boost converter.

The simulation was run for 24 seconds, **Figure A7 16** depicts the simulated response of the output voltage. It can be seen that the DC – DC boost converter has raised the input voltage which was initially at 46V to 372V. Therefore, this simulation, have essentially demonstrated the theoretical realisation of a higher DC output voltage from the lower input voltage, which can be useful for micro – grid applications. The next stage will be to model a power converter which can essentially bring down this voltage to lower voltage, suitable for household appliances.

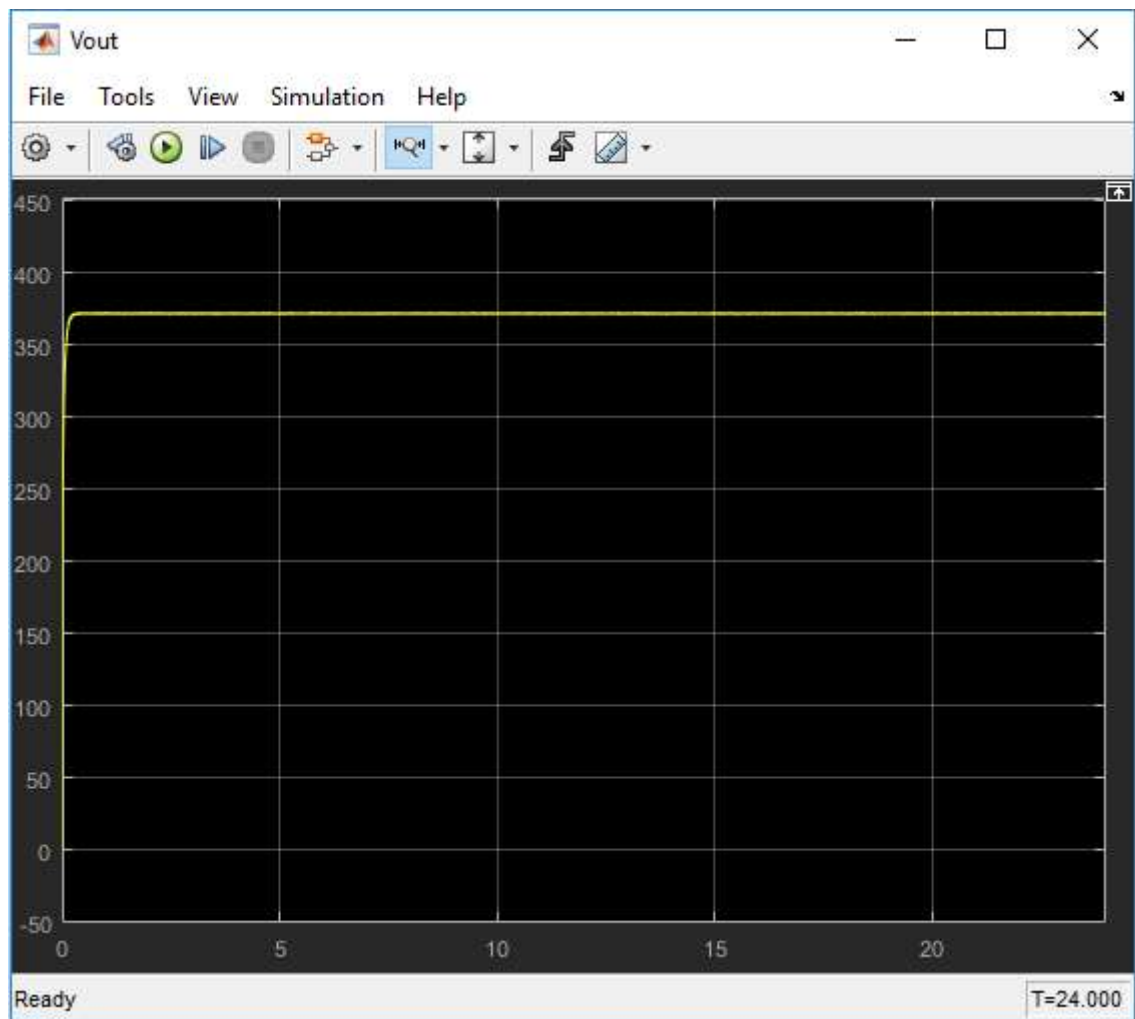


Figure A7 16. 380V output voltage of DC – DC boost converter, from 48Vdc.

7K. Modelling and Simulation of a DC – DC Buck Converter

As previously described, a buck converter can be thought of as a step – down power converter. By connecting the output terminals of a boost converter directly to the input of a buck converter, a DC – DC buck converter can be created. However, DC – DC buck converters can be used to step down the power supply from the high voltage DC transmission line to a lower voltage DC, suitable for the residential home connection. This section presents a modelled DC – DC buck converter. As previously described, the topology of a DC – DC buck converter looks somewhat an inverted form of a DC – DC boost converter. The switch is in series with the inductor and diode in parallel. However, in the DC – DC buck boost converter modelling process, the same modelled DC boost converter presented earlier was used, while the formulas that will be presented in this section will be used to obtain the component parameters of the DC – DC buck converter. The desired output voltage of the DC – DC buck converter was 48V. This means that the 380Vdc output obtained from the PV panel via the DC – DC boost converter will be stepped down to 48Vdc. Ideally, not all household appliances can be powered by 48Vdc, some of the household devices need this voltage to be reduced to 24V, 12V or 5V. The way this can be implemented is explained in detail **later**. In the DC buck converter, in duty cycle calculation the input voltage was used to divide the output voltage thus;

$$Duty\ cycle = \frac{V_o}{V_i} \quad (Equation\ 81)$$

Therefore

$$Duty\ cycle = \frac{380}{48} = 7.92$$

To calculate the specification parameter of the inductor, the following formula was used;

$$L = \frac{(1-D)^2 * R}{2 * F} \quad (Equation\ 82)$$

Where ΔI_r = inductor ripple current, L = inductor, V_o = desired output voltage, V_i = typical input voltage, and f_s = switching frequency. The inductor ripple current can be deduced from the output current as follows;

Since the desired output voltage = 48V and load resistor = 100Ω, then

$$\text{Maximum output current} = \frac{V_o}{R} = \frac{48}{100} = 4.8A$$

But, inductor ripple current = 30% of the output maximum output current. Hence, $\Delta I_r = 1.44A$. Therefore, the inductor value can be derived as;

$$L = \frac{(1 - 7.92)^2 * 100}{2 * 5000} = 0.479H$$

and, the estimated capacitor value was derived from the following relation;

$$C_{min} = \frac{DV_o}{V_r R f} \quad (\text{Equation 83})$$

Hence, the estimated value of the capacitor =

$$C_{min} = \frac{7.92 * 48}{48 * 100 * 5000} = 2\mu F$$

Table A 7 2 lists summary of the component parameters used in the DC – DC buck converter simulation.

Components/parameters	Values
Input voltage	380V
Output voltage	48V
Power Level	230W
Inductor	0.479H
Capacitor	2μF
Switching Frequency	5kHz
Load resistor	100Ω
PWM period	200μs

Table A7 2. DC – DC bulk converter parameters.

These components were selected from the Simulink tool – box and their values adjusted to reflect these values listed. The variable resistor was set to be controlled using a MOSFET switch, pulse signal was supplied to the MOSFET using a PWM generator. The electrical connection was implemented. Simulation was run for 24 second. **Figure A7 17** show the output voltage from the DC – DC buck converter and

Figure A7 18 depicts the modelled DC – DC buck converter. It can be seen as the buck converter stepped down the 380 V input DC voltage to 48Vdc. However, it was observed that the voltage fluctuated between 45V and 48V, but the result was 48.98V. This accounts for the transient response of the inductor voltage due to losses in the MOSFET switch.

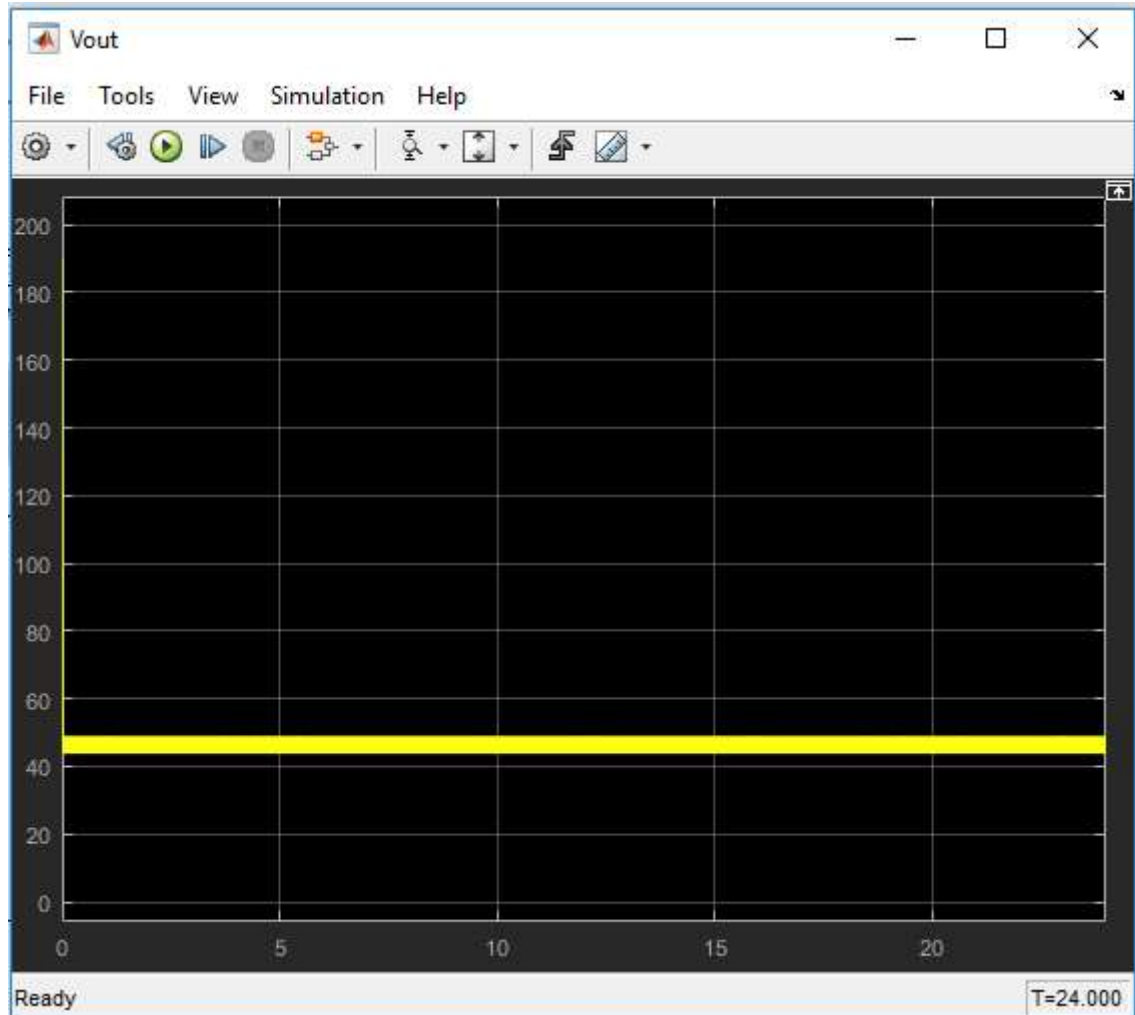


Figure A7 17. 48V output voltage of DC – DC buck converter, from 380Vdc.

From the simulation, it can be seen that a high voltage DC can be regulated to a low voltage suitable for power distribution in a micro – grid arrangement.

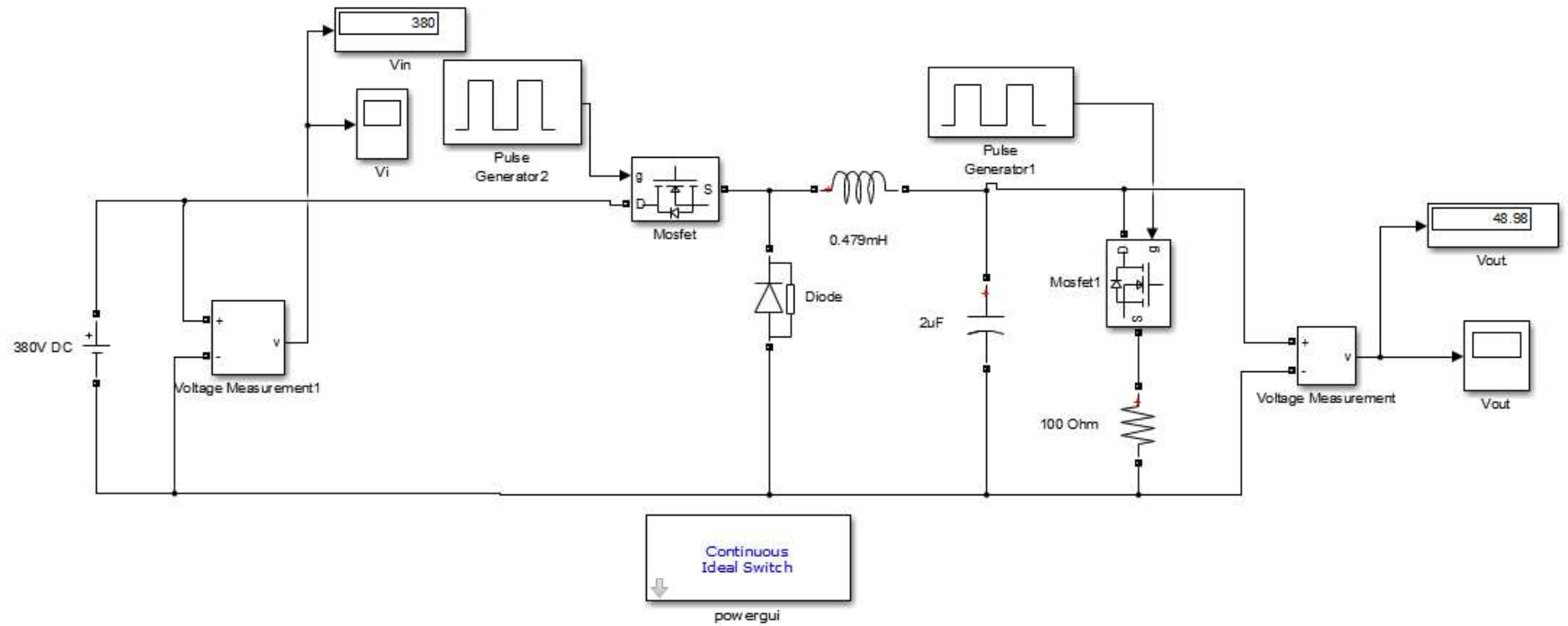


Figure A7 18. A Simulink model of DC – DC bulk converter.

